

UNIVERSITY OF NOTTINGHAM

School of Chemical, Environmental and Mining Engineering



**Treatment of Semi-Synthetic Metalworking Fluids:
Membrane Filtration and Bioremediation**

By

Gérald Thierry Michel Busca

D.E.A. Sciences et Techniques du Déchet

**Thesis submitted to the University of Nottingham
for the degree of Doctor of Philosophy, September 2004**

A ma Mère et à Stacey

ABSTRACT

Waste engineering fluids, such as coolants and cutting fluids, are difficult to treat because they have variable physical natures, are particularly toxic and have a very high Chemical Oxygen Demand. The complex and unknown chemical content of the many different products available is also problematic. Current technologies, such as nanofiltration or chemical treatment, are quite effective at reducing the COD of the waste metalworking fluids before disposal. These technologies remove free or emulsified oil and high molecular weight components, but they have their limitations. In addition, the more stringent legislation on waste disposal and effluent discharge induces an economical stress on engineering industries. It can be anticipated that future legislations will introduce eco-toxicology measurements into industrial effluent discharge consents. A modular on-site treatment plant to treat semi-synthetic metalworking fluids was developed in this thesis. The approach was to combine different technologies and to inter-optimize their performances. The technologies used were membrane filtration, bioremediation and chemical treatment. The use of activated carbon was also studied. Membrane filtration included the study of ultrafiltration and nanofiltration. For the bioremediation process, a bio-consortia was developed and tested over 8 months. A final design of the whole process is given. The proposed treatment plant transforms the waste metalworking fluid into two products: very low chemical oxygen demand aqueous phase at 30 mg/l COD and a recovered oil showing a calorific value of 42 kJ/kg which could be a possible commodity. The whole treatment plant is scaled-up for the treatment of 500 L of waste metalworking fluid per day.

AFFIRMATION

The work submitted in this theses is my own work and has not been previously submitted for any other degree.

SEVEN PAPERS HAVE BEEN PUBLISHED FROM THIS WORK

1- Hilal N., Kochkodan V., Al-Khatib L., **Busca G.**, “Characterization of molecularly imprinted composite membranes using an atomic force microscope”.
SURFACE AND INTERFACE ANALYSIS 33 (8) (2002) pp. 672-675.

2- Hilal N., Kochkodan V., **Busca G.**, Kochkodan O., Atkin B.P., “Thin layer composite molecularly imprinted membranes for selective separation of cAMP”
SEPARATION AND PURIFICATION TECHNOLOGY 31 (3) (2003) pp. 281-289.

3- **Busca G.**, Hilal N., Atkin B.P. “Optimisation of washing cycle on ultrafiltration membranes used in treatment of metalworking fluids”
DESALINATION 156 (1-3) (2003) pp. 199-207

4- Hilal N., **Busca G.**, Talens-Alesson F., Atkin B.P., “Treatment of waste coolants by coagulation and membrane filtration”
CHEMICAL ENGINEERING AND PROCESSING 43 (7) (2004) pp. 811-821

5- Hilal N., **Busca G.**, Hankins N., Mohammed A.W., “The use of ultrafiltration and nanofiltration membranes in metalworking fluids treatment”
DESALINATION 167 (2004) pp. 227-238

6- Hilal N., **Busca G.**, Rozada F., “Use of activated carbon to polish effluent from metalworking treatment plant: comparison of different streams”
DESALINATION (2005) in press.

7- Hilal N., **Busca G.**, Al-Zoubi H., Waller M.P., “Development and test of a bioconsortia for the treatment of metalworking fluids”
Submitted to *JOURNAL OF CHEMICAL TECHNOLOGY & BIOTECHNOLOGY*

ACKNOWLEDGEMENTS

First of all, I would like to express my gratitude to my supervisor, Dr. Nidal Hilal, Reader in Chemical Engineering and Director of Centre for Clean Water Technologies at Nottingham, for his support throughout the project. Nidal, I appreciate your guidance and patience, especially when circumstances were difficult. I also appreciated your advice and encouragement for publishing papers.

I would also like to thank Dr Brian Atkin, former Head of the School and now Vice-president of University of Nottingham-Malaysia Campus, for his support.

All my gratitude to Mr Keith Baker, General Manager of the Environmental Technology Centre, who initiated the project and offered very much-appreciated help at all levels and at any time.

This project was co-founded by Cardev International Ltd, and as such, I am grateful for the company's interest in the research carried out. I would like to thank particularly Mr John Willcock, who has followed conscientiously my progress throughout the work.

Many thanks to all my colleagues and the technicians of Lab L4 Tony, Bill and the super IT team Sue, Phil and Johnnie.

The fun part of my stay in SCHEME includes many people, I will try not to forget anybody! First Windy, you helped me so much to settle in the UK. Thanks to you and to your lovely family for your generosity. Thanks to Neil, Mike and Del for some memorable POETS' days! Fernando who helped me to set up the activated carbon experiments, and for the Salsa dance and the good times we spent while you were here. About Salsa and having fun, thanks to Federico, Ignazi and Smeetha.

The last but the most important acknowledgement goes to Stacey. Stacey, thank you for your support, especially during this difficult end of writing up. All my gratitude for the work you did on my manuscript, cutting my long sentences, teaching me how to use English grammar. Stacey, I will always be grateful and thankful for you being here with me.

TABLE OF CONTENTS

ABSTRACT		i
AFFIRMATION		ii
PUBLISHED PAPERS		iii
ACKNOWLEDGEMENTS		iv
TABLE OF CONTENTS		v
LIST OF FIGURES		xi
LIST OF TABLES		xvii
LIST OF EQUATIONS		xx
LIST OF SYMBOLS AND ABBREVIATIONS		xxii
CHAPTER I	INTRODUCTION	1
CHAPTER II	LITERATURE REVIEW	6
II.1	Introduction	7
II.2	Industrial waste effluent	7
II.2.1	Domestic Sewage	7
II.2.2	Rainwater	8
II.2.3	Trade Effluent	8
II.2.4	Charges for trade effluent	9
II.2.4.1	Consent to discharge	9
II.2.4.2	Discharge to sewer	10
II.2.4.3	Effluent discharges into rivers and other water courses	11
II.2.5	Regulations	11
II.3	Metalworking fluids	12
II.3.1	Brief history of metalworking fluids	12
II.3.2	Uses and chemistry of metalworking fluids	14
II.3.2.1	Types of metalworking fluids	14
II.3.2.2	Chemistry of semi-synthetic metalworking fluids	15
II.3.3	Microbiology of metalworking fluid	17
II.3.3.1	Problems due to microbial contamination of MWF	18
II.3.3.2	Biodegradability	18
II.3.4	Waste metalworking fluids disposal options	19
II.3.4.1	Direct Sewer	20
II.3.4.2	On-site treatment	20
II.4	Membrane technology and applications	22
II.4.1	Definition	22

II.4.2	History	23
II.4.3	Membrane processes	24
II.4.4	General applications	27
II.4.5	Applications in wastewater treatment	28
II.4.6	Filtration of metalworking fluids	28
II.4.7	Water recovery	32
II.4.8	Fouling	33
II.4.8.1	Fouling mechanisms	33
II.4.8.2	Specific type of fouling	34
II.4.8.3	Membrane cleaning	35
II.4.9	Techniques to enhance filtration	36
II.4.9.1	Filtration module and hydrodynamic conditions	37
II.4.9.2	Introducing turbulence	38
II.4.9.3	Surface modification	40
II.4.9.4	Feed Pre-treatment	41
II.4.10	Modelling of filtration for oil waste water	42
II.4.10.1	Permeate flux models	42
II.4.10.2	Membrane surface capture of particles	45
II.5	Atomic force microscopy	45
II.5.1	Introduction	46
II.5.2	Scanning modes	46
II.5.3	AFM applied to membrane	47
II.6	Biological treatment of waste	48
II.6.1	Biodegradation of MWF	49
II.6.2	Bioreactor	49
II.6.3	Scaling-up	51
II.7	Physical chemical method	51
II.8	Activated carbon	53
II.9	Fuel incineration generated from waste	54
CHAPTER III EXPERIMENTAL EQUIPMENT AND PROCEDURES		56
III.1	Introduction	57
III.2	Waste preparation and characterisation	58
III.2.1	The oil: Mobilcut 232	58
III.2.2	Waste simulation and metalworking fluid preparation	59
III.2.3	Waste characterisation	60
III.3	Membranes	62
III.3.1	Ultrafiltration membranes	62
III.3.2	Nanofiltration membranes	63
III.4	Filtrations	63
III.4.1	Small-scale filtration units	63
III.4.1.1	Dead-end filtration cell	64
III.4.1.2	Flat sheet unit	65
III.4.1.3	Cross flow small-scale unit	66
III.4.2	Cross flow large-scale equipment	67
III.4.2.1	Membrane filtration module	67
III.4.2.2	Power	67
III.4.2.3	Waste Coolant tank	67

III.4.2.4	Description of the filtration units	68
III.4.2.5	Filtration operation	71
III.4.2.6	Flushing operation	73
III.4.3	Filtration protocol	74
III.4.4	Washing cycles	74
III.4.4.1	Optimisation of washing cycles	75
III.4.4.2	Washing protocol	77
III.4.5	Cold water flux protocol	78
III.4.6	Temperature tests	78
III.5	Gas injection	79
III.5.1	Experimental apparatus	79
III.5.2	Set of experiments	82
III.6	Chemical treatment	82
III.6.1	Coagulation	82
III.6.2	Acidification	83
III.7	Bioremediation	84
III.7.1	Extraction of indigenous community	84
III.7.2	Flask tests	84
III.7.3	Continuous stirred bioreactor	85
III.7.3.1	Description	85
III.7.4	Small-scale fixed bed bioreactor	86
III.7.4.1	Description	86
III.7.4.2	Bioreactor installation protocol	88
III.7.4.3	Experiment	89
III.7.5	Large-scale Bioreactor	89
III.8	Activated Carbon adsorptions	90
III.8.1	Activated carbon	90
III.8.2	Batch test	91
III.8.3	Columns	91
III.9	Atomic Force Microscope (AFM)	93
III.9.1	Equipment	93
III.9.2	Sample preparation	93
III.9.3	Scan mode	94
III.9.4	Surface analysis	95
III.9.4.1	Geometry	95
III.9.4.2	Roughness	96
III.10	Analysis	97
III.10.1	Measurement of Total Organic Carbon	97
III.10.2	Chemical Oxygen Demand	98
III.10.3	Measurement of pH, Conductivity and Turbidity	98
III.10.4	Calorific Values	98
III.10.5	Ash content	99
III.10.5.1	Producing the ashes	99
III.10.5.2	Ash analyses	100

CHAPTER IV	ATOMIC FORCE MICROSCOPY	101
IV.1	Introduction	102
IV.2	Nanofiltration membrane images	102
IV.3	Determination of pore size distribution	105
CHAPTER V	WASTE CHARACTERISATION, CHEMICAL TREATMENT AND FUEL	108
V.1	Introduction	109
V.2	Fluid characterisation	109
V.2.1	Characterisation of the concentrate	110
V.2.2	Zeta potential measurement	111
V.2.3	Droplets size distribution	112
V.2.4	Concentration stability	118
V.2.5	Fluid viscosity	119
V.2.6	Recapitulation	119
V.3	Chemical treatments	120
V.3.1	Inorganic salts	120
V.3.1.1	Fresh metalworking fluid flocculation	121
V.3.1.2	Concentrate coagulation	124
V.3.2	Acidification	132
V.3.2.1	Concentrate acidification	133
V.3.2.2	Fresh MWF 20% acidification	137
V.3.2.3	Alkaline treatment	138
V.3.3	Calorific value	140
V.3.3.1	Results	140
V.3.3.2	Discussion	141
V.4	Synthesis	145
CHAPTER VI	MEMBRANE FILTRATIONS	146
VI.1	Introduction	147
VI.2	Small-scale filtration	148
VI.2.1	Flat sheet membranes	149
VI.2.1.1	Dead-end filtrations	149
VI.2.1.2	Cross flow flat sheet membrane	152
VI.2.2	Tubular membrane	152
VI.2.2.1	Effect of temperature	153
VI.2.3	Washing cycles	157
VI.2.4	Gas injection	162
VI.2.4.1	Gas injected during demineralised water filtering	163
VI.2.4.2	Gas injected in during MWF5% filtration	167
VI.3	Results obtained with initial instructions	171
VI.3.1	Permeate flux	171

VI.3.2	Permeate quality	173
VI.3.3	Effect of reloading the main tank	175
VI.4	Direct filtration	177
VI.4.1	Effect of transmembrane pressure (TMP)	178
VI.4.1.1	Permeate flux	178
VI.4.1.2	Permeate quality	181
VI.4.2	Effect of feed velocity	185
VI.4.2.1	Ultrafiltration membranes	185
VI.4.2.2	Nanofiltration membrane	189
VI.5	Combination ultra-and nanofiltration	190
VI.6	Model	193
VI.6.1	Ultrafiltration FP200	194
VI.6.2	Ultrafiltration FP100	197
VI.6.3	Nanofiltration AFC30	200
VI.6.4	Oil permeation mechanism	202
VI.7	Synthesis	203
VI.7.1	Small-scale results	203
VI.7.2	Large-scale ultrafiltration	204
VI.7.3	Large-scale nanofiltration	205
VI.7.4	Combining UF and NF	205
VI.7.5	Model	206
CHAPTER VII	ACTIVATED CARBON	207
VII.1	Introduction	208
VII.2	Batch tests adsorption trials	209
VII.2.1	Adsorption isotherms	209
VII.2.2	Fittings to isotherms	210
VII.3	Continuous mode	212
VII.3.1	Column results	212
VII.4	Summary	216
CHAPTER VIII	BIOLOGICAL PROCESS	218
VIII.1	Introduction	219
VIII.2	Experiments carried out in Oxford	220
VIII.2.1	Plate counting	220
VIII.2.2	Bacteria consortia test	221
VIII.3	Experiments carried out in Nottingham	222
VIII.3.1	Development of a home made bio-consortium	223
VIII.3.2	Culturing the Indigenous Community	223
VIII.3.3	Enrichment	227
VIII.3.3.1	Definitions	227
VIII.3.3.2	Strategy adopted	229
VIII.3.3.3	Continuous suspended bioreactor	230
VIII.4	Fixed bed bioreactor	233
VIII.4.1	Optimisation of the ratio COD/flow rate	234
VIII.4.2	Recycling loop	235
VIII.5	Syntheses	236

VIII.5.1	Achievements	236
VIII.5.2	Additional improvements	237
CHAPTER IX	SYSTEM DESIGN	239
IX.1	Introduction	240
IX.2	Initial Design	240
	IX.2.1 Liquid handling	240
	IX.2.2 Concentrate tank and bioreactor feed	241
	IX.2.3 Post bioreactor treatment	242
IX.3	Choice of filtrations	243
IX.4	Treating the concentrate	245
	IX.4.1 UF concentrate	245
	IX.4.2 NF concentrate	246
IX.5	The biological treatment	248
	IX.5.1 Functioning parameters of the bioreactor developed	248
	IX.5.2 Bioreactor scale-up	249
IX.6	Scaling up activated carbon column	250
IX.7	Scale-up of the WHOLE process	252
IX.8	Synthesis	253
CHAPTER X	CONCLUSION AND RECOMMENDATIONS	256
REFERENCES		260
APPENDICES		270

LIST OF FIGURES**CHAPTER II**

Figure II-1: Types of membrane filtration	26
Figure II-2: Membrane filtration control regions	43

CHAPTER III

Figure III-1: Mixing unit	60
Figure III-2: Abacus for oil concentration in water applicable for Mobil cut 232	61
Figure III-3: Dead-end filtration cells	64
Figure III-4: Small scale UF flat sheet unit	65
Figure III-5: Small-scale tubular membrane unit	66
Figure III-6: Side view of the first membrane unit	69
Figure III-7: Top view of the filtration unit 1	69
Figure III-8: Filtration unit 2	70
Figure III-9: Experimental set up used for washing cycle and temperature test	75
Figure III-10: Picture gas injection assembly	81
Figure III-11: Schematic diagram of gas injection assembly	81
Figure III-12: Continuous stirred bioreactor	86
Figure III-13: Fixed bed bioreactor	88
Figure III-14: Activated carbon column set-up	92
Figure III-15: Sample holding technique	94
Figure III-16: Projection of the areas defined by 4 consecutive pixels	98

CHAPTER IV

Figure IV-1: AFM imaging for AFC30 membrane large size	103
Figure IV-2: AFM imaging of AFC30 membrane at nanometric scale	103
Figure IV-3: Three dimensional AFM image for BM05-D with small size surface image.	104
Figure IV-4 Three dimensional AFM image for BM20-D with small size surface image.	104
Figure IV-5: Pore size distribution of AFC30 with fitted equation	106
Figure IV-6: Pore size distribution of BM05-D membrane with the fitted equation	106

Figure IV-7: Pore size distribution of MB20-D with fitted	107
Figure IV-8: Example of line measurement for AFM pore size determination	107

CHAPTER V

Figure V-1: Relationship between refractometry method and concentrate TOC measurements	110
Figure V-2: Microemulsion zeta potential	111
Figure V-3: Measurement of oil droplet using demineralised water at low count rate	114
Figure V-4: Droplet size distribution with demineralised water at high count rate	115
Figure V-5: Droplet size distribution with demineralised water as dilutant high count rate	116
Figure V-6: Droplet size when UF permeate is used as dilutant	117
Figure V-7: Picture of the different oil fraction after standing for 72 hours	118
Figure V-8: pH evolution during addition of aluminium sulphate	124
Figure V-9: Gibbsite Octahedral structure describing the layer of $\text{Al}(\text{OH})_3$	127
Figure V-10: Illustration of aggregated and merged droplets	128
Figure V-11: New emulsion equilibriums case of surfactant impoverishment	131
Figure V-12: New equilibrium case of surfactant enrichment	132
Figure V-13: Waste metalworking fluid after acidification no.2 showing the 3 phases obtained	133
Figure V-14: pH evolution during the fifth acidification vs. volume of acid poured	135
Figure V-15: pH evolution when adding acid progressively	136
Figure V-16: pH evolution after adding acid directly	136
Figure V-17: pH evolution vs. acid addition for fresh MWF20%	138

CHAPTER VI

Figure VI-1: Water flux and effluent flux for BM-05D nanofiltration membrane	151
Figure VI-2: Water flux and effluent flux for BM-20D nanofiltration membrane	151
Figure VI-3: Permeate flux of ultrafiltration membrane FP100 at 3 different temperatures	153
Figure VI-4: Permeate flux of ultrafiltration membrane FP200	

at 3 different temperatures	154
Figure VI-5: Permeate flux vs. feed temperature after 1-hour filtration	155
Figure VI-6: Permeate TOC vs. feed temperature after 1 hour filtration	155
Figure VI-7: Permeate turbidity vs. feed temperature after 1 hour filtration	156
Figure VI-8: Comparison of permeates flux between re-circulation and concentration regime	157
Figure VI-9: Permeate flux during washing cycle and effect of applying pressure	160
Figure VI-10: Filtration of MWF5% after successive washing cycle	161
Figure VI-11: Effect of surfactant used during washing on metalworking fluid filtration	162
Figure VI-12: Permeate flux of demineralised water filtered with FP200 when gas is injected	164
Figure VI-13: Permeate flux when using a two phase flow	167
Figure VI-14: Filtration of metalworking fluid after gas injection has been stopped	168
Figure VI-15: Turbidity of MWF5% when air has been injected at 3.5 bar for 15 min	169
Figure VI-16: Picture of clear tube after MWF filtration with (left) and without (right) gas	170
Figure VI-17: Permeate flux of MWF5% filtration with “cardev filtration conditions”	172
Figure VI-18: Evolution of the permeate turbidity with “cardev filtration condition”	173
Figure VI-19: Permeate turbidity compared to temperature increase during “cardev filtration conditions”	174
Figure VI-20: Permeate turbidity compared to feed concentration increase during “cardev filtration conditions”	174
Figure VI-21: Permeate quality and flux decline during “cardev filtration conditions”	175
Figure VI-22: 3 Semi-batch UF filtrations with “cardev conditions”, comparison between permeate flux, indicating fouling, and feed turbidity, indicating oil permeation	176
Figure VI-23: Permeate flux at different TMP for UF FP100, FP200 and NF AFC 30	

membranes using MWF5% and MWF20% as feed	179
Figure VI-24: Evolution of permeate turbidity with feed concentration for FP100 at low TMP	182
Figure VI-25: Evolution of permeate turbidity with feed concentration for FP200 at low TMP	182
Figure VI-26: Evolution of permeate turbidity with feed concentration for AFC 30 at 6 bar	183
Figure VI-27: Influence of feed velocity on initial permeate flux with feed MWF5% using UF membrane FP100	186
Figure VI-28: Influence of feed velocity on initial permeate flux feed MWF5% using UF membrane FP100 at low TMP	187
Figure VI-29: Influence of feed velocity on initial permeate flux with feed MWF20% using UF membrane FP100	187
Figure VI-30: Influence of feed velocity on initial permeate flux with feed MWF5% using UF membrane FP200	188
Figure VI-31: Influence of feed velocity on initial permeate flux with feed MWF16% using UF membrane FP200	188
Figure VI-32: Influence of feed velocity on initial permeate flux with feed MWF5% using NF membrane AFC30	189
Figure VI-33: Influence of feed velocity on initial permeate flux with feed MWF20% using NF membrane AFC30	190
Figure VI-34: Nanofiltration runs, comparison between UF pre-treated feeds and direct filtration using MWF5% over 40 hours	192
Figure VI-35: Permeate flux plotted against retentate concentration during ultrafiltration using FP200 with a TMP of 2.75 bar and 3 different logarithm fitting curves	195
Figure VI-36: Permeate flux plotted against retentate concentration during ultrafiltration using FP200 with a TMP of 2.75 bar at high feed concentration after regenerating the membrane surface	195
Figure VI-37: Permeate flux plotted against retentate concentration during ultrafiltration using FP200 with a TMP of 3.5 bar	196
Figure VI-38: Permeate flux plotted against retentate concentration during ultrafiltration using FP100 with a TMP of 3.5 bar	198

Figure VI-39: Permeate flux plotted against retentate concentration during ultrafiltration using FP100 with a TMP of 6 bar	198
Figure VI-40: Permeate flux plotted against retentate concentration during ultrafiltration using FP100 with a TMP of 2.75 bar for high retentate concentration	199
Figure VI-41: Permeate flux plotted against retentate concentration during direct nanofiltration using AFC30 with a TMP of 6 bar	201
Figure VI-42: Permeate flux plotted against retentate concentration during direct nanofiltration using AFC30 with a TMP of 6 bar after regenerating the membrane surface and using the concentrate as feed.	201
Figure VI-43: Illustration of gel formation relative to feed concentration increase.	202
Figure VI-44: Phase inversion principle due to oil droplet compaction	203
 CHAPTER VII	
Figure VII-1: Adsorption isotherms	210
Figure VII-3: Concentration treated (C_o) and breakthrough curves for the adsorption process of effluent-e	213
Figure VII-5: Concentration treated (C_o) and breakthrough curves for the adsorption process of effluent-eBF	213
Figure VII-7: Concentration treated (C_o) and breakthrough curves for the adsorption process of effluent-eB	214
Figure VII-9: pH of the effluent collected at the outlet of each activated carbon column	215
Figure VII-11: Picture of effluent bioreactor permeate on the left and the three effluent after activated carbon on the right in order from left to right (-e; -eB and eBF)	216
Figure VII-13: Efficiency of activated carbon on the different effluent tested after 25 litres passed through each column	217
 CHAPTER VIII	
Figure VIII-1: Oxford bio consortia with dilute UF-permeate	222
Figure VIII-2: Nanofiltration permeate test with IC	224
Figure VIII-3: Diluted ultrafiltration permeate flask test with IC	225

Figure VIII-4: Biodegradability comparison between NF and UF permeate	226
Figure VIII-5: Illustration of the impact of enrichment on indigenous population.	228
Figure VIII-6: Indigenous community growth curve	230
Figure VIII-7: Influence of the retention time on the COD removal	231
Figure VIII-8: COD reduction ability of the IC (retention times indicated in day)	232
Figure VIII-9: Reduction in effluent COD	233
Figure VIII-10: Feed COD load and COD removal	235

CHAPTER IX

Figure IX-1: Filtration system	244
Figure IX-2: Acidification process	246
Figure IX-3: Activated carbon column scale-up	251
Figure IX-4: Activated carbon assembly	252
Figure IX-5: Final integrated process	253

LIST OF TABLES**CHAPTER II**

Table II-1: Different types of MWF, their properties and applications	15
Table II-2: Comparison of aerobic and anaerobic systems (+) relative advantage and (-) relative disadvantage	50

CHAPTER III

Table III-1: Steel utilisation of Mobilcut 232	58
Table III-2: Alloy utilisation of Mobilcut 232	59
Table III-3: Value of the washing cycle factors	76
Table III-4: Explicit experimental plan for washing cycle optimisation	76
Table III-5: Surfactant properties	78
Table III-6: Small-bioreactor specifications	87
Table III-7: Bio-decking description	89
Table III-8: Optimised scanning parameters	94

CHAPTER IV

Table IV-1: Constants obtained from fitted curves logNormal distribution	105
--	-----

CHAPTER V

Table V-1: Results from the 4 measurements of the zeta potential of Mobilcut 232 at 5%	111
Table V-2: Refractive index	113
Table V-3: Droplet size analysis	114
Table V-4: Size value of oil droplet	115
Table V-5: Size value of the oil droplets	116
Table V-6: Size value of the particles	117
Table V-7: Description of the different phases found when oil ratio increases	118
Table V-8: Viscosity of different effluent	119
Table V-9: Apparent colloid characteristic constants for fast flocculation	121

Table V-10: Theoretical ratios, $R_{\text{turbid/clear}}$, for complex concentrations forming at the nominal MCl ₃ concentrations leading to the onset of turbid overdosed solution and clear flocculate solution flocculate, for three different complex stoichiometries n.	123
Table V-11: Results from acidification tests	134
Table V-12: Comparison of calorific values	140
Table V-13: Ash analyses of recovered oil	144
 CHAPTER VI	
Table VI-1: Explicit experimental plan and CWF response	158
Table VI-2: Evaluation of the average effect of washing condition on the CWF	158
Table VI-3: Two phases flow pattern corresponding to the gas flow rate	164
Table VI-4: High feed concentration filtration results for the three membranes	183
Table VI-5: Typical nanofiltration performances values	192
Table VI-6: Values calculated from model when filtering MWF using ultrafiltration membrane FP200	195
Table VI-7: Values calculated from model when filtering MWF using ultrafiltration membrane FP100	198
Table VI-8: Values calculated from model when filtering MWF using nanofiltration membrane AFC30	201
 CHAPTER VII	
Table VII-1: Fittings to Langmuir's and Freundlich's models	212
Table VII-2: Recapitulation of effluent before and after activated carbon treatment after 25 litres passed through each column	217
 CHAPTER VIII	
Table VIII-1: Bacteria count	220
Table VIII-2: Experimental plan	224
Table VIII-3: Summary of the bioreactor optimum parameters and performances	236

CHAPTER IX

Table IX-1: Filtration parameters	244
Table IX-2: Evolution of the concentrate quality during the nanofiltration of the UF permeates FP200 and FP100 respectively	247
Table IX-3: 4.5 litres bioremediation optimised parameters	248
Table IX-4: Large-scale bioreactor functioning parameters	250
Table IX-5: Parameters of the large activated carbon filter	251

LIST OF EQUATIONS
CHAPTER II

Equation II-1	Mogden formula	10
Equation II-2	Charge for water course discharge	11
Equation II-3	Gel model	43
Equation II-4	Resistance in series model	44
Equation II-5	Osmotic model	44

CHAPTER III

Equation III-1	Calculation of the total membrane surface area	95
Equation III-2	Roughness RMS	96
Equation III-3	Average height ...	96

CHAPTER IV

Equation IV-1	Log Normal distribution	104
---------------	-------------------------	-----

CHAPTER V

Equation V-1	Schulze-Hardy rule	120
Equation V-2	Volume of spherical droplet or aggregate	125
Equation V-3	Number of droplet	125
Equation V-4	Surface of hydroxide covered by droplets in monolayer	125
Equation V-5	Diameter of sphere covering a surface in monolayer	125
Equation V-6	Number of oil droplets	128
Equation V-7	Protonation of amino ester	138

CHAPTER VI

Equation VI-1	Permeate flux related to TMP for the resistance in series model	178
Equation VI-2	Gel resistance model	179
Equation VI-3	Pressure need to permeate viscous liquid through pores	183
Equation VI-4	Gel resistance model re-arranged	193

CHAPTER VII

Equation VII-1 Langmuir's isotherm 210

Equation VII-2 Freundlich's isotherm 211

CHAPTER IX

Equation IX-1 Feed COD Load 249

LIST OF SYMBOLS AND ABBREVIATIONS*ABBREVIATIONS*

NF	Nanofiltration
UF	Ultrafiltration
RO	reverse Osmosis
MF	Microfiltration
MWF	Metalworking Fluid
MWF5%	Fresh made metalworking fluid at a concentration of 5%
TMP	Trans-Membrane Pressure
IBC	Industrial Bulk Container
IPC	Inductively Coupled Plasma Atomic Emission
STPP	Sodium Tripolyphosphate
CWF	Cold-Water Flux: Flux of demineralised water measured at 20 degree celsius
AFM	Atomic Force Microscope
AC	Activated Carbon
CHP	Combine Heat and Power Plant
PVDF	Polyvinylidene Fluoride
PS	Poly Sulphone
PES	Polyethylene Sulphone
PCS	Photo Correlation Spectroscopy
MWCO	Molecular Weight Cut Off: molecular size rejected by a membrane usually given in Daltons
CCC	critical Coagulation Concentration
IC	Indigenous Community
PBS	Phosphate Buffer Solution
COD	Chemical Oxygen Demand
TOC	Total Organic Carbon
NTU	Nephelometric Turbidity Units
rpm	Rotation per minute
PVC	Polyvinylidene Chloride
Dalton	Molecule masse usually employed in biochemistry equivalent to 1/12 of the mass of carbon

SYMBOLS

pH	Hydrogen Potential
°C	Degree Celsius: (0°C = 273.15K and 100°C=373.15K)
ΔP	Transmembrane Pressure
J	Permeate Flux: flux of fluid passing through the membrane
D	Diffusion coefficient
C	Concentration
Hz	Hertz = $1s^{-1}$
R	Resistance
f	Percentage of pore density
a	mean pore size for a density
d_p	Pore diameter
σ	width of the distribution
cps	centpoise
μS	Microsimens unit of conductance
Π	Osmotic Pressure
δ	Gel Thickness
η	viscosity
μ	Micro in unit 1μ equivalent at 10^{-6}

SUBSCRIPTS

g	Gel values
b	Bulk values
m	Membrane values
0	Initial values

CHAPTER I

INTRODUCTION

CHAPTER I

Introduction

Metalworking fluids are used in the engineering industry to improve machine tools performances and productivity. They are part of a more general product family-called lubricant and are applied in the tooling of metal pieces, cutting (cutting fluid) and many other applications (grinding, drilling, forming, tapping...). Generally, they are composed of oil and organic compounds mixed with water. Once the mixture has been used for a period of time, it degrades and generates a toxic liquid waste. Waste Metalworking fluids as coolants and liquid lubricants are problematic to dispose of in the drain. This is due to their toxicity and high oxygen chemical demand. The toxicity is largely due to biocides added into the blend to prevent bacteriological attack during its lifetime. Other common components such as amines, borate, nitrates, nitrites, polyalkyl sulphonate, glycerol, esters and ester glycols, petroleum based oil or rape seed base oil add to the product toxicity and eco-toxicity. The high chemical oxygen demand of the waste is due to the oil added to the blend and to the accumulation of free oil from the working machinery. The difficulty in developing a system to efficiently treat the waste is due to the large number of different chemical it is composed of.. This waste is becoming increasingly difficult to dispose of and the rising disposal costs make it a financial burden on industry. The combination of rising disposal costs and the government targets to reduce any waste going to landfill makes an enormous impact on the company's bottom line profits. The typical mixture for engineering coolant is 5% oil and 95% clean water. The volume of coolant disposed of in the United Kingdom alone was 400,000 tonnes in 2000 (bio-Wise, 2001).

Different methods have been used to treat waste metalworking fluids. These methods consist mainly of physical-chemical solutions such as coagulation, the disadvantage of this method is that it can only be applied to emulsified oil and requires the use of chemicals. Another method is membrane separation, using ultrafiltration or nanofiltration membranes. The main disadvantage of membrane processes is fouling of membrane elements leading to huge reduction in efficiency. There is a clear need to

develop a cost effective and reliable system for treating metalworking fluids. This system should take into account the regulations imposed on companies for the disposal of the waste and wastewater.

The sponsor of this project is Cardev International Ltd, a leading company in the design and manufacture of industrial filtration systems, providing environmentally friendly systems for the disposal of waste metalworking fluids. Their sponsorship was offered to design a new cost-effective system that fulfils the current regulations on waste disposal. Their current filtration systems are limited by the accumulation of oil during filtration and do not offer a solution for concentrates.

This study proposes an on-site waste water treatment solution to minimise and suppress any disposal and to obtain quality water, allowing direct discharge into a municipal sewage system.

The combination used is an arrangement of ultrafiltration, nanofiltration membranes and bioremediation. Furthermore, acidification and coagulation processes were carried out on the produced concentrate during the membrane filtration stage. Activated carbon was used to polish the final aqueous phase.

Not only did the research culminate in a pilot model which would be suitable for on-site treatment, but also produced a combination of technologies which treated the full volumes of waste fluids and separated the components into two streams. One stream was the concentrated oil (calorific value of 42 kJ/g) which was reduced in volume but could be suitable for use as a fuel and the other was a low chemical oxygen demand (less than 100mg/L after activated carbon) aqueous phase which could be discharged to drain via the companies municipal sewage system at a very low disposal cost.

This thesis is composed of 10 chapters including this introduction chapter.

Chapter II gives a literature review on the different part of the study. The review starts with generality on industrial waste effluent treatment. Then, metalworking fluids are reviewed with their history and nature clarifying the importance of acting on their treatment. The central part of the study deals with membrane filtration and biological treatment. The last three parts review the physical-chemical treatment that can be

applied to spent metalworking fluids. The use of activated carbon in water treatment and the use of spent oil as a fuel have also been reviewed.

Chapter III describes experimental equipment used in this work and all techniques and procedures used during the experimental work. Chapter IV shows three AFM dimensional images of membranes used in this study. It also shows full surface analysis including pore size and pore size distribution. A correlation was developed for the pore size distribution.

Chapter IV presents the atomic force microscopy images and analyses of membrane surfaces.

Chapter V deals with different methods of chemical treatments used. This chapter presents the results on the waste stream characterisation showing that Mobil cut 232 produces a stable microemulsion of fine oil droplets. This emulsion is destabilised when concentrated by membrane filtration. A chemical treatment has been applied to separate the oil from the concentrate. The recovered oil from the chemical treatment has a high calorific value, especially in the case of acidification.

Chapter VI describes the membrane filtration which was carried out at small and large-scales. It shows that the combination of ultrafiltration/nanofiltration is efficient in reducing fouling in the system and therefore improves the overall filtration performance.

Chapter VII investigates the use of activated carbon which was applied to polish the effluent before discharge to the drain. The efficiency of the activated carbon system was tested on three waste streams corresponding to three different stages of the main treatment. The three different stages were just after nanofiltration, after the bioreactor including microorganisms and after the bioremediation without microorganisms.

Chapter VIII deals with biological treatment of the filtration permeate and the development of a bio-consortium in a fixed bed bioreactor. This chapter demonstrates that microorganisms extracted from waste metalworking fluids can be used for efficient bioremediation of the permeate produced during the filtration process.

Chapter IX shows the full detailed integrated design, including the different processes tested in the previous chapters. This design clearly shows the enormous benefits for potential clients and the environment. Cardev International Ltd have recognised the huge benefits from the proposed integrated system and are in the process of developing it (see Appendix A).

The final chapter (X) gives general conclusions and recommendations.

CHAPTER II
LITERATURE REVIEW

CHAPTER II

LITERATURE REVIEW

II.1 INTRODUCTION

This bibliography reviews the different aspects of the project. It gives a general understanding of industrial waste effluent and a more detailed review of the uses and natures of metalworking fluids. The problems and solutions to discharge waste metalworking fluids are described and membrane technologies are dealt with. Their applications to wastewater treatment and waste metalworking fluids' treatment and advantages and limitations of the technique are pointed out. The middle section deals with the atomic force microscopy (AFM) techniques and its application to membrane technology. The next three sections present wastewater treatment technologies that were used, coupled with the membrane filtration system. These three techniques are biological treatment, physical-chemical treatment of emulsion and activated carbon adsorption respectively. The last section introduces what is useful to take into account considering using waste oil as a fuel.

II.2 INDUSTRIAL WASTE EFFLUENT

Three categories of waste waters can be discharged from commercial premises; domestic sewage related effluent, trade effluent and rain waters. This section gives a definition of these different industrial waste effluents. Particular attention is paid to the charge of trade effluent, which is the type of effluent that the work is dealing with.

II.2.1 Domestic Sewage

Domestic sewage on an industrial site are effluents from staff toilets, wash hand basins, showers and kitchen areas. This is also sometimes known as foul drainage and

will usually be kept separate from the trade effluent whilst on the company site, although it is mixed once it reaches the main sewerage system. The charge for this is usually included as part of a water bill from the local water company, as it is for any individual at home.

II.2.2 Rainwater

Industry is also responsible for rainwater from roofs, car parks and other outside areas that discharge into a surface drainage system. This drainage is separate from the foul drainage system and is regulated by the Environment Agency rather than the water company. Rainwater is either channelled to surface drains located in roads adjacent to the property or is sometimes discharged directly to a river or stream. There is not normally a charge for the discharge of rainwater, although companies do have a duty to ensure it is not contaminated by oils or any other substances.

II.2.3 Trade Effluent

Trade effluent is defined as "any liquid, either with or without suspended particles, which is wholly or partly produced in the course of any trade or industry carried out at trade premises". It does not include domestic sewage.

Trade effluents are liquid streams from all processes on the site, including all rinse water, washing water and any other discharge related to the process (even if it is clean water). The local water company charge for this if it goes to sewers, according to a standard Mogden formula. Occasionally, effluent is discharged directly into a river or other water course: in this instance, the Environment Agency gives an agreement and charges the industry.

II.2.4 Charges for trade effluent

All industrial waste waters (trade effluents) are subject to a discharge consent system under either the Water Resources Act 1991 or the Water Industry Act 1991. This first part provides an overview of the charging system based on the Mogden formula.

II.2.4.1 Consent to discharge

The Water Industry Act gives companies the right to discharge to a public sewer but only with the prior consent or agreement of the water company.

Water companies maintain the sewerage system; provide treatment for the waste, and dispose of the final treated effluent. To allow them to do this effectively, they can impose special restrictions on an effluent before allowing the discharge.

These restrictions depend upon the type of treatment provided by the water company, the size of connecting sewers and the capacity of the wastewater treatment works (WWTW). They can also include:

- ❖ The nature and composition of the effluent
- ❖ Temperature and pH
- ❖ Prohibited substances
- ❖ The maximum daily volume allowed
- ❖ The maximum flow rate
- ❖ The sewer into which the effluent is discharged

In addition to the type and quality of the effluent, the Water Industry Act also gives the water companies the right to charge for carrying, treating and disposing of the waste.

II.2.4.2 *Discharge to sewer*

Prices of discharge rise to enable water companies to meet water quality obligations and to manage the global volume increase of fouled water to treat. Charge levied by the water company for discharging trade effluent is calculated using a formula which takes account of the volume and "strength" of the waste and the type of treatment given at the Waste water treatment work. The formula is commonly known as the "Mogden formula" Equation II-1 or "modified Mogden formula" (after the name of the sewage treatment works where it was first used).

The Mogden formula seeks to link charges for discharging trade effluent to the public sewer to the costs imposed by customers, i.e. by paying according to the volume and strength of trade effluent discharged. The values of the different coefficients are set by the water companies. The different values are also adapted upon the type of effluent and volume discharged. More details on UK water company charges are given in (Office of water services 2004). In the UK, the office of water services regulates the rise of the water charges for trade and domestic effluent.

$$C = (R + V + V_b + B \times (O_t/O_s) + S \times (S_t/S_s)) \times V_t \quad \text{Equation II-1}$$

Where:

- ❖ C = Total charge rate for disposal, pence
- ❖ R = Unit cost for conveyance, pence /cubic metre
- ❖ V = Unit cost for volumetric treatment, pence/cubic metre
- ❖ V_b = Additional volume charge if there is no biological treatment
- ❖ B = Unit cost for biological treatment, pence/cubic metre
- ❖ O_t = COD of trade effluent, mg/L; O_s = COD settled sewage
- ❖ S = Unit cost for sludge disposal, pence/cubic metre

- ❖ S_t = Solids value trade effluent, mg/L;
- ❖ S_s = Settled sewage; mg/L
- ❖ V_t = Total volume discharged

II.2.4.3 Effluent discharges into rivers and other water courses

The Environment Agency has introduced a system of charges for the recovery of its costs from companies who discharge effluent in this manner. Charges are calculated according to the composition of the effluent, the quantity discharged and the quality of the receiving water. A banding system is used to classify types of effluent. The bands progress from A to G, where A is the most polluting.

The UK national formula for calculating charges is:

$$\text{Charge} = R (V \times C \times RW) \quad \text{Equation II-2}$$

where:

- ❖ R = Annual charge financial factor (£477 for 1999/2000 England and Wales)
- ❖ V = Banded weighting factor based on consented discharge volume
- ❖ C = Banded weighting factor based on consented discharge content
- ❖ RW = Banded weighting factor based on category of receiving water.

In addition to this charge, companies are required to pay a discharge application fee of £617 (England and Wales) for most new and revised consents.

The fees can be found via the Environmental Agency. Example of weighting factors given by the Environmental Agency are given in Appendix G.

II.2.5 Regulations

More and more pressure on the protection of our environment can be expected from the legislator. It can be read in the Waste Water Frame Work Directive (2000/60/EC)

that achieving a good status of all water by 2015 is aiming at. Even though it does not refer directly to waste effluent, it has an impact on the discharge of effluent to the aquatic environment. A key element that can be seen in this directive is the impact on waste effluent discharges. The set down of discharge limit values are given in Directive (96/61/EC) on IPPC. This directive prefigures more drastic conditions for the discharge of industrial water into the environment and therefore to the discharge of sewage.

The philosophy of the European (and USA) legislations are based on the “Best Available Technology (BAT) principal and the feasibility is not only linked to existing technology, but also to its economical and practical viability. In Europe, the Integration Pollution Prevention and Control, Directive (96/61), indicates to the member states that they have to improve environmental performances on the BAT principle and must focus on waste minimisation. Recycling and therefore, in the case of water treatment, close-loop options for industrial water use are ultimately implicated.

II.3 METALWORKING FLUIDS

Metalworking fluids (MWF) are part of a more general product family called lubricants and are applied in the tooling of metal pieces, cutting (cutting fluid) and any other applications (grinding, drilling, forming, tapping...). As cutting is a major process, MWF are sometimes abusively called cutting fluids.

This section starts with a brief history on the metalworking fluids. The second part presents the metalworking fluids, their use, diversity and chemistry specifically related to semi-synthetic MWF. The third part reviews the microbiology of MWF. The last part presents the different disposal methods available for metalworking fluids.

II.3.1 Brief history of metalworking fluids

Lubricants must have been used as metalworking fluids since the most ancient times, when metal forming appeared especially for weaponry. Even if there are no direct

references to the fluid technology available, it is known that mankind used grease and oil for lubrication. Therefore, it is reasonable to speculate that lubricants have been used in metal crafting. Towards the industrial revolution, scientific studies on friction started to appear and the impact of friction on moving parts and metalworking processes starts to be appreciated. Water and sour beer were used as coolant fluids in cutting and grinding processes, since these processes produce a great amount of heat. The use of MWF was concomitant with the development of machine tools and the need to accelerate manufacturing processes. The need of cooling and lubricating to enhance productivity appeared. Nevertheless, (McCoy, 1994) reports that four elements added to the industrial revolution and the invention of almost all machine tools, led to the development of modern metalworking fluids. The first element is the discovery of petroleum that had a profound impact on the compounding of metalworking fluids. Mineral oil then replaced vegetable and animal based lubricants. The second element is the introduction of better alloys for making harder tools and therefore working at faster speeds and higher pressure, increased the need to use good quality MWF. The third element is the introduction of electrical power source that initiated the design for more powerful and sophisticated machinery. This new development increases stress between tools and workpiece and the need of removing metal parts efficiently led to an even greater need to develop metalworking fluids. The fourth essential element was the growth of industrial chemistry and petrochemistry that allows the manufacture of modern metalworking fluids, leading to the creation of soluble oil, emulsions, sulphurised, chlorinated compounds and additives. During and after the Second World War, progresses on metalworking fluids were made on the same crucial points of productivity and sophistication of the manufacturing processes. Semi-synthetic and synthetic oils were introduced in 1940's (Lijinsky, 2004). The history of development that can be found in (McCoy, 1994), including 94 references, shows that this development is totally interdependent upon the development of machinery and interconnection of sciences as industrial chemistry, friction, lubrication and tribology. Today, metalworking fluids are also developed to take into account workers health, working comfort, environmental and disposal concerns. The advent of modern, complex and diversify MWF has been produced by the need of the metalworking industry. Primarily, modern MWF were introduced to satisfy productivity needs. They responded to continuous advances made in metalworking technologies as tools and machines that took its route during industrial revolution.

Recently, studies on eco-compatible of lubricant have been published. (Sokoavic and Mijanovic 2001) show the use of renewable resources as an alternative to mineral based oils.

II.3.2 Uses and chemistry of metalworking fluids

Lubricants are of many sorts. They can be gas (mainly air), liquids or solids such as organic or inorganic involving surface coating technology. More descriptions can be found in specialised literature such as (Kajdas, 1997). Liquids are of particular concern and are developed below.

II.3.2.1 Types of metalworking fluids

Liquid lubricants are of two different natures. The high viscosity ones are made of different formulation of mineral oil and additives that are classified mainly by their viscosity. The lower viscosity ones include water based lubricants. Metalworking lubricants, the second class of lubricants, are not classified according to their viscosity since other properties such as cooling, lubricating and protection actions of tool and pieces are very important. The purpose of metalworking processes is to tool metallic pieces: to put them into shape, to drill, cut, grind, tap and other different specific operations. Each type of operation, depending on the conditions material tooling, such as tool speed, contact time and heat generated, needs a specific fluid or a different concentration of oil in water. Usually, the process implicates intimate contact between the tool and the workpiece. According to the process, different gradients of pressure, frictions and heat are applied. Therefore, the quality and properties of the MWF are to be tuned to the specific problem encountered in the process. The most important are cooling and lubricating the tool and the pieces tooled. Metalworking fluids are composed of oil derived from petroleum (mineral oil), animal or vegetable oil.

There are three major types of MWF, which are: oil, emulsion and water soluble products. Straight oils are mainly mineral, but also vegetable or animal sources can also be used. They contain various sulphurous additives, chlorinated compounds or

even a mixture of both. Water-soluble MWF are actually soluble chemicals; they do not contain oil and are known to be synthetic soluble oils. Emulsion and micro-emulsion contain oil in the form of suspended droplets dispersed with emulsifiers. Table II-1 recapitulates the main properties of the three types of MWF. The use of MWF depends on each specific application and conditions in which the process is undertaken. The choice of a specific MWF also depends on the properties of the material tooled e.g. hardness and corrosion properties and on the machinery employed. This choice is very critical since MWF are used to enhance productivity and to protect tools and machinery.

Type	Names	Lubricating Properties	Cooling Properties	Directive for applications
	Water	Very Poor	Very Good	Cooling
Solution	Synthetic fluids, Chemical fluids, True Solutions	Poor-Good	Very Good	High cutting speed Drilling Low Pressure Processes
Emulsion	Semi-synthetic fluids	Good	Good	General purposes High cutting speed Drilling
Oil	Oil Straight Oil	Very Good	Very Poor Poor	Tapping / Broaching High Pressure processes

Table II-1: Different types of MWF, their properties and applications

A full range of MWF exist on the market with various chemical compositions.

II.3.2.2 Chemistry of semi-synthetic metalworking fluids

The properties of MWF are important when choosing which MWF to use for a specific application. Semi-synthetic MWF are water-based products that produce an emulsion when mixed with water. The water contains emulsified oil droplets and dissolved compounds. Substances added to metalworking fluids are listed below:

- ❖ Anti-wear additives which form a lubricating film
- ❖ High-pressure additive
- ❖ Antirust additive
- ❖ Foam retardant agent
- ❖ Antifog agent
- ❖ Dispersing agent and surface-active substances (Surfactant and co-surfactant)
- ❖ Biocides
- ❖ Odorous and colouring substances
- ❖ Chemical constituents such as: amines, borate, nitrates, nitrites, polyalkyl sulphonate, glycerol, esters and ester glycols...

(Sokoavic and Mijanovic, 2001) and (Chidlers, 1994) give more details on metalworking fluid chemistry, formulation, and their applications. The following paragraph concentrates on the nature of semi-synthetic fluids.

To produce the oil emulsions, emulsifiers are used. Emulsifiers can be ionic or polymeric and in most of the formulation, both are used. Soluble molecules such as alcohols are introduced into the base. When the base is mixed with water, it forms an emulsion with oil droplets containing a fraction of soluble molecules that pass to the diluting phase (water) so the oil droplets shrink minimising the surface of interaction with the aqueous phase, leading to an even more stable emulsion. The stability of an emulsion depends on the emulsifier, the cocktail of emulsifiers used and on the size of the droplet. Micro-emulsions are stable dispersions of very fine droplets of a liquid in another. The droplet size is below 0.2 μm , but they are not necessarily transparent due to the Tyndall effect. They are created to ensure that they will not achieve equilibrium by separating into two phases.

II.3.3 Microbiology of metalworking fluid

The literature reports a vast variety of microorganisms fouling metalworking fluid. This is due to the variety of oil available and processes that alter the environmental conditions, which can either inhibit or promote the growth of different microorganisms. Temperature, biocide mode action, pH, type of oil base additives agitation, and oxygenation have effects on microbial growth. The majority of articles related to MWF and microbiology are concerned with the health and safety of workers in the metalworking industry.

It seems that primary colonisers are aerobic bacteria, with *pseudomonads* being the predominant population of these micro-organisms. After primary colonisation by *pseudomonads* and other bacteria, the drop in pH allows yeast and fungi to grow.

In (van der Gast *et al.* 2001), 66 bacteria were isolated from 6 different in-use MWF and from tap water used to prepare them. *Pseudomonas pseudoalcaligene* and 14 other *pseudomonas* species were found as follow:

- ❖ 8 from cincinati Cimex
- ❖ 14 from Bostomattic 312
- ❖ 13 from Bosomatic 405
- ❖ 17 from Chipmaster No 1
- ❖ 12 from CVA mill
- ❖ 2 bacteria seen in tap water use to prepare MWF

No fungi were detected because of the high pH encountered in MWF.

The wilder aerobes were pseudomonads; five species were found:

- ❖ *P. aeruginosa*
- ❖ *P. alcaligenes*
- ❖ *P. mendocina*
- ❖ *P. pseudoalcaligenes*
- ❖ *P. stutzeri*

Formatted: Indent: Left: 1.12 cm, Bulleted + Level: 1 + Aligned at: 1.9 cm + Tab after: 2.54 cm + Indent at: 2.54 cm, Tabs: Not at 2.54 cm

II.3.3.1 Problems due to microbial contamination of MWF

Many microorganisms are reported in the literature to be found in various metalworking fluids. This microbial development has a negative effect on the processes using metalworking fluid and enhances a rapid degradation of the fluids (Rossmore and Rossmore, 2003). Contaminations are associated with problems such as corrosion of tools and tooled pieces, odours, putting workers at risk and a lost in fluid performances lead to productivity decreases. The effect of bacteria on metalworking fluids is that they can use most hydrocarbons as a carbon source. Water/Oil emulsions are suitable environments for microbial development because of the presence of water and soluble hydrocarbons. The visible result of such a contamination is the break down of the emulsion, apparition of slime and separation of the oil from the watery phase. Usually, the bacterial activity is followed by a decrease in pH down to neutral or acidic if yeast can establish themselves.

II.3.3.2 Biodegradability

Biodegradation is the break down of chemicals by organisms. This includes two levels of degradation: the first one where the molecule loses its properties because one or more of its active groups has been lost or the molecular structure is changed. The second level is more advanced in terms of remediation. The total breakdown to carbon dioxide, water and mineral salt, is known as complete mineralisation. The limitation in biodegrading lubricants resides in the fact that oil is insoluble in water and tends to make the organic fraction unavailable to the microorganisms. In addition, the complex mixture includes formulation with biocide. In the particular case of water-based MWF, the organic compounds are dissolved or emulsified. Therefore, their constituents are more readily available to microorganisms. Previous studies carried out by CARDEV International Ltd have shown that bio-remediation alone, using an aerobic system is difficult as a treatment method for semi-synthetic metalworking fluids. The synthetic MWF typically have a high Biological Oxygen Demand (BOD) and are therefore difficult to treat biologically.

In the quest for “environmental friendliness”, the choice of biodegradable oil base becomes an alternative to formulate lubricants. In its article, (Willing, 2001) reviews

and discusses the ecological aspects of using synthetic esters in comparison to petrochemical oil based. This interest in lubricants and metalworking fluids, based on renewable resources, has not only its roots in the concern of environmental matters, but also concerns the manufacturing of alternative products not based on petrochemical interest that concerns a very large market. The environmental aspects are of different sorts. The first point is that oil is a non-renewable and a limited resource. The second is that petrochemicals contribute to global warming due to extraction, transport and disposal when incinerated. The third point is that they are more toxic to human type and to the environment than oleo-chemicals etherified as shown by (Willing, 2001) and (Lijinsky, 2004). Petrochemicals based on benzene rings are known to be carcinogenic. The economic aspect is that only 2 to 3 percent of the lubricant market is occupied by products derived from mainly renewable resources. This is because they have only been available since 8 years. In addition, in the early days, they were not so reliable. The second reason is that the multistage synthesis to manufacture these products makes them more expensive than their mineral oil counterparts.

Microemulsion enhances the bio-stability of the product, producing less available oil to the micro-organism due to the larger surface tension presented at the interface with the oil droplet that prevents micro-organisms to approach the oil droplet. Therefore, the direct bioremediation of semi-synthetic MWF is rather unlikely and a stage enabling the removal of the oil droplet is needed.

II.3.4 Waste metalworking fluids disposal options

UK industries produce around 400,000 tonnes per year of metalworking fluids with an estimated disposal cost of £8 - 16 million in 2000 alone (Bio-Wise, 2001). This figure is similar for France, Germany and Italy. Manufacturing industries in Europe are under increasing pressure from regulators to take more responsibility for their waste. The increase of waste disposal cost contributes to this pressure. Therefore, engineering industries face a particular challenge to treat the waste effluent that they produce. Metalworking fluids miscible with water is one of the most complex and polluting problems because it is based on a large mixture of components, such as mineral oil or synthetic products and most of them form an emulsion or microemulsion. They have a

high COD and contain pollutant chemicals. The treatability of the waste depends on its nature. Anionic additives can be removed generally by acidification or reactions with cationic coagulants.

II.3.4.1 Direct Sewer

To directly dispose of metalworking fluids in the sewer poses many problems to the municipal wastewater treatment plant. The typical problems are reported in Sutton and Mishra, 1994. The nature of the waste, emulsion and presence of oil may clog screening processes and interfere with skimming operations and the mechanical part of the municipal wastewater treatment plant. The presence of large amount of surfactant can compromise the efficiency of the wastewater treatment plant physical separation process, by emulsifying oil and particles. Metalworking fluids typically represent a very large amount of oxygen demand and contain toxic organic compounds in non-negligible concentrations that can affect the performances of the biological process. In the late 1970's, in the USA and Europe, law started to enforce pre-treatment by limiting the amount of grease that can be put down the drain. Regulations concerning toxic chemicals, heavy metals and pH of the waste effluent started appearing. Nowadays, the cost of disposal of such waste increases tremendously. Sewage costs increase according to the volume needed to be treated and improvement of technologies. Therefore, on-site treatment can be an effective way for solving this problem; such treatments are recognised as good environmental practice and a positive step in environmental strategies.

II.3.4.2 On-site treatment

Oily waste streams can be treated in three different ways; physical, chemical and biological or any combination of these three technologies. The treatment is carried out in three steps. Primary treatment separates the floatable oil, also call non-emulsifiable oil, from the main stream fine particulates that can be separated or by gravity of mesh filtration of size 100 to 300 μ m. This step allows the treatment plan to be buffered. The flow and concentration of the wastewater fluctuates with time. Therefore, the first step

is to buffer the variations. Because they are tuned to work at an optimum that is related to inlet flow and concentration, the secondary and tertiary treatment steps will benefit directly from this equalization. This step is critical when large fluctuations in daily volume and quality of the wastewater are present. Knowing the magnitude fluctuations, designing accordingly a sufficient holding volume tank and using a spent holding tank should stand and smooth fluctuations in the original inlet. The free oil should be removed at this stage in order to minimise mixing and the liquid that may be mechanically re-emulsified. Avoiding mixing is general practice, not always followed (Thomas and King, 1991), in the treatment of oily wastewater. Because the waste water can be mixed with surfactant coming from for example, washing water of the workshop floor and machinery contains a lot of surfactant, therefore, creating emulsion and even more problems downstream.

For the secondary treatment, several technologies can be used. When dealing with an emulsion it can be broken down by centrifugation. The spent oil must be treated before its disposal, and different physico-chemical methods have been investigated such as settling, chemical treatment, floatation, centrifugation and membrane techniques such as Microfiltration, Ultrafiltration and Reverse Osmosis have been reported (Bilstad and Espedal, 1996). A review of these methods is shown elsewhere (Benito *et al.* 1998).

Increasing attention is now paid to the selection of environmentally-friendly products and disposal solutions due to the multiplicity of negative effects which the cutting fluids waste place on man and the environment. Usually, the emulsion has to go through a separation process. The concentrated oil is incinerated in the cement or steel industry or in special industrial incinerators. The watery phase is conditioned and goes to a sewage treatment plant. The three most common methods of disposal of spent metalworking fluids are evaporation, chemical treatment and membrane filtration. (Burke, 1991) shows performance and cost parameters of each method. The treatment of this waste has been addressed by several techniques such as chemical destabilisation by inorganic compounds as described by (Rios, *et al.* 1998) and will be reviewed in section II-6. Even electrical methods have been patented. Finally, membrane filtration processes have been used for a long time for waste MWF treatment (Belkacem, M. *et al.* 1995, Benito, J. *et al.* 1998, Benito J.M. *et al.* 2001 and Hu X, *et al.* 2002,).

The effluent after treatment can be discharged to surface water, sanitary sewer facility process for recycling or processing or to atmosphere via incineration or activated carbon regeneration.

Even if a biodegradable metalworking fluid is employed, a pre-treatment is necessary prior to any discharge into sewage in order to eliminate free oil and particles as well as reduce to a minimum COD level that is an important parameter used to calculate the disposal cost. Previous studies have shown that bioremediation alone is difficult as a treatment method for metalworking fluids. There are some alternative and environmentally friendly lubricants coming to the market, that are usually biodegradable (Willing, 2001). This also justifies the choice of using biotechnology to solve the problem linked to the waste metalworking fluids.

II.4 MEMBRANE TECHNOLOGY AND APPLICATIONS

This section defines what membranes are, gives an overview of the advances made in membrane technology, the principal applications, limitations of the technology and techniques employed to overcome the limitations and improve membrane processes. After defining what a membrane is, a brief history of membrane technology is depicted. Then, a general overview of all membrane technology is given. Finally, polymeric pressure driven membranes are described, including the four types of technologies known as microfiltration (MF), ultrafiltration (UF), nanofiltration (NF) and reverse osmosis (RO).

II.4.1 Definition

Membranes are engineered barriers that exclude or separate colloids, molecules or salt (Baker, 2000). The key property exploited in membrane technology is the ability of the membrane to control the permeation of a chemical species through the system. In fact, a membrane is nothing more than a thin discrete interface that moderates permeation of chemical species in contact with it. It is different from a filter which is limited to separate particles larger than 10 μ m and only because of their size. Membranes separate

particles, molecules and chemical species because of their size, shape and their chemical and physical properties. Membranes are able to control the rate of chemical permeation; this effect is widely used in medicine to relieve chemicals in the human body.

II.4.2 History

Studies of membrane properties have been recorded since the 18th century. In 1748 Abbé Nolet had described the permeation of water through a diaphragm and called it osmosis. Until 1945, membranes were only used in the laboratory or for small-scale specific applications. After The Second World War, micro-porous membranes were used to access the quality of water. This became possible by the earlier development and improvement of nitrocellulose (collodion) material for membrane applications. The major advance in membrane technology was made by Loeb and Sourirajan, who produced the first asymmetric reverse osmosis membrane giving a permeate flux 10 times higher than the membrane then available. This technology is based on the deposition of a thin polymeric film (called active layer) on a much thicker and porous substrate that gives mechanical strength to the assemblage. Loeb-Sourirajan advanced open reverse osmosis to commercial water desalination and to the development of ultrafiltration and nanofiltration membranes. The second advance was made by medical applications like artificial kidneys by W.J. Kolf in 1945, with the technique being completely refined in the 1960's. The other important medical application is the control drug delivery systems. Medical applications account for the largest part of the membrane market including the biggest amount in total membrane surface sold. Then between the 1960's and 1980's, numerous formations based on the Leob-Sourirajan method were developed. The type of modules diversified from dead-end to cross flow filtration, the latter including large membrane areas of tubular, spiral wounded, hollow fine fiber and flat sheet. Advances were made at the same time on polymers used to produce membranes. In the 1980's, new technology was developed such as gas separation and pervaporation. Nowadays, more and more engineered polymers are used to improve membrane performances. Recently, less conventional material appeared to produce microfiltration and ultrafiltration membranes. Using ceramic

materials that have great thermal and chemical resistance and even dense metallic (palladium), are used for gas separation.

II.4.3 Membrane processes

The development of polymeric membranes created two types of membrane structure, isotropic and anisotropic membranes. Anisotropic membranes are based on the Loeb-Sourirajan design and their properties rely on the thin active layer, allowing the development of high flow rate polymeric membranes, using microporous or dense polymers as active layers. The membrane media is generally manufactured as flat sheets or as hollow fibers and then configured into membrane modules. The most common membrane module configurations are hollow-fiber (consisting of hollow-fiber membrane material), spiral wound (consisting of flat sheet membrane material wrapped around a central collection tube), and cartridge (consisting of flat sheet membrane material that is often pleated to increase the surface area). In addition, to the various module configurations, there are a number of different types of membrane materials, hydraulic modes of operation and operational driving forces that can vary among the different classes of membrane filtration. Each of these characteristics of membrane filtration systems may be considered by a manufacturer and used to meet the particular treatment objectives for a given application. The membranes used in all four processes are most commonly made of polymeric materials. In the early years of membrane development, nitrocellulose and cellulose acetate were the most often used, but were increasingly replaced by more sophisticated materials such as polyamide, polysulfone, polycarbonate and a number of advanced polymers (Mulder, 1988). These synthetic polymers offer improved chemical stability and higher resistance to microbial degradation and thus are suitable for use in a wide range of applications such as wastewater treatment.

This review pays particular attention to four filtration processes: microfiltration (MF), ultrafiltration (UF), nanofiltration (NF) and reverse osmosis (RO). All of them are well-established technologies developed at small and large industrial scales. They are pressure driven filtration processes that use membrane technology to allow the passage

of water and the passage or retention of particles, molecules or salts. Figure II-1 illustrates the principals of filtration processes using this type of membranes.

Microfiltration is a low-pressure process used for the retention of suspended material particles down to size $0.05\ \mu\text{m}$ (Ripperger and Altmann, 2002). Typical operating pressures range from 0.5 to 3 bar. They usually have a symmetrical pore structure, with porosities as high as 80%.

Ultrafiltration is a medium pressure process offering retention of proteins, colloids and biological materials. Typical operating pressures for ultrafiltration range from 1 to 15 bar. UF membranes are also porous membranes with an asymmetric pore structure comprising a 1-2 μm thick top layer of very fine pore sizes supported by a 100 μm thick openly porous layer. Both layers may be made from the same material. The thin-film composite membrane is another type of UF membrane. It consists of an extremely thin layer, typically 1 μm thick, deposited on an open porous matrix. Microfiltration membranes and ultrafiltration membranes are mainly described as pore flow microporous membranes.

Nanofiltration is built on the same principal, a less open structure material is used as the active layer and charges may be added to the surface in order to control the passage of solute salts. Nanofiltration is used for the removal of dissolved material in the molecular range of 100 to 500 kDa. Nanofiltration membranes with small nominal pore diameters between $0.001\mu\text{m}$ and $0.01\ \mu\text{m}$ are described as intermediate pore flow/solution diffusion membranes (Baker, 1992) and (Noble and Stern, 1995). Salts and charge species are transmitted through the membrane preferentially. The typical operating range for nanofiltration membrane is from 10 to 40 bar.

Reverse Osmosis is a high pressure driven process up to 60 bar, allowing the retention of almost all particles and ionic species. RO membranes are generally considered to have no macroscopic pore structures but to consist of a polymer network (dense active layer) in which solutes can be dissolved. The permeation through RO membranes are described with the solution diffusion model.

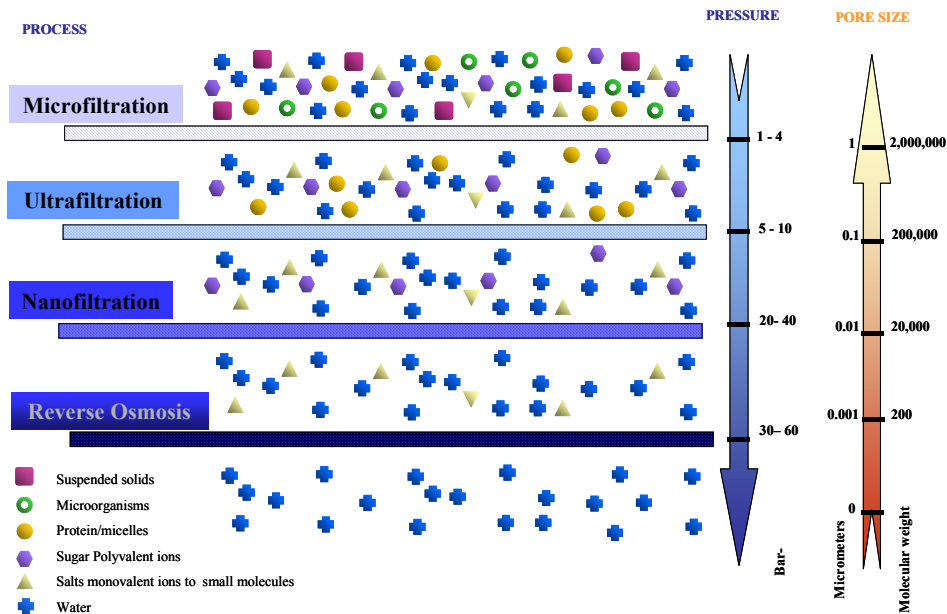


Figure II-1: Types of membrane filtration

Cross flow membrane filtration is now a mature technology, regularly employed as a standard technique for liquid processing to effect clarification, product isolation, concentration and separation duties in a large number of manufacturing industries. Benefits of this type of membrane technology include:

- ❖ Selective and consistent separation
- ❖ Increased product yield
- ❖ Low energy consumption
- ❖ Small footprint
- ❖ Established technology
- ❖ No additives, flocculating agents or percolates chemicals required
- ❖ Large variations in feed quality have little influence on permeate quality
- ❖ Easy retrofitting
- ❖ Low maintenance

II.4.4 General applications

There are various membrane technologies (Scott and Hughes, 1996). Microfiltration is mostly used for filtration and sterilisation and to remove small-suspended solids and microorganism in milk pasteurisation. Ultrafiltration membranes are used to separate colloidal suspensions, oil emulsions, viruses and proteins from solutions. They are used in the food industry for sugar recovery and cheese production for example. Some examples of water treatment that can be given are water recycling processes, dye recovery and oil-water emulsion separation. There is a wide range of use of ultrafiltration in biotechnology as cell harvesting enzyme production (Weatherley, 1994) and (Wang, 2001). The last UF application is usually done at small or medium scale. Water desalination is the oldest industrial application for drinking water to obtain ultra pure water.

Other types of membrane systems are for gas separation used primarily in separation of uranium 235 from uranium 237 in the enrichment process to obtain nuclear fuel. Other gas separation processes are used to separate nitrogen from air, carbon dioxide from natural gas and hydrogen can be separated from a gas mixture using metallic palladium.

Pervaporation is used for the dehydration of ethanol and recently an application for the removal of trace amounts of volatile organic compounds from contaminated water.

More recently, membrane reactors are used to control the product of chemical reactions. Membrane reactors use the separative properties; the membrane shifts the equilibrium of a chemical reaction by removing products from the reactor such as catalytic gas-phase reactions, chiral drug separation and cell culture and fermentation processes.

For a long time, membranes were used in case of high value compound recovering because of cost considerations. Therefore, they were used in pharmaceutical industries and then food industries. Nowadays, membrane technology is more efficient and industrially well established. Applications to less economically valued processes like wastewater treatment take place and are recognised to be effective.

II.4.5 Applications in wastewater treatment

Industrial water uses membrane technology up front of a process to guarantee water quality. This is of importance as it prevents corrosion in cooling system as sensitive as nuclear power stations and ensures quality water that enters food-processing industries. On the other hand, membrane technology is used to minimise fresh water consumption in a process and the typical example is the paper mill industry. This industry used to consume 300 m³ in early twentieth century down to 30 m³ today of fresh water per ton of paper (Nuortila-Jokinen, *et al.* 2003). Evaporation and floatation have been widely used to treat the effluent. Since the 1980's, membrane technology has been used. Ever since, along with improvement performance and decrease in prices, membrane technology replaces the traditional effluent treatment. The advantages are numerous; adaptability, small footprint and low energy consumption. The versatility of the membrane process allows its use at any stage of paper pulp manufacturing for treatment of water, for product recovery, chemicals, water and pulp.

II.4.6 Filtration of metalworking fluids

This part develops Section II.3.4 (“Waste metalworking fluids disposal options”) and focuses exclusively on membrane technology applied to waste metalworking fluids treatment. The treatment of MWF from wastewater is of environmental and commercial importance (Cheryan and N.Rajagopalan, 1998). Generally, membrane technology is used here to reduce the volume of waste to be disposed of via a contractor. Some examples of studies on MWF filtration for recycling purposes are also given.

a) *MWF filtration for disposal*

Pressure on companies to minimise their waste production helped in the development of such technology. Economical reasons lead in the choice of using membrane technology rather than other methods. Membrane technology is more likely to be used where the flux of wastewater is less than 190 m³ per day (Cheryan and Rajagopalan, 1998). The capital investment increases when membrane processes have to be scaled

up because the surface area of the membrane is linearly related to the throughput and therefore the cost of a plant rises more steeply than other processes when scaled up (Stevenson, 1997). Membrane technology is versatile and can be used in combination with other technologies such as coagulation or biotechnology. These combinations are excellent choices for the treatment of waste metalworking fluids (Xing et al. 2001) and (Cheryan and Rajagopalan, 1998). This technology is suitable, and is already used for on-site wastewater treatment (Bio-Wise2001; Willing2001). It is obvious that UF or NF treatments are not sufficient to obtain a perfectly clean permeate with an acceptable organic content to treat metalworking waste effluent, (Belkacem *et al.* 1995).

In the 1970's, the first investigation on cutting oils ultrafiltration were published. At this early stage, the efficiency of the treatment of such waste compared to traditional methods was recognised. Limitations and problems imposed by ultrafiltration were also pointed out by (Lee, *et al.* 1984). In this article, the author shows that concentration polarisation is due to an oil gel that has a concentration of 40% and membrane fouling is due to adsorption of oil at the membrane surface which modified its wettability.

(Benito *et al.* 2001) investigates the filtration of emulsified cutting oil using a dead-end ultrafiltration cell. Four parameters were studied; Trans-Membrane Pressure (TMP), oil concentration, temperature and rotation speed. They showed that with increasing TMP, the permeate flux first increases at low pressure, then the permeate flux becomes independent of the pressure applied, and at higher pressure the permeate flux can decline. They attribute this behaviour to the formation of an oil layer that has a specific resistance to the permeate flow that increases with the TMP. Because of the compaction of the oil droplet, this specific resistance is measured without stirring. The increase in oil concentration decreases the permeate flux. Two reasons are given for this happening. Firstly, the viscosity of the solution increases and secondly, the specific resistance of the oil layer increases. The temperature and stirring speed are reported to increase the permeate flux. The authors explain this by the fact that a high stirring rate leads to an increase in shear rate, therefore there is less chance for a gel formation to take place.

(Hu, *et al.* 2002) investigate the fouling of oil in water emulsion by ultrafiltration and described mechanisms of the oil droplets fouling the membrane surface. Accumulation

of oil droplets at the membrane surface, due to concentration polarisation, increases the concentration of the emulsion towards the membrane surface, increasing the collision frequencies. Then, at a point the interaction becomes such that oil droplets aggregate and leads to the formation of a gel layer that finishes covering the whole membrane surface. Scanning electronic microscopy images show such aggregates and infrared analysis show that the major fouling material was oil.

(Belkacem, *et al.* 1995) have an interesting approach in treating waste MWF and enhancing reactive salts (CaCl_2). This treatment is reported to enhance ultrafiltration permeate flux, to reduce the concentration polarisation layer and by making the permeate flux independent of the concentration ratio. The authors destabilised the oil emulsion by using coagulant to increase the size of the droplet. The membrane surface is seen to be used as a coalescing media. In this study, the employed MWF forms an emulsion showing a droplet size of 180 to 630 μm when destabilised. This technique is interesting, the argument being that a small amount of chemicals are used. The authors showed that 30 to 60% of the chemicals can be saved (this is the difference between the concentration needed to destabilise and to break the emulsion). However, membrane separation processes are more cost effective when no chemicals are used and furthermore, the technique cannot be applied to more stable micro-emulsions or soluble oils.

(Atsushi and Mitsutoshi 2002) used a simulated waste effluent containing mineral oil emulsified with alkylphenolthoxylate. This waste simulation allowed the authors to simplify the system, to assess and to measure the retention rate of the mineral oil and the non-ionic surfactant. They showed that even though the MF process substantially reduces the turbidity of the permeate compared to the feed emulsion, the mineral oil was rejected at only 39-61% and the surfactant at 16-19%. For the UF membrane the oil rejection was 97% and the surfactant rejection rate was 8-14%. It can be seen that in both cases, oil was not totally removed. The permeate flux is shown to be reduced with time and volume reduction. The authors used the notion of Volume Reduction Factor that they define as $\text{Volume initial} / \text{Volume of concentrate}$. They compared the UF MF with an adsorption method and found that UF has better performances than the adsorption process. Nevertheless, they suggest that the adsorption process could be used to complete the ultrafiltration as a secondary disposal technique.

Membrane filtration can be coupled with different technologies as it can be seen in (Chang, *et al.* 2001). They proposed a method using an ultrafiltration of oily wastewater with post-ozone treatment to enable the UF permeate of cutting oil to be reused as process water.

Ultrafiltration is found to be an effective method for the treatment of oily effluents. This technique allows the separation of oil and organic compounds from the aqueous phase and results in two effluents, a concentrate and a permeate. The concentrate is the heaviest part containing concentrated oil and pollutants. The permeate is the result of the filtration process that is lighter than the concentrate. The limitation is due to concentration polarisation and the resulting fouling of the membrane surface by the droplet of oil. Generally, in all studies the resistance is due to concentration polarisation increasing with pressure. This is due to the compaction of the oil droplet that aggregates and forms an oil gel at the membrane surface. Dissolved organic molecules pass through the membrane pores. Microfiltration and ultrafiltration membranes are also used for recycling synthetic metalworking fluids (Mahdi and Skold, 1991). Membrane systems are recognised for the treatment of oily streams such as wastewater from metalworking fluids and are cost effective.

b) *Recycling of MWF*

The last advance in MWF filtration is to apply the process in order to recycle most of the fluid. (Mahdi and Skold, 1991) and more recently (Skerlos *et al.* 2000) investigate the microfiltration of synthetic MWF with ceramic membrane in the view of recycling waste MWF by separating contaminants such as tramp oil, micro-organisms and particles from the MWF. In the first part of the study, the authors investigated the flux decline induced by the filtration of unspoilt metalworking fluid. They observed identically a flux decline during filtration operations. This decline is identified as adsorption of MWF ingredients leading to pore diameter reduction. The restriction to the technique is due to fouling of additive and oil and therefore the “de-formulation” of the blend. Molecules and additives are of different molecular size and physical-chemical nature and have different retention rates. Therefore, the recycled product is not like the primary product. The quality of the recycled product has to be assessed. This solution is appealing from an environmental point of view because it

could cut down the needs of frequent waste MWF disposal. However, the study can only be carried out on specific MWF involving a precise tuning of the filtration process and the secrecy of MWF formulations make the study of additive retention difficult, all the most that is not in the interest of manufacturer to market recyclable MWF.

II.4.7 Water recovery

Water reuse takes place principally in the worry of freshwater conservation. The water recovery for reuse in industry can be done in two different manners, recycling and reclamation. Reclamation is the treatment of recovered water made available for reuse. Recycling means the recovery, with or without treatment, to and from a specific process. The parallel that can be made is that glass bottles are recycled (as bottles) and the glass from the bottles can be reclaimed as glass. In the last case, the glass is reprocessed to manufacture different items and not necessarily bottles. In industry, water reuse is motivated by legal requirements such as legal pressure upon discharge, or by economic interests. Water reuse in industry is straight forward, as long as it is reliable and cost-effective. The challenge in reusing water in industry arises from the fact that wastewater comes from different processes and/or at different stage of a process. The wastewaters are blended together and result in a mixture that varies greatly in flow and load, making it difficult for a system to treat and to provide a reliable treated effluent suitable for reuse. Membrane technology is very promising because of its versatility and effectiveness in buffering the permeate stream in load and flow. Recycling waste water in re-making metalworking fluids found its difficulties in the standards needed in the specific application. Two problems can be foreseen. First an excess of surfactant may affect the foaming of the product and its quality. The second problem is the low organic content present in membrane permeate which makes it ideal for biological contamination that would be transmitted to the product with the dramatic consequences reviewed in II.3.3.1.

II.4.8 Fouling

Fouling is associated with the decline of permeate flux and of retention-rate. Actually, these are not only due to membrane fouling, but also to operating conditions. Intrinsic fouling describes an irreversible process that requires the filtration process to be stopped, the membrane surface to be regenerated, and this regeneration should be associated with total or partial permeate flux and a rejection-rate recovery. The level of recovery shows the severity of fouling as well as the effectiveness of the cleaning method. The severity of fouling experience under specific conditions can be assessed by measuring under the same conditions, the water flux of the fouled membrane and comparing it to the original water flux done before filtration. Only limited progress in controlling these problems has been made in the last 20 years. Fouling affects the performance of the plant because of the permeate flux decreasing. Fouling can affect the plant by changing specific species permeability. In an ideal case, during filtration, only the membrane opposes a resistance to the flux. (Viadero, *et al*, 1999) state that fouling occurs when additional resistance to the permeate flux are experimented other than the intrinsic membrane resistance.

II.4.8.1 Fouling mechanisms

There are four types of fouling linked to four additive resistances to the membrane intrinsic resistance. Concentration polarisation, this phenomenon always appears in membrane separation system due to accumulation of rejected compounds at the surface of the membrane. The concentrations of the accumulated solute can be high enough to form a gel-layer that adds another resistance to the flux. In the case of porous membranes, it is possible for solutes to penetrate into pores and accumulation leads to pore blocking so the membrane rejection properties can be dramatically changed. Adsorption of molecules at the membrane surface or within the pores of the membrane block the membrane as well. The adsorption of molecules at the membrane surface occurs as soon as the membrane is in contact with the solution and equilibrium takes place. Under the pressure of the feed side, an additional deposition of solute can take place due to the increase in concentration of rejected solute next to the membrane

surface. It can be noted that the blocking process does not occur for non-porous membranes.

II.4.8.2 Specific type of fouling

This section describes specific mechanism of membrane fouling such as biofouling scaling and cake formation.

Biofouling is due to the deposition and adhesion of bacteria at the membrane surface or in pores following the mechanisms described above. In addition, biofouling leads to the formation of a biofilm onto the membrane surface in the worst case. Bio-fouling occurs in three phases described in (Le Thi, 2000). It starts with the adsorption of chemical compounds such as polysaccharides and proteins that happens as soon as the membrane is in contact with the liquid. The bacteria adhesion happens in 2 stages. First stage is a reversible process involving the approach of the cell next to the surface by diffusion or convection. The second stage is the adsorption and linkage of the bacteria to the surface, this stage is called irreversible bacteria adhesion. In the third phase, the whole surface is colonised and a biofilm is formed.

The scaling phenomena are the precipitation, deposition and growth of mineral crystals at the surface of the membrane. It is generally due to calcium or magnesium carbonate or sulphate and occurs more likely in RO processes. Other precipitates can also cause fouling. This is encouraged by the concentration polarisation that induce a high concentration of solutes at the membrane surface. Specific mechanisms can be found in (Linnikov, 2003). Linnikov considers the growth of crystal in supersaturated salts in solution, so the control of seed crystal in the solution is a factor to diminish the scale growth rate. (Sheikholeslami and Ong, 2003) examines the kinetics and thermodynamics of calcium carbonate and calcium sulphate sodium chlorine solution as encountered in desalination plants.

Cake or film formation is due to the accumulation of material on the membrane surface leading to the formation of a layer that can compact. The nature of the cake is very different to the dispersed bulk solution and can lead to the formation of a strong

adhesive layer that compacts. The compaction reduces the membrane permeability and tends to solidify the cake that will become difficult to remove.

In the case of oil emulsions, that constitute metalworking fluids the main mechanism has been described in Section II.4.6.

II.4.8.3 Membrane cleaning

Fouling induces a decline in the permeate flux and rejection rate and is the main limitation in membrane application. Whatever the technology used or the application, membrane fouling always occurs; it may be limited by using the right type of membrane by applying good hydrodynamic conditions, introducing turbulences such as particles in the concentrate or a gas phase while filtration takes place. These points are reviewed in Section II.4.9. Nevertheless, at a point, membranes have to be regenerated. The solution used to clean the membrane must not damage the membrane or introduce any conditions that lead to problems like precipitation that can happen when, for example the pH of the washing solution is changed. Therefore, the washing conditions are of great importance.

Fouling due to oily waste water can be cleaned with surfactant. (Mahdi and Skold, 1991) used surfactant and alcohol in water micelle solution to regenerate membrane surfaces fouled by oil. The cleaning effect is explained by re-emulsification of the oil that can then be removed from the surface. In this case, 96% of flux recovery was measured.

(Benito, *et al.* 2001) in a study of cutting oil ultrafiltration investigating a commercial biodegradable cleaning agent (Derquim+) containing ionic and non-ionic surfactants, it was found to be very effective to regenerate the membrane after fouling to a total initial flux recovery. (Lee, *et al.* 1984) showed that micellar solutions were effective in cleaning membrane used for the filtration of cutting oil. A total regeneration was possible using micelles. Other authors (Belkacem, *et al.* 1995) found it effective to use micellar solution in order to clean membrane surfaces that are fouled with oil. Micellar solutions are composed of surfactant dissolved in water and are used to re-emulsify the oily layer, which fouls the membrane surface. The use of micellar solutions as a

cleaning method is considered for higher flux recovery without changing the membrane properties, fouling the membrane or even causing damage to the membrane surface.

It is not always recommended to use cleaning agents. If used, they must be chosen carefully as to not alter the membrane surface. Frequently using cleaning agents and chlorinating the membrane does not necessarily prevent the biofouling of the membrane, it can reinforce biofouling problems. Microorganisms subject to low levels of biocides generate large amounts of extra-cellular polysaccharides (EPS) for protection and tend to live or survive within a protective biofilm. EPS have two main fouling actions. Firstly, they adsorb onto the membrane surface and into pores. Secondly, they promote microorganisms to adhere and colonise the surface. Many plants work satisfactory with a biofilm. Performances of the plant depend on the nature and the structure of the biofilm. In some cases the presence of bacteria on the membrane surface leads to less organic compounds fouling (Fillaudeau and Carrere, 2002b) because bacteria degraded them. The resistance of the biofilms to chemical cleaning will increase if their use is not adapted. (Baker and Dudley, 1998) recommend that shock dose of non-oxidising biocides should always be applied.

Membrane cleaning is time consuming and the use of chemicals adds to the cost of the membrane filtration process. Therefore, the frequency and duration of cleaning cycles must be limited. This can be achieved by optimising the membrane filtration process to limit membrane fouling and have it less dramatic.

II.4.9 Techniques to enhance filtration

Besides cleaning and regenerating membrane surfaces, several methods can be used to minimise membrane surface fouling during filtration.

This section deals with methods that can be used to enhance filtration process by increasing permeate flux and/or the retention rate during filtration. In contrast to cleaning, filtration is not stopped and the enhancing process takes place at the same time as the filtration. The methods fall into three categories. The first category proposed in the literature is based on the principle of introducing turbulences into the

feed stream (hydrodynamic control). The second category consists of modifying the surface of membrane in order to minimise the interaction between membrane surfaces and fouling materials. The third technique consists of pre-treating the effluent in order to remove or modify the fouling material.

II.4.9.1 Filtration module and hydrodynamic conditions

Hydrodynamic considerations must be taken into account among the various methods proposed to limit membrane fouling and biofouling.

a) *Filtration modules*

The first step was to use cross flow filtration instead of dead-end filtration. This is of historical interest nowadays as all industrial filtrations are carried out in cross flow mode. In 1907, Bechhold carried out filtration with a flow parallel to the membrane surface. He found an increase in volume filtered before the membrane was blocked. Cross flow, filtration became popular later when membrane separation took off in the industry in the 1960's. The effect of the feed velocity has been reviewed in the previous section. Cross flow filtration employs tangential flow across the membrane surface which provides a continuous scouring action and hence reduces the membrane fouling layer due to feed stream debris and macromolecules. Particles and filtered molecules are not pushed directly onto the surface. Different configurations of cross flow filtration can be found such as flat sheet, spiral membrane and tubular membrane modules. In conventional filtration, the feed flow is perpendicular to the membrane surface, which causes a build up of debris at the membrane surface, causing a reduction in fluid permeation.

b) *Velocity*

Velocity of the cross flow is a very important condition, especially for large particles, bacteria, yeast and flocks (Fillaudeau and Carrere, 2002b). In addition, the nanofiltration of fine particles is affected by feed velocity as shown by

(Manttari, *et al.* 1997) studying the NF of paper mill effluent. They showed that the critical flux of the membranes was dependent on the flow velocity.

c) *Trans-membrane pressure*

The pressure applied is another parameter that leads to a kick blocking of the membrane. With the trans-membrane pressure increasing, the permeate flux is expected to increase. However, it is not always the case when the critical pressure is reached the permeate flux reaches a plateau and may decrease. The critical pressure depends on the type of membrane used, the feed nature and velocity. The decrease occurs when materials are deposited onto the membrane surface, forming a gel-layer or a cake. Opened membranes such as microfiltration are more affected than reverse osmosis membranes. Therefore, adjusting the TMP can improve the permeate flux and diminish the effect of fouling.

II.4.9.2 *Introducing turbulence*

This has an effect by minimising the concentration polarisation layer and removing particles depositing onto the membrane surface. As an example, dead-end filtration can be dramatically enhanced by adding agitation just on top of the filtering surface.

a) *Gas injection*

Gas injection is used to enhance the permeate flux in membrane filtration and the retention rate. (Li *et al.* 1998) found that both flux and protein retention were improved by gas injection. The technique is based on the principle of introducing turbulences towards the membrane surface by creating a multiphase flow within the membrane tube. The bubbles have the effect of reducing the boundary layer, therefore reducing the resistance to the permeate flux and of harder fouling (adsorption onto the membrane surface) by removing particles from the surface creating local mixing next to the membrane surface. This effect is well known and adequately studied. However, the understanding of the multiphase flow impact on the permeate flux and retention rate is not totally understood. The nature of the fluid and the membrane geometry has an impact on the bubble formation. This technique is more likely to be applied in UF

or MF when the resistance to the permeate flux is highly affected by the concentration polarisation layer of particles, as for (Sur and Cui, 2001).

(Li, *et al.* 1997) enhanced the ultrafiltration of proteins by gas sparging and studied the bubble sizes and frequencies. They found that the permeate flux increases with the bubbling frequency. The effect of bubble size was found to affect the filtration as for smaller bubbles and a plateau region was reached for larger slugs.

(Um *et al.* 2001) found that some of the gas was partially masking the membrane surface and therefore decreased the overall permeate flux. In other cases bubble can be trapped in the membrane pores and decreases the permeate flux by reducing membrane porosity.

b) *Other turbulence promoters*

The other turbulence promoters can be divided into two types, the static promoters that are linked to the module design and the non-static that are particles added to the feed stream. Particles added to the feed streams may damage the membrane surface and may be undesirable for concentrate treatment. Nevertheless, the application of fluidised bed systems can be attractive in highly viscous systems in which energy consumption can be a problem. (Panpanit and Visvanathan, 2001) studied the effect of the addition of bentonite to the feed in the UF treatment of oily waste water generated by car washing. The improvement of the filtration is attributed to the aggregation of the oil droplets on the clay particles and a limit in clay concentration and flock size is found. Beyond the limit of 300mg/L of bentonite, the flux declined due to particle fouling. The formation of large aggregates is found to have a beneficial effect by promoting turbulences next to the membrane surface.

(Kim *et al.* 2002) studied the effect of both by adding glass balls to a vortex-flow microfiltration system. The system was applied to the treatment of oil in water emulsion. It was found that the insertion of glass balls was effective at high flow rate and high oil concentration. This indicates that in this case the enhancement of the filtration is due to the disturbances of the gel layer that forms at the membrane surface during filtration.

II.4.9.3 Surface modification

Membrane surface properties are another important factor. (Hamza *et al.* 1997) used modified polyethersulfone ultrafiltration with surface modifying macromolecules to filtrate oily water. They found that the modified polyethersulfone membranes have a superior performance and that the oil gel layer resistance of the membranes decreased with an increase in the surface modifying macromolecules. (Bowen and Sharif, 2002a) have shown the importance of membrane shape in the fouling process. Rough surfaces have been shown to be more likely to foul. On one hand, roughness gives a larger surface area and slows down the liquid film moving at the membrane surface. On the other hand, it can create turbulences at the membrane surface and local mixing. The presence of charges at the surface of the membrane, their nature (positive or negative) and density are important factors (Pasmore *et al.* 2001). Hydrophilicity has been shown by (Benito, *et al.* 2001) and is obviously a factor to take into account for oil-water separation, especially when oil droplets are likely to foul the membrane surface. The chemical nature of membranes influences the interaction and adsorption/desorption equilibrium with solutes. The pore size can lead to different type of fouling. (Fillaudeau and Carrere, 2002b) have shown in the case of microfiltration of beer, that for the 1.4 μm the predominant fouling mechanism was due to the yeast cell layer building up or yeast pore blocking, probably because the 1.4 μm pores is the same as the yeast size. For the membrane with smaller pore size 0.1, 0.45 and 0.8 μm , the retention and adsorption of compounds such as proteins and polyphenols was the predominant mechanism. High molecular weight cut-off ultrafiltration membranes were more suitable for harvesting *Esterichia coli* and *Saccharomyces cerevisiae* than microfiltration membranes. They attributed these results to the size of the microorganisms in relation to the membrane pore size because the yeast cells have a similar size to microfiltration membranes pores. Therefore, the microorganisms became embedded directly into the pore and created a blockage. On the same principal, in flock filtration, the size of the flocks is a very important factor. This size is linked to the fluid velocity and shear rate within the tube, so hydrodynamic conditions are likely to be major factors for particle filtration. (Tardieu *et al.* 1998) showed that at the deposition of sludge on the membrane surface of an MBR is of a very different nature

depending of the hydrodynamic condition applied. In this article, at low feed velocity, they found that the sludge forms a cake layer, whereas at high feed velocity the progressive fouling was attributed to convective back-transport phenomena in the fouling processes. In their article, (Fillaudeau and Carrere, 2002a) attributed the main fouling mechanism of the large pore microfiltration membrane to the build up of a yeast cell layer which was very sensitive to cross-flow velocity.

Membrane surface modification aims at lowering the energy between the fouling material and the membrane surface in order to avoid adhesion. The best example is the role played by hydrophilic molecules added to the membrane cast or grafted afterwards to the membrane surface. The change in membrane surface wettability and avoid lipophilic material to spread onto the membrane surface. Other molecules are added to the membrane surface in order to modify their surface properties and specifically their charges. To avoid biofouling, biocides may be added to the membrane surface in this case, the effect is to kill micro-organisms that approach the membrane surface, avoiding the formation of a biofilm.

II.4.9.4 Feed Pre-treatment

(Kim, *et al.* 2002) studied three modes of stream pre-treatment prior to the filtration of the effluent by a spiral wound RO membrane. The three systems proposed were: UF membrane filtration; granular activated carbon (GAC) adsorption and organic flocculation coupled with the GAC. The best pre-treatment was found to be the UF system and this performance is attributed to the best turbidity retention by the pre-treatment system. The pre-treatment aims at removing the fouling material from the feed stream. This technique is largely applied for seawater desalination using different filters that remove large particles and microorganisms and the nanofiltration membrane to remove poly-charged and large ions prior the RO membrane unit.

Other method such as centrifugation is proposed by (Turano, *et al.* 2002). In that case, the effect of the pre-treatment is effective leading to a higher permeate flux, a much longer steady state and a slower permeate decay. The effect is also found to be beneficial to the membrane regeneration efficiency.

II.4.10 Modelling of filtration for oil waste water

This part of the chapter deals with the permeate flux modelling and fouling mechanisms.

II.4.10.1 Permeate flux models

Three main general physical models predict the permeation through a pressure driven membrane; the gel model, the resistance in series model and the osmotic pressure model. Figure II-2 illustrates a general view of the improvement of permeate flux with the increase in Trans-Membrane Pressure (TMP). The permeate flux is the flow of permeate stream produced per unit of membrane surface, usually given in litre per hour per square metre (L/h.m²). The TMP is the driving force that pushes the fluid through the membrane and is the difference in pressure between the feed side and the outside of the membrane. It can be seen that when pure water is used, the permeate flux increases linearly with the TMP the slop of the line represents the resistance of the membrane to the water. When a solute is present in the solution, two behaviours can be noticed. First the permeate flux increases with the TMP until it reaches the critical pressure. This first part of the graph is called the pressure control region. The second part is when the TMP reaches a critical pressure and the permeate flux does not continue to increase linearly with the TMP and eventually reaches a plateau. This second part of the graph is said to be gel control region (Baker, 1992).

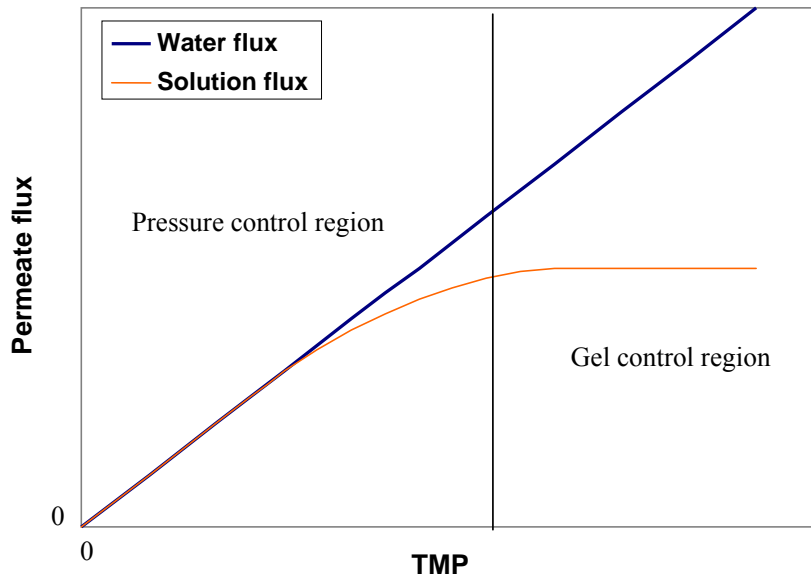


Figure II-2: Membrane filtration control regions

The gel model

The gel model assumes that a gel layer forms on the membrane surface where the solute concentration is constant and only depends on the solute. This model can predict a limiting flux and can not predict the flux in the pressure control region. This model is represented by Equation II-3.

$$J = (D/\delta) \ln(C_g/C_b)$$

Equation II-3

Where:

- ❖ **J** is the permeate flux
- ❖ **D** is the coefficient of diffusion of the solute
- ❖ **δ** is the gel thickness
- ❖ **C_g** is the gel concentration
- ❖ **C_b** bulk concentration

The resistance in series model

The resistance in series model relates permeate flux to a series of resistance, adding to the intrinsic membrane resistance, due increase in increase in TMP and the formation of a concentration polarisation layer and fouling of the membrane. This model is represented by Equation II-4

$$J = \Delta P / \eta (R_m + R_{gel}) \quad \text{Equation II-4}$$

Where:

- ❖ **J** is the permeate flux
- ❖ **ΔP** is the trans-membrane pressure
- ❖ **R_m** is the membrane intrinsic resistance to the permeate flux
- ❖ **R_{gel}** is the gel resistance to the permeate flux
- ❖ **η** is the permeate viscosity

The osmotic pressure model

The osmotic pressure model justifies the limitation of the permeate flux by the increase of osmotic pressure due to the increase of solute concentration at the membrane surface. Equation II-5 represents the osmotic pressure model.

$$J = (\Delta P - \Pi) / R_m \quad \text{Equation II-5}$$

Where:

- ❖ **ΔP** is the trans-membrane pressure
- ❖ **Π** is the osmotic pressure

- ❖ R_m is the membrane resistance

II.4.10.2 Membrane surface capture of particles

Many different parameters intervene in membrane fouling. Particle-wall interaction is an important parameter to model membrane fouling. The understanding of how the particles approach the membrane surface is important. The particle adhesion depends strongly on particle-wall interaction and of the becoming of the particle after the collision. The capture, deposition and detachment are determined by a combination of colloidal and hydrodynamics factors. (van de Ven, 1998) shows the importance of each factor that intervenes in particle wall interactions. It seems evident that the approaching angle (particle-wall) has an influence on the particle adhesion to the surface. The distribution (between: wall, fluid, particle and into adhesion process) of the particle energy after the collision depends on the collision angle.

(Munson-McGee, 2002) relates this to the force of adhesion measured by the atomic force microscope. It is clear that particles in cross flow filtration, arrived at an angle to the membrane wall, contrary to dead-end filtration where we can assume if there is no stirring, that the particles come to the membrane wall at a right angle. In the literature, it can be seen that particles hit the tubular wall quite tangentially and roll along the wall or return back to the bulk solution or/and stick to the surface. (King and Hammer, 2001) showed how leucocytes are captured by the membrane surface and how they role onto the membrane before immobilisation (Lu, *et al.* 2002).

II.5 ATOMIC FORCE MICROSCOPY

Atomic Force Microscopy (AFM) allows the scanning of any type of surface, conductive or non-conductive, with very little sample preparation and can be done directly in air. Therefore, it is found to be very useful to study the structure of membrane surfaces. Besides imaging surfaces, AFM can be used to measure forces of interaction between the tip or probes and surfaces in different environments.

II.5.1 Introduction

AFM is a technique of surface scanning. In atomic force microscopy, it is commonly the repulsive force between the tip attached to the end of a cantilever and the sample that is measured by the cantilever deflection. Because the repulsive force is universal, the technique can be applied to any type of material, conductive, non-conductive, biological, hard or soft such as polymers (Shakesheff, 1995). In general, AFM enables one to detect surface morphology, nanoscale structures and molecular/atomic scale lattices. AFM can be used in three different modes. In contact mode, the tip approaches the surface until contact between the sample and the tip is realised. Originally, this technique was used to get high-resolution surface profiles specifically for non-conductive material. With advances in this technique, it appears that for many materials, the tip surface interaction must be minimised, so non-contact was introduced. The real power of atomic force microscopy is its ability to directly quantify forces of interaction between the AFM tip and surfaces in both air and liquid environments. The creation of the colloid probe, coated colloid-probe and cell probe techniques make it possible to measure (bio)colloidal interactions with membrane surfaces (Bowen, *et al.* 1999a) and (Hilal, *et al.* 2002).

II.5.2 Scanning modes

There are three different modes to generate an image using an AFM. In contact mode, the tip of the cantilever scans across the sample surface, being in direct physical contact with the sample. The force of the contact is set up when the cantilever approaches the sample surface. As the scan goes on, the topographic features cause the deflection of the cantilever and the light beam, reflected from the back of the cantilever into a photodetector. The amount of deflection of the cantilever can be calculated from the difference in light intensity on the photodetector sector. In non-contact mode, the cantilever is made to oscillate at its resonance frequency. As the oscillating cantilever gets closer to the sample surface, it experiences a change in the force gradient that provokes a change in oscillation amplitude and phase. Both changes in amplitude and phase can be tracked via the deflection of the laser beam reflected from the back of the cantilever to the photodetector. The two modes are the classic modes used in AFM

imaging. The latter, non-contact, is preferred when soft samples or biological material are imaged. This is done in order to minimise sample tip interaction or to avoid dragging material that may be picked up in contact mode. In any case, during imaging, minimising the interaction between tip and sample is always preferable. The third mode presented here is the profiled mode. This mode of imaging has been used and presented in (Hilal *et al.* 2002) and (Hilal *et al.* 2003) when imaging imprinted and grafted membranes surfaces. This mode gave much greater results than contact and non-contact mode because of the loose material that can be found at the modified membrane surfaces.

Profile mode allows acquiring an image using the feed back Z-height at each data point to establish a topographic profile of the sample surface. The image is obtained by the tip approaching the surface at a defined speed until the laser beam signal becomes equal to or more positive than the set point. The Z-level is then recorded as topographic data. Then, the cantilever is withdrawn above the surface at a defined fixed distance, the scanner is moved laterally to the next point, and the cycle is repeated. The great advantage here is that the topographic image of the sample can be obtained without any lateral interaction between the tip of the cantilever and the sample as long as the Z-pullout chosen is large enough and it can be performed with a classic contact pyramidal tip. The minor disadvantage is that it is a little time consuming, taking approximately half an hour to produce a complete scan as opposed to few minutes with the conventional scanning mode.

II.5.3 AFM applied to membrane

In this part, the key points that AFM imaging brings to the membrane study and the technique used to image membrane surfaces are reviewed.

The key advantage of AFM above other techniques is its ability to produce images in both non-conducting and conducting surfaces, in air or liquids, without special sample preparation. This is why AFM has been shown to be a versatile tool for the determination of important key properties of polymer membranes (Magonov and Myung-Hwan, 1996) including pore size and surface roughness (Bowen *et al.* 1996b) and (Calvo *et al.* 1997a) and (Calvo *et al.* 1997b). Atomic force microscopy can

indicate key properties of the membrane under many different conditions. By surface analysis, it is possible to give the pore size distribution, porosity and roughness, which are key points in modelling membrane permeation (Bowen, *et al.* 1997) and fouling (Ochoa, *et al.* 2001) understanding. Ahead of these common AFM measures, it is possible to spot a single pore and describe its shape at a nanoscale (Bowen, *et al.* 1996a) that we know has an important impact on fouling characteristics (Bowen and Sharif, 2002b). Coupled with probe preparation technique, AFM is a powerful tool to measure adhesion forces (Bowen *et al.* 1998). Probes are prepared by adding a silica, polystyrene or sphere made from other material of different diameters or even bacteria (Bowen *et al.* 1999b) to the end of a cantilever without a tip. The technique is even more powerful when it is possible to coat the probe (sphere) with polymer (Hilal and Bowen, 2002) or protein (Butt, *et al.* 1995).

II.6 BIOLOGICAL TREATMENT OF WASTE

It has to be considered that biotechnology is one of the key elements among a panel of techniques implemented in a waste treatment. It is used for soil remediation *in-situ* or in a bioreactor, or solid waste treatment such as composting liquid waste treatment and energy production such as methane produced from landfill or in a bioreactor. Waste treatment processes always show multidisciplinary characteristics and the techniques involved are physical, chemical and biological.

Bioremediation takes place in two stages and both are of importance from a remediation point of view. The primary degradation corresponds to the lost of the one or more functional groups. The other stage is the mineralisation, in which the entire molecule is oxidised to carbon dioxide, water and mineral salts (for aerobic processes).

One of the main gains that can be seen through the use of biotechnology is the reduction in COD and the detoxification of the effluent such as denitrification, bioreduction of metal as chrome IV into chrome III. In contrast to other techniques, such as oxidation processes, biological processes stabilise the waste stream, as the case in solid waste treatment such as composting or liquid waste effluent that produce sludge. The advantage here is that the processed effluent is less toxic than the ingoing

effluent. In certain cases, oxidation processes involve reaction paths that produce toxic co-products, besides a global reduction in organic content. The other advantage of bioremediation compared to oxidation processes, is when they can be competitive treatment solution. The cost of oxidation processes (involving UV light, ozone production, use of chemicals hydrogen peroxide, Fenton reagent or titanium oxide) is higher than that of biological treatment.

The use of micro-organisms for degrading waste effluent has been used for decades to treat domestic sewage. During the last 20 years, the rapid development of microbiology and biochemistry allows very effective treatment of toxic industrial waste effluents such as MWF to be obtained.

II.6.1 Biodegradation of MWF

It has been shown in Paragraph II.3.3 that metalworking fluids are colonised by a number of micro-organisms. The extraction and selection of the microorganism from waste MWF leads to the development of micro-organism consortia able to degrade MWF (van der Gast *et al.* 2002).

The biodegradation of MWF, when assisted by membrane filtration, is mainly based on the bioremediation of the surfactants and oil that permeates through the membrane.

Primary biodegradation of surfactant results in the loss of its functionality. Therefore, it can be expected to lose the undesirable properties of foaming, dissolving grease and forming emulsion, which are phenomenon of the effluent and even more difficult to treat.

II.6.2 Bioreactor

Bioreactors are enclosed vessels in which various parameters can be controlled and in which the biodegradation takes place. The immobilisation of micro-organisms in biofilms has great advantages that can be summarised as follows:

- ❖ Maximises the retention time of the biomass
- ❖ It enhances the productivity per unit of biomass
- ❖ System can sustain higher flow rate without washout
- ❖ The fixed systems are more resistant to contamination by microbes or overdosed contaminant, making the overall process more robust.

Different types of bioreactors can be used to treat industrial waste effluent. Two systems of bioremediation can be found aerobic or anaerobic. When oxygen is provided to the bioreactor, the system is aerobic and when the bioreactor is deprived of oxygen, the system is anaerobic. The differences between aerobic and anaerobic system is fundamental from a microbiology point of view. For the engineering side the difference resides essentially into 8 main technical considerations as presented in Table II-2

	Aerobic system	Anaerobic sytem
Rate of degradation	+	-
Organic load acceptance	-	+
Complex organic degradation	-	+
Oxygen	Imperative	NO
Heating	Facultative	Needed
Robustness/simplicity/maintenance	+	-
Odour and gas treatment *	+	- Methane
Biomass production	-	+
Running cost	+	-
Cost investment	+	-

Table II-2: Comparison of aerobic and anaerobic systems (+) relative advantage and (-) relative disadvantage

* except for methane production plant

II.6.3 Scaling-up

From flask test to laboratory scale fermenter to industrial size, all parameters of the biological process have to be scaled up cautiously in order to ensure performance repeatability at each stage. Good control of the bioremediation parameters at each scale can lead to performance improvement. As a simple example, the oxygen intake in 100 ml flask will be improved dramatically when the same biologic system is set-up in a 2 litres batch reactor, agitated, and in which air is bubbling due to the great improvement of exchange surface area between the gas phase and the liquid phase. In order to ensure good repeatability of remediation performances, inocula of consistent quality, which provide sufficient quantity, are necessary. For the inoculation of a large vessel, it is necessary to provide a large volume broth, 10% of the vessel volume that is going to be inoculated (Asenjo and Merchuk, 1995). To ensure success, the micro-organisms should be in their exponential growth phase. This can be assessed by following the measurement of the broth turbidity.

II.7 PHYSICAL CHEMICAL METHOD

Physico-chemical processes are used to destabilise cutting oil emulsion. These processes can be divided into two categories, one that uses inorganic salts and those that use polymers. The first one is not effective for the removal of truly soluble organic chemicals. Chemical treatment of waste metalworking fluids can be easily adapted to any scale. Both techniques are aimed at flocculating the oil droplet to separate the oily phase of the emulsion from the aqueous phase. Coagulants may cause the removal of colloids in wastewater by two different primary mechanisms. One theory involves the neutralisation of the surface charges on the particle so that they can aggregate and form larger particles to be separated from the aqueous phase by difference in density in a reasonable time. The other mechanism is referred to as the "sweep flock" mechanism. This is based on the coagulant precipitation; the resulting nascent particles and flock collide with the colloids that adsorb on their surface. Both mechanisms are involved in colloid flocculation.

The acid-alum method is the most common method of chemical treatment of metalworking fluid. This technique uses sulphuric acid, aluminium sulphate and the addition of sodium sulphate and the process is described in five steps by (Burke, 1991) as follows:

- ❖ Add sulphuric acid in order to lower the pH down to a range of 2.5 to 3.
- ❖ Add aluminium sulphate, preferably as a 50-60% in weight concentrate solution.
- ❖ Allow the addition of sulphuric acid and aluminium sulphate to react for five minutes.
- ❖ Slowly add sodium hydroxide 50% concentrate solution in order to adjust the pH.
- ❖ After ideal pH is reached, allow solution to continue mixing for more than five minutes, then turn off mixing and let solution stand for as long as the flocculate rises to the surface.

It is worth noting here that the agitation is kept mild.

Although, this technique uses aluminium sulphate, other inorganic salts can be used. A study is presented in (Rios, *et al.* 1998). In their article the authors used CaCl_2 and AlCl_3 as coagulants. Sometimes the technique is supported by UF system that removed the large colloids. The down side of the technique is the usage of chemicals. These chemicals add cost to the process and may contaminate the supernatant (clear aqueous phase) and the oily phase. The effect of cations such as iron on further treatment may lead to some problems. Problems in fouling of NF or RO system and to the degradation of membrane polymers as it is reported in (Gabelich *et al.* 2002). The other difficulty in using chemical techniques is the control of the doses of chemical to be used, especially when the inlet stream varies in concentration, not only for economical reasons, but also for process efficiency. Excess of chemical may lead to re-emulsification.

II.8 ACTIVATED CARBON

This part presents a brief review of the use of activated carbon in remediation technology.

Activated carbon is a matrix that presents a large surface area and a strong adsorption potential. The manufacture of activated carbon involves the creation of carbon matrix by pyrolyse of material rich in carbon. Activated Carbon (AC) is prepared from nut shells, wood, coal, or other carbonaceous material. Waste such as tyres or sludge may be used, this step is a pathway for waste valorisation.

The quality of the AC is relative to the carbon content of the source that may contain contaminant and minerals. The rates of pyrolyse and the activation process are of importance. These factors influence the porosity, pores size and active surface area of the activated carbon. The ability of activated carbon to adsorb pollutant is linked to its characteristics.

There are two classes of activated carbon:

Powder Activated Carbon (PAC) consists of fine particles, showing a very large external surface and a short length of diffusion.

Granular Activated Carbon (GAC) consists of large particles superior to 100 μm , they show therefore, a smaller external surface than the powder one. The adsorption is strongly dependent of the diffusion of the contaminant into the pores of the activated carbon surface.

Activated carbon may be used as a catalyst or catalyst support improving reactant concentration to its surface. Generally AC is used as a separation process that remove contaminant from the stream. The technique can be used to treat gas and is particularly effective at removing odours and Volatile Organic Compound (VOC) to recycle solvents. It is also used to treat aqueous phases. It can be used to remove trace contaminant.

Activated carbon is capable of being recycled using thermal reactivation techniques. This process offers very significant advantages to an activated carbon consumer;

- ❖ The best environmental option available
- ❖ Removal of expensive waste disposal costs
- ❖ Conservation of existing landfill provision
- ❖ Reduction in operating costs as regenerated material is often less expensive than virgin adsorbent

Reactivation restores the activated carbon to a state where it is virtually identical to the properties of the virgin pre-cursor.

Activated carbon is used in batch stirred systems or in continuous mode. Batch systems are efficient to treat small volumes and achieve equilibrium rapidly. Continuous systems need to be implemented when a permanent stream needs to be treated.

II.9 FUEL INCINERATION GENERATED FROM WASTE

Two important aspects of burning waste oil have to be taken into account. The total amount of energy that can be recovered has to be balanced against the total energy employed in the collection and refining of the used oils. The second aspect is emission; the major problems are PCBs, HAPs, dioxins and heavy metals. If the legal requirements are not met then a treatment can be done or the waste oil has to be considered as a hazardous waste and treated accordingly. As an example of oil treatment, (Bhaskar *et al.* 2004) presents a study on recycling waste lubricant oil using thermal and catalytic techniques for desulphurisation. Hazardous waste demands an incineration process that ensures a total oxidation of PAHs, PCBs and dioxins and a post gas treatment to remove heavy metal.

A good alternative is to burn the oil in cement factory. The advantage of this method of disposal is that the flux of gases produced during the oil combustion mixes with the cement and reacts, absorbing and retains within heavy metals. There are limits on the

amount of contaminants to be retaining legally and technically (e.g. chlorine and zinc are known to have a strong effect on cement quality).

This recovered oil is suitable and can be blended with fuel and used on site in a boiler or a Combine Heat and Power (CHP) plant. A lower European limit of one Megawatt has recently been introduced, below which it is not advisable to burn used oil (Department of the Environment, Good practice guide 1993)

	<u>Error! Bookmark not defined.</u>	Deleted: 7
II.1	Introduction	7
II.2	Industrial waste effluent	7
II.2.1	Domestic Sewage	7
II.2.2	Rainwater	8
II.2.3	Trade Effluent	8
II.2.4	Charges for trade effluent	9
II.2.4.1	Consent to discharge	9
II.2.4.2	Discharge to sewer	10
II.2.4.3	Effluent discharges into rivers and other water courses	11
II.2.5	Regulations	11
II.3	Metalworking fluids	12
II.3.1	Brief history of metalworking fluids	12
II.3.2	Uses and chemistry of metalworking fluids	14
II.3.2.1	Types of metalworking fluids	14
II.3.2.2	Chemistry of semi-synthetic metalworking fluids	16
II.3.3	Microbiology of metalworking fluid	17
II.3.3.1	Problems due to microbial contamination of MWF	18
II.3.3.2	Biodegradability	18
II.3.4	Waste metalworking fluids disposal options	19
II.3.4.1	Direct Sewer	20
II.3.4.2	On-site treatment	20
II.4	Membrane technology and applications	22
II.4.1	Definition	22
II.4.2	History	23
II.4.3	Membrane processes	24
II.4.4	General applications	27
II.4.5	Applications in wastewater treatment	28
II.4.6	Filtration of metalworking fluids	28
II.4.7	Water recovery	32
II.4.8	Fouling	33
II.4.8.1	Fouling mechanisms	33
II.4.8.2	Specific type of fouling	34
II.4.8.3	Membrane cleaning	35
II.4.9	Techniques to enhance filtration	36
II.4.9.1	Filtration module and hydrodynamic conditions	37
II.4.9.2	Introducing turbulence	38
II.4.9.3	Surface modification	40
II.4.9.4	Feed Pre-treatment	41
II.4.10	Modelling of filtration for oil waste water	42
II.4.10.1	Permeate flux models	42
II.4.10.2	Membrane surface capture of particles	45
II.5	Atomic force microscopy	45
II.5.1	Introduction	46
II.5.2	Scanning modes	46
II.5.3	AFM applied to membrane	47
II.6	Biological treatment of waste	48
II.6.1	Biodegradation of MWF	49
II.6.2	Bioreactor	49
II.6.3	Scaling-up	51

II.7	Physical chemical method	51
II.8	Activated carbon	53
II.9	Fuel incineration generated from waste	54

CHAPTER II

Figure II-1: Types of membrane filtration	26
Figure II-2: Membrane filtration control regions	43

CHAPTER II

Table II-1: Different types of MWF, their properties and applications	15
Table II-2: Comparison of aerobic and anaerobic systems (+) relative advantage and (-) relative disadvantage	50

CHAPTER III

EXPERIMENTAL EQUIPMENT

AND

PROCEDURES

CHAPTER III

Experimental Equipment and Procedures

III.1 INTRODUCTION

This chapter describes materials, equipment and protocols adopted for each experimental part of the project. It is divided into ten sections including this introduction giving details of the process.

Firstly, Section III.2 explains the preparation, characterisation and simulation of the waste effluent that is used throughout this thesis.

The second part deals with the filtration process. This part is divided into three sections detailing the different membranes used, the filtration equipment at small and large-scale, and finally describes the method used to inject gas in the tubular membrane during filtration.

The third part describes the two methods of chemical treatment in Section III.6.

The fourth part concerns the description of the bioremediation process, including details of the creation of a bio consortium adapted to the waste used and the bioreactors.

The fifth part of the chapter describes in Section III.8 the process that uses activated carbon.

The last three sections describe analysis techniques. Section III.9 describes the Atomic Force Microscopy technique used to image and analyse the surface of the membranes. Finally, Section III.10, details the five analytical techniques used to assess the performance of the treatment process.

III.2 WASTE PREPARATION AND CHARACTERISATION

Throughout the study, Mobilcut 232 is used as a waste stream. This section describes the characteristic of the oil, how the waste streams are simulated and finally, how the waste is characterised.

III.2.1 The oil: Mobilcut 232

Mobilcut 232 is a multipurpose semi-synthetic metal working fluid with a high oil content and excellent bio-stability donated by Exxon-Mobil. This oil formed a microemulsion when mixed with water for a wide range of oil concentrations.

Table III-1 and Table III-2 show the principal usages recommended by Mobil.

In these tables, concentration rates are given as percentage in volume and the letters stand respectively for: (E) Emulsion; (M) Micro-emulsion; (S) Solution. Mobilcut 232 used during this work is highlighted in grey.

OPERATION	Steels			
	Mild steels	Mid-hard Steels	Hard steels	Alloyed steels
Turning - Screw cutting	Mobilcut 222 5 / M	Mobilcut 222 5 / M	Mobilcut 232 5 / M	Mobilcut 242 5 / M
Milling	Mobilcut 222 5 / M	Mobilcut 222 5 / M	Mobilcut 232 5 / M	Mobilcut 242 5 / M
Drilling - Boring	Mobilcut 222 5 / M	Mobilcut 222 5 / M	Mobilcut 232 5 / M	Mobilcut 242 5 / M
Tapping	Mobilcut 222 5 / M	Mobilcut 222 5 / M	Mobilcut 242 5 / M	Mobilcut 242 5 / M
Grinding	Mobilcut 321 3 / S			
Sawing	Mobilcut 222 5 / M	Mobilcut 242 5 / M	Mobilcut 242 5 / M	Mobilcut 242 5 / M
Gear shaping	Mobilcut 232 5 / M	Mobilcut 232 5 / M	Mobilcut 232 6 / M	Mobilcut 151 6 / E
Broaching	Mobilcut 232 6 / M	Mobilcut 242 6 / M	Mobilcut 242 7 / M	Mobilcut 151 8 / E
Honing	Mobilcut 232 5 / M	Mobilcut 232 5 / M	Mobilcut 242 4 / M	Mobilcut 242 5 / M

Table III-1: Steel utilisation of Mobilcut 232

Operation	Alloys		
	Aluminium and alloys	Copper and alloys	Cast-iron
Turning - Screw cutting	Mobilcut 232 4 / M	Mobilcut 122 4 / E	Mobilcut 232 4 / M
Milling	Mobilcut 232 4 / M	Mobilcut 122 4 / E	Mobilcut 232 4 / M
Drilling - Boring	Mobilcut 242 5 / M	Mobilcut 122 4 / E	Mobilcut 232 5 / M
Tapping	Mobilcut 242 5 / M	Mobilcut 122 4 / E	Mobilcut 232 5 / M
Grinding	Mobilcut 232 3 / M	Mobilcut 321 3 / S	Mobilcut 321 3 / S
Sawing	Mobilcut 242 4 / M	Mobilcut 122 4 / E	Mobilcut 232 4 / M
Gear shaping	Mobilcut 242 5 / M	Mobilcut 232 5 / M	Mobilcut 232 5 / M
Broaching	Mobilcut 242 6 / M	Mobilcut 242 6 / M	Mobilcut 232 6 / M
Honing			Mobilcut 232 4 / M

Table III-2: Alloy utilisation of Mobilcut 232

The oil concentration varies between 3% and 6% of oil in volume depending on the application and for some specific applications this concentration may rise to 10%. The concentration of the waste metalworking fluid (MWF) is also dependent upon the water loss during cooling and mode of collection of the waste fluid. In an industrial environment, the oil concentration is variable and a fixed oil concentration must be chosen in order to study the filtration behaviour. An initial oil concentration is fixed at 5% in volume to study the microemulsion filtration and to simulate the waste stream.

III.2.2 Waste simulation and metalworking fluid preparation

Typically, the waste has an oil concentration that varies from 1% to 10% in volume. Therefore, in order to simulate the waste, a microemulsion of Mobilcut 232 is mixed at 5% of oil in volume with tap water. Figure III-1 shows the coolant-mixing unit OSCAR CMS (CARDEV Ltd). This mixing unit allows the production of a constant

microemulsion freshly made when needed. In the rest of the work, the effluent is identified by MWF (MetalWorking Fluid) followed by a percentage showing the part of oil in volume measured by refractometry. MWF 5% stands for an emulsion at 5% in volume of Mobilcut 232 as described in this paragraph. The blend is done using tap water.

Other filtration tests are carried out using the retentate that has a concentration of 20% (MWF 20%). This retentate is obtained after filtration with FP100 ultrafiltration membrane of original MWF 5% prepared as above.

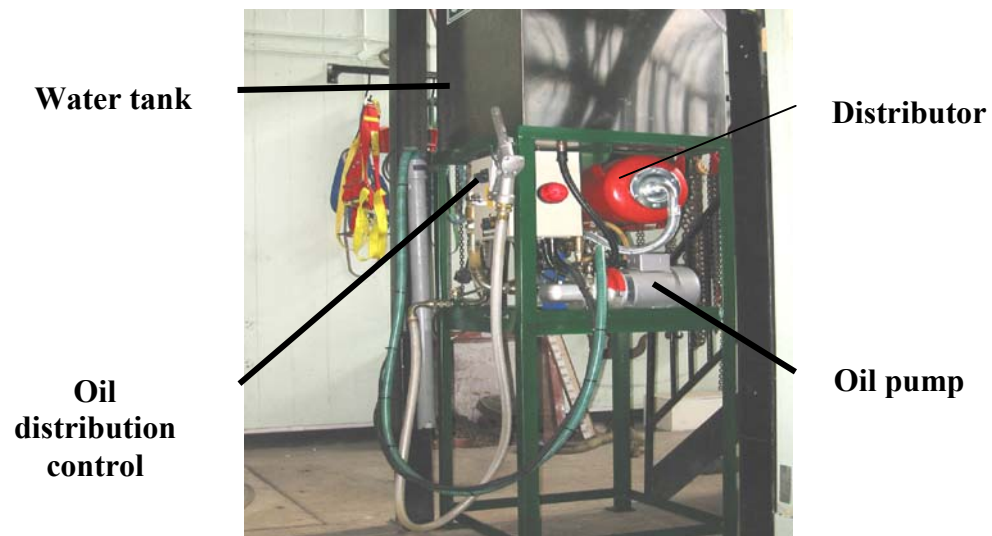


Figure III-1: Mixing unit

III.2.3 Waste characterisation

a) *Oil content*

A refractometer enables the direct measure of the oil content of the microemulsion when between 0% and 15%. The abacus is shown in Figure III-2. When the oil concentration is over 15%, the microemulsion is diluted with tap water at 50%, then the reading is taken and the result multiplied by two to calculate the actual oil concentration. The reading is accurate at $\pm 0.2\%$.

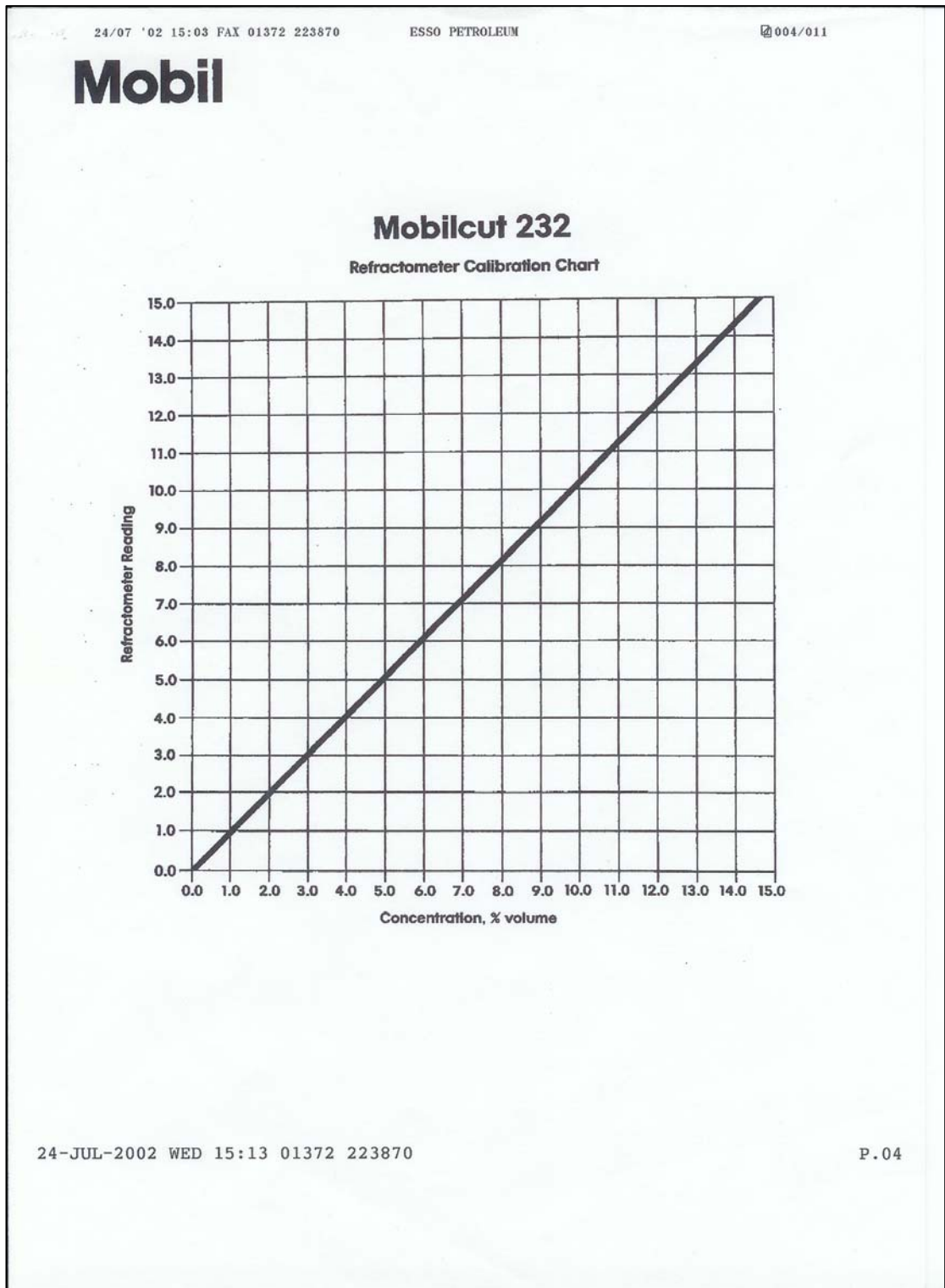


Figure III-2: Abacus for oil concentration in water applicable for Mobilcut 232

b) *Oil droplet size*

Oil droplet sizes are measured by Photon Correlation Spectroscopy (PCS) using a ZETASISER 3000 from Malvern Instrument Ltd, UK.

The PCS technique relies on the measurement of the movement of particles undergoing Brownian motion.

c) *Oil and emulsion viscosity*

The viscosity of the metal working fluid is measured with a BOHIN Rheometer C-VOR using double gap geometry. The temperature is set and controlled by a water bath.

III.3 MEMBRANES

Six different types of membranes were used in this work. They fall into two categories, ultrafiltration (UF) and nanofiltration (NF) membranes.

III.3.1 Ultrafiltration membranes

Three UF membranes, two tubular membranes and one flat sheet membrane are used.

PCI Membrane System provided both the NF and UF tubular membrane. These membranes have an inner diameter of 1.27 cm and can be cut in length to fit the module in which they are used. Two Polyvinylidene fluoride (PVDF) tubular ultrafiltration membranes FP100 and FP200 with respective Molecular Weight Cut Off (MWCO) of 100,000 and 200,000 Dalton were used. These membranes are chosen for their chemical resistance and hydrophobic properties in order to minimise fouling. The manufacturer recommends operating temperatures between 10°C and 60°C.

Nadir membrane GmbH provided the flat sheet UF membrane UF-PS-100H made of polysulphone (PS) with a MWCO of 30,000 Dalton.

III.3.2 Nanofiltration membranes

Three nanofiltration membranes are used, two flat sheets and one tubular membrane.

The two flat sheet nanofiltration membranes are BM-05D and BM-20D from Berghoff Filtration, Germany. They have a MWCO of 500 and 2,000 Dalton respectively. These membranes are negatively charged nanofiltration membranes made of polyamide.

The tubular nanofiltration membrane AFC30 from PCI Membrane System has a MWCO of 3,000 Dalton. It is a thin polyamide film composite nanofiltration membrane used for purifying solutions of low molecular weight organics, achieving high retention of organics with salt passing. AFC30 exhibits good retention for organic molecules above 200 Dalton. The operational range recommended by PCI is at pH between 4 and 9.5, a temperature range between 10°C and 60°C and is resistant to most solvents.

III.4 FILTRATIONS

This section describes the equipment used for the filtration of MWF. Filtrations were carried out at both small and large-scale. Two types of filtration were carried out, ultrafiltration (UF) and nanofiltration (NF). The first part, III.4.1, describes the three small-scale units used in this work. In Section III.4.2, the two large-scale units and the filtration protocols are detailed. Finally, specific filtration procedures are given, starting with washing cycles, cold-water flux (CWF), pressure excursion and temperature tests.

III.4.1 Small-scale filtration units

Membrane filtrations were carried out using the different membranes mentioned in Section III.3.

III.4.1.1 Dead-end filtration cell

The dead-end filtration cell is used with the nanofiltration flat sheet membrane.

a) Description of the cell

The dead end filtration work was conducted with a stirred cell model 8010 from Millipore Corporation, USA. The cell, described in Figure III-3, has a capacity and hold-up volume of 10 and 0.2 millilitres respectively. It holds a membrane disc of 25 millimetres in diameter and the effective membrane area is 4.1 cm². The maximum operating pressure of the cell is 5.17 bar. A magnetic stirrer assembly is mounted inside the cap assembly. The design of the body allows the stirrer to be as close as possible, just above the membrane.

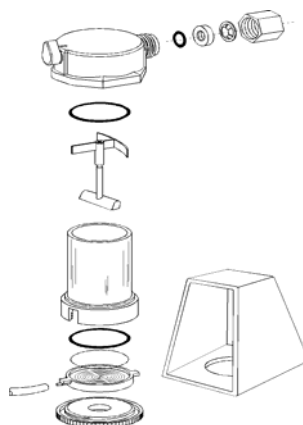


Figure III-3: Dead-end filtration cells

b) Operation of the cell

When operating the cell, the membrane is mounted on the membrane holder then the O-ring gasket locks the membrane in place. The rest of the body is assembled and the 10 millilitres of solution is poured into the cell. With the magnetic stirrer in place and the cap assembly locked, the cell is stirred for 15 minutes to allow the membrane to be wetted with the solution stirred above it. The pressure relief knob is closed and turning on the nitrogen gas cylindrical valve sets the operating pressure.

c) *Protocol*

The applied pressure was set at 4.8 bar, the stirring rate at 300 rotation per minute (rpm) and the permeate flux was measured volumetrically. The permeate was collected in a graduated cylinder and the time to collect a certain volume of permeate was measured in order to determine the flux. The flux was determined by measuring the time for 1 ml of permeate to pass through the membrane. The flux was measured 4 times and the mean of these measurements was then calculated. A Cold Water Flux (CWF) was measured before and after filtration. The CWF is the measurement of the membrane permeate flux of demineralised water at 20°C and is described in Section III.4.5

III.4.1.2 Flat sheet unit

Figure III-4 shows a dual ultrafiltration membrane cell. This cell was mounted with two sheets of Polysulfone Nadir membrane described in III.3.1. The total filtration surface area is 0.0135 m². These sheets are mounted in the filtration unit in series. The filtration was carried out at a pressure of 1.5 bar, using MWF 5% for feed.



Figure III-4: Small scale UF flat sheet unit

III.4.1.3 Cross flow small-scale unit

The tubular cross flow small-scale unit enables some preliminary experiments to be carried out with tubular ultrafiltration membranes and to determine optimum parameters of washing cycles. This unit was also used to study the effect of temperature on the filtration of MWF and to study the injection of gas during the filtration of MWF.

Figure III-5 shows the small cross flow filtration unit. This unit is fitted with two tubular ultrafiltration membranes 1.27cm inner diameter and 30cm long situated side by side and connected by a U bend. The total length covered from the inlet manometer to the outlet is 70 cm. The membrane tubes in this configuration show a total effective filtering area of 0.024 m². The pump used is from Mono Pump Ltd, Manchester model CMM253/H13F and delivers a maximum pressure of 3.45 bar. The pump is fitted with a motor from Brook Compton Ltd, Doncaster Model KP 7575. At the maximum inlet pressure, the maximum flow rate measured is 0.277.10⁻³ m³/s (1000 L/h).

The pump recycles the feed solution from a 20 litre feed tank through the membrane unit. It is possible to recycle the permeate in order to undertake a constant feed solution concentration or to withdraw the permeate from the re-circulation loop to undertake a concentration filtration. The concentrate tends to heat up during filtration therefore, to ensure a constant feed temperature a cooling coil is placed in the feed tank. An electrical resistance, controlled by a thermostat, may replace the cooling coil when experiments are carried out at higher temperatures.



Figure III-5: Small-scale tubular membrane unit

III.4.2 Cross flow large-scale equipment

This part is concerned with the two large-scale filtration units as well as a comprehensive methodology to run the two units.

III.4.2.1 Membrane filtration module

The membrane module is the same for both units, shown as **1** in Figure III-6 (page 69) and consists of 18 tubes, each 95 cm centimetres long in which the membranes are fitted. The membranes have a total surface area of 0.64 m². The filtered fluid goes through the 18 tubes in sequence. The end caps of the filtration module U-bends fitted to each membrane so that the fluid enters the first membrane and is distributed via a U-bend to the second and so on. It finally enters the eighteenth and leaves the filtration module. All appends as if the fluid is following a single multi-bend tube of 17.10 m long. A diagram of the module is given in Appendix C.

III.4.2.2 Power

Power for the entire system is provided via one 415V "3-phase and neutral" plug, which is located on the first membrane system. Power to membrane system two is switched on via the main control panel located on the first unit.

III.4.2.3 Waste Coolant tank

The waste coolant tank has a capacity of 2000 litres, with a glass window indicating the fluid level. Fluid is drawn from the waste oil tank via a floating pick up, drawing fluid from the top. The fluid then passes through the clear hose into the long stainless steel pre-filter on system Unit 1. This pre-filter is fitted with a re-usable nylon mesh bag filter rated at 300 microns.

III.4.2.4 Description of the filtration units

This part describes each pump and the valves used to operate both membrane system units.

a) *System unit 1*

This unit is composed of six different tanks that are described in Figure III-7.

The first membrane system unit consists of six tanks and five pumps. The main tank (1) is charged with 180 litres of waste. The waste is then pumped to a coalescing tank (2) filled with plastic beads that help to remove tramp oil. Then it overflows back up into the inner process tank (3). From that tank, the waste is driven to the membrane module. Tank (4) is used to collect the permeate, tank (5) is used to contain nutrient to feed the bioreactor and tank (6) is used to collect the oil from the coalescing tank.

A Grundfos pump, type CR2 110, drives the first and second membrane units. The membrane back-pressure can be tuned with a valve. A bypass is added to the pump outlet and when the bypass is opened, the membrane can be operated at lower pressure and different cross membrane pressures (XMP) can be applied to the system. Two pressure gauges allow the TMP and the XMP to be set. The TMP is the pressure average across the membrane unit, calculated as the average between inlet pressure and outlet pressure. The XMP is the pressure drop across the membrane unit. At the membrane unit outlet, a flow meter allows the fluid velocity to be calculated.

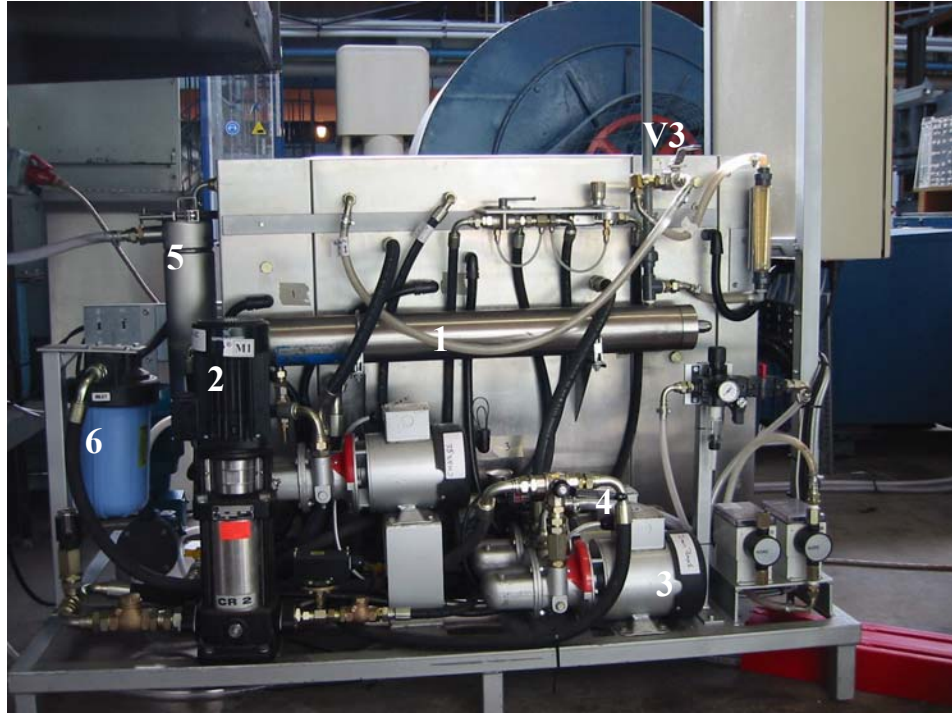


Figure III-6: Side view of the first membrane unit

1: membrane module; 2: M1 process pump; 3: charge pump; 4: circulation pump behind (3);
5: prefilter 300 μ m; 6: prefilter 100 μ m; V3 permeate diverting valve

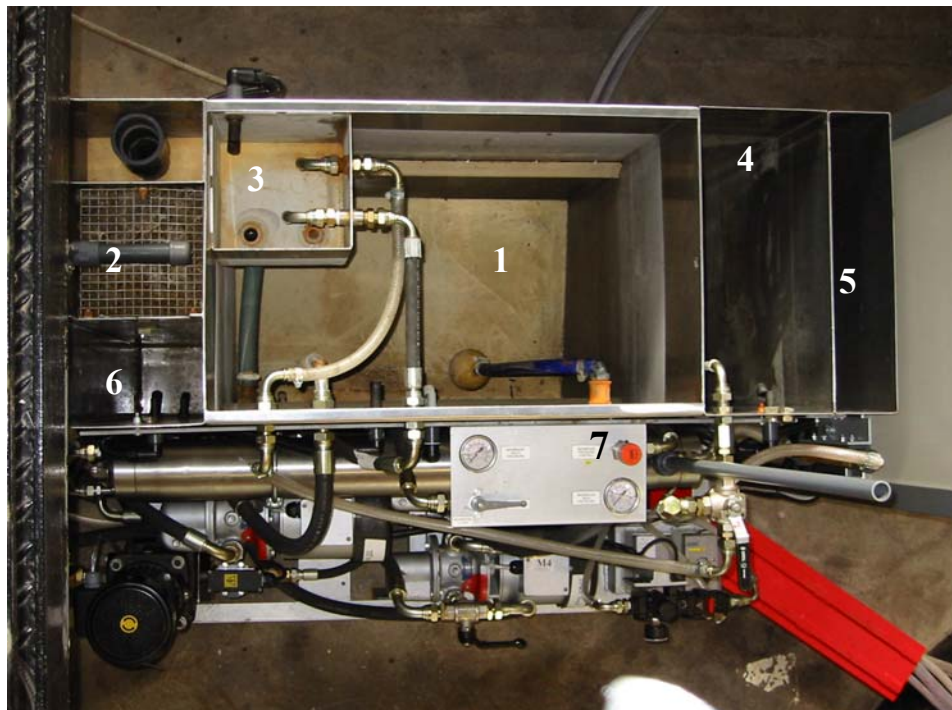


Figure III-7: Top view of the filtration unit 1

1: main tank; 2 coalescer tank; 3 process tank; 4 permeate tank; 5 nutrient tank; 6: tramp oil tank; 7: back-pressure valve

b) System unit 2

Figure III-8 shows the membrane filtration unit 2. This unit consists of three tanks and three pumps. The main tank has a capacity of 600 litres. The effluent is pumped into an internal process tank through a 100 μ m filter. From the process tank, the fluid is pumped to the membranes. To wash the membrane, an external tank is used that is driven by the process pump. Both the main tank and washing tank can be flushed with the third pump.



Figure III-8: Filtration unit 2

1: main tank; 2: process tank 3: external washing tank; 4 process pump; 5: circulation pump; 6: back-pressure valve; 7: Process/ flushing valve

This unit has its own control panel and an external flushing tank. The large double valve, shown as (7) on Figure III-8, must be facing outwards during processing, and downwards during flushing.

III.4.2.5 Filtration operation

This part explains how each unit described in III.4.2.4 can be operated.

a) *System unit 1*

From the pre-filter, the fluid is drawn through the charge pump (pump M3, operated via charge pump stop/start switches on main control panel) into the main tank of system 1. The charge pump will continue to run until the fluid level in the main tank rises to the bottom of the internal process tank, at which point, the high level float switch is made and the pump is stopped. Each charge allows 180 litres to enter the main tank. With this system, the filtration is carried out in semi-batches of 180 litres.

Once the main tank is full **(1)**, the circulation pump **(4)** can be started using the circulation pump start button on the main control panel. The circulation pump draws the fluid from the floating pick up in the main tank of system 1 through a large plastic filters, fitted with a re-usable bag rated at 100 microns into the coalescing tank. A pressure switch is fitted to the pump to stop the pump when the pressure reaches 3.5 bar (i.e. when the blue filter **(6)** is blocked), as well as a pressure gauge to give visual confirmation. Once the fluid sprays over the coalescing tank **(2)**, it passes down through the coalescing media, returns up through the rear chamber and floods into the internal process tank **(3)**. When the internal process tank is full and overflows into the main tank, the process can be started. A full description of the coalescing medium is given in Appendix D.

Once running, the membrane pressure control valve can be carefully closed until the membrane inlet reaches the desired pressure. The XMP may be adjusted by opening the bypass valve positioned at the membrane inlet, which diverts part of the flow back into the process tank. The process pump now feeds from the internal process tank and pumps through the membranes, returning the concentrate to the internal process tank and the permeate via a flow meter and a valve V3 to the permeate tank if V3 set to process mode, or back to the internal process tank if V3 is set to flush mode.

During normal operation, processing continues until the level in the main tank drops so the pump is not able to feed the internal process tank. Then the process tank level slowly drops until the process tank float switch is no longer made, at which point the process pump also stops.

b) *System unit 2*

When the second membrane system is "full" (i.e. level just meets bottom of internal float tank), the circulation pump (M2A) should be started. This pump draws from the bottom of the main tank through a filter into the internal process tank. The filter is fitted with a re-usable nylon mesh bag filter rated at 100 μ m to retain all the large biological material that escapes from the bioreactor.

When the internal process tank is full, the process pump can then be started. Before starting the process pump, ensure that the membrane pressure control valve is fully open and that the membrane valve opposite is set to "membrane open". Once running, the membrane pressure control valve can be carefully closed until the membrane pressure is satisfactory.

Fluid from the main tank is pumped through the membrane pod. Concentrate is returned to the internal process tank, whilst permeate is fed into an IBC, via a flow meter. This process continues until the low-level float switch is reached. At this point, the process pump cuts off and the level in the internal float tank drops until its float switch breaks contact - this cuts off the process pump. The resulting concentrate can then be drained via drain pump 2, which is controlled from the main panel.

III.4.2.6 Flushing operation

This section describes the flushing operation that are carried out when the membrane requires cleaning.

a) *System unit 1*

A hosepipe is attached to the cam-lock fitting on the inlet of the process pump. Clean water is passed through until the water spilling out of the internal process tank is relatively clean. Surfactant is then added to the process tank, and the process pump started as described in Section III.4.2.5. Valve V3 has to be turned to the flush position to divert permeate back into the process tank. This processing continues until the system is turned off (usually 30 - 60 minutes is sufficient time). The full washing protocol has been studied and optimised in this work and is given in III.4.4. The concentrated solution can then be drained from the system using drain pump 1 via valve V10 - when V10 is turned clockwise, the coalescer is drained. When the valve is fully turned anti-clockwise, the main tank is drained. The internal process tank is drained into the main tank via valve V6.

b) *System unit 2*

To flush system 2, the external flush tank must be used. The external flush tank is filled with fresh water until the top float switch is reached. The membrane module is flushed, then surfactant is added to the water. Valve V21 is turned to divert permeate back into the external washing tank. The large double valve underneath the flush tank is turned downwards for flushing. This diverts the process pump and changes over the control of the float switches from the internal flush tank to the external flush tank.

The external flush tank can be drained via V19B, using drain pump 2 controlled on main panel of the first unit.

III.4.3 Filtration protocol

Prior to any experiment or when a new membrane set is used, a washing cycle is carried out as follows.

- ❖ The content of the membrane unit (process tank, pump and membranes) is emptied via the pump to the main tank.
- ❖ The unit is flushed with 25 litres of tap water at 45°C via the concentrate tap.
- ❖ 1% of surfactant is added to another 25 litres of tap water at 45°C to wash the membranes.
- ❖ The permeate valve is opened in order to recycle the permeate back into the process tank.
- ❖ The washing cycle runs as described in III.4.4.2, page 77.
- ❖ The liquid present in the membrane, pump and process tank are flushed after 20 minutes.
- ❖ The system is rinsed with 25 litres of tap water at 45°C and the re-circulation lasts 5 minutes.

III.4.4 Washing cycles

Membranes are washed when they are fouled or when they need to be regenerated, in order to ensure the same state of the membrane surface when a new set of filtration starts. This washing cycle has been studied and optimised. Therefore, this part describes how the optimisation of the washing cycle has been conducted and explains the washing cycle used for each filtration experiment.

III.4.4.1 Optimisation of washing cycles

This optimisation is carried out with the tubular small-scale unit fitted with ultrafiltration membrane FP100, this unit was describe in Section III.4.1.3. Figure III-9 shows a diagram of the experimental set up.

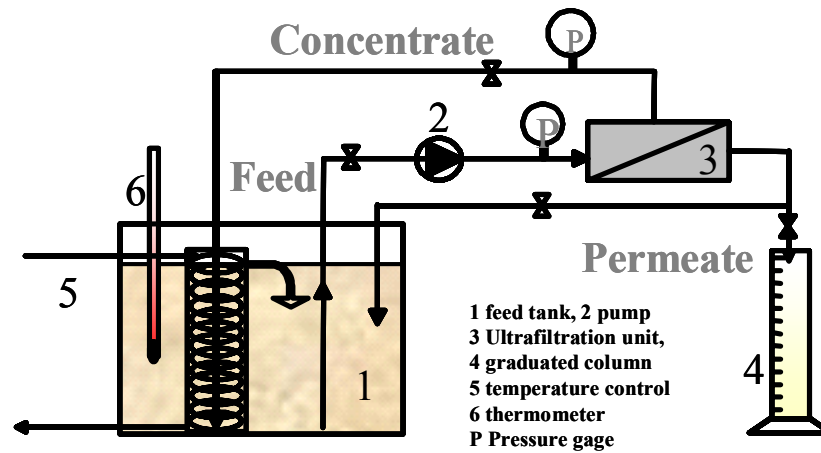


Figure III-9: Experimental set up used for washing cycle and temperature test

The efficiency of the washing cycle of the membrane surface is evaluated using six factors; surfactant concentration, washing solution temperature, re-circulation velocity, washing cycle duration, volume of washing solution and the application of pressure during the washing cycle. The screening of these factors is undertaken using eight trials where each factor is varied between two values (state -1 and state $+1$) defining the experimental domain. The experimental domain is set up regarding the membrane characteristics and surfactant use recommended by the manufacturer. Table III-3 shows the values taken for each factor and defines both states. Experiments are structured using an optimal experimental plan based on Plackett and Burman matrix (Lanteri and Longerey 1998) and (Plackett and Burman 1946) to reduce the large number of trials. To study these six factors, a minimum of eight experiments are necessary. A further two experiments are added to the experimental program, one at the centre of the domain where each factor takes a middle value and the other with no surfactant added. Table III-4 shows the experimental program with the two extra trials in the last two rows (9 and 10). The importance of each factor is calculated by the sum of the cold water fluxes of each experiment taking into account the sign of the state

(State -1 or State +1). This sum is then divided by the number of experiments. The first column of the matrix consists of only +1 state so this calculation leads to the average response over the experimental domain.

Factor		State (-1)	State (+1)
Surfactant concentration (%)	X1	0.5	1.5
Washing temperature (°C)	X2	40	60
Washing time (minutes)	X3	15	45
Volume of solution (litres)	X4	5	15
Application of pressure (no units)	X5	No	Yes
Re-circulation velocity (m/s)	X6	2.7	3.6

Table III-3: Value of the washing cycle factors

Experiment number	X1	X2	X3	X4	X5	X6
1	1.5	60	45	5	Yes	2.7
2	0.5	60	45	15	No	3.6
3	0.5	40	45	15	Yes	2.7
4	1.5	40	15	15	Yes	3.6
5	0.5	60	15	5	Yes	3.6
6	1.5	40	45	5	No	3.6
7	1.5	60	15	15	No	2.7
8	0.5	40	15	5	No	2.7
9	0	60	30	10	No	3.6
10	1	50	30	10	No	3.6

Table III-4: Explicit experimental plan for washing cycle optimisation

The washing solution is prepared in a clean container where the surfactant is mixed with tap water at the correct temperature (60 or 40°C) in the required volumetric proportions (0.5 or 1.5%). The washing temperature is maintained with a thermostat. When needed to be applied, a 3.5 bar pressure is maintained for one minute prior to the last five minutes of washing. The velocity of the washing solution is controlled with a valve placed before the pump inlet; allowing variation of the velocity between 2.7 m/s and 3.6 m/s.

III.4.4.2 Washing protocol

This section describes the washing cycle protocols used to regenerate the membrane surface and to ensure that in-between sets of filtration, the surface membrane is in an identical condition each time that a filtration experiment takes place. The washing protocol has been set after an investigation carried out by (Busca, Hilal, and Atkin 2003) and similar protocol was used by (Chen, Kim, and Ting 2003) to investigate the optimisation of washing cycle. This investigation looked at six parameters that have been thought to influence the effectiveness of a washing cycle. The results of the investigation are presented in Chapter IV.

The protocol followed in this work to regenerate membrane surface is applied to both UF and NF tubular membranes in the small and large-scale units and can be described as follows. The membrane unit is fully flushed with 45°C tap water, then the process or feed tank is filled up with a surfactant solution (1% of surfactant) Surfactant SURFACT HDL manufactured by **Surfactem Ltd**: United Kingdom. Surfact HDL is a caustic, biological, heavy-duty laundry liquid containing sodium tripolyphosphate (STPP). Table III-5 recapitulates the main properties of the surfactant. This surfactant is mixed with tap water to the required concentration at 45°C. The filtration process then takes place without the application of back-pressure for at least 20 minutes. The permeate is re-circulated into the feed tank. After cleaning, the membrane unit is flushed and tap water at 45°C and is re-circulated to desorb the surfactant adsorbed at the membrane surface. Then the membrane unit is flushed with cold water to bring back the temperature of the unit to 20°C.

Appearance at 20°C	White liquid
Total solid content	35%
Total surfactants content	10%
STPP content	25%
Density at 20°C	1.24 kg/L
pH (0.5% aqueous solution)	9
Viscosity at 20°C	11000 cps

Table III-5: Surfactant properties

III.4.5 Cold water flux protocol

This paragraph describes the protocol used to measure Cold Water Flux (CWF). CWF is used to assess to what extent the membrane recovers the water flux after filtration or after the cleaning cycle. 10 litres of reverse osmosis (RO) water at 20°C are used to flush the system. The RO water has an original conductivity of 0.11 μ S, at 20°C. The RO water is filtered at 20°C and under constant conditions of pressure. The permeate is not returned to the feed tank to avoid any contamination of surfactant or permeate that may be left in the membrane unit. After having taken a series of permeate flux, (CWF) the conductivity in the process tank is checked. If it is below 10 μ S, the test is acceptable. If not, the unit is flushed again and a new CWF is measured, applying the same procedure.

III.4.6 Temperature tests

The small-scale tubular membrane unit shown in Figure III-5 and adapted as shown in Figure III-9, is used to study the effect of temperature on the ultrafiltration. An electrical resistance, controlled by a thermostat, replaces the cooling coil when experiments are carried out at higher temperatures. The membrane is cleaned after each trial. The MWF is filtered at a constant inlet pressure of 3.6 bar. Experiments are

carried out at three feed temperatures 20°C, 30°C and 45°C. Flux, permeate turbidity and TOC are reported for both FP200 and FP100 membranes.

For each temperature, two types of filtration take place. The first set of experiments is carried out at constant feed concentration and the permeate is therefore recycled into the feed tank. The second set is carried out with increasing concentration ratio in the re-circulation loop. The permeate is kept separated from the feed stream resulting in an increase in the feed stream oil concentration during the filtration process. In the second case, a process tank containing 6 litres of metalworking fluid is used, allowing a rapid enrichment of the concentrate in oil.

The filtration experiments in the concentration loop mode last 65 hours, resulting in membrane fouling. The unit is flushed with 10 litres of tap water at 45°C. Then a washing cycle takes place, followed by flushing the system again with 10 litres of tap water at 45°C. Finally, 10 litres of RO water with a conductivity of 0.11µS is flushed through the system in order to rinse and cool down the membrane unit to prepare for cold water flux measurements.

III.5 GAS INJECTION

Gas injection is used to enhance the permeate flux in membrane filtration. The technique is based on the principle of introducing turbulence within the membrane tube. Tests are performed using the small tubular unit fitted with a single tube. The circulation flux in the membrane is horizontal.

III.5.1 Experimental apparatus

A picture of the experimental apparatus is shown in Figure III-10 and a schematic diagram is shown in Figure III-11. The assembly consists of a single horizontally mounted tubular polyvinylidene fluoride membrane (FP200) as described in III.3.1, page 62. The membrane tube has a length of 0.30 m. In this configuration, the filtration surface area is 0.0117 m². The tested solution is driven from the feed tank by a pump

and circulated through the membrane module. The tests are carried out at inlet pressure of 3 bar and outlet pressure of 2.5 bar and the liquid velocity is 2.3 m/s.

When the gas is used, compressed air is injected one metre away from the membrane inlet via a T piece of 6 mm internal diameter. The airflow rate is set using the rotameter's valve. Adjusting the back-pressure valve controls the applied TMP. A clear Perspex tube, of identical internal diameter as the piping, is set between the T junction and the membrane module to give a clear view of the two phase flow. A reservoir (2 in Figure III-11) maintained at the same pressure as the membrane outlet 2.5 bar collects the mixture of gas and liquid. The volume of gas injected via the T-junction is vented from the reservoir. The difference in pressure between gas inlet and gas outlet is taken into account. When no gas is used, the TMP is set using the back-pressure valve on the membrane unit.

The permeate flow is measured using a graduated cylinder and then the permeate is returned to the feed tank to maintain the constant feed concentration. Two tanks of 15 and 25 litres respectively and open to atmospheric pressure, have been added in series after the pressurised reservoir. The liquid is pumped to the membrane module from the second tank.

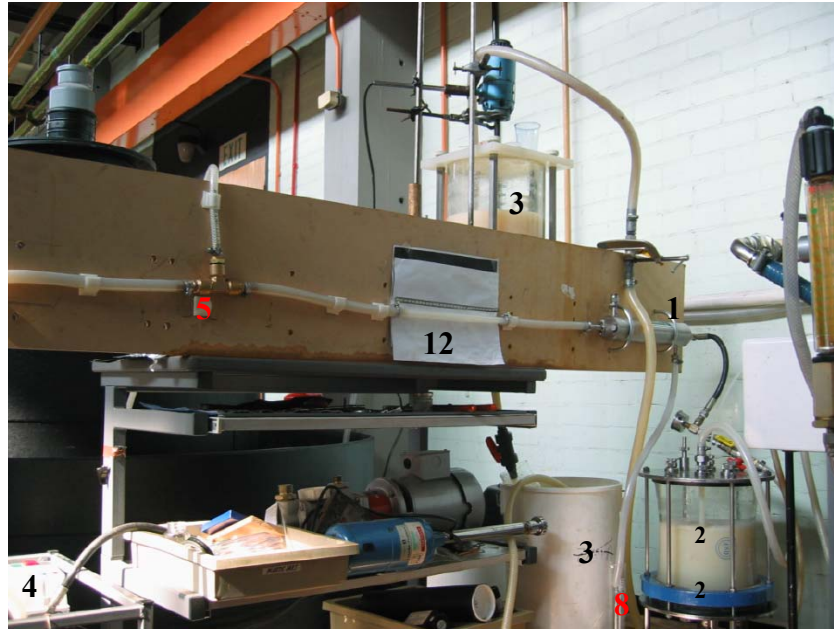


Figure III-10: Picture gas injection assembly

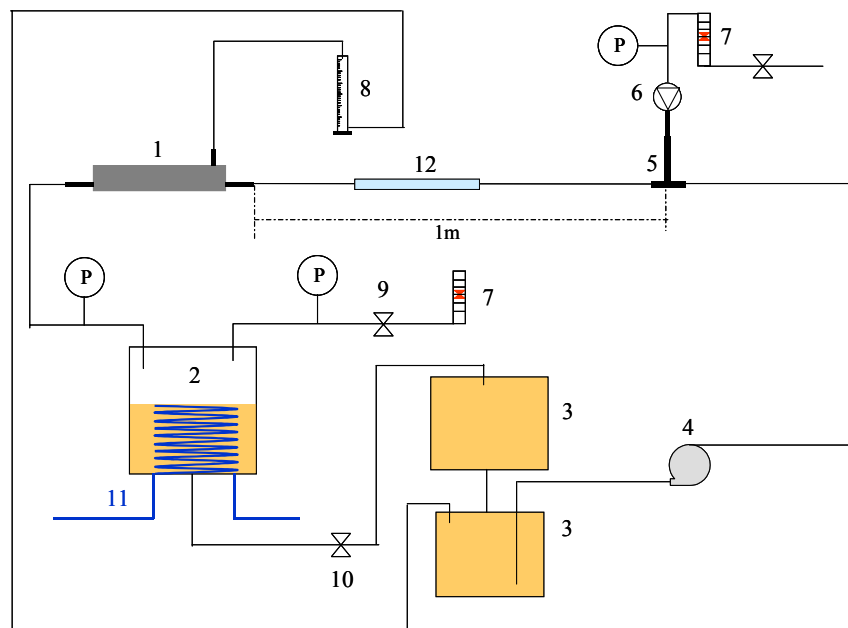


Figure III-11: Schematic diagram of gas injection assembly

1: Membrane; 2: Reservoir; 3: De-foaming Tanks; 4: Pump; 5: T-junction; 6: Solenoid Valve; 7: Air-Rotameters; 8: Graduate cylinder; 9: Gas outlet valve; 10: Back-pressure Valve; 11: Cooling System; 12: Perspex tube; P: Pressure Gauge

III.5.2 Set of experiments

The first set of experiments used demineralised water, measuring water flux when gas is injected at different flow rates. The flow pattern and shape of bubbles are observed via the clear Perspex tube. Pictures are taken using a digital camera. The second set of experiments used MWF 5%.

Between each experiment using MWF 5%, the membrane unit is flushed with tap water at 45°C and washed for 20 minutes according to the washing protocol described in Section III.4.4.2. Before starting any filtration, the membrane unit is fully flushed with tap water and a CWF is taken at 20°C with reverse osmosis water at an inlet pressure of 3 bar and outlet pressure of 2.5 bar as the experiment was run.

III.6 CHEMICAL TREATMENT

This part describes the two methods used for the chemical treatment of the emulsion. This treatment is applied to MWF 5% and to an UF concentrate at 20%.

III.6.1 Coagulation

The effluent used is MWF 5%. Four coagulants were tested: aluminium sulphate hydrate, at 98% purity $(\text{Al}_2(\text{SO}_4)_3)_x \text{H}_2\text{O}$ ($x=14\sim 18$) F.W.342.15; aluminium chloride, 98% purity AlCl_3 , F.W. 133.34; iron sulphate pentahydrate at 97% purity $\text{Fe}_2(\text{SO}_4)_3 \cdot 5\text{H}_2\text{O}$, F.W. 489.94; and iron chloride FeCl_3 at 97% purity, F.W. 162.21; all coagulants are from Sigma Aldrich Chemicals. The coagulation of the micro-emulsion produces two phases, an aqueous phase called supernatant and a coagulated oily phase floating on top of the aqueous phase.

The Critical Coagulation Concentration (ccc) is evaluated by a simple technique, which consists of a series of test tubes each of 10 ml volume where the waste coolant is prepared and an increasing quantity of coagulant is added. The content of the tube is energetically shaken and left to stand for two hours followed by gentle mixing. The mixing allows the large flocks produced in the initial coagulation phase to collect all

residual colloids. After mixing, the samples are left to stand for a further 15 minutes. The critical coagulation concentration is determined at the point where the supernatant is clear and below this point, a slightly cloudy supernatant remains. The coagulated oil and the supernatant are separated by filtration using a paper filter of 2.6 μm pore size.

III.6.2 Acidification

Sulphuric acid has been used to separate the oil from the aqueous phase of the concentrate. The sulphuric acid is from Argos Organic of a purity 97% and a density of 1.84 kg/L. It has been used to prepare a 5 normal sulphuric acid solution. This 5N solution is used in a series of acidification of concentrate MWF 20.8%.

500 ml of concentrate collected from UF filtration with an oil concentration measured at 20.8% is placed in a beaker on a magnetic stirrer and the acid is added into the beaker with a burette as the quantity of acid can be monitored. The stirring speed is set at high (300 rpm) or low (50 rpm). Five experiments were carried out:

Experiment 1: 5 Normal of acid is added ml per ml to the 500 ml of MWF 20.8%, stirring 300 rpm.

Experiment 2: 5 Normal of acid is added ml per ml to the 500 ml of MWF 20.8%, stirring 50 rpm.

Experiment 3: 10 ml of 5 normal acid is directly added to 500ml of MWF20.8%, stirring 50 rpm.

Experiment 4: 10 ml of 5 normal acid is directly added to 500ml of MWF20.8%, stirring 300 rpm.

Experiment 5: 5 Normal of acid is added ml per ml to the 500 ml of MWF 20.8%, stirring 50 rpm only 10 ml over all of acid is poured then stirring is completely stopped.

Experiment 5 bis: The aqueous phase obtained in Experiment 4 is brought back to pH 9.5 by adding potassium hydroxide (KOH) flakes.

For each experiment the pH and phase separation are measured.

Progressive addition of acid means that 1 ml of acid is added under experimental condition the pH is measure and the next ml is added when the pH is stabilised. In the case of direct addition of acid the volume of acid is poured and the evolution of the solution pH value is followed over time.

III.7 BIOREMEDIATION

This part describes the methods used to extract Indigenous Community (IC) of micro-organisms from waste metalworking fluid, how the IC is enriched to ensure good degradation of the permeate produced in the filtration stage.

III.7.1 Extraction of indigenous community

Indigenous Community is extracted from a real industrial waste metalworking fluid generated from “Mobilcut 232”.

The waste effluent is divided into 15ml centrifuge tubes and centrifuged at 4,000 tours per minute for 15 min. The supernatant oil is withdrawn with a pipette; the rest of the solution is extracted, leaving the micro-organisms at the bottom of the tube. The pellet is re-suspended with Phosphate Buffer Solution pH=7 (PBS) (15 ml added). Solutions are centrifuged for a second time in the same conditions as above. The residual supernatant oil and the PBS are discarded. The pellets are re-suspended with PBS into ten 2 ml Eppendorf tubes. Four of them are frozen at -80°C . The micro-organisms are re-suspended in 2ml of effluent for testing.

III.7.2 Flask tests

Flask tests are used to explore the feasibility of remediation of the filtered effluent by the micro-organisms collected in the waste, the indigenous community.

10 ml of pellet suspensions are added to 100 ml effluent in 250 ml conical flasks. A hydrophobic cotton plug closes the top of the flask and the flasks are shaken for 7 days at room temperature. The COD is recorded at the start, day 3, 5 and 7. At the same time the number of bacteria are counted with a haemocytometer count technique. This count will allow the determination of when the Indigenous Community (IC) starts growing exponentially and the rate of bacterial growth.

III.7.3 Continuous stirred bioreactor

The continuous stirred bioreactor is used to develop a bio consortium from the IC when working with a continuous culture. Figure III-12 shows a schematic diagram of the continuous stirred bioreactor.

III.7.3.1 Description

In practice, steady state is achieved when biomass, substrate and product concentration are constant with time. Theoretically, a chemostat will have reached steady state when the culture has undergone at least three residence time (Faibish and Cohen 2001). Once steady state has been established, step changes in dilution rate must be small otherwise, oscillation will occur. Enrichment allows the microorganisms to adapt to higher COD contents in the feeding effluent. The continuous stirred bioreactor is used to select the microorganisms that grow fast enough and use the effluent as a sole carbon source.

Nanofiltration permeate diluted at 50% with tap water (M50/50) showing a global COD of 6,000 mg/L is primarily used as a feed for the bioreactor. Then, the concentration of the feed of the bioreactor is increased until it reaches the typical NF permeate of 12,000 mg/L in COD. The pH and the COD are measured at the outlet of the stirred bioreactor.

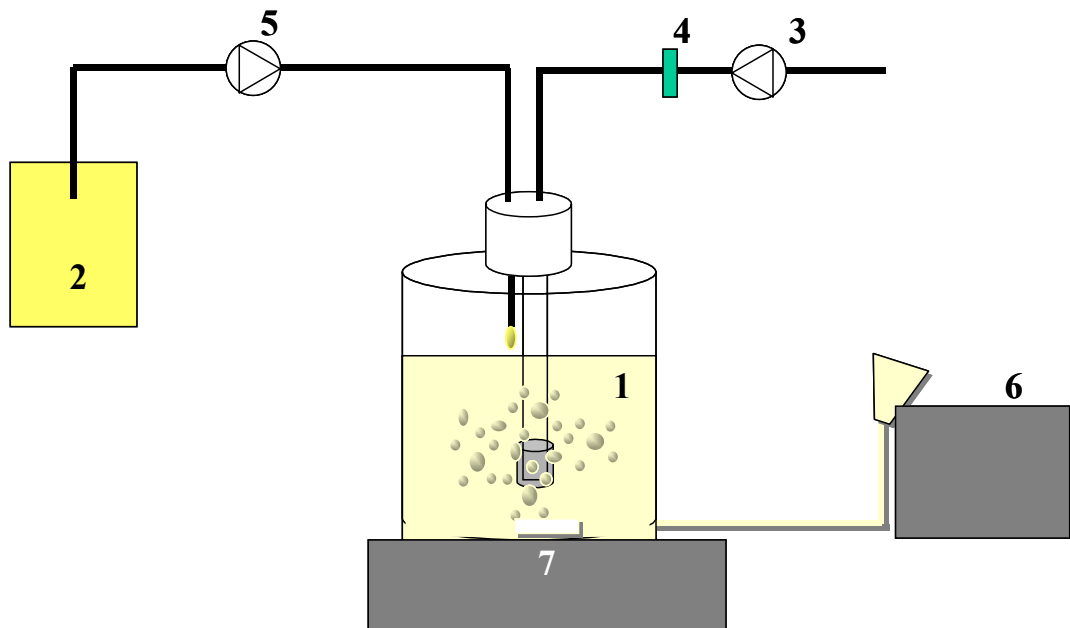


Figure III-12: Continuous stirred bioreactor

1: Bioreactor; 2: Feed tank; 3: Air pump; 4: 0.22µm filter; 5: peristaltic pump; 6 collecting tank;
7: magnetic stirrer

III.7.4 Small-scale fixed bed bioreactor

The small-scale fixed bed bioreactor is used to study the bio-consortium developed with the continuous stirred bioreactor. Figure III-13 shows a schematic diagram of the fixed bed bioreactor, including the re-circulation loop.

III.7.4.1 Description

Reactor specifications are shown in Table III-6. The bioreactor is a five litre cylinder 153 mm diameter packed with plastic pall ring from Koch-Glisch, UK. Ten stages of heighten pall rings are mounted. In order to avoid any preferential route through the packed bed, each stage is rotated in comparison to the previous one so that an upper pall ring sits onto two of the previous stage Figure III-13 shows the assembly. Air is

injected via a porous stone at a rate of 1.2 litres per minute ensuring good agitation and aeration in the bioreactor.

Reactor diameter (m)	0.153
Reactor total height (m)	0.3
Total volume (m ³)	5.515 · 10 ⁻³
Collector volume (m ³)	0.552 · 10 ⁻³
Collector effective volume (m ³) (minus air distributor volume)	0.54 · 10 ⁻³
Packing Volume (m ³)	4.596 · 10 ⁻³
Top volume (m ³)	0.367 · 10 ⁻³ (2 cm above the bed)
Void ratio (%)	77.8
Effective volume (m ³)	4.5 · 10 ⁻³
Specific surface area (m ² /m ³)	390

Table III-6: Small-bioreactor specifications

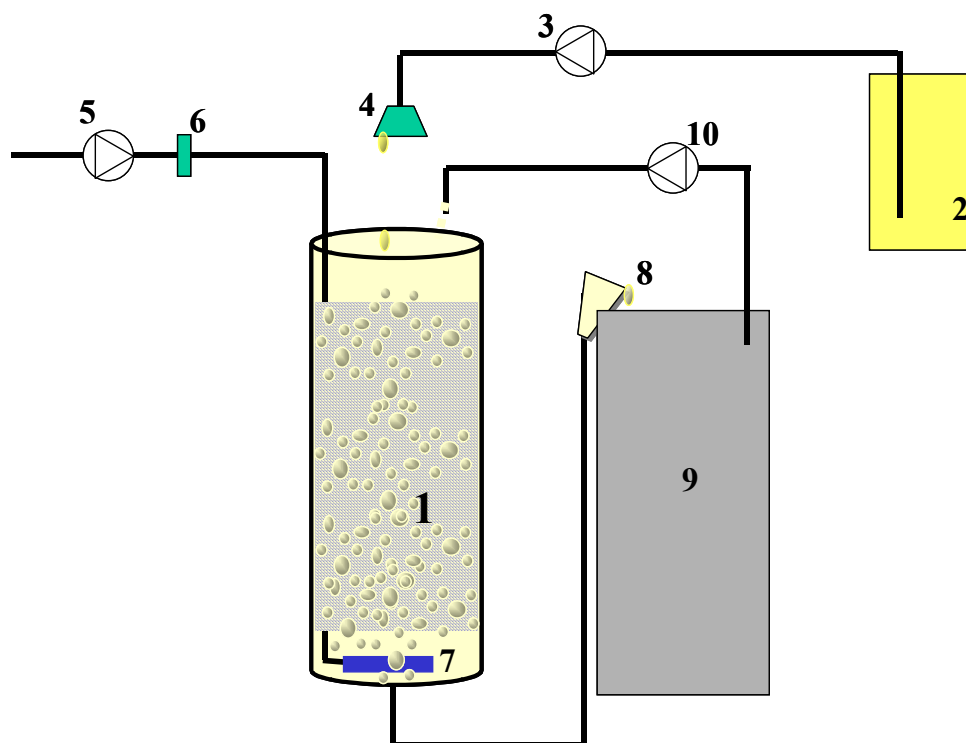


Figure III-13: Fixed bed bioreactor

1: pall ring matrix; 2: feed tank; 3: peristaltic pump; 4: liquid distributor; 5: air pump;
6: 0.22µm filter; 7: air stone; 8: effluent outlet; 9: collecting tank; 10: re-circulation pump

III.7.4.2 Bioreactor installation protocol

Three 250 ml conical flasks containing 50% NF permeate, 50% tap water and 3% Minimal medium are inoculated with the frozen bio-consortium. The prepared mix is filtered through a sterile filter 0.22 µm. The flasks are shaken (200 rpm) for three days until sufficient growth occurs. The pH of the broth is maintained above 8.5. After three days, all the flasks are split into six new flasks and the volume is brought to 150 millilitres with fresh filtered new M50/50 mix. After two days at 25°C and 200 rpm the flasks show a pH of 8.7. Substantial growth is observed in the bulk and on the wall of the flasks. The bioreactor is filled up with 4 litres of the mixture (M50/50) and the content of each flask is poured in the bioreactor. The complement of mixture is added to top up the bioreactor. Air is supplied via the air-stone, the fluid is recycled at 2.75 litres per day to ensure good mixing and the pH is measured every 12 hours to control that it is not dropping below 8.5.

III.7.4.3 Experiment

When the pH of the bioreactor reaches 8.5 and a turbid growth is observed, the continuous mode is started. A peristaltic pump feeds the bioreactor with the effluent.

Then the COD, pH, turbidity are monitored at the outlet and inlet of the bioreactor. The parameters studied are flow rate and NF permeate (effluent) COD concentration.

III.7.5 Large-scale Bioreactor

The large-scale bioreactor outlet set slightly lower than the inlet to allow a gravity feed on the outfall. The tank is partitioned across the middle to ensure that all fluids must feed in through the top, flow down through the bio decking and then back up through the bio-decking before they can escape. Table III-7 shows the data of the large-scale bioreactor.

Specific surface area		100 m ² /m ³
Number of internal mixing points		6000 / m ³
Void ratio		97%
Standard dimension ± 10 mm	Length	1160 mm
	Width	600 mm
	Height	600 mm
Material		PVC
Sheet thickness		0.7 mm
Average dry weight		30 kg

Table III-7: Bio-decking description

Sample points taps are fitted to the permeate inlet and the reactor outlet.

Permeate is pumped from the first membrane unit's permeate tank into the bioreactor via pump M5 (permeate pump start). The permeate rate can be varied via the knob adjuster between 0 and 100% of its maximum flow rate, which is 1.8 litres per minute.

Nutrients are pumped from the nutrient tank in the first membrane unit via pump M7 (nutrient pump start). Again, the rate at which the nutrient is delivered is variable (via the knob adjuster) between 0 and 100% of its maximum flow rate, which is 4 litres per hour.

Air is delivered to the bioreactor via the air regulator mounted on the first membrane unit: air pressure/volume can be adjusted via the knob on the top of the regulator. Air passes through one-way valves and into each side of the bioreactor, where the air is injected through a ceramic air stone. One air stone is installed on each side of the central partition.

III.8 ACTIVATED CARBON ADSORPTIONS

This section deals with the tests using activated carbon. Activated carbon is used to polish the effluent that leaves the bioreactor. Another test is set to try directly to remediate the NF permeate. Two types of tests have been set up. The first is batch tests allowing the assessment of the feasibility and to get information about the adsorption isotherms. The second involves continuous process in columns.

III.8.1 Activated carbon

The activated Carbon used is a grade CC65/12/40 from CPL Environment Limited, Carbon Division "Carbon Plant", is a granular activated carbon with a density of 300kg/m³. The surface area, meso- and micro- pore volumes and average pore diameter of the samples have been calculated from adsorption and desorption

isotherms. These were obtained by measuring the volume of N₂ adsorbed on and desorbed from the samples over a range of pre-selected pressures from near-vacuum to ca. atmospheric pressure at a temperature of 77K using an ASAP 2010 unit. The pressure was increased incrementally to produce the adsorption isotherm, and then reduced incrementally to obtain the desorption isotherm (Perry, 2003). The value for the surface area was obtained using the multi-point BET (Brunauer, Emmett and Teller) equation, and used points obtained within the relative pressure range 0.05-0.35. The BET surface measured was 846m²/g. The full report of the measurement is shown in Appendix E.

III.8.2 Batch test

Three series of batch tests are carried out, one with the effluent collected from the bioreactor not filtrated with microorganisms and the second one with the same effluent but microfiltrated at 0.45µm and a third one with nanofiltration permeate. Five flasks are prepared with 0.5 grams of activated carbon and 100 ml of effluent at different concentrations. This procedure is done separately for each type of the effluents described above. Different concentrations are obtained by dilution of the effluent with RO water. The concentrations are 100% pure effluent, 75% (75 ml of effluent and 25 ml of RO water), 50%, 25% and 10%. The flasks are closed to avoid any evaporation. They are stirred at 20°C ±1°C for 72 hours to ensure that equilibrium is reached. After 72 hours, the samples are centrifuged for 10 min at 6000 rpm. Then the supernatant is collected and COD measured.

III.8.3 Columns

Three columns are assembled in parallel. Each is 0.935 meter long and 3 cm of inner diameter containing 212 grams of activated carbon. They are fed separately in three different ways:

- ❖ The first column is fed with bio-permeate that has been microfiltered at $0.45\mu\text{m}$ beforehand via a small cross membrane unit specially designed to ensure a constant feed to the column.
- ❖ The second column is fed directly with the bio-permeate containing residual microorganisms.
- ❖ The third column is fed with the NF permeate from the AFC30 filtration of the MWF 5% pre-treated with UF FP100.

All columns have an identical supply rate of 0.7 litres per day. The samples are collected daily from the bottom of the column and analysed.

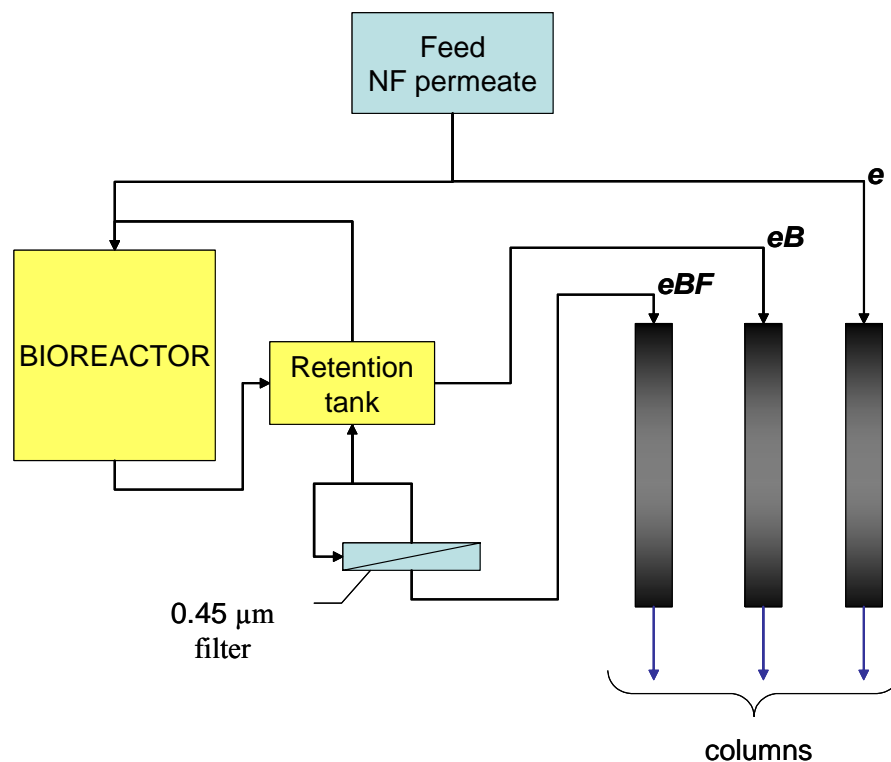


Figure III-14: Activated carbon column set-up

Figure III-14 shows the activated carbon set-up used to compare the efficiency of activated carbon using the three effluents described.

III.9 ATOMIC FORCE MICROSCOPE (AFM)

Atomic force microscopy allows the imaging of conductive and non-conductive surfaces, with very little sample preparation in air and in liquid environments. This technique is found very useful to study the structure of membrane surfaces. A number of imaging modes may be used to generate an image using an AFM. These modes are reviewed in Chapter II.

III.9.1 Equipment

The AFM used is an Explorer (TMX 2000), a commercial device from Veeco Instruments (USA). Silicon cantilevers (Ultralevers, Park Scientific Instruments) with a high aspect ratio tip of typical radius and curvature of 10 nm have been used to produce the membrane surface images. The only preparation required is to solidly attach the membrane to a steel disc with double-sided scotch tape without any alteration to membrane surface properties. For the analysis of surface pore characteristics, the integrated software of the AFM image processing is used.

III.9.2 Sample preparation

The membrane samples are placed in 500 ml of RO water for 20 minutes in order to clear them of any preservative substances. This procedure is repeated three times.

Then the sample is stuck to a metallic chip that can be magnetically held on the AFM sample holder. For the tubular membranes, two techniques can be used. The active layer can be peeled off and fixed on the double-sided scotch tape. Alternatively, as shown in Figure III-15, it can be cut longitudinally, fixed directly on the metallic chip and orientated parallel to the cantilever the scan then takes place at the edge of the tube with a scan orientation of 90°. To eliminate the effect of the curvature on the membrane image, a second order levelling along the Y axis is applied.

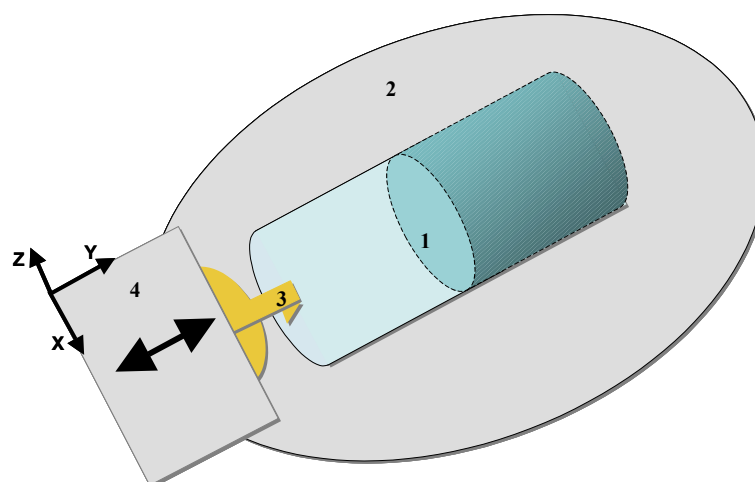


Figure III-15: Sample holding technique

1: tubular membrane cut longitudinally; 2: metallic chip; 3: cantilever; 4: scanner;
 ←→ scanning motion

III.9.3 Scan mode

Profile mode is used, allowing an image to be generated using the feed back Z-height at each data point to establish a topographic profile of the sample surface. Table III-8 shows the scanning parameters used to produce the images. These parameters have been optimised experimentally.

Set point	0 nA
Z-pullout	1 μm
Tip approach speed	10 $\mu\text{m/s}$
Pullout speed	250 $\mu\text{m/s}$
Scan frequency	1Hz

Table III-8: Optimised scanning parameters

III.9.4 Surface analysis

Imaging the surface of membranes enables the determination of surface characteristics and membrane properties such as surface roughness, ratio geometric surface versus total surface, pore size distribution and pore geometry. The value of the projected area is the X scan range multiplied by the Y scan range. The measures and calculations are generated through the AFM software.

III.9.4.1 Geometry

The value of the surface area is calculated including the height (Z Data). It is calculated using the height (Z_1 , Z_2 , Z_3 and Z_4) of every four adjacent pixels. The surface of the rectangle described as Z_1 , Z_2 , Z_3 and Z_4 is computed by dissecting the rectangle into triangles and then computing the area of each triangle.

Then the surface of a single triangle is calculated as:

$$S = \sqrt{p(p-a)(p-b)(p-c)} \quad \text{Where } p = \frac{1}{2}(a+b+c) \quad \text{Equation III-1}$$

Where:

$$a = \sqrt{(\Delta x)^2 + (\Delta Z_{12})^2} \quad \text{Where } \Delta Z_{12} = Z_1 - Z_2$$

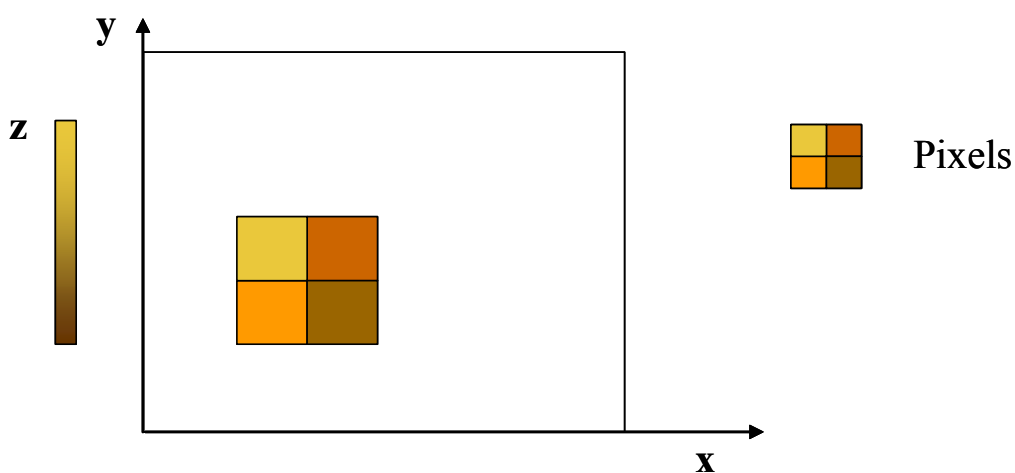
$$b = \sqrt{(\Delta y)^2 + (\Delta Z_{24})^2} \quad \text{Where } \Delta Z_{24} = Z_2 - Z_4$$

$$c = \sqrt{(\Delta z)^2 + (\Delta Z_{14})^2} \quad \text{Where } \Delta Z_{14} = Z_1 - Z_4$$

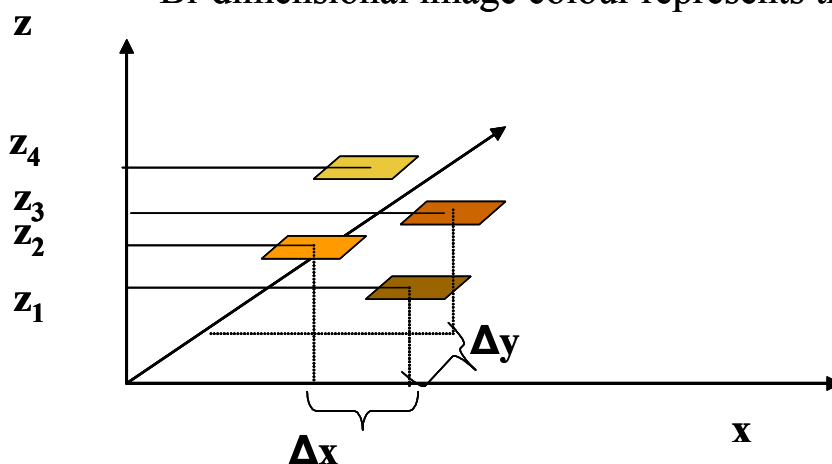
Where Δx , Δy and Δz are the steps made in the x,y and z directions respectively for each triangle defined.

This calculation is applied to all the surface in order to get the total surface area including the Z variations. Therefore, the ratio of the projected area on top of the surface area gives a good indication of the sample's surface area deviation to the geometric flat surface.

Peak and valley spacing measurements give the mean value of spacing between a peak and a valley consecutively. For the calculation, peak spacing is defined as the spacing between neighbouring peaks is set at zero nm. Any peak is taken into account by setting minimum peak height at zero nm. The calculation is done for each 10 lines across the picture that counts 300 lines.



Bi-dimensional image colour represents the high z



Tri-dimensional image the pixels are projected on axis z

Figure III-16: Projection of the areas defined by 4 consecutive pixels

III.9.4.2 Roughness:

The area RMS –root-mean-square roughness is defined as the square root of the mean value of the squares of the distance of the point from the image mean value over each data point.

$$RMS = \sqrt{\frac{1}{N} \sum_{i=1}^N \langle Z_i - Z \rangle^2} \quad \text{Equation III-2}$$

Average height give the arithmetic mean, defined as:

$$|Z| = \frac{1}{N} \sum_{i=1}^N Z_i \quad \text{Equation III-3}$$

III.10 ANALYSIS

Analyses are carried out in order to assess the performance of each component of the system and the system as a whole.

III.10.1 Measurement of Total Organic Carbon

Total Organic Carbon (TOC) and pH are used to characterise both the permeate of membrane filtration and the supernatant streams from coagulation. TOC is measured using a UIC Carbon Coulometer by combusting 20 µl of solution in an oven at 950 °C in a saturated oxygen environment. The CO₂ produced by the combustion is collected after filtration and quantified by coulometric analysis. In the reactor vessel, the carbon dioxide reacts with ethanolamine to form hydroxyethylcarbamic acid. A current is applied to the reactor vessel to regenerate the ethanolamine and the current is measured. This measurement can be recalculated to indicate the number of carbon dioxide molecules that is reacted.

III.10.2 Chemical Oxygen Demand

The Chemical oxygen demand (COD) test is a fundamental test for assessing the quality of effluents and waste water prior to discharge. It predicts the oxygen requirement of the effluent and is used for assessing treatment plant performance. The COD is measured using premixed preparation from Palintest Ltd. In this test, the sample is oxidised by digesting in a sealed reaction tube with sulphuric acid and potassium dichromate in the presence of silver sulphate catalyst. The amount of dichromate reduced is proportional to the COD. The transmittance of the sample is measured against a reagent blank prepared in the same condition as the sample but with distilled water. The blank gives 100% transmittance.

The COD after filtration depends principally upon MWF used and its concentration in the emulsion.

III.10.3 Measurement of pH, Conductivity and Turbidity

A Mettler Toledo Inlab 420 probe, suitable for use in oil and colloidal solutions, is used to measure the pH of all solutions e.g. Waste MWF, permeates and concentrate as well as bio-permeate and is used to follow the pH evolution during chemical tests acidification and coagulation.

The conductivity is measured using a conductivity meter RS 180-7127.

The turbidity is measured with the Hach Model 2100An Laboratory Turbidimeter. Turbidity is reported in Nephelometric Turbidity Units (NTU) and the turbid meter is calibrated using formazine standards.

III.10.4 Calorific Values

The calorific value of the floating oil obtained after coagulation of the micro-emulsion is measured using a Perfect Calorimetry C5000 Control from IKA.

For the coagulation experiments that use metallic (Al^{3+} and Fe^{3+}) coagulants, the following procedure is applied. The oil is collected on a paper filter, placed in a Petri dish and then placed in an oven at 80°C for 48 hours for drying before the measurement of its calorific value is taken. Two measurements are taken for each determination and reproducibility of the data is very good.

In the case of acidification, regarding that clear oil is recovered, no drying is included in the procedure. Nevertheless, a gel is recovered in some cases and its calorific value is measured by adding a standard tablet of benzoic acid used to ignite the gel. This tablet produces a known quantity of energy withdrawn from the total amount measured.

III.10.5 Ash content

Ashes are produced from oil that has been recovered in the acidification process.

III.10.5.1 Producing the ashes

The sample is weighed into a dish and organic matter is combusted. The dish containing the residue is cooled in a desiccator and the amount of total ash determined by weighing. Platinum dishes are used as it is widely used crucible material. Platinum has a high melting point (1773°C), good heat conductivity and high chemical inertness.

Procedure is done as follows. A sample of approximately 2-3 grams of oil is taken and weighed exactly in a crucible. This sample stands in an oven at 850°C for 5 hours. After 5 hours, the oven is turned off and the dishes are left to cool down. Then they are weighed, the difference between the weight before and after combustion give the mass of ashes collected. This procedure is repeated 20 times in order to collect enough ashes to analyse. The weight of ashes can be related then to the quantity of oil burned.

III.10.5.2 Ash analyses

The ashes collected are transferred to a ceramic crucible and dissolved with HF/HNO₃/HCl cocktail in a microwave then boric acid solution is added and mixture microwaved again. The resultant is brought to 100 ml volumetric flask. Metal analysis is then carried out by ICP.

The results are given in gram per litre in the 100 ml solution that can be easily related to the quantity of ashes and therefore to the quantity of oil.

CHAPTER III EXPERIMENTAL EQUIPMENT AND PROCEDURES	57
III.1 INTRODUCTION	57
III.2 WASTE PREPARATION AND CHARACTERISATION	58
III.2.1 The oil: Mobilcut 232	58
III.2.2 Waste simulation and metalworking fluid preparation	59
III.2.3 Waste characterisation	60
III.3 MEMBRANES	62
III.3.1 Ultrafiltration membranes	62
III.3.2 Nanofiltration membranes	63
III.4 FILTRATIONS	63
III.4.1 Small-scale filtration units	63
III.4.1.1 Dead-end filtration cell	64
III.4.1.2 Flat sheet unit	65
III.4.1.3 Cross flow small-scale unit	66
III.4.2 Cross flow large-scale equipment	67
III.4.2.1 Membrane filtration module	67
III.4.2.2 Power	67
III.4.2.3 Waste Coolant tank	67
III.4.2.4 Description of the filtration units	68
III.4.2.5 Filtration operation	71
III.4.2.6 Flushing operation	73
III.4.3 Filtration protocol	74
III.4.4 Washing cycles	74
III.4.4.1 Optimisation of washing cycles	75
III.4.4.2 Washing protocol	77
III.4.5 Cold water flux protocol	78
III.4.6 Temperature tests	78
III.5 GAS INJECTION	79
III.5.1 Experimental apparatus	79
III.5.2 Set of experiments	82
III.6 CHEMICAL TREATMENT	82
III.6.1 Coagulation	82
III.6.2 Acidification	83
III.7 BIOREMEDIATION	84
III.7.1 Extraction of indigenous community	84
III.7.2 Flask tests	84
III.7.3 Continuous stirred bioreactor	85
III.7.3.1 Description	85
III.7.4 Small-scale fixed bed bioreactor	86
III.7.4.1 Description	86
III.7.4.2 Bioreactor installation protocol	88
III.7.4.3 Experiment	89
III.7.5 Large-scale Bioreactor	89
III.8 ACTIVATED CARBON ADSORPTIONS	90
III.8.1 Activated carbon	90
III.8.2 Batch test	91
III.8.3 Columns	91
III.9 ATOMIC FORCE MICROSCOPE (AFM)	93
III.9.1 Equipment	93
III.9.2 Sample preparation	93

III.9.3	Scan mode	94
III.9.4	Surface analysis	95
III.9.4.1	Geometry	95
III.9.4.2	Roughness:	97
III.10	ANALYSIS	97
III.10.1	Measurement of Total Organic Carbon	97
III.10.2	Chemical Oxygen Demand	98
III.10.3	Measurement of pH, Conductivity and Turbidity	98
III.10.4	Calorific Values	98
III.10.5	Ash content	99
III.10.5.1	Producing the ashes	99
III.10.5.2	Ash analyses	100

CHAPTER III

Figure III-1:	Mixing unit	60
Figure III-2:	Abacus for oil concentration in water applicable for Mobilcut 232	61
Figure III-3:	Dead-end filtration cells	64
Figure III-4:	Small scale UF flat sheet unit	65
Figure III-5:	Small-scale tubular membrane unit	66
Figure III-6:	Side view of the first membrane unit	69
Figure III-7:	Top view of the filtration unit 1	69
Figure III-8:	Filtration unit 2	70
Figure III-9:	Experimental set up used for washing cycle and temperature test	75
Figure III-10:	Picture gas injection assembly	81
Figure III-11:	Schematic diagram of gas injection assembly	81
Figure III-12:	Continuous stirred bioreactor	86
Figure III-13:	Fixed bed bioreactor	88
Figure III-14:	Activated carbon column set-up	92
Figure III-15:	Sample holding technique	94

CHAPTER III

Table III-1:	Steel utilisation of Mobilcut 232	58
Table III-2:	Alloy utilisation of Mobilcut 232	59
Table III-3:	Value of the washing cycle factors	76
Table III-4:	Explicit experimental plan for washing cycle optimisation	76
Table III-5:	Surfactant properties	78
Table III-6:	Small-bioreactor specifications	87
Table III-7:	Bio-decking description	89

Table III-8: Optimised scanning parameters

94

CHAPTER IV

ATOMIC FORCE MICROSCOPY

CHAPTER IV

Atomic Force Microscopy

IV.1 INTRODUCTION

This Chapter presents the result obtained using the atomic force microscope to characterise membrane surfaces.

The results present the images and pores size distribution of the nanofiltration membrane used during the work these results were partially presented in

IV.2 NANOFILTRATION MEMBRANE IMAGES

Figure IV-1 to Figure IV-4 show the atomic force microscope images of the nanofiltration membrane surface used in the treatment of metalworking fluids. AFC30 was used with the large-scale equipment, filtration are studied in chapter VI section VI-4. MB05-D and MB20-D membranes were used with the dead-end filtration unit to polish the aqueous phase obtained from chemical treatment of semi-synthetic metalworking fluids the filtration are presented in Chapter VI Section VI-2.1.1.

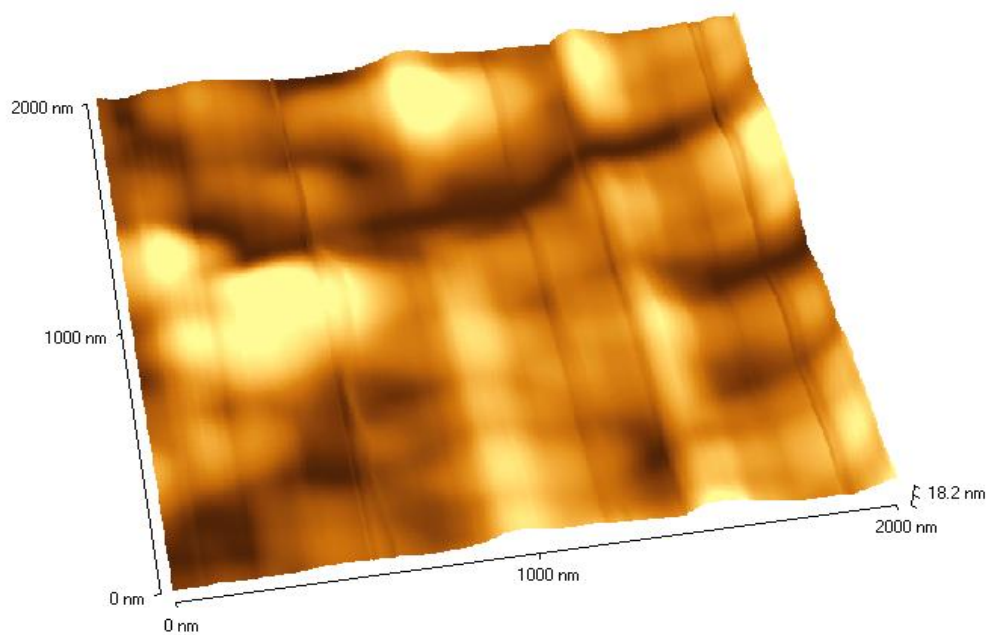


Figure IV-1: AFM imaging for AFC30 membrane large size ($2\mu\text{m} * 2\mu\text{m}$)

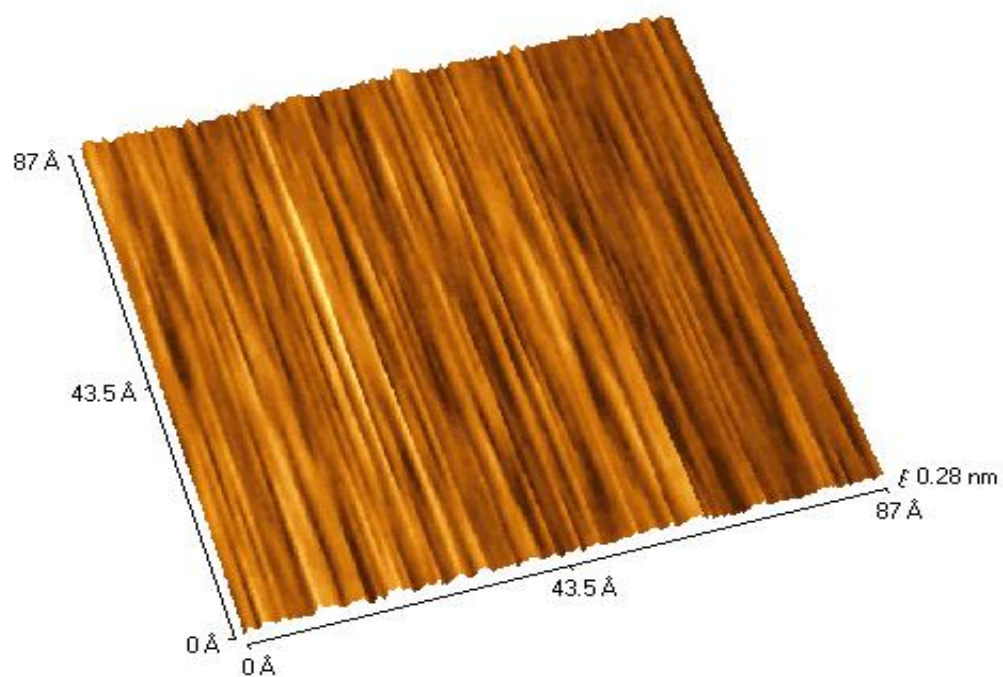


Figure IV-2: AFM imaging of AFC30 membrane at nanometric scale.

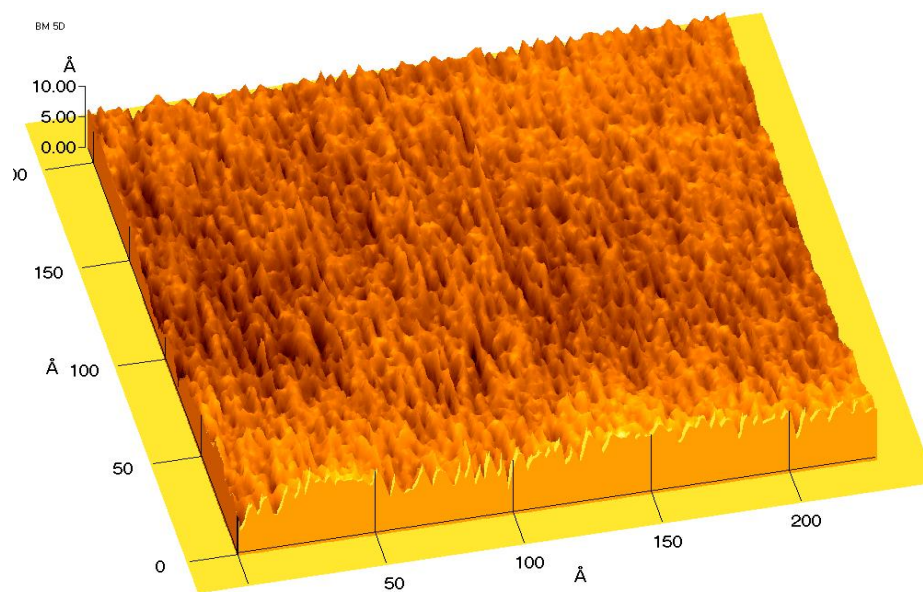


Figure IV-3: Three dimensional AFM image for BM05-D with small size surface image.

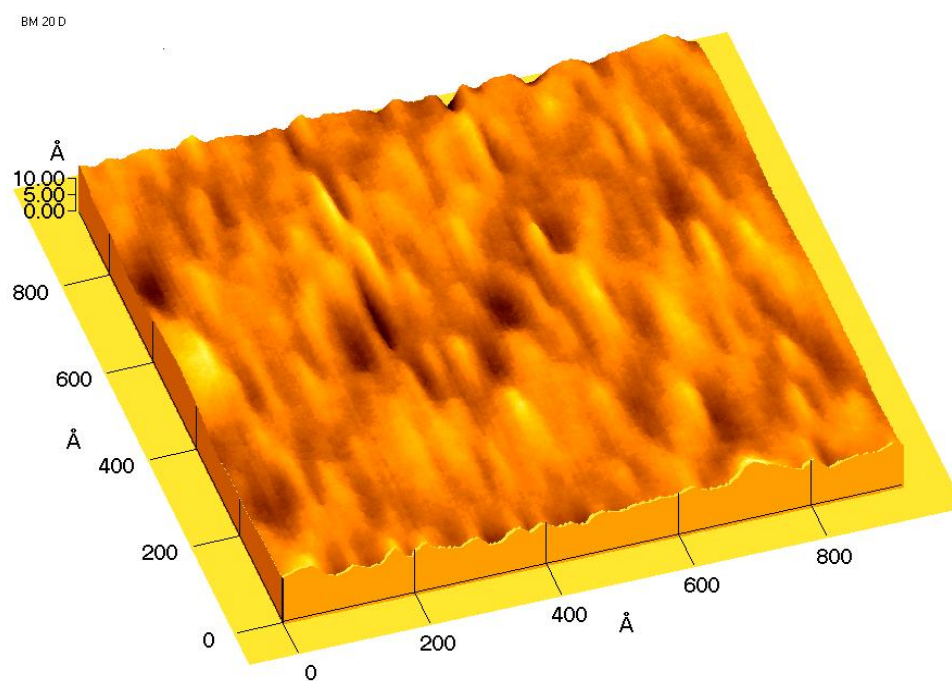


Figure IV-4 Three dimensional AFM image for BM20-D with small size surface image.

IV.3 DETERMINATION OF PORE SIZE DISTRIBUTION.

Pore size and size distributions of each membrane, which are shown in Figures IV-1 to Figure IV-2, have been determined using line analysis software. Figure IV-8 illustrates the principle of the measure. The pore size distribution identifies the pore size width of the membrane. Fifty to one hundred pores were measured for each membrane. In order to represent the pore size of all membranes with the suitable fitted equation, lognormal distributions have been chosen for fitting the data. This was found to give a good fitting to the pore size distribution data. The lognormal distribution shown in Equation IV-1 was represented by the percentage frequencies f .

$$f = f_{\max} \exp[-0.5(\ln(d_p/a) / \sigma)^2] \quad \text{Equation IV-1}$$

where f is the percentage of pore density, f_{\max} is the maximum of f , d_p is a pore diameter, a is the mean value of the pore diameters that makes f_{\max} maximum (most probable d_p), and σ is the standard deviation or width of the distribution.

Figure IV-5, Figure IV-6 and Figure IV-7 present the pore size distribution of the three nanofiltration membranes each fitted with Equation IV-1. A good fitting was obtained. The diameters μ obtained by the fitting Equation IV-1 is very close to the mean diameter obtained by AFM while the values of σ represent the width of the pore size of the membranes.

Membrane	R-value	f_{\max}	a (nm)	σ (nm)
AFC30	0.961	17.25 ± 1.16	0.551 ± 0.012	0.224 ± 0.023
BM05/D	0.904	33.92 ± 5.45	1.09 ± 0.029	0.140 ± 0.026
BM20/D	0.978	28.56 ± 2.17	4.15 ± 0.120	0.298 ± 0.030

Table IV-1: Constants obtained from fitted curves lognormal distributions

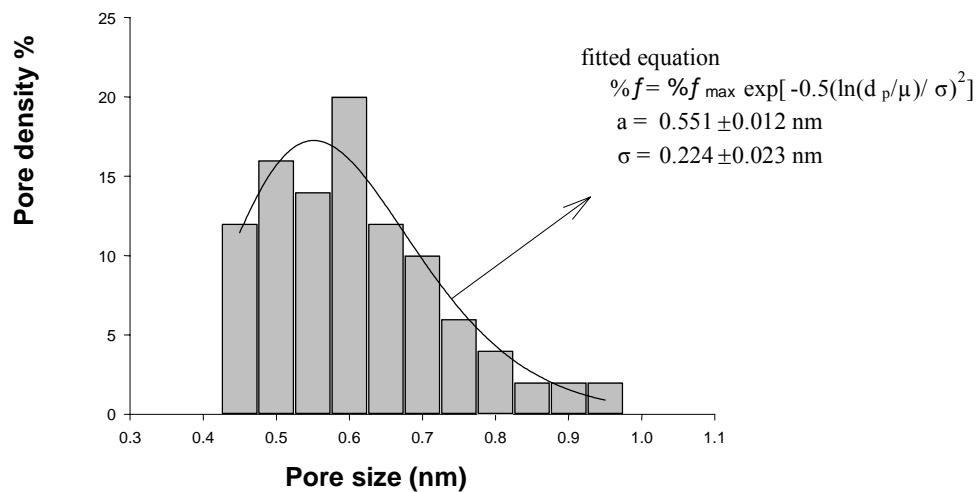


Figure IV-5: Pore size distribution of AFC30 with fitted equation

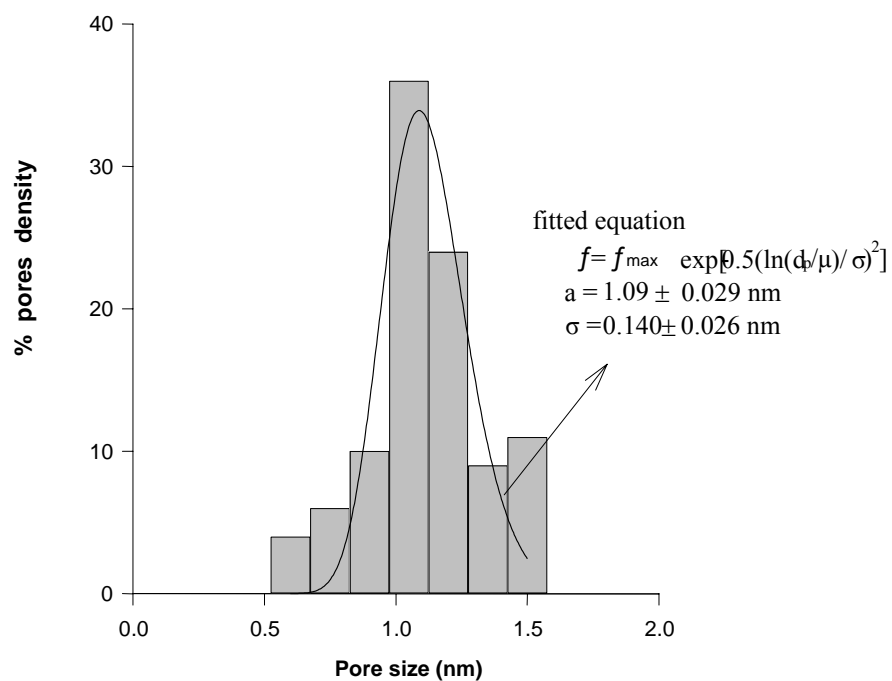


Figure IV-6: pore size distribution of BM05-D membrane with the fitted equation

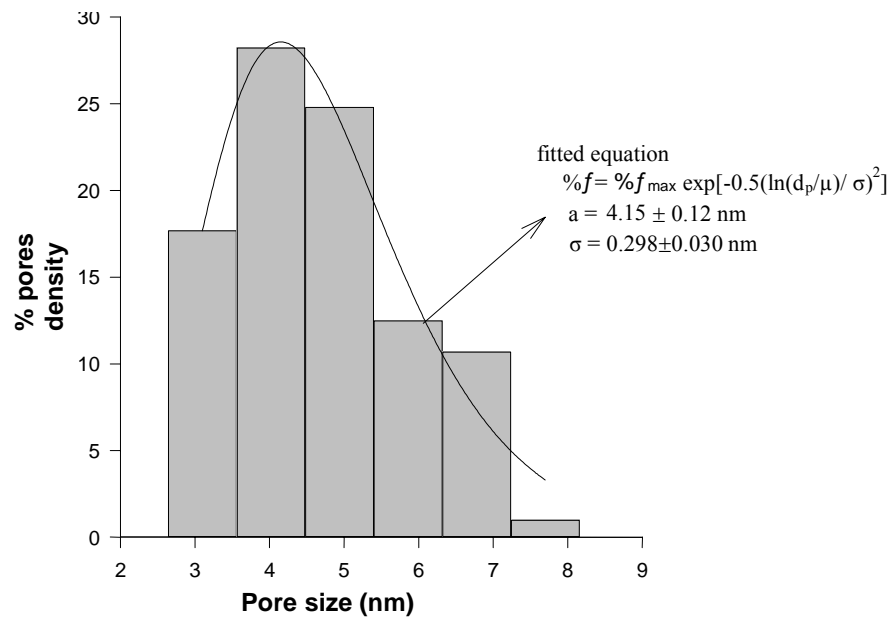
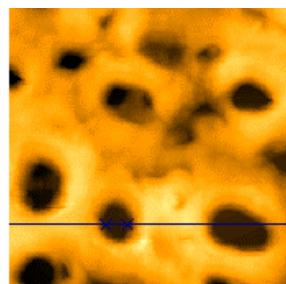


Figure IV-7: Pore size distribution of MB20-D with fitted equation



	X(nm)	Y(nm)	Z(nm)
Point1:	1196.5	2697.6	82.2
Point2:	1475.0	2697.6	85.6
Diff:	278.4	0.0	3.4
Length:	278.458 nm		
Pt Angle:	0.70°		

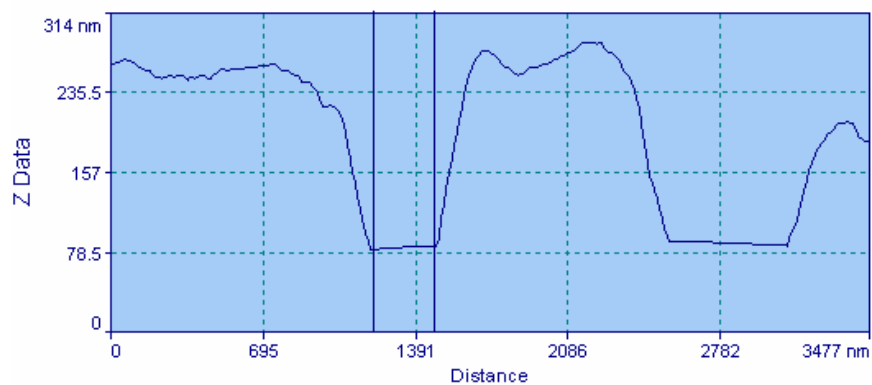


Figure IV-8: Example of line measurement for AFM pore size determination

CHAPTER IV Atomic Force Microscopy 102

IV.1	Introduction.....	102
IV.2	Nanofiltration membrane images.....	102
IV.3	Determination of pore size distribution.....	105

CHAPTER IV

Figure IV-1:	AFM imaging for AFC30 membrane large size (2 μ m *2 μ m).....	103
Figure IV-2:	AFM imaging of AFC30 membrane at nanometric scale.....	103
Figure IV-3:	Three dimensional AFM image for BM05-D with small size surface image.....	104
Figure IV-4:	Three dimensional AFM image for BM20-D with small size surface image.....	104
Figure IV-5:	Pore size distribution of AFC30 with fitted equation.....	106
Figure IV-6:	pore size distribution of BM05-D membrane with the fitted equation..	106
Figure IV-7:	Pore size distribution of MB20-D with fitted.....	107

CHAPTER IV

Table IV-1:	Constants obtained from fitted curves lognormal distributions	105
--------------------	--	------------

CHAPTER V

Waste Characterisation,

Chemical Treatment and Fuel

CHAPTER V

Waste Characterisation, Chemical Treatment and Fuel

V.1 INTRODUCTION

This chapter presents the results of the experiments that have been carried out to assess the feasibility of processes involved in the final design. The first part of this chapter presents the characterisation of the original microemulsion. The second part presents the results on chemical treatments. Two chemical treatments were studied inorganic salt flocculation and acidification. This part also discusses the application of chemical treatment of the concentrate generated during the filtration process and its benefits.

V.2 FLUID CHARACTERISATION

The fluid used is Mobilcut 232 as described in Chapter III, its data sheet is given in Appendix I. This fluid is emulsifiable oil that forms a microemulsion when it is mixed with water. This part gives more details than what can be found on the data sheet and is an essential step towards the understanding of the waste that is going to be treated.

V.2.1 Characterisation of the concentrate

Figure V-1 shows the linear relationship between Total Organic Carbon (TOC) measured in the concentrate effluent and the reading given by refractometry. The data obtained here fit a straight line of $y(\text{TOC}) = 7860.4x(\text{oil}\%)$ with a r^2 of 0.9896. It can be seen that the TOC is proportional to the amount of oil measured by refractometry. Therefore, the refractometry method was used in this work to establish the TOC of the waste effluent and of the concentrate obtained during filtration processes.

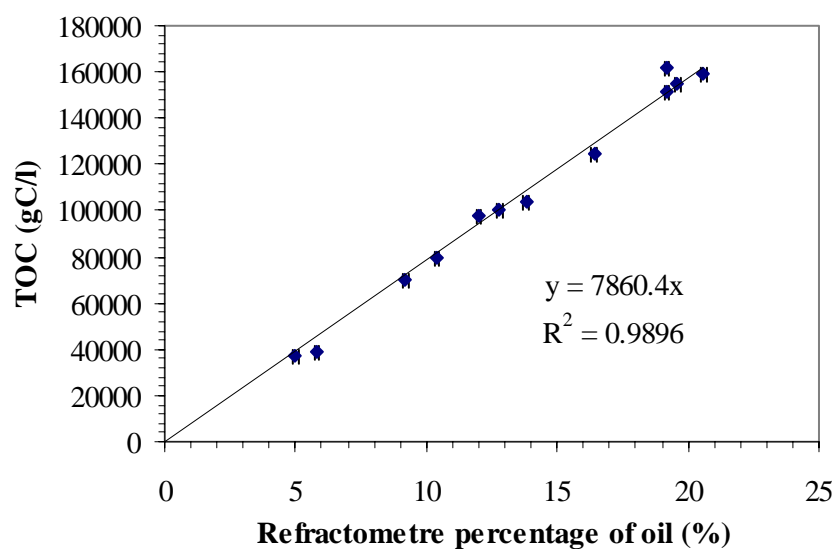


Figure V-1: Relationship between refractometry method and concentrate TOC measurements

V.2.2 Zeta potential measurement

The zeta potential measures the magnitude of repulsion or attraction between particles. Its measurement is the key to electrostatic dispersion control. Figure V-1 and Table V-1 show the results obtained after four measurements.

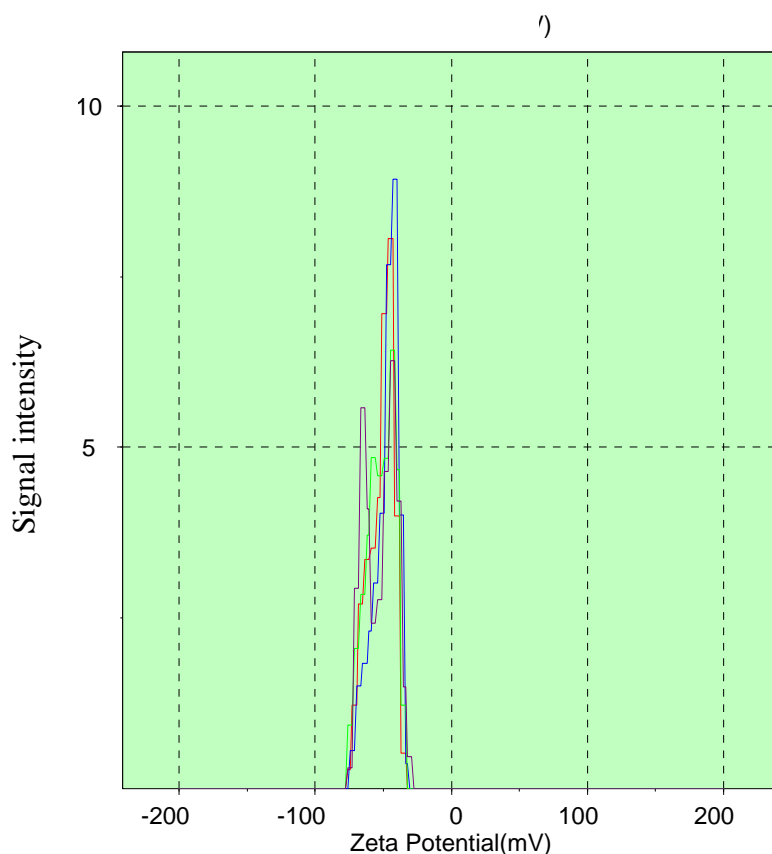


Figure V-2: Microemulsion zeta potential

Run n ^o	Mobility $\mu\text{mcm/Vs}$	Zeta potential mV	Width
1	-4.101	-51.7	5.9
2	-3.835	-48.4	5.7
3	-4.087	-51.6	7.9
4	-4.283	-54.0	9.5
Average	-4.076	-51.4	7.2
+/-	0.184	2.3	1.8

Table V-1: Results from the 4 measurements of the zeta potential of Mobilcut 232 at 5%

The zeta potential of the microemulsion droplet is -51.4 mV on average. This value is characteristic for a stable emulsion. Emulsions stabilised by electrostatic charges are considered to be stable when the absolute value of their zeta potential is over 30 mV. The charges supported by the droplet are negative and therefore positively charged molecules or ions can easily be adsorbed onto the droplets surface and induce destabilisation of the microemulsion by reducing the electrostatic repulsion forces between oil droplets.

V.2.3 Droplets size distribution

Particle size measurements are estimated by Photon Correlation spectroscopy (PCS). The PCS technique rely on the measurement of the movement of particles undergoing Brownian motion. Semi-synthetic oil Mobil cut 232 is mixed with tap water at 5% in oil to produce a micro-emulsion of oil in water. As dilutant, ultrafiltration permeate was proposed. The permeate is obtained after filtration on FP 100 (MWCO of 100,000 kD) was diluted 4 times and filtered again with a Millipore filter 0.025 μ m to avoid any dust contamination.

The size measurement of the oil droplets was duplicated. The sample of oil microemulsion needed to be diluted. The chosen dilutant was demineralised water and in the second case, clear UF permeate, filtered at 0.22 μ m just before use and diluted with RO water until the count rate on the dilutant is below 3000 counts per second as advised by Malvern Instrument. The second dilutant was chosen in order to make sure that there was no significant influence on the distribution size when diluting the micro emulsion with RO water.

Table V-2 presents the refractive index measure of the raw oil and dispersing medium, the refractive indices are entered in the software to calculate the oil size distribution.

	% of UF permeate	Refractive index
RO + UF Permeate	0%	1.332(0)
	33%	1.334(0)
	50%	1.334(2)
	66%	1.334(6)
	100%	1.334(9)
Oil	#	1.476(5)
	#	1.476(3)

Table V-2: Refractive index

The three first size measurements are presented respectively in Figure V-3, Figure V-4 and Table V-5, the numerical results reported respectively in Table V-3, Table V-4 and Table V-5, have been carried out using RO water at different dilutions. Figure V-3 shows the results obtained when a count rate of 50 kCps (kilo count per second) is used. The red and blue curves are of the same sample measured at 5-minute intervals. As indicated in Table V-3, two distinct droplet sizes are found respectively at 476 and 670 nm. It can be seen that after 5 minutes, the size of droplet increases and the width measurement increases, indicating an aggregation of the oil droplet. It can be concluded that diluting the emulsion in RO water has an effect on the oil droplet size distribution. This can be explained by the fact that the ionic strength of the solution is changed and that the concentration in the surfactant is considerably diminished, leading to an aggregation of the oil droplets. Nevertheless, to measure a size distribution, the 5% emulsion has to be diluted. In that particular case, Malvern indicated that it is possible to make the measurement by changing the ionic strength of the dilutant phase by adding some salts. However, the addition of salt may also interfere with the droplet size and the increase in ionic strength may not overcome the problem of surfactant dilution.

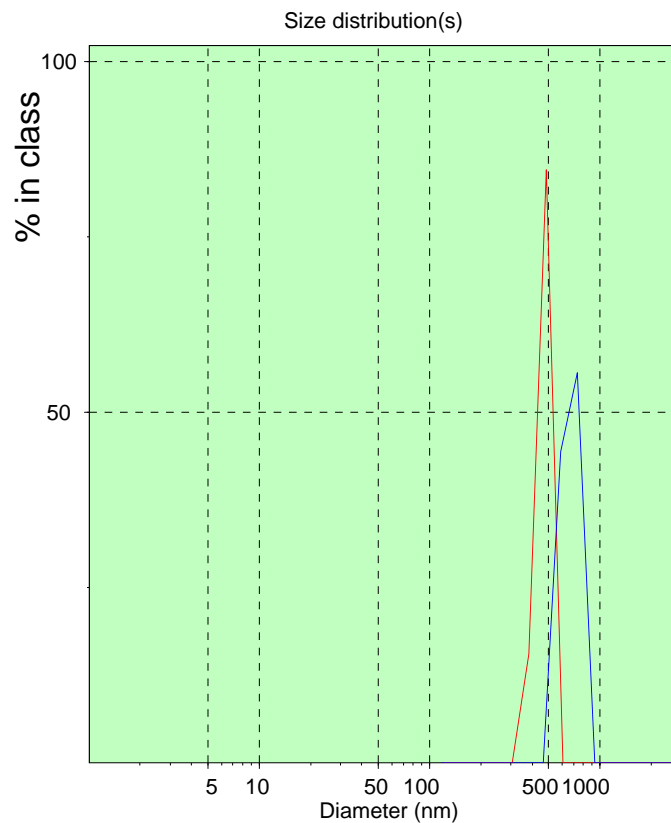


Figure V-3: Measurement of oil droplet using RO water at low count rate

Peak Analysis by intensity			
Peak	Area (%)	Mean (nm)	Width (nm)
1	100.0	467.6	123.3
2	100.0	670.4	292.4

Table V-3: Droplet size analysis

Figure V-4 shows measurements obtained when the count rate is over 250kCps in the range recommended by Malvern. In this case, the size between the two measurements does not vary as much as previously. However, the width of the peak changes and this indicates that the droplet size change, probably slower than in the first case.

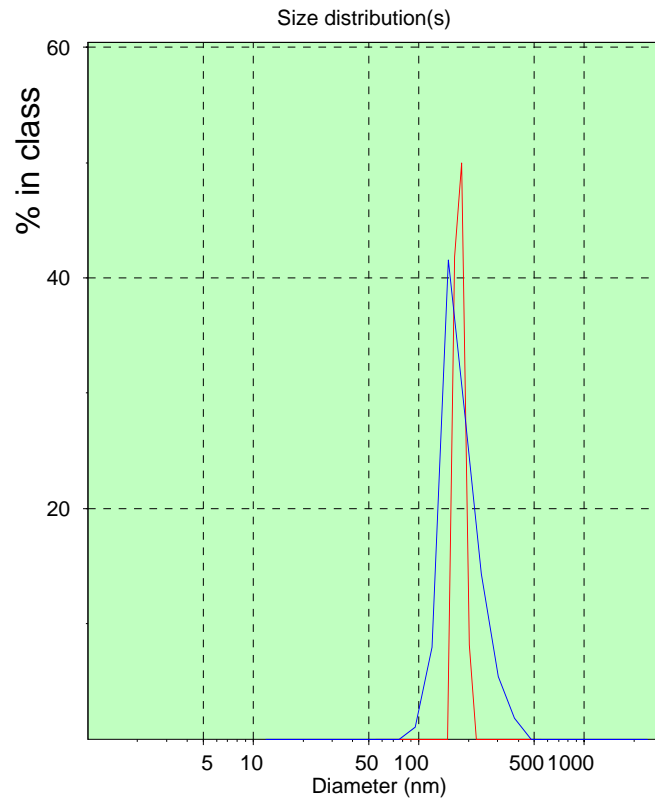


Figure V-4: Droplet size distribution with RO water at high count rate

Peak Analysis by intensity			
Peak	Area %	Mean (nm)	Width (nm)
1	100	176.8	35.2
2	100	184.2	84.4

Table V-4: Size value of oil droplet

Figure V-5 and Table V-5 show the measurement carried out at high oil concentration leading to a particle count rate of 550kCps over the range recommended. A single peak is shown, indicating that the droplet size does not vary with time (if it does, it is much slower than at the low count rate). This measure gives the first estimate of droplet size distribution of 168.4nm.

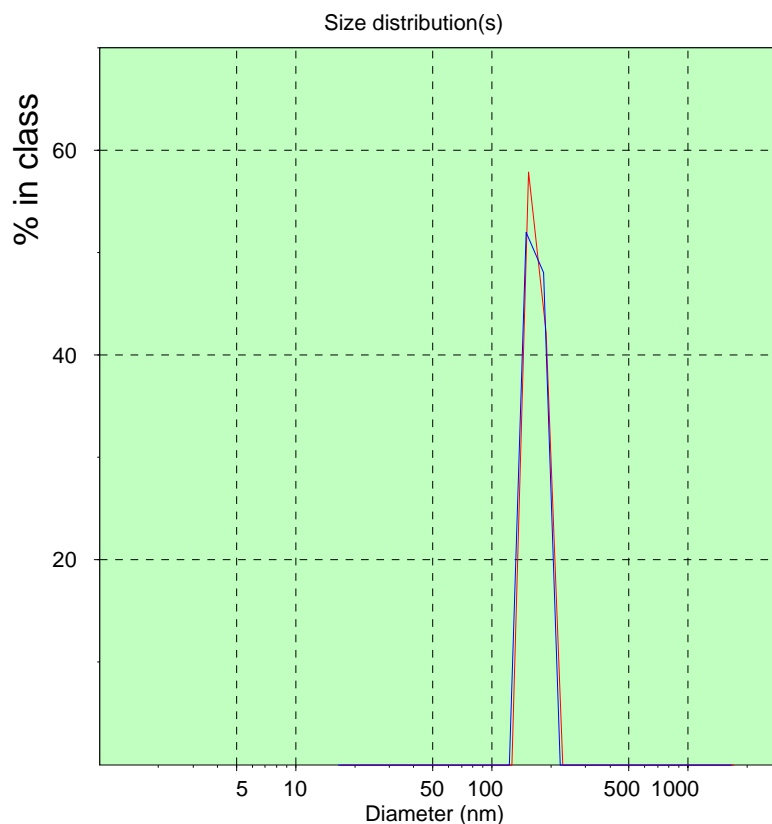


Figure V-5: Droplet size distribution with RO water as dilutant high count rate

Peak Analysis by intensity						
Run	Angle	KCps.	Z _{average} (nm)	Polydispertion	Fit	Time
1	90.0	558.0	171.6	0.084	0.000334	10:47:58
2	90.0	565.4	165.3	0.078	0.000256	10:52:15
Average		561.7	168.4	0.081		

Table V-5: Size value of the oil droplets

A measurement is carried out using UF permeate as dilutant. In this case, the concentration in surfactant is high and may help in preserving the size of the droplet in spite of the dilution. The problem with this technique is that the permeate contains micelles which can interfere with the measurement. Figure V-6 shows the results of emulsion size distribution when UF permeate is used as dilutant. Two sizes are observed. The first size, at 39.9 nm this can be attributed to large micelles that are

present in the permeate and in the original emulsion. The software calculated a molecular weight of 0.9 to 1.1 kDa, that is the limit of the membrane used (FP100). The second size is comparable to the size measured in the third case when using RO water and can be reasonably attributed to the oil drop size when Mobilcut 232 produces a microemulsion in water. (Um et al. 2001) found a similar result using another semi-synthetic oil and gave size droplet distribution between -100 and 400 nm.

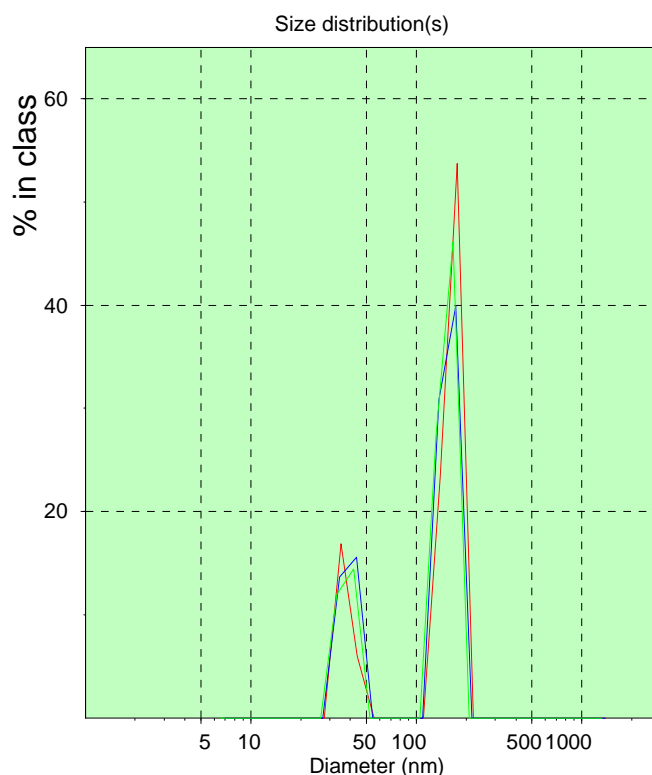


Figure V-6: Droplet size when UF permeate is used as dilutant

Peak Analysis by intensity			
Peak	Area	Mean (nm)	Width (nm)
1	31.8	39.9	18.5
2	68.1	161.6	89.3

Table V-6: Size value of the particles

V.2.4 Concentration stability

The stability of emulsion/microemulsion depends upon the concentration in oil in surfactant and water producing different phases; emulsion, microemulsion, water in oil emulsion or gel. Therefore, a series of mobilecut 232 have been prepared at different concentrations using tap water. Figure V-7 shows the result of phase separation after 72 hours standing in the test tubes. Over 50% of oil in the emulsion is stable for a few minutes and then separated into a gel phase and an aqueous phase. The 5 different phases are described in more detail in Table V-7

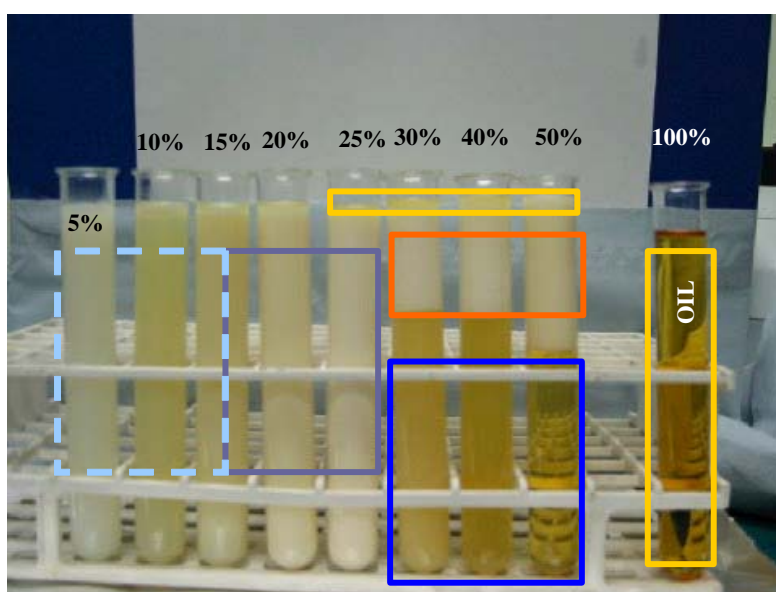


Figure V-7: Picture of the different oil fraction after standing for 72 hours

Sign	Phase designation	Characteristics
	Microemulsion	Translucent homogenous phase of oil in water
	Emulsion	Opaque emulsion phase increase of particle size leads to opacity of the homogenous phase
	Gel	May be due to phase inversion containing a large amount of water
	Aqueous phase	Water containing soluble molecules as the yellow dye from Mobilcut 232
	Oil	May contain water as an inverted water in oil micro emulsion.

Table V-7: Description of the different phases found when oil ratio increases

V.2.5 Fluid viscosity

Table V-8 shows the results of the viscosity measurements. The viscosity values shown are the mean values over a range of shear rates that can be found in the tubular membranes. Emulsion viscosity was not sensitive to the range of temperature applied. The UF concentrate is twice as viscous than the fresh metal working fluid MWF5%. The raw Mobil oil cut 232 viscosity decreases with temperature.

Fluid	MWF5%	UF concentrate 20%	Oil Mobil cut 232
Temperature °C	Viscosity (Pa.s ⁻¹)		
20	1.66E-03	3.54E-03	1.52E-01
30	1.40E-03	2.98E-03	9.00E-02
40	1.57E-03	3.04E-03	5.56E-02

Table V-8: Viscosity of different effluent

V.2.6 Recapitulation

Mobilcut 232 is a stable microemulsion showing an average droplet size of 162 nm. This micro emulsion is not only stabilised by the very small size of its droplet, but also by strong electrostatic repulsion forces showing a zeta potential of -51.4mV . When the concentration in raw oil is increased, the oil droplet size seems to increase too, as the homogenous phase becomes opaque. After 72 hours, a thin oily layer appears at the top of the tubes test when the concentration is above 20% and the stability of the emulsion starts to break down. For higher oil concentrations, a gel is formed on the top of a clear aqueous phase. Over 50% of oil, the same pattern is observed, except that the separation takes place in minutes rather than hours. The oily phase grows very slowly from the gel phase that can be considered as stable.

V.3 CHEMICAL TREATMENTS

Chemical treatment of waste metalworking fluids can be easily adapted to any scale. This second part presents the results obtained using independently common inorganic salt separation and sulphuric acid. Both techniques are aimed at flocculating the oil droplet to separate the oily phase of the emulsion from the aqueous phase. Coagulants may cause the removal of colloids in wastewater by two different primary mechanisms. One theory involves the neutralisation of the surface charges on the particle so that they can aggregate and form larger particles to be separated from the aqueous phase by the difference in density within a reasonable time (Lissant, 1973) and (Walstra, 1996). The other mechanism is referred to as the "sweep flock" mechanism. This is based on the coagulant precipitation as the resulting nascent particles and flock collide with the colloids that adsorb on their surface with them. Both mechanisms are involved in colloid flocculation.

This part is divided into 3 sub-parts including the inorganic salts treatment, the acidification treatment and finally the measurement and comparison of the calorific values of sub-products generated during chemical treatment.

V.3.1 Inorganic salts

Flocculation of metalworking fluids is widely used in the industry, especially when dealing with oil emulsion. The principles of the technique have been described in Chapter II. In this paragraph, the minimum flocculation concentration of MWF5% is determined and the flocculation behaviour of Mobil cut 232 is discussed. In a second part, the quantity of flocculant needed to flocculate the concentrate MWF resulting from ultrafiltration membrane process is measured. The mechanism and difference in nature between the fresh metalworking fluid at 5% in oil and the concentrate are also discussed.

V.3.1.1 Fresh metalworking fluid flocculation

a) Results

Table V-9 shows the results of fast flocculation that have been carried out with MWF 5%. The critical flocculation concentrations found for each flocculant are in the same order of magnitude [10^{-2} mole per litre of metal (M^{3+})]. However, aluminium sulphate is more efficient than iron sulphate, 33% less metallic ions are needed to flocculate the waste.

Salt	Apparent C_{crit} (eq M^{3+} per litre)	$K_{colloid}$
$Al_2(SO_4)_3$	1.50×10^{-02}	10.935
$AlCl_3$	1.80×10^{-02}	13.122
$Fe_2(SO_4)_3$	2.00×10^{-02}	14.58
$FeCl_3$	1.80×10^{-02}	13.122

Table V-9: Apparent colloid characteristic constants for fast flocculation

b) Discussion

The investigated system has an alkaline pH and is composed of a mixture of hydrophilic compounds. This means that the flocculation process is the consequence of the precipitation of $Al(OH)_3$ and $Fe(OH)_3$ in colloidal form and the adsorption of the organic components present. Flocculation of nascent $Al(OH)_3$ by anions follows the Schulze-Hardy rule, which describes the relationship between the concentration of electrolyte required to initiate the fast flocculation of a colloid and the charge of the said electrolyte (Nowicki W. and Nowicka G., 1994). The empirical rule is Schulze-Hardy rule, given in Equation V-1

$$C_{crit} = K_{colloid}/z^6$$

Equation V-1

Where z is the charge of the electrolyte which causes the flocculation, K_{colloid} is a characteristic of the colloid and C_{crit} is the concentration required for fast flocculation. Estimates for C_{crit} for each flocculants are shown in Table V-9.

The similarity between the constants is indicative of the compliance with the Schulze-Hardy rule. The procedure used for the verification of the rule is not rigorous, because it treats the system as if Al^{3+} or Fe^{3+} were used to flocculate the colloidal system. This is not the case because at an initial pH of 9.5, the important flocculation agents are the hydroxides formation and its polymerisation and structure. What is actually happening is that the organic content from the colloidal system (which is a constant quantity) is being used to adsorb onto the nascent aluminium and iron hydroxide that forms. This means that the colloid is able to cause fast flocculation when interacting with a given concentration of nascent hydroxide. The condition fulfilling the Schulze-Hardy rule is met for these unknown concentrations, which corresponds to the nominal ion and aluminium salt concentrations, causing fast flocculation for the coolant micro-emulsion at the given dilution. Therefore, when the Schulze-Hardy rule is tested, the results will indicate that it is being met (the constant has the same value for electrolytes of the same charge) even though the actual constant values are implicit in the apparent constant values.

Another interesting factor is the different behaviour of sulphates and chlorides. Addition of further aluminium chloride provokes turbidity in the solution, while this effect is not seen in the presence of an excess of aluminium sulphate. This is a more complex issue. Some work on flocculation of organic matter shows that the residual concentration of aluminium increases with the increase of concentration of some organic compounds in neutral-alkaline solutions. If more aluminium is added, then the residual aluminium concentration decreases. This is connected to the formation of complexes between organic compounds and aluminium, which may be either soluble or insoluble (Cathalifaud, *et al.* 1997). In the same way, organic acids or their conjugated bases would be affecting the flocculation of the cutting oil. This is not likely to be the case here as the effect is only observed with chlorides. The potential effect of sequestering/complexation of cation by formation of complexes $[\text{MCl}_n]^{+3-n}$ must be the cause. This is observed as the concentration of $[\text{Cl}^-]$ increases, leading to a clear solution and flocculate and then, at higher concentrations, to turbid solutions.

They may be an indication of the influence of chloride concentration on the formation of complexes of the form $[MCl_n]^{+3-n}$ if a ratio is defined $R = [Cl^-]_{\text{turbid}}^n / [Cl^-]_{\text{clear}}^n$, as the ratio of the equilibrium concentrations of a said complex at the concentration at which turbidity reappears over the concentration at which a clear flocculate is obtained. This assumes a constant concentration of the cation M^{3+} . As pH decreases with higher concentration of the flocculant salt, $[M^{3+}]_{\text{turbid}}$ must be higher than $[M^{3+}]_{\text{clear}}$. Table V-10 shows theoretical ratios, $R_{\text{turbid/clear}}$, for complex concentrations forming at the nominal MCl_3 concentrations leading to the onset of turbid overdosed solution and clear flocculate solution, for three different complex stoichiometries n .

n	R_{FeCl_3}	R_{AlCl_3}
4	16.3	8.2
5	32.9	13.9
6	66.1	23.6

Table V-10: Theoretical ratios, $R_{\text{turbid/clear}}$, for complex concentrations forming at the nominal MCl_3 concentrations leading to the onset of turbid overdosed solution and clear flocculate solution, for three different complex stoichiometries n .

$$[\text{FeCl}_3]_{\text{clear}} = 2.19 \cdot 10^{-2} \text{M}; [\text{FeCl}_3]_{\text{turbid}} = 3.59 \times 10^{-2} \text{M}$$

$$[\text{AlCl}_3]_{\text{clear}} = 1.85 \cdot 10^{-2} \text{M}; [\text{AlCl}_3]_{\text{turbid}} = 3.72 \cdot 10^{-2} \text{M}$$

The calculations ignore the change in chloride concentration due to complexation, or the effect of other organic compounds present in the competitive formation of aluminium or iron complexes containing both chloride and organic ligands. It is a reasonable argument for the phenomenon observed that complexes are likely to reduce the effective cation concentration and deflocculate part of the material, or maybe created insoluble complexes with organic, aluminium or iron and chloride. Finally, the effect of the alkali/aluminium ratio in the solution is independent of pH. (Bottero., 1989) reported that when the ratio $\text{NaOH}/\text{AlCl}_3$ is raised above 2.3 by the addition of NaOH to a solution, AlCl_3 aggregation begins, with larger aggregates occurring for ratios above 2.6. Therefore, when a system in which the ratio $\text{NaOH}/\text{AlCl}_3$ is reduced by the addition of aluminium salts, as shown in Figure V-8, the ratio $\text{NaOH}/\text{AlCl}_3$ may have the effect of moving from initially larger flocks to smaller dispersed aggregates. Chloride may effectively take part in some kind of

complex formation. The ratio $\text{COD}/[\text{M}^{3+}]$ was measured and was found to be greater for both aluminium and iron chlorides. This can also be interpreted by the formation of chloride organic complexes that diminish the dissolved COD level in the clear supernatant. For the sulphate to give the same COD removal level, the flocculant has to be overdosed.

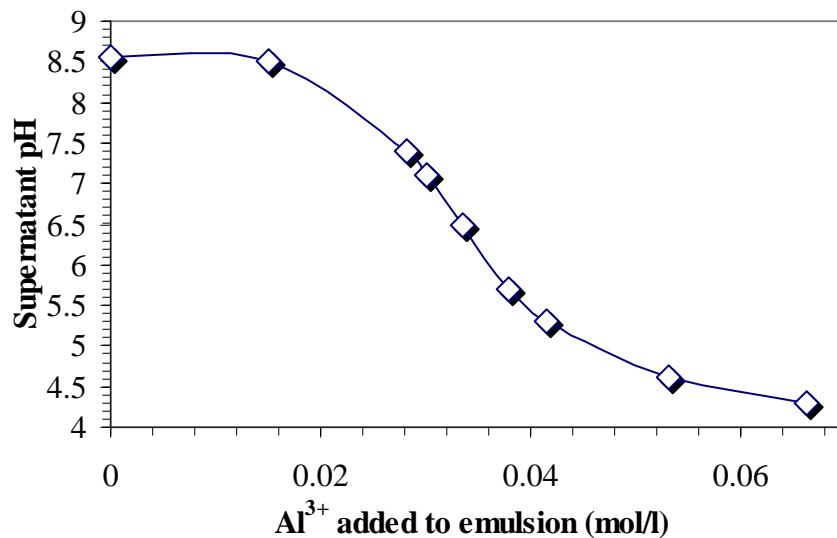


Figure V-8: pH evolution during addition of aluminium sulphate

V.3.1.2 Concentrate coagulation

a) Results

Flocculation tests were carried out using aluminium sulphate to flocculate metalworking fluid concentrate at 20.8% in oil content. The concentrate has been obtained by filtering fresh metalworking fluid, MWF5%, until it reaches the value of 20.8%. The results show that 2.56×10^{-2} mol/L of Al^{3+} were needed to flocculate the concentrate. This is equivalent to 7.9 g of aluminium sulphate per litre of concentrate against 4.7 g required to flocculate the raw emulsion at 5% in oil content. This represents a ratio 39.5 g of aluminium sulphate per litre of oil in the concentrate against 94 g of aluminium sulphate per litre of oil in the MWF5%. This increase in flocculant needed can be explained by the fact that the quantity of oil to flocculate is

much more important in the concentrate than in the fresh metalworking fluid (5% against 20.8%). The flocculation is driven by the adsorption of oil droplets onto the surface of aluminium hydroxide that forms in the alkaline environment (pH 9.3). Nevertheless, four times more oil is flocculated with only 40% more flocculant. Two reasons can be given to explain this fact. The first is to consider that smaller hydroxide particles were formed when flocculating the concentrate. In this case, a larger surface area per gram of aluminium sulphate would have been created and therefore more droplets could have been adsorbed onto the nascent hydroxide. This is unlikely, regarding that both rapid flocculation in the case of fresh MWF5% and concentrate at 20.8% have been carried out in the same conditions in a solution at pH 9.3 by shaking a test tube containing $\text{Al}_2(\text{SO}_4)_3$ and the effluent. Therefore, this first possibility can be dismissed. The second reason is that the concentrate is a less stable emulsion than the fresh MWF5%. This destabilisation can be explained by the fact that the concentration of oil droplets increase bringing them closer to each other forcing them to aggregate. This is similar to the experiment in Section V.2.4. This mechanism is reinforced by the fact that the surfactant and micelles have been discarded with the permeate during the filtration process. Even if the size of the oil droplets contained in the concentrate can not be measured (due to dilution problems, knowledge of the ionic pressure and surfactant concentration) it is not unrealistic to presume that they aggregate, which also explains why the concentrate becomes white-opaque instead of amber translucent as it is shown in Figure V-7 on page 118.

If the oil droplets adsorb onto the nascent aluminium hydroxide forming a nonolayer of adjacent spherical droplets of diameter d , then the diameter of the oil droplet in the concentrate phase can be calculated. This calculation can be done in two steps. At first from the droplet size in MWF5%, it can be calculated what the surface produced per gram of aluminium sulphate in the experimental condition is. Then, working of the same set of equations gives the size of the aggregate in the concentrate at 20.8% of oil, assuming that the adsorbing surface area per gram of aluminium sulphate is identical in both situations.

b) Discussion

Initially, a set of equations used to perform the calculations are given. Then, by comparing the calculations and the experimental values, the assumptions made previously in the results section are discussed. The hypothesis of concentrate's emulsion destabilisation is confirmed. The hypothesis of an increase in hydroxide surface is also investigated and rejected. Finally, the nature of the destabilisation is discussed. The surface area of the aluminium hydroxide is based on the surface occupied by the adsorbed oil droplets and does not take into account the adsorption of other organic compounds and so should be considered inferior to the real surface area.

The volume of a spherical droplet or aggregate is calculated using the equation of the volume of a sphere as follows:

$$V = \frac{4\pi r^3}{3} = \frac{\pi d^3}{6} \quad \text{Equation V-2:}$$

where d is the droplet diameter in meters. The number of droplets for a given volume of oil (V_{total}) is calculated as follows:

$$N_{droplet} = \frac{V_{total}}{V_{droplet}} = \frac{6 \times V_{total}}{\pi d^3} \quad \text{Equation V-3:}$$

The surface of hydroxide covered by droplets of size d in monolayer is calculated using Equation V-4 and the reverse Equation V-5 is used to calculate the diameter of a droplet covering a known surface area in monolayer.

$$S_{cov} = N_{droplet} \times d^2 \quad \text{Equation V-4}$$

$$d = \frac{6V_{total}}{\pi S_{Cov}} \quad \text{Equation V-5}$$

Calculation of aluminium hydroxide surface area:

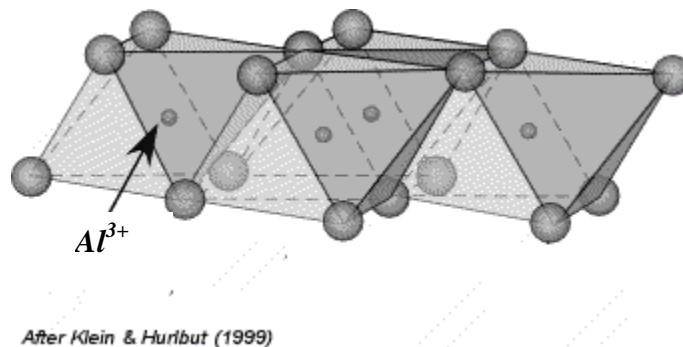
The surface covered by the oil droplet in the case of fresh MWF5% can be calculated because the droplet size is known to be $162 \times 10^{-9} \text{m}$ (measured in part V.2.3.). Using Equation V-3, the number of oil droplets of size 162 nm obtained with $5 \times 10^{-5} \text{m}^3$ of oil contained in 1 litre of MWF5% is N_{droplet}

$$N_{\text{droplet}} = 2.246 \times 10^{16} \text{ droplet per litre of MWF5\%}.$$

Considering that all the droplets are adsorbed onto the aluminium hydroxide, generated by 4.7g of $\text{Al}_2(\text{SO}_4)_3$ used under specific experimental conditions, this surface can be calculated using Equation V-4. Therefore, the surface generated by one gram of aluminium sulphate used under the experimental conditions is known.

$$S_{\text{cov}} = 589.46 \text{ m}^2 \text{ for 4.7g of aluminium sulphate is } \underline{125 \text{ m}^2/\text{g}}.$$

The formation of aluminium hydroxide gel precipitate consists of thin gibbsite layer of aluminium hydroxide in which every third octahedral site is occupied by an aluminium cation and the distance between hydroxide is 0.29nm.



From: <http://www.tulane.edu/~sanelson/geol211/phyllsilicates.htm> accessed 2003

Figure V-9: Gibbsite Octahedral structure describing the layer of $\text{Al}(\text{OH})_3$

The value of $125 \text{m}^2/\text{g}$ of aluminium sulphate is small but realistic regarding the conditions in which it is formed, and is a value for the surface area involved in the oil droplet adoration.

Calculation of the oil droplet size in the concentrate:

Substituting $N_{droplet}$ in Equation V-4 by its expression given by Equation V-3, the oil droplet size or aggregate size can be calculated, assuming that conditions of spherical shape mono-layer adsorption of adjacent spherical shaped aggregate are realised.

The surface to cover is the one produced by 7.9g/L of aluminium sulphate introduced into the emulsion, which is $990.8 \text{ m}^2/\text{L}$ ($7.9\text{g/L} \times 125.46\text{m}^2/\text{g}$). The total volume of oil at 20.8% in 1 litre is $2.08 \times 10^{-4} \text{ m}^3/\text{l}$. Therefore, the diameter of the oil droplets aggregated is $d_{20\%}$, calculated using Equation V-5.

$$d_{20\%} = 401 \times 10^{-9} \text{ m}$$

Nevertheless, the overall quantity of oil adsorbed on the hydroxide should correspond to the experimental value to validate the hypothesis of emulsion destabilisation. This raised the question of aggregate structure. Two structures can be proposed, a large coagulated oil droplet of 401nm diameter or a pack aggregated structure 401 nm wide of n original droplets as illustrated in Figure V-10. In order to answer this question, the quantity of oil in an aggregate in a close pack system has to be calculated and compared to the quantity of oil effectively adsorbed onto the hydroxide surface in the experiment.

Quantity of oil in an aggregate

Figure V-10 represents the oil droplet of 162nm and the merge droplet of 401 nm

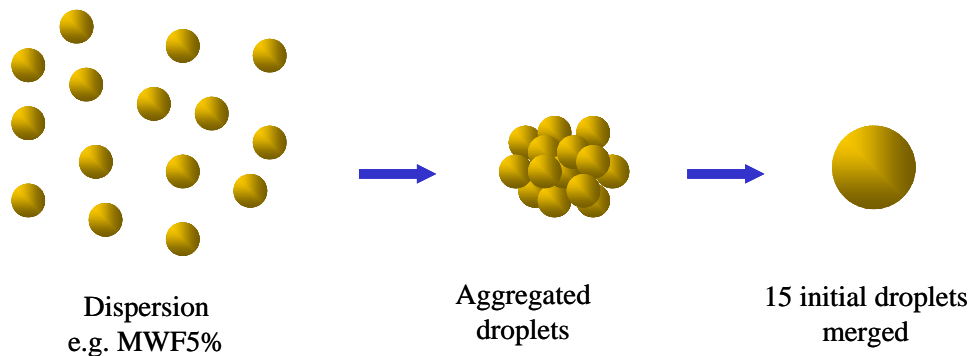


Figure V-10: Illustration of aggregated and merged droplets

If the droplets were only aggregated (droplets would not be merged), they could at best form a closed packed structure containing a void ratio of 26%. This would lead to a structure of 401 nm diameter containing only 11.2 original droplets, as calculated with Equation V-6 below with a void ratio of 26%.

$$N_{\text{Original-droplet}} = (\text{Volume}_{\text{structure}} - \text{Volume}_{\text{Void}}) / \text{Volume}_{\text{Original-sphere}} \quad \text{Equation V-6}$$

The same calculations using Equation V-4 and a ratio of 125.46m²/g of aluminium sulphate shows that 10.88g of aluminium sulphate would have been used. In this case, using the best-packed structure, the calculation deviates from the experimental value (+27.11%). Therefore, it should be considered that the original oil droplet merged to form a larger droplet.

The hypothesis is that the oil droplet merges to form a larger droplet of 401 nm in diameter with a volume of 3.375x10⁻²⁰ m³. This volume is equivalent to the volume of oil of 15.16 original droplets of 162 nm diameter (e.g. the 15.16 droplets coagulate together to give a larger droplet of 401 nm diameter). It has been calculated earlier that the concentrate at 20.8% in oil should contains 9.34x10¹⁶ original droplets per litre. If it is assumed that the original droplets (d=162nm) have merged in the concentrate to produce larger droplets of d=401 nm diameter, then the concentrate should contain 9.34x10¹⁶/15.16 = 6.227x10¹⁵ large droplets per litre. These droplets would adsorb according to Equation V-4 onto a surface of 990.4 m². This result is very close to the surface found previously corresponding to less than 7.89g of aluminium sulphate. There is a perfect correlation between the calculated value, 7.89g, and the experimental value, 7.9g (-0.16%). Therefore, it can be concluded that the concentrate is an emulsion of the larger droplets formed on average by 15.16 original droplets merged to produce a single larger droplet 401nm in diameter.

The hypothesis of hydroxide surface increase

To effectively reject the case of aluminium hydroxide surface effect, let's assume that the oil droplet does not aggregate and keeps a diameter of 162nm. Then the number of droplets in the concentrate at 20.8% would be $N_{droplet} = 9.34 \times 10^{16}$ droplets per litre of concentrate and would cover a monolayer surface of 2452.16 m^2 . This would have needed 19.55g of aluminium sulphate (producing $125.42 \text{ m}^2/\text{g}$ under the experimental conditions). These calculated results are far from the experimental value (+247%) and would correspond to an increase of 247.4% in surface. No reasons can be given for such a surface increase. Therefore, the hypotheses involving a surface increase of the hydroxide can be objectively rejected.

How stable droplets merge

The concentration in oil is not the only reason and should not be enough to force the original droplets to coagulate. An increase in concentration brings the droplets closer and increases droplets interaction, creating aggregate. It is unlikely that the aggregates formed are able to spontaneously coagulate. Therefore, a mechanism enabling the small solid droplets, to coagulate must be explained. To explain this mechanism, another element has to be taken into account, the surfactant and micelles dissolved in the aqueous phase ensure the equilibrium between oil and water as illustrated on Figure V-11. In this case, an impoverishment of the concentration in surfactant (e.g. the surfactants permeate the membrane) has to be considered. The study of the droplet size at the beginning of the chapter shows that oil droplet size is sensitive to surfactant content. Diluting the microemulsion leads to an increase in size as shown in Figure V-3. In the concentrate, 15.16 original droplets would present a surface of $12.524 \times 10^{-14} \text{ m}^2$ and the larger droplet representing the same volume of oil (e.g. 15.16 original droplet merged) show a surface of $2.02 \times 10^{-12} \text{ m}^2$ that is four times smaller. Therefore, less surfactant molecules can cover the surface of the large droplet and a new equilibrium oil-surfactant can be established. The opposite case is enrichment of surfactants in the concentrate (e.g. surfactants are rejected by the membrane). As shown on Figure V-12, water would be trapped in-between close oil droplets creating a gel. This is not observed as the concentrate at 20.8% is a stable emulsion and does not form a gel. Therefore, it can be concluded that the concentrate surfactants

concentration decreases during ultrafiltration. Following the mechanism described in Figure V-11 and based on Le Chatelier's principal, surfactants present at the surface of the droplets re-dissolved to maintain *equilibrium 1*. The droplet-droplet electrostatic and steric forces of repulsion decrease, destabilising the droplets structure. At the same time, the oil droplet concentration increased. Both phenomena lead to oil droplets aggregation and coagulation into a larger droplets to reach a new equilibrium.

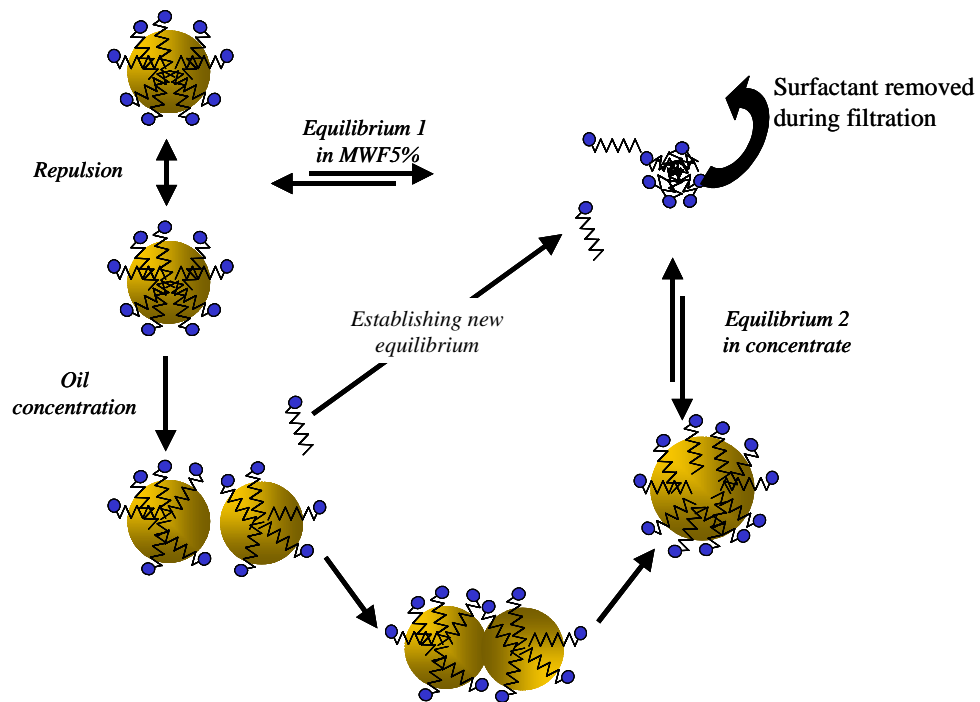


Figure V-11: New emulsion equilibria case of surfactant impoverishment

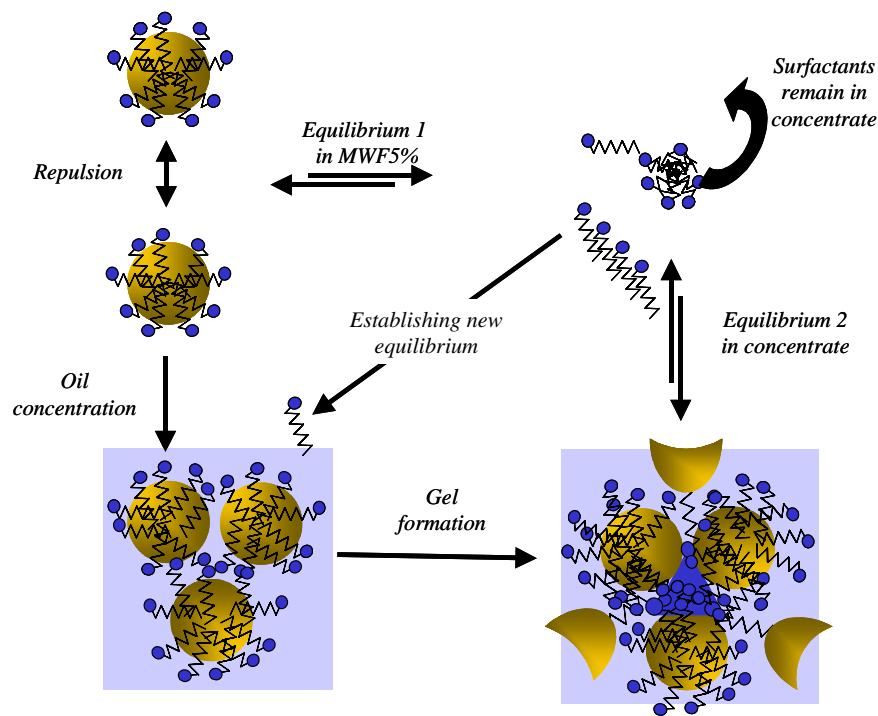


Figure V-12: New equilibria case of surfactant enrichment



V.3.2 Acidification

Acidification is a different flocculation process, based on the principle that the charges at the droplet surface can be neutralised by adding protons to the system regarding that oil droplets are stabilised by electrostatic forces. The acid will also neutralise the pH of the alkaline concentrate (pH 9.3). This variation in pH can have an effect on the solubility of certain molecules that are in or at the surface of the oil droplets.

A different experimental approach was undertaken for the study of the acidification process. Results obtained during salt flocculation show that the concentrate is less stable than the fresh MWF. Acidification has been carried out directly with the concentrate MWF20.8%. The different phases obtained during the acidification, the behaviour of pH and mode of operation are discussed. Acidification is also carried out using fresh MWF20% and results are compared with those obtained with the concentrate. Finally, the effect of potassium hydroxide addition to the aqueous phase is discussed.

V.3.2.1 Concentrate acidification

a) Results

Five tests have been carried out; the results are shown in Table V-11. The results show that three phases are obtained when the MWF 20.8% is mixed with sulphuric acid. These phases are; an oily phase, a gel and a yellow aqueous phase as shown in Figure V-13. They are denoted respectively as **O**, **G** and **W** in Table V-11. It can be seen from this table that the calorific value of the gel is much less combustible than completely coagulated oily phase.

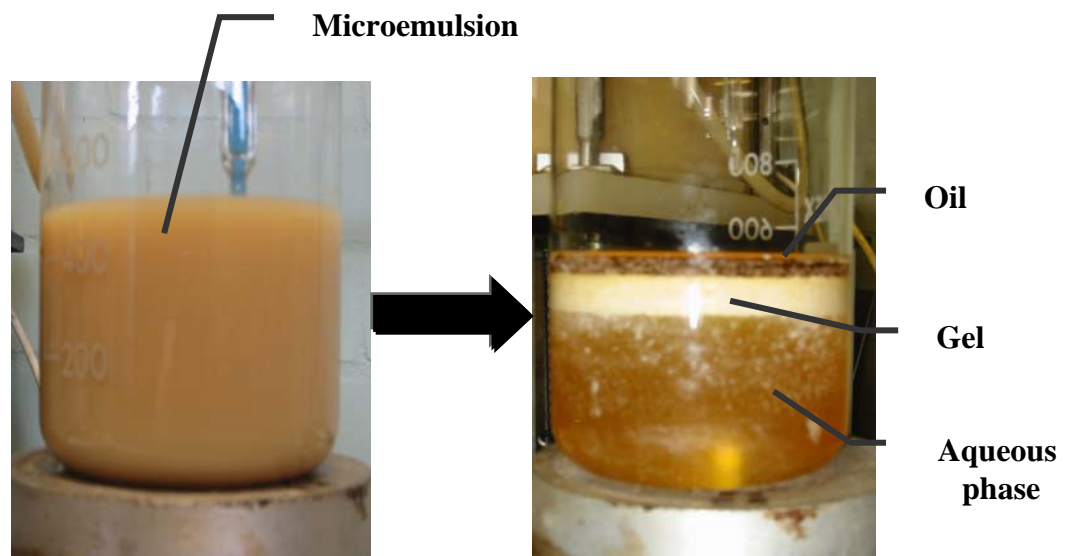


Figure V-13: Waste metalworking fluid after acidification n°2 showing the 3 phase obtained

<i>Product</i>	<i>Calorific value (J/g)</i>	<i>quantity of acid (ml)</i>	<i>pH after 24h</i>	<i>turbidity (NTU)</i>	<i>TOC (mg/l)</i>	<i>acid introduction</i>	<i>Agitation speed rpm</i>	<i>agitation time (minute)</i>	<i>Product fraction after 24h (%)</i>
<i>Oil Mobilcut 232</i>	31953	32019							
<i>O1</i>	#	#							0%
<i>G1</i>	20919	20259.1	13.5	1.3		Progressive	300	20	18%
<i>W1</i>				1.7	14.4				82%
<i>O2</i>	41742	41693		5.75					4%
<i>G2</i>	22367		10.25	6.25		Progressive	50	20	20
<i>W2</i>				3.68	59				76%
<i>O3</i>	41707	41659		6.15					5%
<i>G3</i>			10	6.3		direct	50	15	95%
<i>W3</i>				6.4	217				0%
<i>O4</i>	41999	41953							14%
<i>G4</i>			10			direct	50	15	6%
<i>W4</i>				6.3	268				80%
<i>O5</i>	41932	41942		6.8					20%
<i>G5</i>			10			Progressive	50	15	0%
<i>W5</i>				5.45	228				80%
<i>W5bis</i>			KOH flakes	10.5	2	#			#

Table V-11: Results from acidification tests

Results reported in Table V-11 show that obtaining oil separated from the aqueous and coagulate phases depends on three different factors. These factors are (i) the quantity of acid added, (ii) the agitation rate and (iii) the mode of acid addition (direct is that the all quantity of acid is added to the emulsion at once and progressive means that the acid is introduced millilitre by millilitre over 15 minutes).

b) Discussion

Figure V-14 shows the evolution of pH of the experiment number 5. The pH is neutralised when 6 ml of acid are added to the metalworking fluid concentrate. When the oil starts to separate, more acid is added up to 10 ml of H₂SO₄ 5N. Then, stirring is stopped and the pH of the aqueous phase is measured. Figure V-15 shows the evolution of pH with time after adding the 10 ml of sulphuric acid and stopping the stirring. The pH decreases during the next 90 minutes. The values reached after 24 hours are pH 5.4 and turbidity 228 NTU as shown in Table V-11.

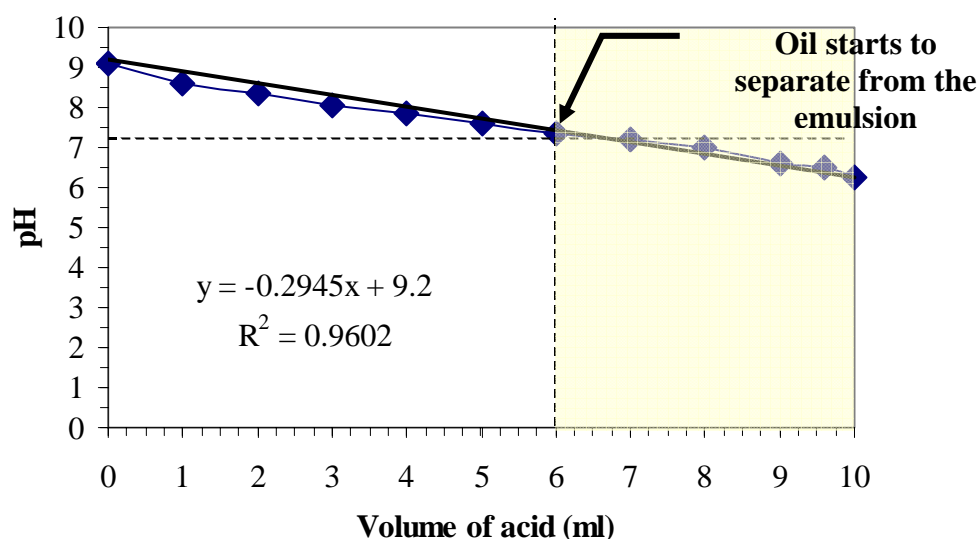


Figure V-14: pH evolution during the fifth acidification vs. volume of acid poured

Figure V-15 and Figure V-16 show the evolution of pH with time in two cases respectively: when 10 ml of acid is added progressively and when acid is added directly to 500 ml of concentrate at 20.8%.

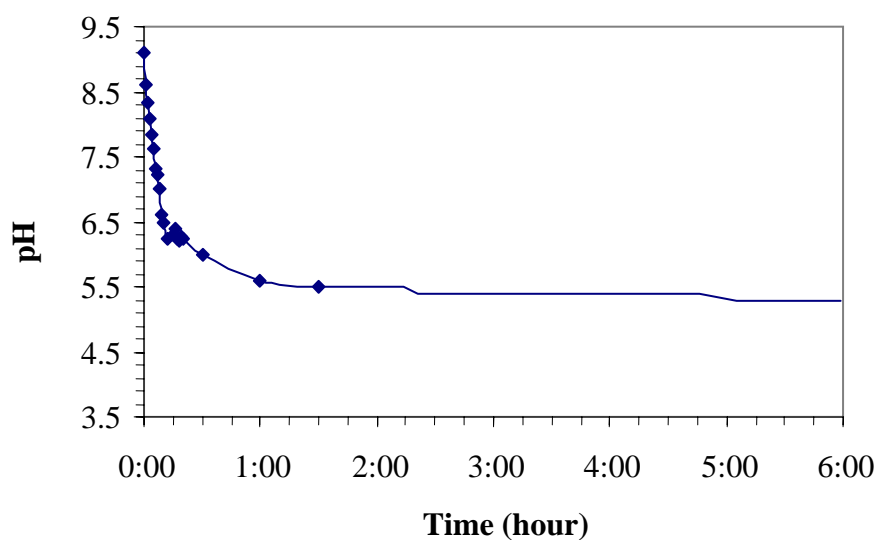


Figure V-15: pH evolution when adding progressively acid

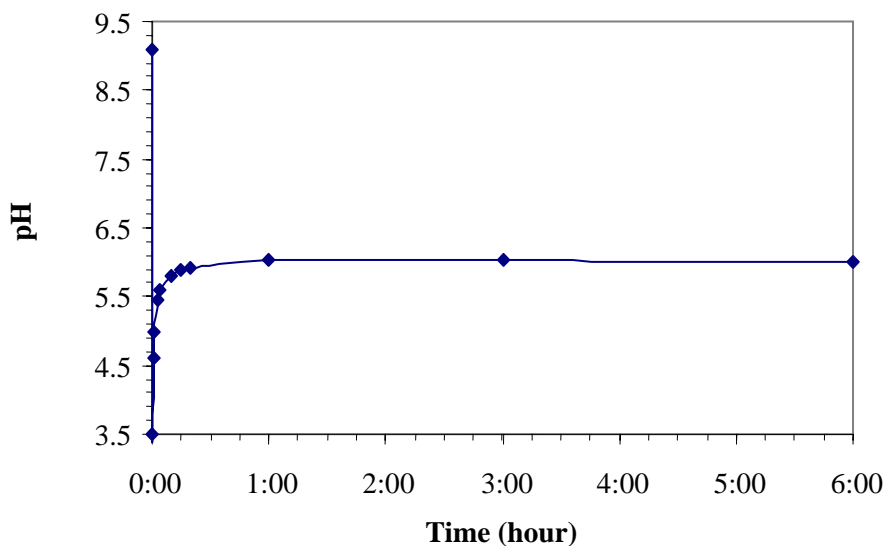


Figure V-16: pH evolution after adding acid directly

In both cases, the addition of 5% of H₂SO₄ at 5N leads to an aqueous phase with very similar pH values, 5.6 and 5.8. The difference resides in the quality of the flocculated phase obtained. The products obtained are, in order of combustible quality gel, mixture gel/oil and fully coagulated oil. In the first case the acid is slowly added to the concentrate and a coagulated oily phase is obtained. In the second case the acid is added at once, a gel is obtained. Gels are stable after 24 hours when the ratio (W/O/G) are measured. It took 3 to 12 weeks to break the gel into an oily phase and an aqueous phase. Reaction kinetics and the coagulation process can explain the difference in behaviour between the two types of acid introduction mode. Figure V-16 shows the pH falls down to 3.5 in one second and is followed by a rapid increase to 5.5 within 30 seconds. Figure V-15 shows a completely different pattern, in which the final pH is obtained after one and half hours. First, in this case, the addition is controlled and 1 ml is allowed when pH-meter stabilised (each minute 1 ml of acid was added). Secondly, when 10 ml of acid was added, the pH was 6.8 and decreased down to 5.6 after 1.5 hours letting the coagulation take place and uncharged molecules to leave the surface of the droplet dissolving into the acidic aqueous phase.

V.3.2.2 Fresh MWF 20% acidification

A sixth experiment has been conducted to compare the behaviour of the concentrate with a fresh MWF20%. The same parameters as in experiment number 5 were used to allow a direct comparison. H₂SO₄ 5N was added progressively to 500ml of fresh MWF20% with 50 rpm stirring, then stirring was stopped after adding all the acid. The pH of the aqueous phase was then measured.

a) Results

Figure V-17 shows the evolution of pH during the addition of the acid. It can be seen in the figure that a larger quantity of acid is needed to neutralise and to start observing the oil separation compared to the concentrate acidification. The oil effectively starts to separate after 9.5 ml of acid. That is, +160% more acid than in experiment number 5. Neutralisation occurs at 16 ml of acid added and that is +60% compared with experiment number 5. 20 ml of acid added, after 20 hours a gel and a turbid aqueous

phase 2200NTU with a pH value of 5.8 were obtained. Figure V-8 shows that the emulsion breakage starts at a pH value of 8.4 whereas it took place at pH 7.2 in the previous case using concentrate.

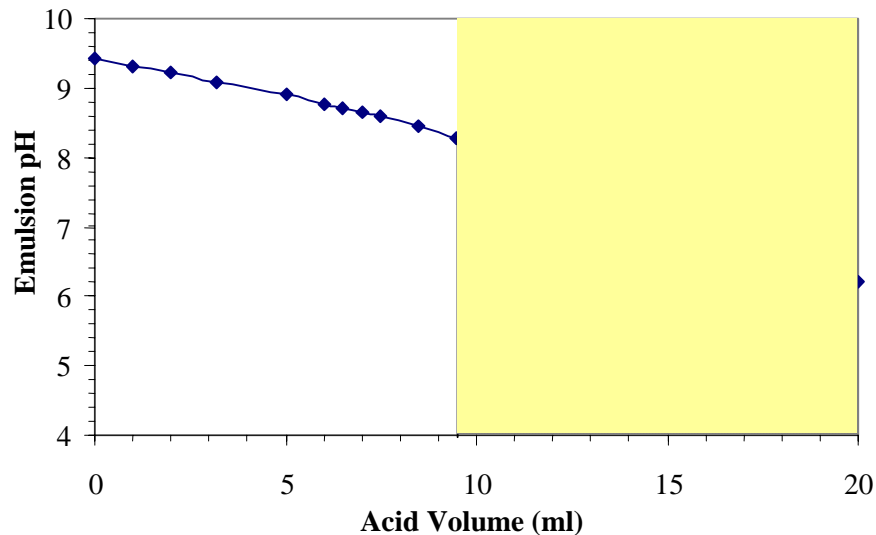


Figure V-17: pH evolution vs. acid addition for fresh MWF20%

b) Discussion

Results obtained with 20% concentrated fresh made fluid are very different to those obtained in experiment number 5 with the concentrate. The main difference is that a gel is obtained in the case of freshly made fluid even though the experiment took place in the best conditions that have been found previously for the concentrate acidification. It can be concluded that the acidification of the fresh metalworking fluid is not as efficient as the acidification of the concentrate of the same oil content.

V.3.2.3 Alkaline treatment

The alkaline step is often used to chemically treat metalworking fluids; this is the final step in the Acid Alum method described by (Rios, *et al.* 1998). In the study, the solid can be attributed to the removal of an excess of aluminium sulphate. In this work, the caustic treatment has been carried out with the aqueous phase collected from

acidification experiment number 5. The pH of the aqueous phase has been brought to an alkaline pH by adding potassium hydroxide pellets.

a) *Results*

The pH value of the solution has been brought from 5.8 to 10. Addition of KOH flakes to the aqueous phase of experiment number 5 induces the formation of a white precipitate and a large decrease in turbidity from 228 to 2 NTU.

b) *Discussion*

The precipitate that forms can be attributed to amine and organic compounds soluble in an acidic environment when the solution is brought back under alkaline conditions. This indicates that the action of sulphuric acid is not only to neutralise charges present on the oil surface but also react with some components. Alkanesulfonate of general formula $R-SO_3^- : Na^+$ or K^+ can be electrically neutralised by proton contribution. Actions of acid on organic molecules that stabilise the emulsion (emulsifiers) make them more hydrophilic as shown in Equation V-7 protonation of an aminoester. Part of the emulsifiers dissolved into the aqueous phase leading to emulsion break down. This phenomenon is described by (Lissant, 1973). Mobil cut 232 contains different amine, amino esters. The product data sheet in Appendix B shows that it contains 15 to 25% in weight of alkanolamine and 5 to 15% in weight of diethanolamine esters of rapeseed oil.

The drop in turbidity is due to the formation of the solid that wipes the solution of the remaining oils and other complexes that have been created during the acidification process.



V.3.3 Calorific value

The calorific values of the different phases recovered were measured and compared with each other and with other types of fuel. The purpose of these measurements was to determine if the recovered oil could be used as a fuel.

V.3.3.1 Results

Table V-12 shows the different calorific values found for the raw commercial oil, the aluminium flocculated oil, acid coagulated oil and the gel (highlighted in blue).

Type of Fuel	Fuel	Calorific value	
		kJ/g	kwh/kg
Solid	Charcoal	33	9.2
	Coal	25.33	6.9 to 9.2
	Wood	17	4.7
	Dung cake	6 to 8	1.7 to 2.2
Liquid	Kerosene	48	13.3
	Petrol	50	13.9
	Diesel	45	12.9
	Acid treated Oil	42	11.7
	Raw Mobilcut 232	31	8.6
	Ethanol	30	8.3
	Aluminium treated oil	26	7.2
	Acid treated Gel	20.2 to 20.9	5.6 to 5.8
Gas	Bio Gas	35 to 40	9.7 to 11.1
	Butane (LGP)	50	13.9
	Methane	55.3	13.9
	Hydrogen	150	41.7

Table V-12: Comparison of calorific values 1 kJ=0.0002777 kWh

Results show that the oil recovered by acidification has very good calorific value and it is comparable to other types of fuel such as Diesel. The raw oil has a lower calorific value than the acid recovered oil. Both aluminium treated oil and gel have a poor calorific value inferior to ethanol. The great advantage here is that oil recovered by acidification may be used as fuel (use full product) due to its high calorific value of 42,000 kJ/kg.

V.3.3.2 Discussion

The discussion is divided into 3 parts. The first part discusses the calorific values. The second part deals with the use of the energy and gives some solutions for using the recovered oil on site. The third part deals with the pollution that may be generated by the oil combustion including, as an example, the ash analyses of the acid oil recovered from MWF20%.

a) Results analysed

The three following paragraphs discuss the calorific value of the acid recovered oil compared to raw “Mobil cut 232”, aluminium recovered oil and the gel obtained during the acidification process respectively.

The difference of +11kJ/g in calorific value between the acid recovered oil and original “Mobil cut 232” is that raw oil “Mobil cut 232” does not contain only hydrocarbons but also other molecules like surfactants, biocides, emulsifiers and alcohol. These components have a lower calorific value for the same mass hydrocarbons due to their content in oxygen, sulphur and nitrogen. In the case of the acid recovered oil, part of these components were removed from the oily phase. This removal takes place in two stages. First, component parts are dissolved in the aqueous phase when the fluid is prepared. Secondly, the acidification process further dissolved components in the aqueous phase. It had been shown earlier in V.3.2.3, in the hypothesis, that during acidification, some components of the metalworking fluid are dissolved at a lower pH as surfactants and emulsifiers leave the surface of the oil droplets enabling coagulation. The difference in calorific values also shows that no water is dissolved in the oily phase. This indicates that the acidified oil is fully coagulated and composed mainly of hydrocarbons.

The aluminium-recovered oil has a low calorific value of -38%, compared to the acid recovered oil. This can be attributed to aluminium hydroxide polymerised present in the oily phase. However, it can be calculated that the aluminium hydroxide represents less than 2% of the oil mass. Therefore, another reason should explain the important difference in calorific value. The coagulation process involving the formation of aluminium hydroxide is different from the one using acid. The method is based on the

adsorption of the oil droplets on the nascent hydroxide and water may be trapped the aluminium hydroxide structure. In the case of aluminium flocculation, the oil droplet flocculated but did not totally coagulate, so the water content is more important than for the acidification process.

The gel obtained from the acidification method has the lowest calorific value and has a difficult ignition (Chapter III). This can be explained by the presence of a large amount of water within the gel structure.

b) *Use of the energy*

Under the European recommendations for installing a Combine Heat and Power (CHP) a minimum power of 1MW should be installed for the plant to be efficient (Chapter II). An installed power of 1 MW can be achieved by burning 94 kg of oil per hour with an efficiency of 90%. This quantity of oil corresponds to 45.1 m³ of waste MWF5% treated per day. This corresponds to a relatively large plant. In comparison General Motors in Mansfield, Ohio, USA employed 3,500 people and produced 151 m³ per day in 1989. Nowadays, economical and environmental considerations lead companies to recycle their fluid, cutting the fluid spent by 30 to 50 %.

Three solutions to solve the issue of discrepancy between the amount of oil needed to be recovered and the minimum installed power.

The exclusive use of the recovered oil as a fuel can be seen if a boiler or CHP is already in place in the plant and to complement and cut down the amount of fuel used. In the case of General Motors, the treatment would produce 88.5 MWh and suppress the disposal cost associated with oil.

For smaller volumes, the same principle is applicable when an existing system is in place. In the case where a combustion unit (boiler or CHP) needs to be installed, it may be possible to advise a group to burn recovered oil and other waste in a common plant, for example from an estate. Hot water and electricity would be redistributed back to the estate.

The third solution may be implemented when onsite combustion is not possible. The solution consists of finding a contractor that would take the recovered oil for no cost regarding its energetic value of the waste such as a cementery.

c) *Ash analysis*

To be able to use the recovered oil onsite as a fuel, the toxicity of fume and ashes has to be assessed. The ash content measured was 13 grams of ashes per kg of recovered oil. Table V-13 shows the ICP analyses carried out on the ashes. The two main compounds found were iron and sulphur. Vanadium may cause corrosion problems but appears in very little quantity. Toxic metallic compounds (shown in bold in Table V-13) that are present in little quantity apart from lead.

The oil has been burned at 850°C and therefore some volatile metals such as mercury may have been lost during calcinations. Nevertheless, zinc which is also a volatile, low boiling point metal, is measured at a non negligible quantity. Therefore, despite high temperature used to burn the reclaimed oil the loss in volatile metal may be considered to be minimum.

The values give an example of the composition of bottom ashes from reclaimed oil after acidification. The main concern is the presence of sulphur, which indicates the production of sulphur oxides in the combustion exhaust gases that may need post treatment. Some studies proposed catalyse ways to remove the sulphur of lubricant recovered oil to remove sulphur (Bhaskar, *et al.* 2004) proposed a system using ion oxide.

The trace element found in the reclaimed oil will strongly depend on the oil history. The process and the nature of the metal tooled will play a major role in the metal content of the oil. Therefore, any consideration to use the reclaimed oil as fuel on site must be followed by strict analyses of the ashes and fumes content. Nevertheless, if any element is found in excess, using the reclaimed oil blended with another fuel may eliminate the problem, especially if an existing boiler or CHP plant is in used within the plant. This method has two effects; diminishing the quantity used it cuts down the

fuel cost and by diluting the reclaimed oil, a suitable blend for combustion can be achieved.

Analyte	Analyte per gram of ash ($\mu\text{g/g}$)
Vanadium	1
Chromium	6
Ion	1260
Nickel	18
Copper	336
Zinc	160
Cadmium	Below LLD
Calcium	770
Sodium	820
Lead	473
Aluminium	647
Sulphur	2865
Gold	4
Potassium	630
Magnesium	96
Palladium	Below LLD

Table V-13: Ash analyses of recovered oil

LLD; Lower Limit of Detection

V.4 SYNTHESIS

These experiments helped in the understanding of each step of the completed process, giving indications on the nature of the waste effluent and its behaviour. Two methods of chemical treatment have been studied and were proposed as an alternative to membrane separation technology. Both chemical methods are proven to be even more effective when used with the filtration concentrate. Therefore, chemical treatment can be used as an onsite treatment for the concentrate produced during filtration of the waste metalworking fluid. This method can be justified by the volume reduction of the waste to be chemically treated, by the production of a valuable fuel and finally by the possibility of returning the aqueous phase back into the filtration process.

CHAPTER V Waste characterisation, chemical treatment and fuel 109

	V.1	Introduction	109
	V.2	Fluid characterisation	109
V.2.1		Characterisation of the concentrate	110
V.2.2		Zeta potential measurement	111
V.2.3		Droplets size distribution	112
V.2.4		Concentration stability	118
V.2.5		Fluid viscosity	119
V.2.6		Recapitulation	119
	V.3	Chemical treatments	120
V.3.1		Inorganic salts	120
V.3.1.1		Fresh metalworking fluid flocculation	121
V.3.1.2		Concentrate coagulation	124
V.3.2		Acidification	132
V.3.2.1		Concentrate acidification	133
V.3.2.2		Fresh MWF 20% acidification	137
V.3.2.3		Alkaline treatment	138
V.3.3		Calorific value	140
V.3.3.1		Results	140
V.3.3.2		Discussion	141
	V.4	Synthesis	145

CHAPTER V

Figure V-1: Relationship between refractometry method and concentrate TOC measurements	110
Figure V-2: Microemulsion zeta potential	111
Figure V-3: Measurement of oil droplet using RO water at low count rate	114
Figure V-4: Droplet size distribution with RO water at high count rate	115
Figure V-5: Droplet size distribution with RO water as dilutant high count rate	116
Figure V-6: Droplet size when UF permeate is used as dilutant	117
Figure V-7: Picture of the different oil fraction after standing for 72 hours	118
Figure V-8: pH evolution during addition of aluminium sulphate	124
Figure V-9: Gibbsite Octahedral structure describing the layer of $\text{Al}(\text{OH})_3$	127
Figure V-10: Illustration of aggregated and merged droplets	128
Figure V-11: New emulsion equilibriums case of surfactant impoverishment	131
Figure V-12: New equilibrium case of surfactant enrichment	132
Figure V-13: Waste metalworking fluid after acidification n°2 showing the 3 phase obtained	133
Figure V-14: pH evolution during the fifth acidification vs. volume of acid poured	135

Figure V-15: pH evolution when adding progressively acid	136
Figure V-16: pH evolution after adding acid directly	136
Figure V-17: pH evolution vs. acid addition for fresh MWF20%	138

CHAPTER V

Table V-1: Results from the 4 measurements of the zeta potential of Mobilcut 232 at 5%	111
Table V-2: Refractive index	113
Table V-3: Droplet size analysis	114
Table V-4: Size value of oil droplet	115
Table V-5: Size value of the oil droplets	116
Table V-6: Size value of the particles	117
Table V-7: Description of the different phases found when oil ratio increases	118
Table V-8: Viscosity of different effluent	119
Table V-9: Apparent colloid characteristic constants for fast flocculation	121
Table V-10: Theoretical ratios, $R_{\text{turbid/clear}}$, for complex concentrations forming at the nominal MCl_3 concentrations leading to the onset of turbid overdosed solution and clear flocculate solution flocculate, for three different complex stoichiometries n .	123
Table V-11: Results from acidification tests	134
Table V-12: Comparison of calorific values	140
Table V-13: Ash analyses of recovered oil	144

CHAPTER VI

MEMBRANE FILTRATION

CHAPTER VI

Membrane Filtration

VI.1 INTRODUCTION

The first part deals with the results obtained during the small-scale filtration study. The feasibility of using membrane filtration technology is discussed. Antifouling methods are studied. The first method is the optimisation of membrane washing cycles using micellar solution and the second is the use of two phase flow. The results of gas injection during metalworking fluid filtration are discussed.

Membrane filtration is used for separating oil from water and treating waste metalworking fluids. This work presents two different filtration systems. The first system consists of direct filtration of MWF using two ultrafiltration (FP100 and FP200) and one nanofiltration (AFC30) membrane. The second system consists of ultrafiltration membranes followed by a nanofiltration membrane. Filtration experiments are carried out in a large-scale, semi-batch process of volume 180 litres described in Chapter II. The performances of each filtration system are discussed and compared. A number of factors, such as concentration polarisation and fouling via deposition, pore blocking and macromolecular adsorption can limit this technique. Oil droplets are transported and eventually captured at the membrane surface, causing a drastic increase in the local concentration of particles, a gradual fouling and a consequent reduction in permeability.

In this study, a large-scale tubular membrane unit is used for the treatment of a semi-synthetic MWF. The effects of a number of parameters affecting permeate flux and quality are investigated. These parameters include trans-membrane pressure (TMP), fluid velocity in the membrane tube, concentration ratio in the re-circulating feed stream and the molecular weight cut-off (MWCO) of the membranes.

Two models are investigated; the resistance in series theory and the gel polarisation theory. The study deals with filtration of high oil concentration aiming at increasing the retentate concentration using industrial conditions. This implies that the original

concentration in oil in the feed stream was 5% and increased up to 20% during filtration. The feed temperature increases during filtration with varying permeate flux and membrane retention as it has been shown in Chapter IV. Under these conditions, the gel layer plays an important role.

The aim of this study is to optimise the filtration operation in order to obtain a permeate quality level acceptable for treatment using an aerobic bioreactor. Performances of the filtration stage limit fouling and improve permeate quality.

The experiments at large scale were first carried out as recommended by the rig manual (Appendix C). These conditions are referred to as “cardev conditions” the results are presented and discussed in section VI.3. The second part presents the results obtained during direct MWF filtration carried out under lower TMP conditions. The third part presents the results obtained using the combination UF-NF filtration, using independently FP100 and FP200 as NF pre-treatment.

VI.2 SMALL-SCALE FILTRATION

This section deals first with the filtration carried out using flat sheet membranes, dead-end nanofiltration and flat sheet cross flow ultrafiltration membranes. The second part presents the results from small-scale tubular membranes.

VI.2.1 Flat sheet membranes

These experiments helped to assess the feasibility of treating Mobil cut 232 fluids using membrane technology. The experiments that have been carried out are described in this section. Their performances are compared with the flocculation process in the conclusion of this chapter.

VI.2.1.1 Dead-end filtrations

The dead-end filtration was used to filter the supernatant produced by flocculation using two nanofiltration membranes BM-05D of 500 Da and BM-20D of 2000 Da. AFM images and pores size distribution of these membranes are shown in chapter IV.

The initial water flux was determined for both membranes used in this study, BM-20D and BM-05D. The demineralised water used here has a conductivity of 0.3 μs . The measured water fluxes had values of $6.94 \pm 0.01 \text{ L/h/m}^2$ for BM-05MD and $12.79 \pm 1.09 \text{ L/h/m}^2$ for BM-20D.

After determining the water fluxes for both membranes, the obtained supernatant from the flocculation step (section V3.1.1. chapter V) had a TOC of 5715mg/L and was used as the feed. Filtration was carried out in a dead-end filtration unit at 4.75 bar and stirrer speed of 300 rpm. The resultant permeates from the BM-05D membrane have fluxes of $2.54 \pm 0.25 \text{ L/h/m}^2$ and TOC of 4356 mg/l, while BM-20D membrane has a flux of $6.65 \pm 0.73 \text{ L/h/m}^2$ and a TOC of 3832 mg/l.

The water flux was measured again through both membranes; the data from these measurements were compared with initial water fluxes to assess the extent of the fouling of both membranes. As shown in Figure VI-1, the water flux was reduced for the BM-05D membrane whereas an increase was noticed for this flux when the BM-20D membrane was used, shown in Figure VI-2. Similar behaviours were observed when both membranes were reused for filtering the supernatant from flocculation for the second time; again the water flux was noticed to increase slightly for BM-20D and decrease for the BM-05D.

The water flux experiments have been repeated several times for each case. The experimental errors are shown as error bars in Figure VI-1 and Figure VI-2 which show the data for all experiments.

For the BM-20D membrane, the values of water flux shows that the flux has been fully recovered with a slight increase each time when the membrane was filtered with demineralised water as shown in Figure VI-2. The most probable reason for that is that the fouling occurring from supernatant filtration is a surface fouling, causing a layer of

deposited material on the membrane surface. Subsequent filtration with demineralised water managed to remove this layer.

In the case of the BM-05 D membrane, the fouling is a combination of both surface fouling and pore blocking. Subsequent filtrations with demineralised water recovered some of the flux, 66% of the initial demineralised water flux after the first effluent filtration and 52% after the second effluent filtration was recovered. These two demineralised water fluxes were still higher than the flux of the effluent. This increase in flux is due to the removal of the fouling layer on the membrane surface. However, the recovery of demineralised water flux was not 100% compared with the initial demineralised water flux. This is likely to be due to fouling occurring through pore blocking. Figure VI-1 shows a further decrease in demineralised water flux. It is believed that this decrease is due to more pores being blocked after each supernatant filtration through the membranes.

The permeation increase for any run with water that follows a run with effluent for the BM-20D membrane, shown in Figure VI-2, may be a consequence of molecules larger than 2000 Dalton entering the membrane. This may affect the structure of the membrane causing pore enlargement. The structural changes result in increased permeability to small molecules and overall fouling simultaneously. Because of the complex and non-characterised nature of the effluent, information cannot be given on the effect of this process on changes in the cut-off of the membrane with respect to larger molecules.

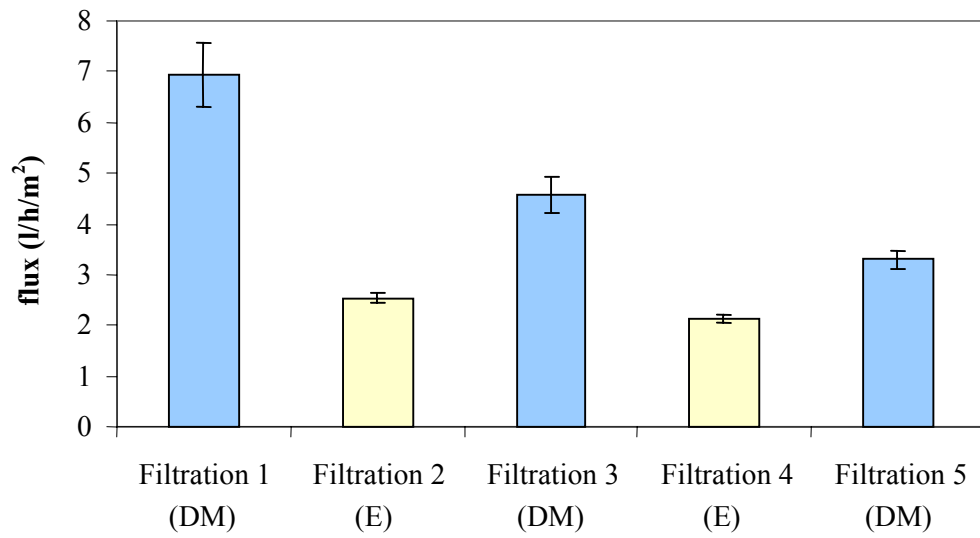


Figure VI-1: Water flux and effluent flux for BM-05D nanofiltration membrane

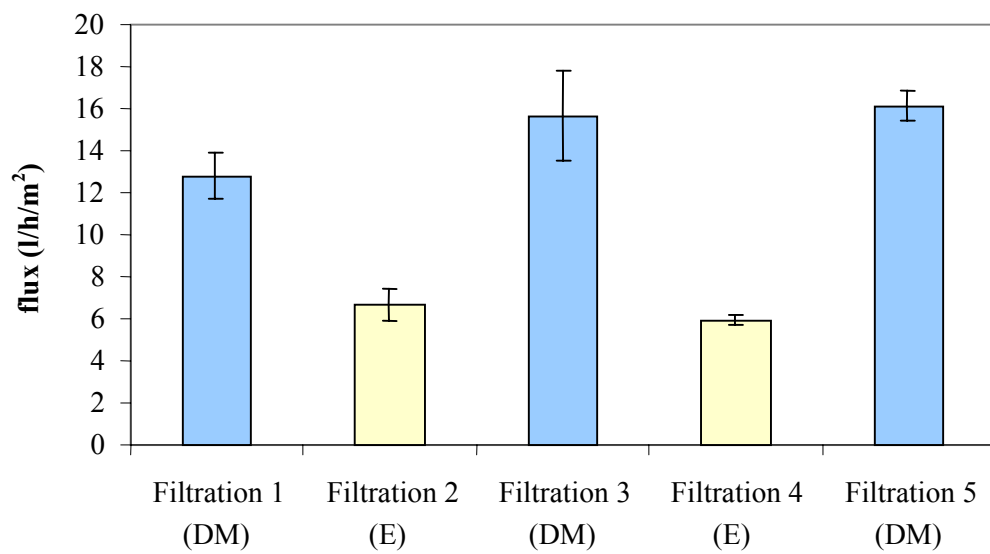


Figure VI-2: Water flux and effluent flux for BM-20D nanofiltration membrane

Where (DM) stands for Demineralised Water and (E) for Effluent

VI.2.1.2 Cross flow flat sheet membrane

The cross flow membrane unit has been used to treat waste metalworking fluid oil concentration of 5%. This has been carried out to compare UF performances with the chemical treatment performances as it has been published by (Hilal, *et al*, 2002). At this stage, no measurement of permeate flux has been carried out in detail.

a) Results

After carrying out the crossflow filtration using Polysulphonate ultrafiltration membrane of 100,000 Dalton, the collected permeate was analysed. Total organic carbon (TOC) was found to be 5,374 mg/L with a pH of 9.6. The resultant permeate from this membrane had much lower TOC than the feed which has a TOC of 44,209 mg/l. The pHs of both the feed and the permeate were the same at 9.6. It is worth noting that the permeate has a yellowish colour and was much clearer compared to the feed which has a milky appearance.

b) Discussion

These preliminary tests show that ultrafiltration is an effective way of treating oily wastewater. The technique shows similar performances to the one found for the chemical treatment employing aluminium sulphate. However, more investigations presented below using tubular membranes were carried out to improve the technique.

VI.2.2 Tubular membrane

The large-scale filtration system described in Chapter III uses a cross flow tubular membrane. Therefore, a study of the cross flow filtration of Mobil cut 232 has been carried out in order to determine the effect of different parameters on the ultrafiltration of the waste effluent. The study of the effect of temperature and pressure has been carried out as well as an optimisation of the washing cycle.

VI.2.2.1 Effect of temperature

The effect of increasing feed temperature on the permeate has been studied using FP100 and FP200 ultrafiltration membranes. Figure VI-3 and Figure VI-4 show the filtration of MWF5% at different temperatures using ultrafiltration membranes FP 100 and FP200 respectively. In both cases, increasing the feed temperature increases the initial permeate flux. Nevertheless, concentration polarisation establishes itself and the permeate flux decreases progressively. This decrease is due to the feed concentration increasing which induces the effect of concentration polarisation.

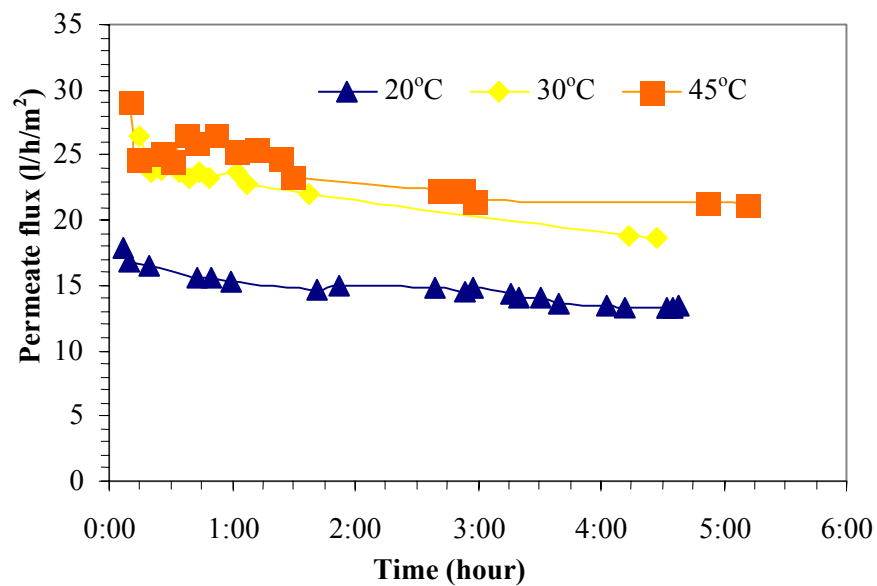


Figure VI-3: Permeate flux of ultrafiltration membrane FP100 at 3 different temperatures

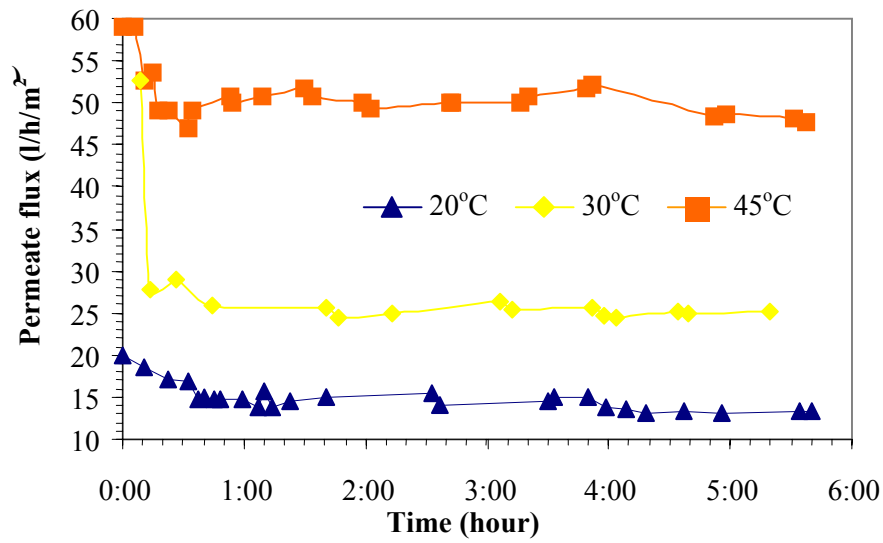
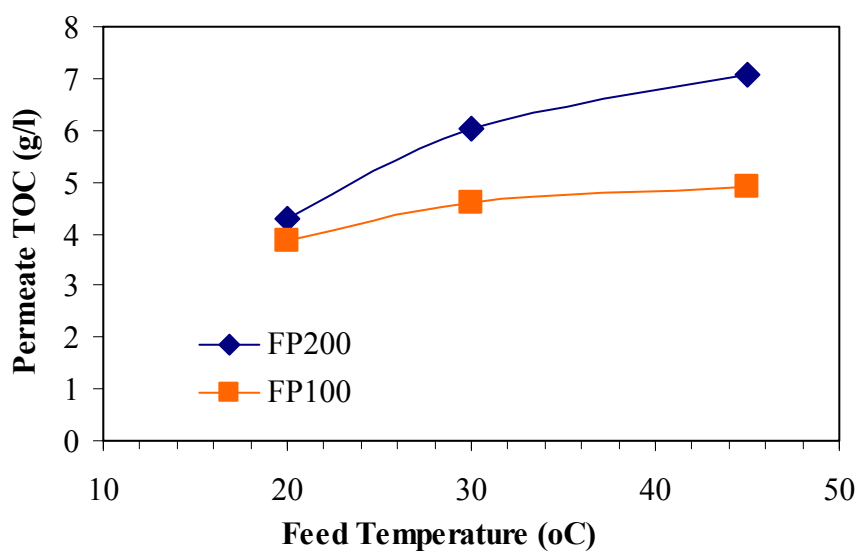


Figure VI-4: Permeate flux of ultrafiltration membrane FP200 at 3 different temperatures

Figure VI-5 compares the fluxes obtained from both membranes at temperatures 20°C, 30°C and 45°C. The values shown in Figure VI-5 were the average flux over 200 ml of collected permeate. It can be seen from Figure VI-5 that the FP200 ultrafiltration membrane has a flux 40% higher than the FP100 at 20°C. Figure VI-5 also shows the flux has increased by more than 50% for both membranes when the feed temperature was raised from 20°C to 45°C. At the same time, the quality of permeate was dramatically affected.



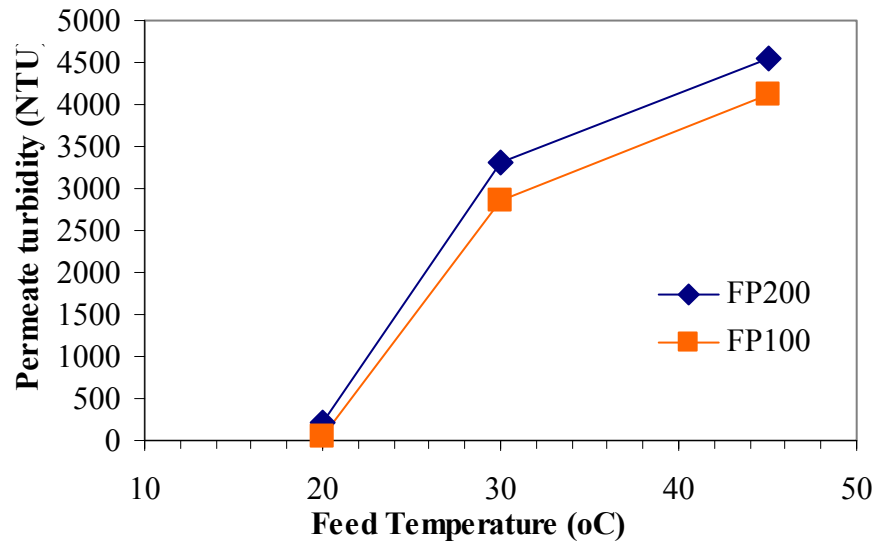


Figure VI-6 and

Figure VI-7 show the Total Organic Carbon (TOC) and the turbidity of the permeate from both membranes. More oil and organic matter were passing through the membrane pores when the feed temperature was increased. This may be attributed to the solubility of the oil in the hot water was better and the viscosity of the fluid decreased with the temperature, allowing the oil to pass through the membrane and produce an emulsion with lower oil concentration on the permeate side (Simon and Tragardh, 2000).

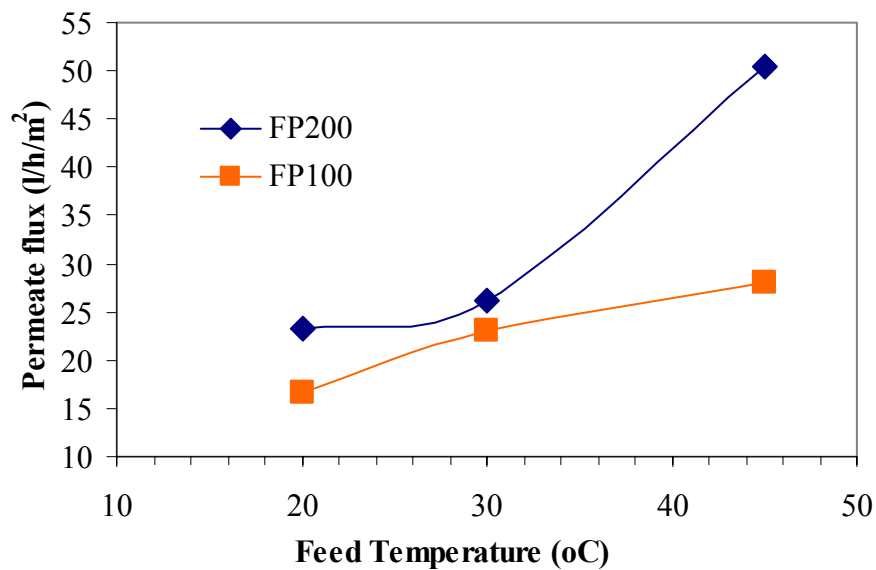


Figure VI-5: Permeate flux vs. feed temperature after 1-hour filtration

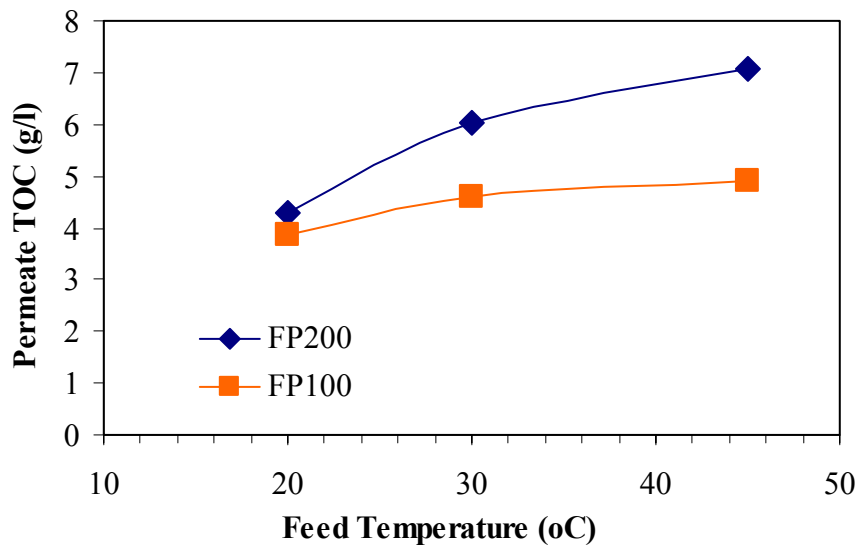


Figure VI-6: Permeate TOC vs. feed temperature after 1 hour filtration

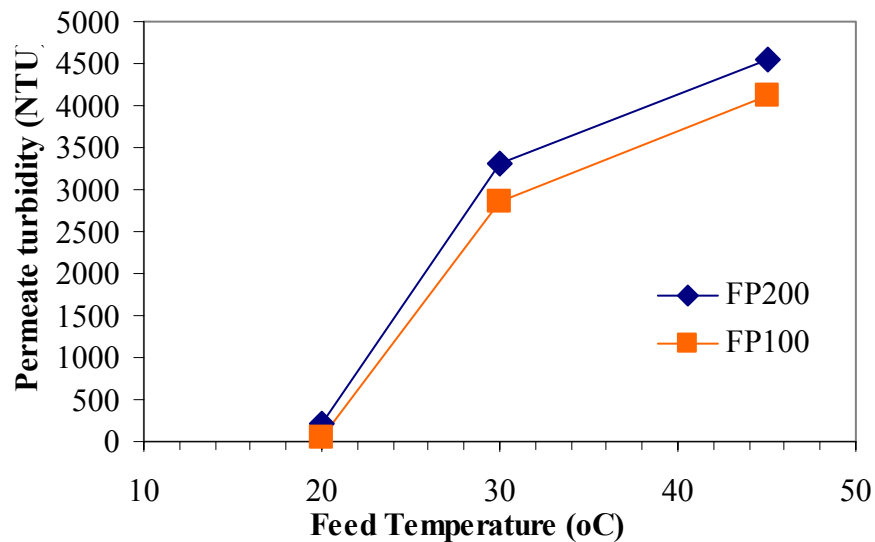


Figure VI-7: Permeate turbidity vs. feed temperature after 1 hour filtration

In industrial membrane processes, the permeate is not usually recycled into the filtration process. Therefore, the feed stream, which only consists of the re-circulated concentrate, is concentrated and rejected species increased. In this case, the oil concentration increases during the filtration. Figure VI-8 shows a comparison between the resultant permeates from FP200 UF membrane in both recycling and concentration systems. Both curves in Figure VI-8 were almost identical until a point where the feed stream concentration has an impact on the permeate flux, leading to a larger decrease

than recycling. The start of the rapid decrease in permeate flux was caused by the concentration polarisation, due to the accumulation of oil droplets on the membrane surface. Then the rate of flux decrease slows down due to membrane fouling. In the case where the permeate was recycling, the permeate flux arrives at a steady state with the fouling effect at 15 L/h/m^2 . A further decrease in the permeate flux, when there was no recycling, was due to an increase in the concentration ratio in the re-circulation loop with an increase in the gel layer resistance (Lee, *et al.* 1984).

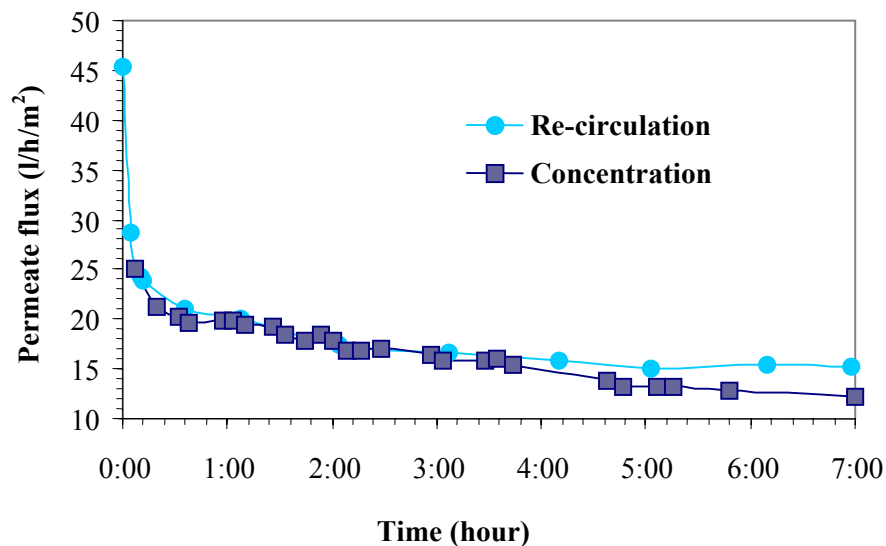


Figure VI-8: Comparison of permeates flux between re-circulation and concentration regime

VI.2.3 Washing cycles

The efficiency of washing cycles and the effect of surfactant on MWF filtration are studied in this section. The experimental plan used is presented in Chapter III. Results obtained from this study show that Cold water Flux (CWF) of demineralised water varies from 805 to 362 L/h/m^2 . This wide variation in the results indicates that at least one of the factors studied has an important effect on the efficiency of membrane regeneration. Table VI-2 shows the estimation of the importance of each factor investigated. Table VI-2 shows that the washing temperature (factor X2) was the predominant factor and when the washing temperature was raised from 40°C to 60°C , the CWF increased on average by 177 L/h/m^2 . The circulation velocity (factor X6) was

surprisingly negative. This means that when the velocity of washing solution in the membrane tube was raised from 2.7 to 3.6 m/s, the CWF decreases by 101 L/h/m² on average. An increase in feed velocity will increase the turbidity of the fluid. This was a favourable condition to wash away the oil from the membrane surface (Darko, *et al.* 2002) and (Noordman, *et al.* 2002). These results can be explained by the fact that when the valve was fully open to give full speed of 3.6 m/s, an inlet pressure of 1.3 bar and an outlet pressure of 0.7 bar were measured during the whole washing cycle. At lower velocities, no inlet or outlet pressures were noticed. This may be attributed to the fact that surfactant fouls the membrane when pressure exists in the system at high velocity. Washing time (factor X3) and applied pressure during the washing cycle (factor X5) have similar importance and were both positive as shown in Table VI-2. As for the application of pressure (factor X5), it was more difficult to interpret because of interactions between pressure variations and the velocity of washing solution. The surfactant concentration (factor X1) has the smallest value as shown in Table VI-2 and does not seem to be significant.

An increase in surfactant concentration from 0.5% to 1.5% led to a small increase in CWF by 51 L/h/m² as shown in Table VI-2. It was evident that surfactant was crucial to clean the membrane as illustrated by the weak performance of a cleaning cycle without surfactant experiment (Table VI-1, experiment 9). This means that a minimum amount of surfactant was needed to clean the membrane. The last parameter, the volume of the washing solution (factor X4), has the smallest effect, as shown in Table VI-2, and therefore should be kept as small as possible in the system under study. Five litres was the minimum volume used in this case. The experimental data taken in the centre of the domain (10th row in Table VI-1) shows a smaller CWF flux to the average CWF calculated in the first column of Table VI-2. This was due to the pressure applied by the system running at full speed causing a higher surfactant fouling.

<i>Experiment number</i>	<i>Factors</i>						<i>Response (CWF L/h/m²)</i>
	<i>X1</i>	<i>X2</i>	<i>X3</i>	<i>X4</i>	<i>X5</i>	<i>X6</i>	
1	1.5	60	45	5	Yes	2.7	805
2	0.5	60	45	15	No	3.6	597
3	0.5	40	45	15	Yes	2.7	362
4	1.5	40	15	15	Yes	3.6	487
5	0.5	60	15	5	Yes	3.6	484
6	1.5	40	45	5	No	3.6	509
7	1.5	60	15	15	No	2.7	611
8	0.5	40	15	5	No	2.7	436
9	0	60	30	10	NO	3.6	207
10	1	50	30	10	NO	3.6	326

Table VI-1: Explicit experimental plan and CWF response

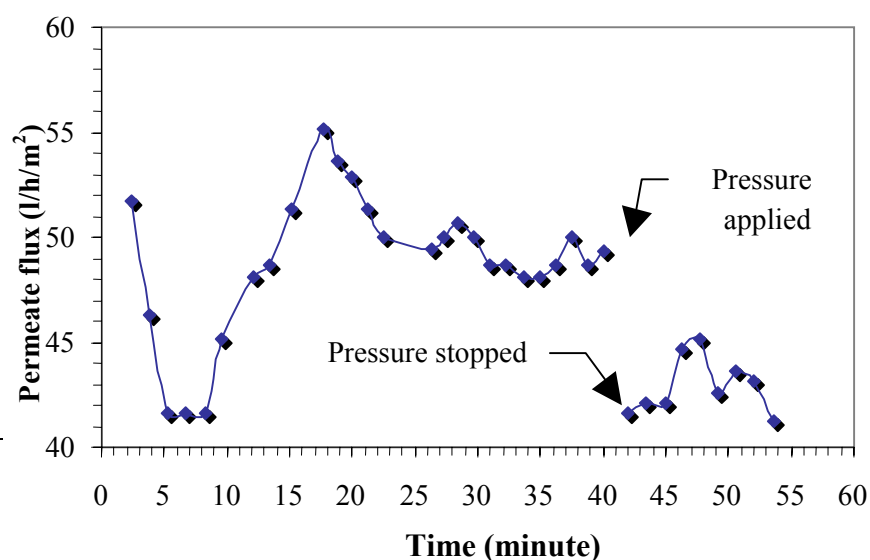
Average of CWF (L/h/m ²)	X1	X2	X3	X4	X5	X6
536.5	25.5	88.5	35.3	14.1	34.8	-50.5

Table VI-2: Evaluation of the average effect of washing condition on the CWF

- ❖ X1: surfactant concentration
- ❖ X2: Washing temperature
- ❖ X3: washing time
- ❖ X4: Volume of the washing solution
- ❖ X5: Pressures Applied
- ❖ X6: Fluid velocity in the membrane tubes

A FP200 membrane was used to filter MWF for six hours, which led to a large reduction in permeate flux, indicating fouling of the membrane. This was followed by a washing cycle without pressure. Figure VI-9 shows the permeate flux of a washing cycle and the effect of pressure. It can be seen from Figure VI-9 that the washing cycle takes place in three phases before applying the pressure. At first, the flux declines for five minutes where the surfactant molecules accumulate near the membrane surface (concentration polarisation) until it reaches a steady state, leading to stabilisation of the flux for three minutes. During this stabilisation, the surfactant interacts with the oil, (2nd phase) which fouls the membrane surface and finally produces a rapid increase in the flux (3rd phase). This was due to the removal of oily fouled material from the membrane surface after which the maximum flux was obtained and the washing permeate flux decreased gradually.

A sudden decrease of 16% in permeate flux can be seen after a pressure of 3 bar was applied for one minute. This decrease was not recovered with time. This sudden decrease may be interpreted by the fact that the washing materials have fouled the



membrane.

Figure VI-9: Permeate flux during washing cycle and effect of applying pressure

Figure VI-10 shows the filtration of MWF using FP200 with eight periodic washing cycles each after 6 hours using a concentration loop mode. The regeneration of the membrane was efficient in all cases. The permeate flux decreased sharply in the first few minutes. This decrease was less sharp as the number of washing cycles increased and may be due to the adsorption of surfactant onto the membrane surface or within the membrane pores. The quantity of permeate collected during the first hours was 500ml for the initial filtration when the membrane surface was not in contact with the surfactant. This increased with washing cycles to reach 800 ml after the eighth washing cycle (Belkacem, *et al.* 1995).

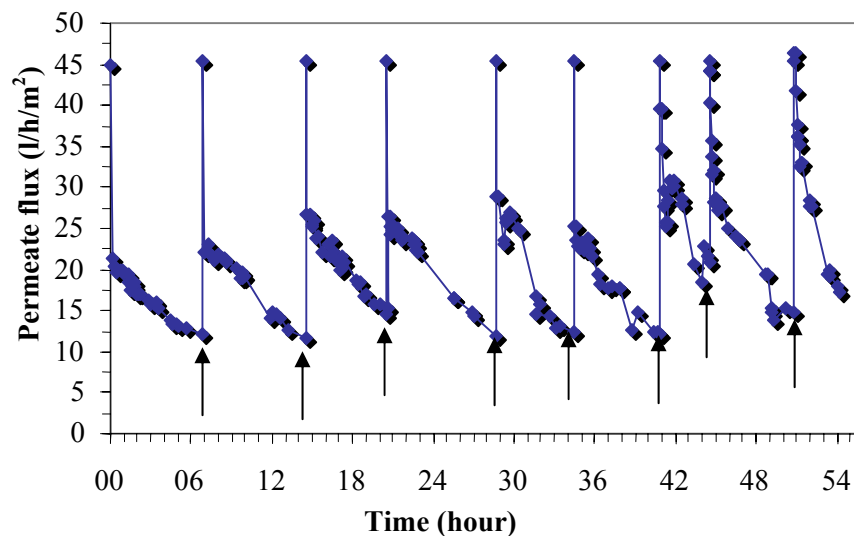


Figure VI-10: Filtration of MWF5% after successive washing cycle

Figure VI-11 presents a comparison between the permeate flux of metalworking fluid using two FP200 membranes, one pre-washed with surfactant, the other pre-washed with tap water. The data was collected over a three hour period. Figure VI-11 shows the protective effect of the surfactant used to pre-wash the membrane compared with that pre-washed with water. The most probable reason for this was that the surfactant

was effectively adsorbed onto the membrane surface preventing fast fouling by the oil emulsion. It can be seen from Figure VI-11 that the permeate flux started to increase after 3 minutes, a behaviour that has been seen earlier in Figure VI-9.

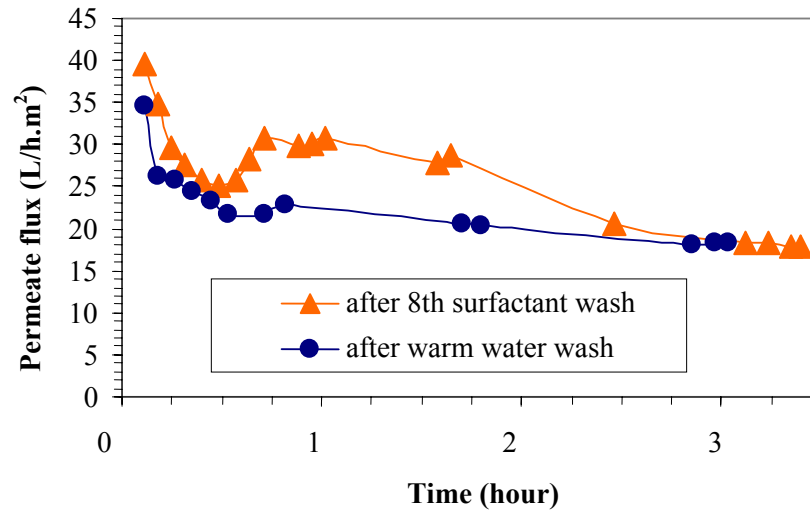


Figure VI-11: Effect of surfactant used during washing on metalworking fluid filtration

The necessity of using a surfactant (Micellar solution) to clean the surface of the PVDF ultrafiltration membranes has been demonstrated and found to be effective. However, the amount and concentration of surfactants play a crucial role in membrane fouling. In addition, they have a preventive anti-fouling effect that has been observed and two major factors have been identified for cleaning membrane surface after the filtration of metalworking emulsions: temperature of the washing cycle and an optimal concentration of surfactant.

The study of the mechanism to regenerate the membrane surface fouled by the microemulsion using micellar solution indicates that an oily layer build-up onto the membrane surface during filtration. This layer can be removed efficiently by dissolving it into the washing solution.

VI.2.4 Gas injection

Turbulence in a tubular module can be introduced by injecting air in the membrane unit via a T-junction in order to create gas slug flow during filtration process. The small-scale equipment presented in Chapter III was modified (Figure III-10) to enable the testing of injecting gas in the filtration system of ultrafiltration of MWF in order to enhance the filtration by removing or disturbing the concentration polarisation layer (Cui and Wright, 1996). A diagram has been presented in the experimental equipment and procedures chapter (Figure III.11). The modified module is fitted with a single tube ultrafiltration membrane FP200 29.4 cm long. Firstly, the behaviour of the permeate water flux when injecting air during filtration was investigated and the effect of gas injection on the permeate flux during MWF5% filtration was studied.

VI.2.4.1 Gas injected during reverse osmosis (RO) water filtering

The influence of gas injection on permeate flux of filtering a two phase water/air flow is tested using reverse osmosis water with a conductivity of $0.11\mu\text{S}$. Reverse osmosis water gives no concentration polarisation and has a constant permeate flux under constant TMP. Therefore, any variation in permeates flux that appears during RO filtration can be interpreted as a gas phase effect.

a) Results

Figure VI-12 shows the result of reverse osmosis water filtered at a TMP of 2.75 bar and a temperature of 20°C . During gas injection, a drop in cross membrane pressure is observed. This is corrected by opening the back pressure valve. The gas is injected at 3 bar at a distance of 1 meter from the membrane inlet. This pressure is taken as membrane inlet pressure and the pressure measured at the outlet is 2.5 bar. RO permeate flux variations during gas injection show a difference of 5% at most.

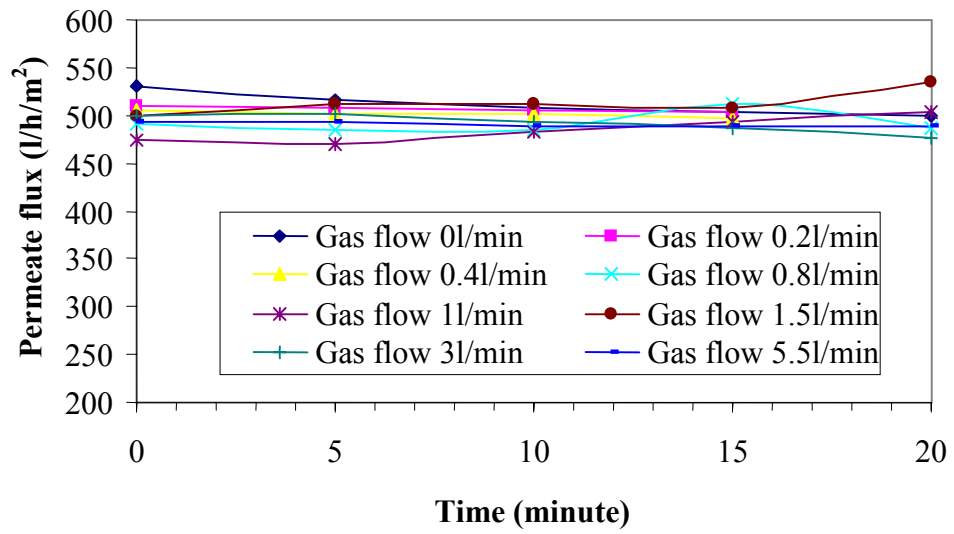
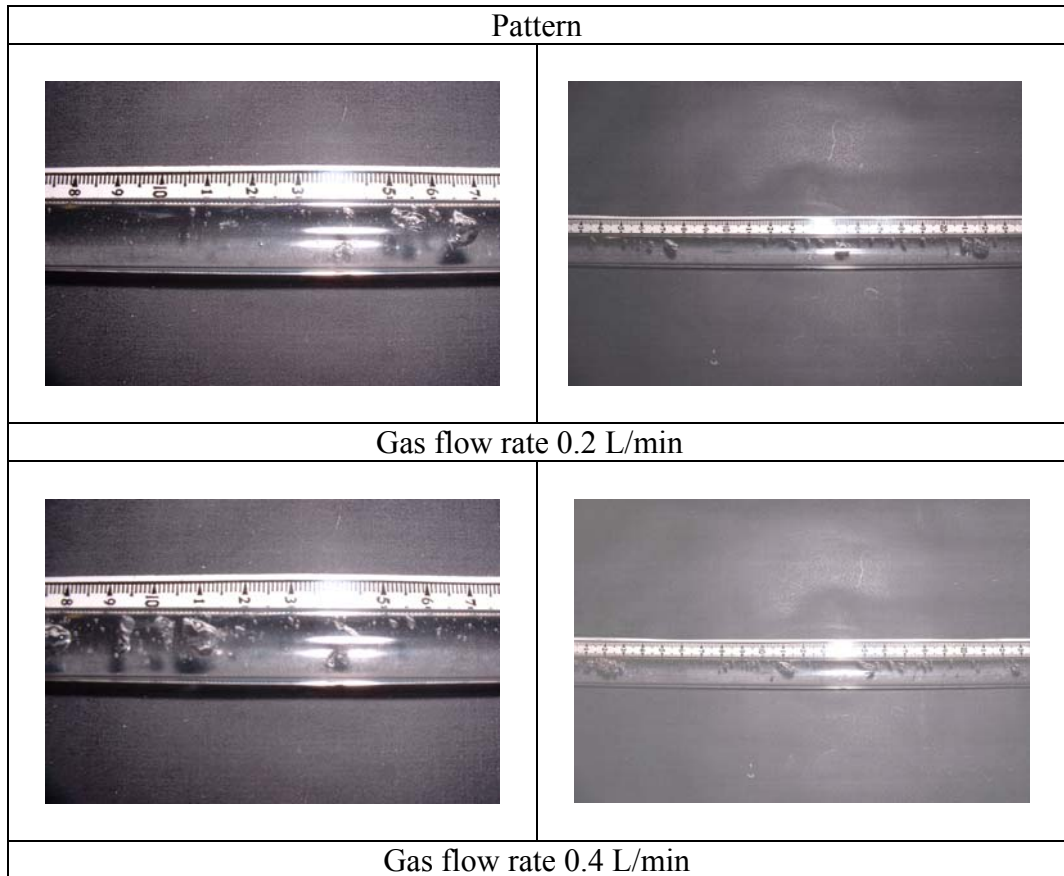


Figure VI-12: Permeate flux of demineralised water filtered with FP200 when gas is injected

Table VI-3 shows photographs taken in the clear tube placed prior the membrane unit (as describe in Chapter III Figure III-11). The flow pattern and the size of bubbles created were measured.



	
Gas flow rate 0.8 L/min	
	
Gas flow rate 1.0 L/min	
	
Gas flow rate 2.0 L/min	
	
Gas flow rate 3.0 L/min	

Table VI-3: Two phases flow pattern corresponding to the gas flow rate

Table VI-3 shows the range of flow pattern that may be produced by the system set up. This range varied from 0.5 cm individual caps shape bubbles running at top of the horizontal tube to 5 cm slug flow when the gas flow rate increases.

The turbulence created by the wake of the passing air bubble is expected to disturb the gel layer that is formed on the membrane surface during filtration.

b) Discussion

The injection of gas at low or high rates under of the experimental conditions does not affect the water permeate flux. This result was expected because demineralised water filtration does not induce any concentration polarisation effect. Nevertheless, the experiment shows that the small bubble created and the gas dissolved in the water do not affect the permeate flux under the experimental conditions. Adjusting the backpressure valve to correct the TMP to its original value compensates the pressure drop induced by the injection of gas. The gas flow rate induces a different flow pattern as shown in Table VI-3. Small bubbly flow to slug flow was observed. The gas dissolved in the water does not interfere with the water flux during filtration. Therefore, any effects observed during metalworking fluid filtration when gas is injected can be attributed to the injection of gas.

VI.2.4.2 Gas injected in during MWF5% filtration

Turbulences created by the wake of the passing air bubble are expected to disturb the gel layer that is formed on the membrane surface during filtration.

a) Results

Figure VI-13 below shows the permeate flux measured when MWF5% is filtered with an ultrafiltration membrane FP200. It also shows that the flux is enhanced when gas bubbles are introduced. Nevertheless, increasing gas flow do not affect the filtration permeate flux.

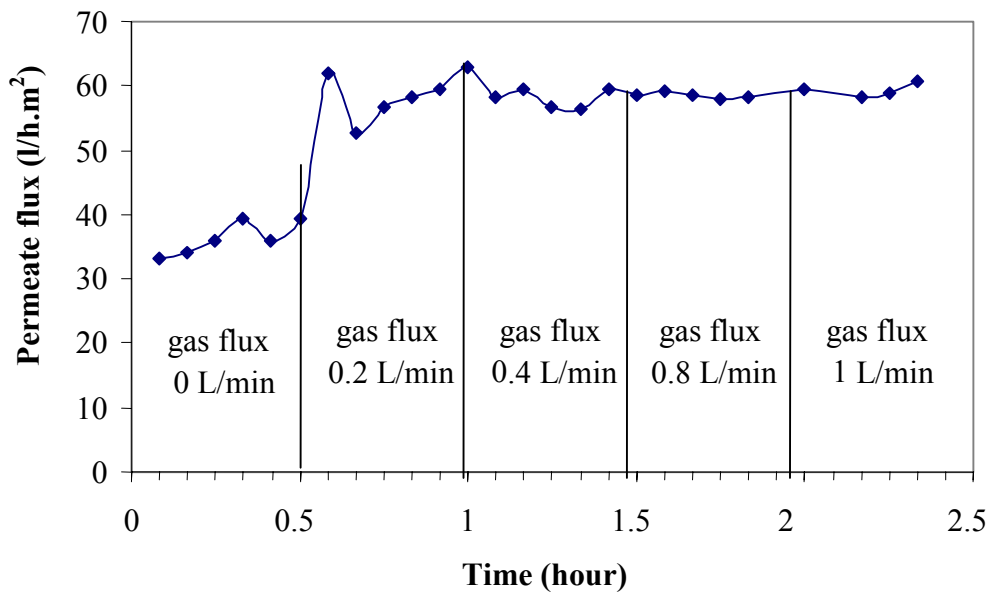


Figure VI-13: Permeate flux when using a two phase flow

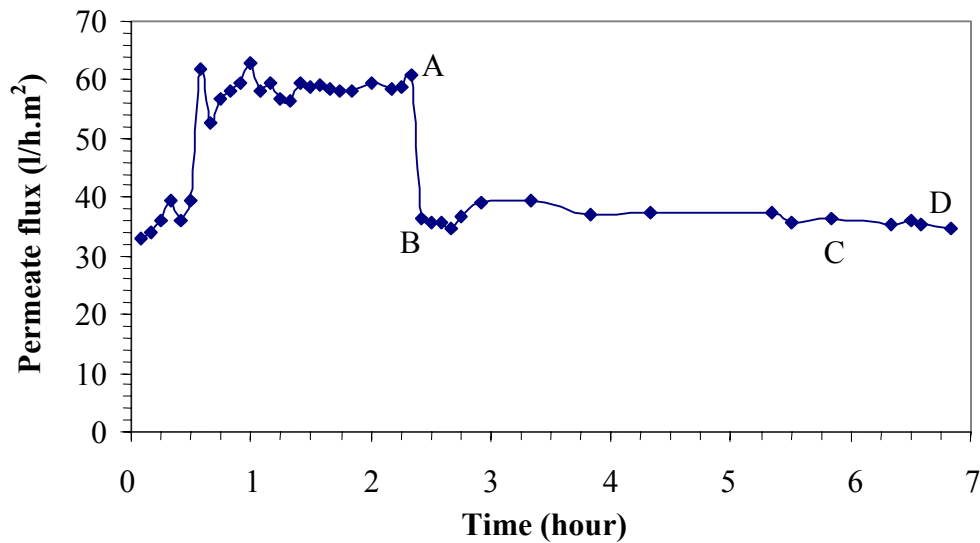


Figure VI-14: Filtration of metalworking fluid after gas injection has been stopped

Figure VI-14 shows MWF5% filtration after stopping the gas injection filtration overnight in **A** and started the next day in **B**. From **B** to **C** no gas is injected. Without any gas injection, no difference in permeate flux is noticed, the permeate flux of MWF5% is similar to the one measure the previous day. At **C** gas is injected at a flow of 1.0 L/min and at **D** the filtration is terminated after 7 hours. In this last case between **C** and **D**, no effect of the gas injected is observed.

Figure VI-15 shows the evolution of the MWF5% turbidity after it has been mixed with gas at 3.5 bar for 15 min. Then sample turbidity is immediately measured. During the first seconds of turbidity measurement the solution gas/emulsion is so turbid that the measure is saturated. At 30 seconds, a turbidity value of 6500 NTU was measured. The solution lost its gas and returned to its original turbidity value of 1200 NTU in 3 minutes. This experiment shows that when the microemulsion is mixed with pressured gas, part of the gas dissolved in the liquid phase and stayed locked in solution. It took 3 minutes for all the bubbles to separate from the emulsion, whereas for demineralised water this is practically instantaneous.

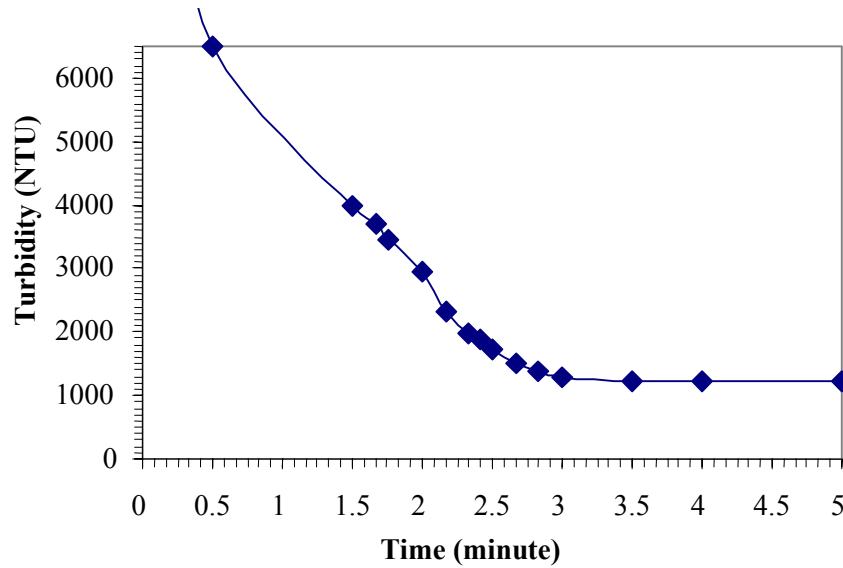


Figure VI-15: Turbidity of MWF5% when air has been injected at 3.5 bar for 15 min

b) Discussion

There is no improvement in MWF filtration when gas is injected into the tubular membrane. Difficulties appeared because of the gas trapped in the emulsion. This is specific to the metalworking fluids. The reason for this is the presence of surfactant that trapped the dissolved gas delaying the release of the gas bubbles formed when the pressure is released at the outlet of the system. Despite the attempt to release the gas at the same pressure as in the membrane, the enrichment in dissolved gas in the MWF during filtration was inevitable.

The results from both experiments of gas injection during the filtration of demineralised water and of MWF5% show that using gas injection to enhance the filtration of metalworking fluids and more generally of surfactant solutions is not straight forward. Negative effects during filtration process arose from the dissolution of gas in the liquid phase that is sequestered by the surfactant creating a sol-gel.

A second explanation that can be given for the drop in permeate flux is when gas is injected. The formation of a film was observed on the clear tube when metalworking fluid was filtrated and gas injected. Figure VI-16 show the photograph of the clear tube after MWF filtration and after demineralised water has been used to flush the system.

A thin film of material remains on the tube (left picture) whereas a clean tube is obtained in the case of filtration without gas injection (right picture).

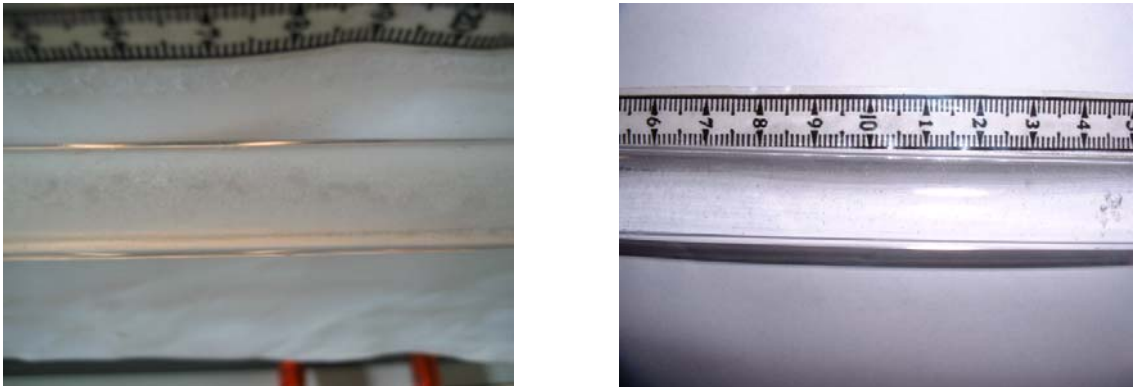


Figure VI-16: Picture of clear tube after MWF filtration with (left) and without (right) gas

(Um, *et al.* 2001) came to similar conclusions in that injecting gas in oily wastewater containing surfactant has a positive effect in promoting turbulences. A negative effect attributed to the masking effect of the effective membrane surface area and occupancy of pores by bubbles. The authors related this negative effect to the gas fraction within the solution.

Tests using MWF5% and higher gas flow rates were briefly setup. An increase in the emulsion gasification when it returns to atmospheric pressure was observed. No immediate benefit on the permeate flux was noticed as shown by (Um, *et al.* 2001). The difference between this work and the work carried out by (Um, *et al.* 2001) is that in this work, the filtration is operated at a much higher TMP of 2.75 bar as opposed to 1 bar. In the present study, the limitation of the gas effect expected is attributed to the change in nature of the fluid filtrate that contains dissolved gas when gas is injected, plugging the pore of the membrane and contributing to the membrane surface fouling.

VI.3 RESULTS OBTAINED WITH INITIAL INSTRUCTIONS

The following experimental parts deal with the large-scale equipment.

The first filtration unit described in Chapter IV, fitted with ultrafiltration membrane FP100, was used according to the instruction manual. The instructions were to filter the waste MWF at inlet and outlet pressure of 8.5 and 7 bar respectively.

Two types of results are presented, the effect of “cardev condition” filtration on the permeate flux and on the permeate quality. In addition, a full filtration process is presented, including three successive batches of filtration. Using FP100 ultrafiltration membrane under “cardev conditions” the 180 litres batch is concentrated, then the tank is replenished with fresh MWF5%.

VI.3.1 Permeate flux

Figure VI-17 shows the permeate flux of fresh metalworking fluid MFW5%. The filtration was carried out at a TMP of 7.75 bar. The initial permeate flux is 64 L/h/m² which decreased dramatically down to 30 L/h/m² after 2 minutes. After 15 minutes, the permeate flux increased to 40 L/h/m², then a constant flux of 34 L/h/m² was observed. After 1 hour and 45 minutes, the flux decreases from 34 L/h/m² down to 22 L/h/m².

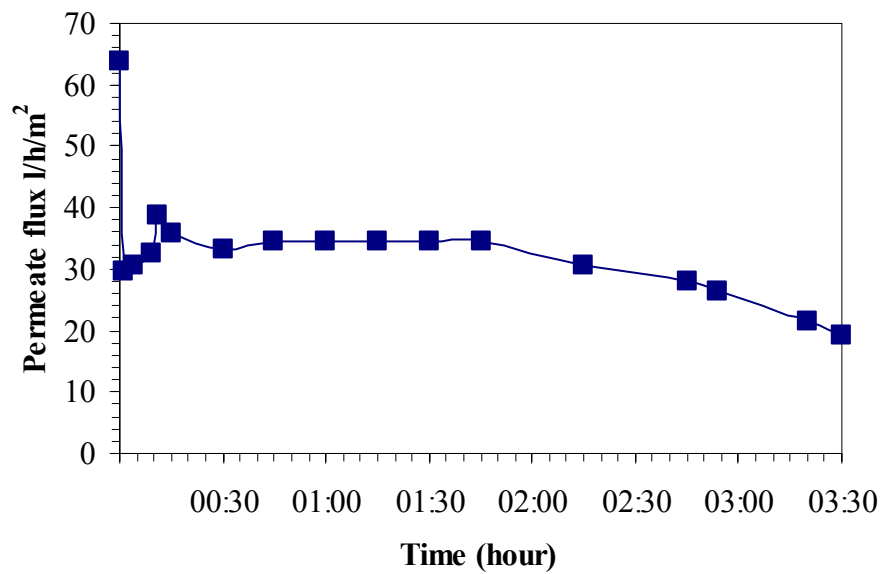


Figure VI-17: Permeate flux of MWF5% filtration with “cardev filtration conditions”

The sharp decrease in permeate flux as soon as the pressure is operated, indicates that under the experimental conditions, the membrane filtration is controlled by concentration polarisation. The increase in permeate flux that follows can be attributed to the fact that the membranes were washed with surfactant solution and flushed before use. The presence of surfactant adsorbed onto the membrane surface can cause an increase in permeate flux during MWF5% filtration. This phenomenon was explained in Chapter IV and it lasted only 15 minutes. Another explanation is that on the large-scale equipment, the temperature cannot be controlled. The feed temperature rises from 21°C to 36°C after 3.5 hours. The study of the effect of temperature on the permeate flux carried at small scale, explained in Chapter IV, indicates that the permeate flux increases with the feed temperature. After 2 hours the permeate flux decreases by 43% from the plateau at 34.5 L/h/m² down to 19.8 L/h/m². The decrease in permeate flux is due to the increase in feed concentration coupled with a stabilisation of the feed temperature.

VI.3.2 Permeate quality

Figure VI-18 shows the evolution of the permeate turbidity during the filtration of the MWF with recommended filtration conditions. The turbidity stays between 200 and 400 NTU during the 2 first hours. After 2 hours, the turbidity increases rapidly until it reaches a value of 1438 NTU.

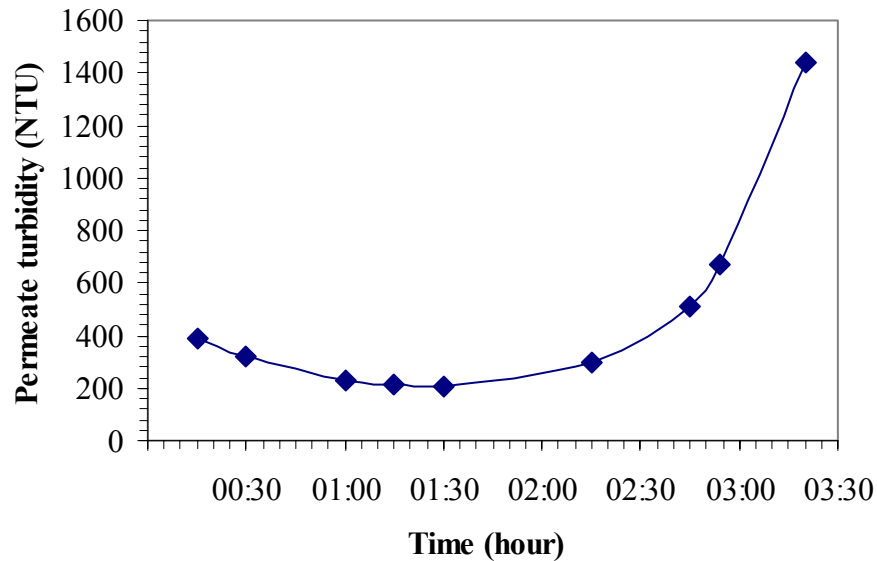


Figure VI-18: Evolution of the permeate turbidity with “cardev filtration condition”

Figure VI-19 and Figure VI-20 show the increase of permeate turbidity in relation to the increase in feed temperature and concentration. Both feed physical properties increases linearly from 21 to 36 °C and from 5 to 12% respectively during the filtration. The increase in feed temperature is due to the pump. The feed concentration increases during filtration.

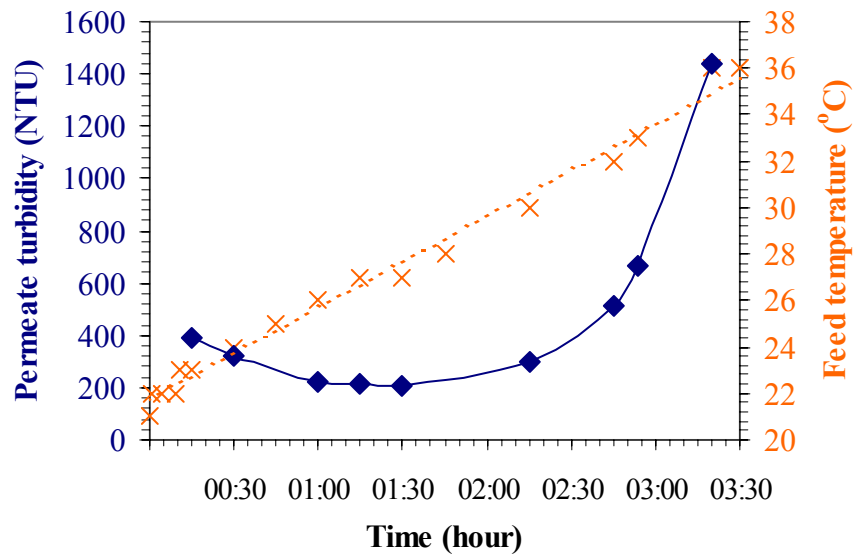


Figure VI-19: Permeate turbidity compared to temperature increase during “cardev filtration conditions”

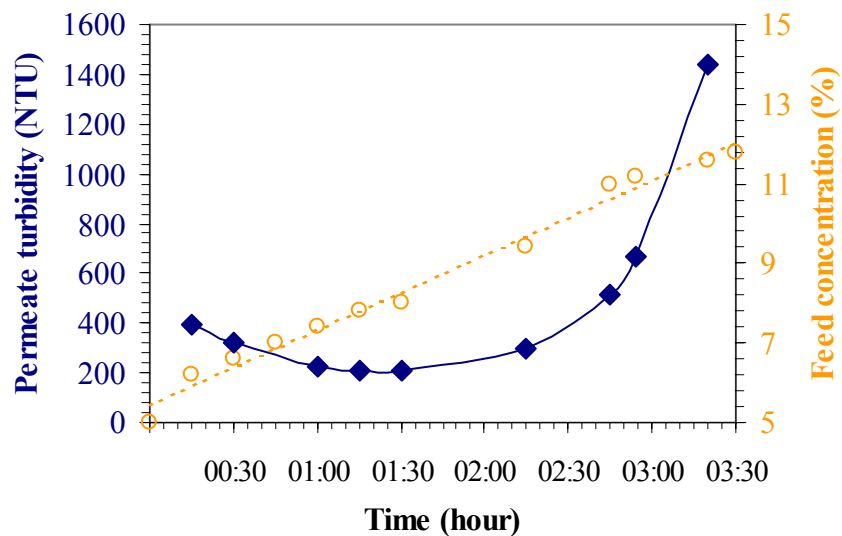


Figure VI-20: Permeate turbidity compared to feed concentration increase during “cardev filtration conditions”

The permeate quality is altered when compared to the filtration done at small-scale. In chapter IV, the permeate was found to have a turbidity of 40 NTU, using in that case a TMP of 2.5 bar. The increase in TMP considerably affects the quality of the permeate that is now at best between 200 and 400 NTU. Three factors contribute to the increase in permeate turbidity. The first factor is temperature, as seen in chapter IV. The second

factor is the feed concentration that also increases during the filtration. Both factors increased linearly during the filtration, whereas the permeate was increasing exponentially after 2 hours of filtration. Therefore, a third factor may be responsible for the increase in permeate turbidity: membrane surface fouling. Figure VI-21 shows the membrane permeate flux (orange curve) and the permeate turbidity (blue curve). After 2 hours, the permeate flux starts to decline due to membrane fouling, in parallel after 2 hours, the permeate turbidity starts to increase. Therefore, the main reason that depletes the permeate quality, under the experimental conditions, may be linked to membrane fouling and more explicitly to the deposition of oil at the membrane surface.

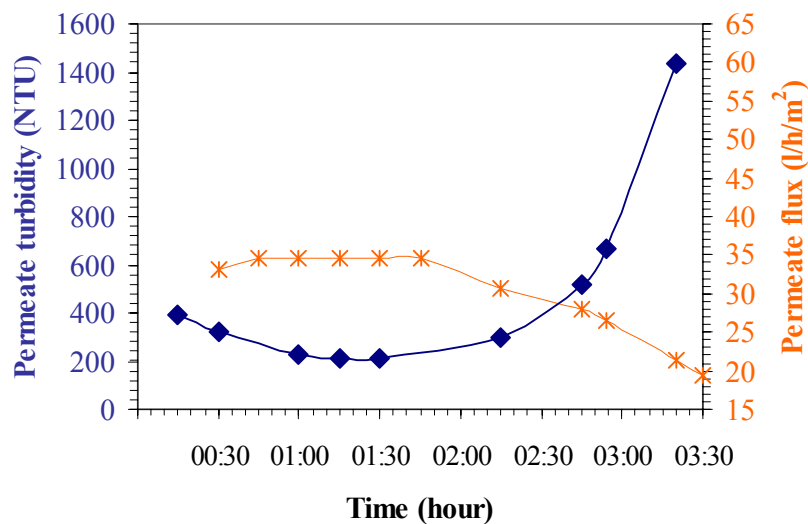


Figure VI-21: Permeate quality and flux decline during “cardev filtration conditions”

After 3.5 hours, 105 litres of permeate has been filtered and 75 litres of concentrate, with an oil concentration of 12%, is left in the filtration unit’s main tank. The filtration process stopped because enough liquid could not be processed. Therefore, the main tank is recharged with 105 litres of fresh MWF5% in order to continue the filtration.

VI.3.3 Effect of reloading the main tank

The new feed obtained has an oil concentration of 8.6% and a temperature of 30°C. The filtration is started again and this process has been carried out twice after 3.5 hours

and 6.5 hours, the main tank is reloaded with fresh MWF5%. Figure VI-22 shows the evolution of the permeate flux (blue curve) and turbidity (orange curve) during MWF filtration using the “cardev conditions” settings (e.g. the filtrations after recharge continue). The black arrows indicate the point at which the main tank was reloaded. After each reload, the permeate flux increases to 35.7 L/h/m² after 5 minutes from the first reload and after 30 minutes from the second reload. In both cases, after the flux increases, the permeate flux declines over the 3 hours of filtration. This decline is due to fouling and retentate concentration.

Figure VI-22 shows that the permeate turbidity increases sharply when the permeate flux decreases. Two maxima turbidity values are measured at 1438 and 1822 NTU just before reloading the main tank. After reload, the permeate turbidity decrease to values below 300 NTU after 45 minutes, and 1 hour after the first and second reload respectively. Three minimum values of permeate turbidity were observed for each part of filtration 209, 210 and 192 NTU.

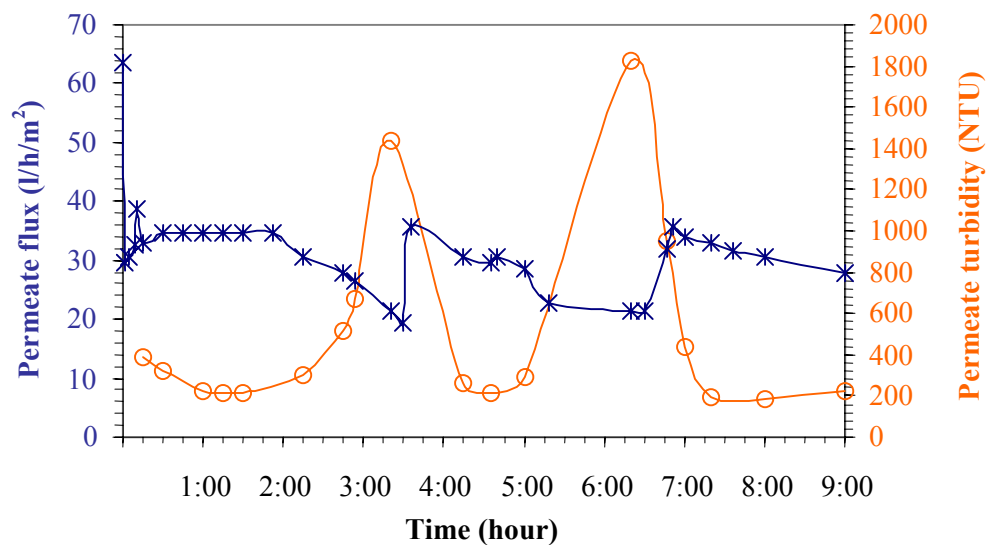


Figure VI-22: 3 Semi-batch UF filtrations with “cardev conditions”, comparison between permeate flux, indicating fouling, and feed turbidity, indicating oil permeation

Reloading with MFW5% dilutes and lowers the temperature of the remaining retentate. The concentration polarisation effect is reduced and less oil fouls the membrane surface. Therefore, the flux and quality of the permeate improved. This phenomenon can be explained by the fact that lowering the retentate concentration lowers the

concentration polarization and helps to dissolve the gel layer. In addition, the permeate quality also improves because of the temperature decrease.

A lag in permeate quality improvement can be observed. This is due to the permeate retained in the membrane housing. The difference in time for permeate flux partial recovery between first reload (5 minutes) and second reload (30 minutes) is due to membrane fouling and pore are blocking. The more the filtration continues, the more the membrane surface fouls and pores become blocked. The oil needs to be removed from the surface and pores to be unblocked. The pores are effectively unblocked at a TMP of 8 bar because the flux is recovered after reloading the feed with fresh MWF5% to a value of 34.5 L/h/m².

Under “cardev conditions”, FP100 ultrafiltration membrane at high TMP is used. The filtration is rapidly controlled by concentration polarisation. The permeate flux decreases with the retentate concentration increasing. The permeate quality is not quite as good as the permeate obtained during small-scale filtration, the main difference being the operational TMP. The maximum concentration ratio achievable is 12%. Above this value the flux decreases and the permeate quality deteriorates rapidly. Therefore, the ultrafiltration of the MWF has to be optimized. The optimisation should take place at a lower TMP and under operating conditions that allow a reduction of the concentration polarization layer.

VI.4 DIRECT FILTRATION

Having carried out MWF5% ultrafiltration using the operational parameters recommended, it has been found that these operational conditions were not optimal. Therefore, improvements of the operational parameters were investigated using FP100 and FP200 ultrafiltration membranes. Filtration of MWF5% and MWF20% were also carried out using the nanofiltration membrane.

It was decided that the study should be made at an initial feed oil concentration of 5% and using the concentrate resulting from complete MWF filtration. The concentrates

have an oil concentration of 20% and 16% respectively for FP100 and FP200. The TMP and cross flow velocity are studied using the two UF membranes.

VI.4.1 Effect of transmembrane pressure (TMP)

The effect of TMP on the initial permeate flux was studied by increasing TMP from 1 to 7 bar. The effect of TMP is tested with both feed MWF5% and MWF20%. The permeate flux and the permeate quality are assessed. Data is presented for two ultrafiltration membranes, FP100 and FP200, and one nanofiltration membrane, AFC 30.

VI.4.1.1 Permeate flux

a) Case of the ultrafiltration membranes

Figure VI-23 shows the initial permeate flux versus TMP for two different feed concentrations, 5% and 20% oil. It can clearly be seen from Figure VI-23 that the initial flux for both UF membranes increases with TMP to a maximum value and then gradually reduces with a further increase in TMP. A maximum value of 49 L/h/m² was reached at 2 bar when using the FP200 UF membrane; this value was sustained up to 5 bar and then gradually decreased with a further increase in TMP. For the FP100 UF membrane, a maximum value of 39 L/h/m² was reached at 4 bar and then gradually decreased with increasing TMP. Similar behavior was noticed when using feed concentrations of 20 % oil. The existence of a maximum value for the initial permeate flux in the case of the FP100 and FP200 UF membranes is due to the formation of a concentration polarisation layer on the membrane surface. The initial permeate flux was found to increase monotonically with TMP when using a feed concentration of 5% oil and the AFC30 nanofiltration membrane. In the case of a feed concentration of 20% oil, a maximum permeate flux was reached at 3 bar in all cases and remained at this value with further an increase in TMP.

It may be seen from Figure VI-23 that the permeate flux decreases dramatically when using a feed concentration of 20% in oil. This decrease was by 75% for AFC30, and 80 % for FP100 and FP200.

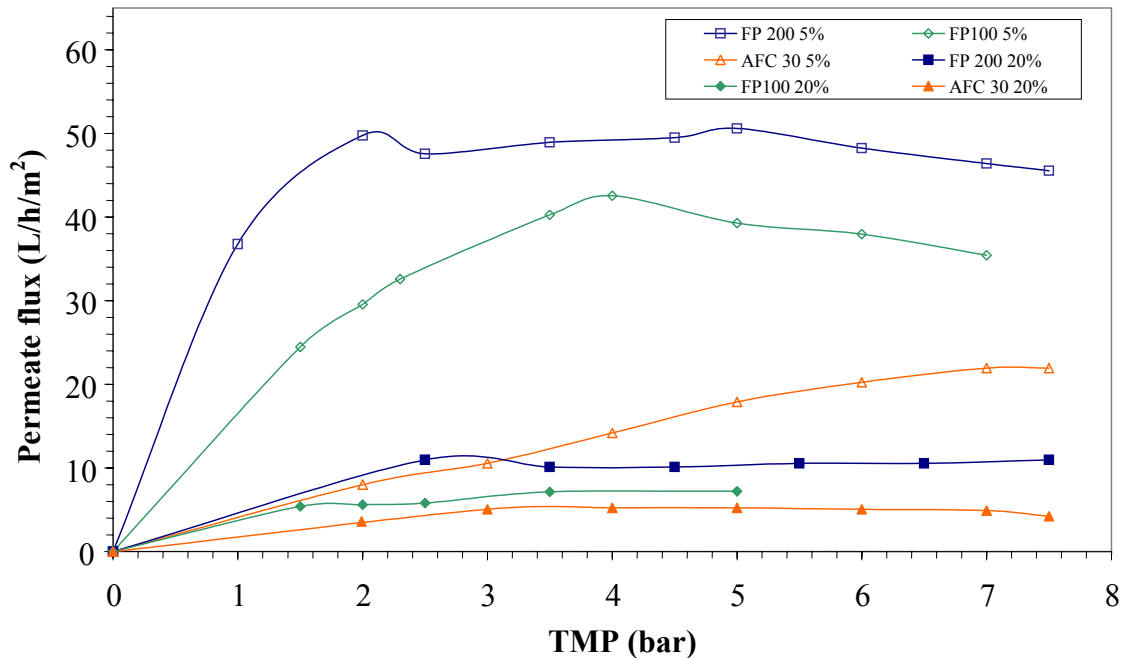


Figure VI-23: Permeate flux at different TMP for UF FP100, FP200 and NF AFC 30 membranes using MWF5% and MWF20% as feed

The permeate flux of an oil in water can relate to the TMP by the relation expressed in Equation VI-1 using the gel resistance model.

$$J = \text{TMP}/\eta(R_m+R_g)$$

Equation VI-1

Where J is the permeate flux, η is the permeate viscosity, R_m is the intrinsic membrane resistance and R_g is the gel resistance added to the intrinsic membrane resistance.

The UF filtrations are carried out at different TMP and gel resistance increased with the TMP. This is because at higher TMP, more oil droplets came towards the membrane surface. Therefore, the thickness of the gel layer increases and the resistance to the permeate flux is increased.

At higher TMP and higher feed concentration, the relationship between TMP, gel resistance R_g and the permeate flux J are more complex. The permeate flux becomes directly dependant on the gel layer resistance rather than the TMP and can be expressed as in Equation VI-2.

$$J = (D/\delta) \ln(C_g/C_b)$$

Equation VI-2

Where J is the permeate flux, D is the diffusion coefficient of the solute in water; δ is the thickness of the polarisation layer, C_g is the gel concentration and C_b is the feed concentration.

In the case where the concentration at the membrane surface reaches the gel concentration, the permeate flux is no longer related to the TMP, and in identical thermal and hydrodynamic conditions the permeate flux stays constant. Nevertheless, during filtration, the temperature increases then the concentrate viscosity decreases and membrane properties change, leading to an increase in permeate flux. In addition, during filtration the emulsion concentration and properties change as it has been seen in Chapter IV. The changes in emulsion properties (concentration, aggregation) lead to a decrease in permeate flux due to the thick set of the gel layer and emulsion destabilization. In extreme case it can be seen using Equation VI-2 that when C_b tends to equal C_g the permeate flux tends to zero. This explains the limitation observed during ultrafiltration of MWF in the retentate concentration that can be obtained; 20% for FP100 and 16% in the case of FP200. Over these values, the permeate flux decreases and the permeate quality deteriorates rapidly. In addition, Equation VI-2 shows that the permeate flux declines linearly with the logarithm of the feed concentration.

As shown in Figure VI-23, at low TMP the flux is linear with the pressure applied as predicted by Equation VI-1. When the TMP increases, the permeate flux reaches a plateau and tends to decrease the plateau as predicted by Equation VI-2. The decrease in permeate flux is indicative of the fact that the gel concentration, C_g , is also related to the TMP and increases with increasing TMP.

b) Case of the nanofiltration membrane

In the case of the nanofiltration membrane, a difference can be seen between high and low feed concentrations. At 5% feed concentration, the permeate flux increases linearly with TMP until 6 bar. At 20% feed concentration, the permeate flux increases with the TMP until 3 bar then the permeate flux reaches a plateau. In the first case (between 0 and 6 bar) the permeate flux follows the resistance-in-series model. However, in the second case at high concentration the gel polarisation controls the filtration.

VI.4.1.2 Permeate quality

The permeate quality has been assessed by measuring the value of its turbidity. The more turbid the permeate, the more oil goes through the membrane. This section presents the results of permeate turbidity obtained during the filtration of MWF5% and of MWF20%.

Figure VI-24 and Figure VI-25 respectively show the evolution of permeate turbidity at low TMP during filtration of MWF using FP100 and using FP200 respectively as the concentration loop takes place. Figure VI-26 shows the nanofiltration permeate turbidity during filtration, at a TMP of 6 bar, as the concentration ratio increases. In all three cases, the permeate turbidity increases strongly with the feed concentration. The difference resides in the turbidity values obtained.

a) Ultrafiltration

For FP100 the value reaches at 2.75 bar TMP is 50 NTU compared to the 4700 NTU obtained with FP200 under the same operational conditions. This indicates that the membrane molecular weight cut off has an effect on the permeate turbidity. On Figure VI-24, the turbidity value measured at 3.5 bar is seven times higher than at 2.75 bar. In addition, when comparing FP100 performance at high TMP (Figure VI-18 page 173)

where the turbidity was initially between 200 and 400 NTU and reached 1438 NTU for a feed concentration of only 12.6%. This indicates that the TMP also has an effect on the level of permeate turbidity.

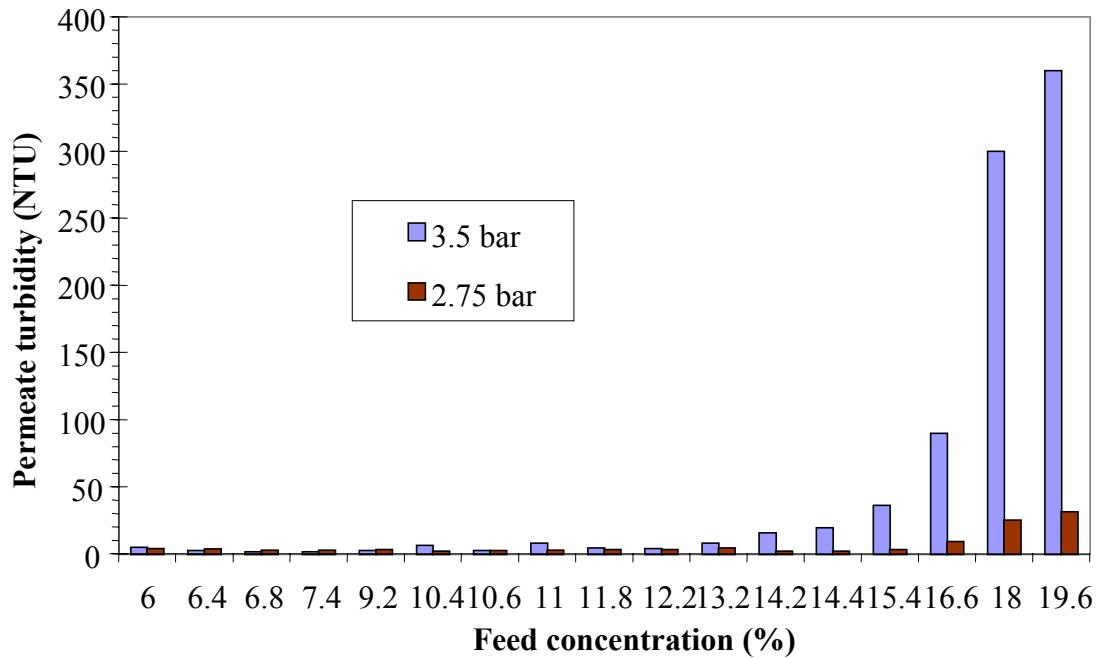


Figure VI-24: Evolution of permeate turbidity with feed concentration for FP100 at low TMP

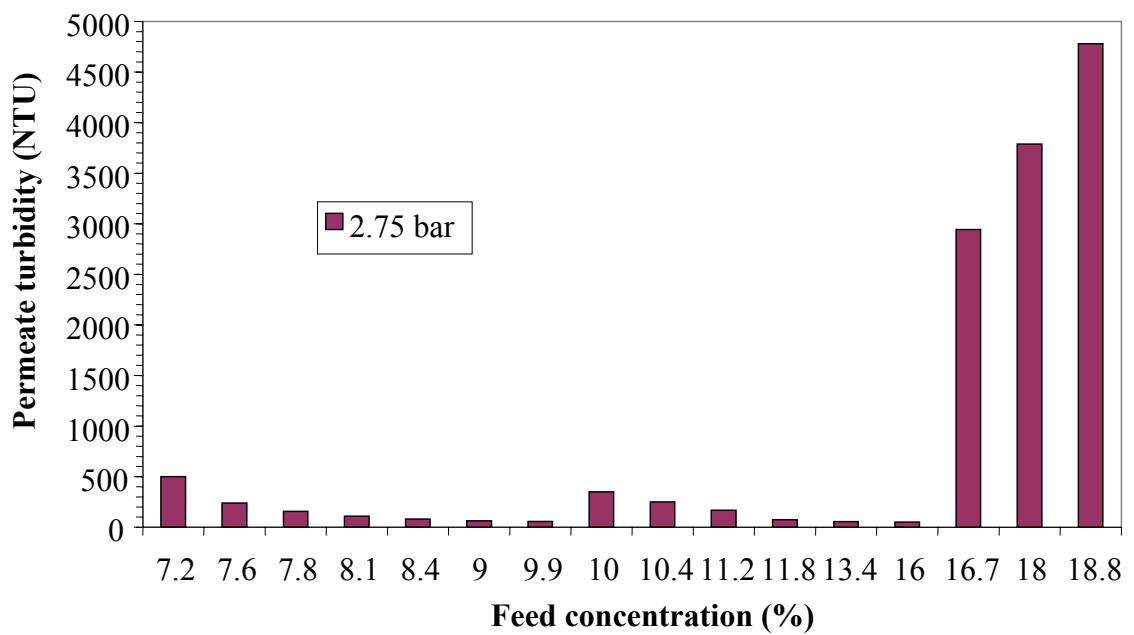


Figure VI-25: Evolution of permeate turbidity with feed concentration for FP200 at low TMP

b) Nanofiltration

The evolution of the nanofiltration permeate turbidity during MWF5% filtration is shown on Figure VI-26. The permeate turbidity reaches at most 7.6 NTU, despite the high TMP of 6 bar used. In that case the smaller molecular weight cut off of the nanofiltration membrane prevents the oil to permeate through the membrane. Nevertheless, the turbidity increases with the feed oil concentration and with fouling. The black arrow shows at which point the membrane unit was washed with surfactant and restarted with using the same feed as previously.

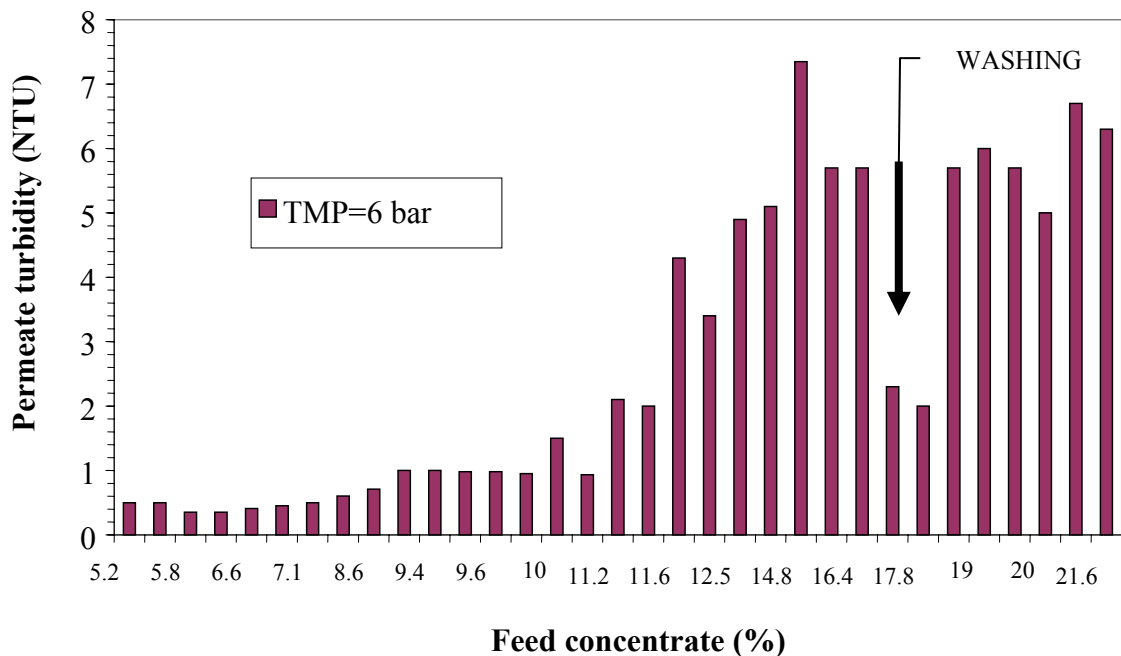


Figure VI-26: Evolution of permeate turbidity with feed concentration for AFC 30 at 6 bar

Permeate at high feed concentration

All membranes have been regenerated and filtration is restarted with the high oil concentration retentate obtained during the MWF5% filtration.

Filtration experiments at feed concentrations of 20% and 16% oil result in poor permeate quality, even if the membrane is washed and the filtration restarted, as shown

in Table VI-4. The NF permeate turbidity has an order of magnitude lower than the value found for the UF membrane permeate; however, its TOC has increased by 88% compared with the permeate obtained using 5% feed concentration.

	Feed concentration (oil %)	Permeate flux (L/h/m ²)	Permeate Turbidity (NTU)
FP200	16%	9	4780
FP100	20%	6.2	500
AFC30	20%	4	6

Table VI-4: High feed concentration filtration results for the three membranes

The permeate deterioration at high feed concentration is the result of the oil layer covering the membrane surface, leading to its permeation through the membrane pores. Table VI-4 shows that the permeate turbidity depends on the membrane molecular weight cut off used. In addition, the feed at 20% oil concentration that comes from concentration loop is less stable than the original emulsion. Therefore, the gel layer is more likely to coagulate and to form an oily film at the membrane surface.

Synthesis

In all cases beside temperature three parameters increase the permeate turbidity; (i) the feed concentration, (ii) the degree of fouling and (iii) the increase in TMP. This is due to the fact that at high feed concentration and at high TMP the oil that fouls the membrane surface is pressed through the membrane pores.

TMP contributes by two means to the phenomenon; by increasing the number of oil droplet coming towards the membrane surface (increasing the concentration polarisation) and by forcing the oil to pass through the membrane. The pressure needed to force oil through a pore can be expressed as Equation VI-3.

$$\Delta P = 4\gamma \cos(\theta) / D_m$$

$$\text{Equation VI-3}$$

Where γ is interfacial tension between oil and the solvated surface, θ is the contact angle, D_m is the membrane pore diameter and ΔP is the pressure required to push the oil through the pore.

Pore size affects the permeate turbidity because according to Equation VI-3 larger the pore sizes, smaller the pressure needed to push the oil through is.

The oil concentration in the feed increases the gel formation by bringing larger aggregates onto the membrane surface. Therefore, oil fouling takes place and the oil can permeate the membrane. This can be seen on Figure VI-26, the black arrow shows the point at which the filtration has been stopped and the membrane regenerated. The filtration was continued using the same feed at 17%. The permeate turbidity stays high despite the membrane regeneration. The turbidity values decreases at first because the gel layer has been removed due to the regeneration process. However, a quick increases in permeate turbidity is observed because of the gel layer rebuilding on the membrane surface. This shows that the turbidity of the nanofiltration permeate increases with the feed concentration independently of the original state of the membrane surface. At high feed concentration the membrane fouls rapidly due to large aggregates dragged to the membrane surface.

VI.4.2 Effect of feed velocity

The other filtration parameter studied in this work was the feed velocity. Figure VI-27 to Figure VI-33 show the effect of feed velocity at different TMPs. The increase of feed velocity in the membrane tube increases the shear stress at the membrane surface. This increase in shear stress creates turbulences at the membrane surface that disturbed the concentration polarisation layer. The tests were carried out using two feed MWF5% and MWF20%.

VI.4.2.1 Ultrafiltration membranes

Figure VI-27 presents the ultrafiltration results for a feed concentration of 5% oil and for different transmembrane pressures from 3 to 7 bar. It can be seen in Figure VI-27 that permeate flux increases with velocity, regardless of TMP, from 10-15 L/h/m² to 48 L/h/m². Similar behaviour was found when using a feed concentration of 20% oil (Figure VI-29).

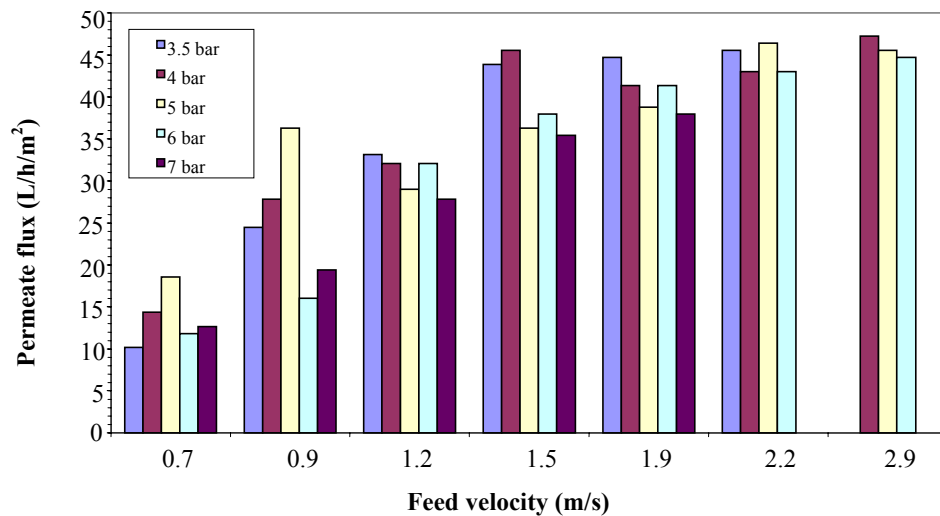


Figure VI-27: Influence of feed velocity on initial permeate flux with feed MWF5% using UF membrane FP100

When looking in more detail at Figure VI-27, increasing the TMP does not necessarily result in a permeate flux improvement. The same behaviour was found previously, shown in Figure VI-23. The permeate flux is limited by the concentration polarisation when TMP reaches 4 bar. Nevertheless, increasing the feed velocity improves for small TMP (at 3.5 bar the permeate flux rises from 10 to 46 L/h/m² when the feed velocity rises from 0.7 to 2.2 m/s) as well as high TMP (at 7 bar the permeate flux rose from 12 to 35 L/h/m² when the feed velocity rise from 0.7 to 1.9 m/s). When the flow velocity reaches 1.5 m/s, the permeate flux does not increase any more, but the TMP controls the permeate flux.

Figure VI-28 shows the effect of cross flow velocity on the permeate flux for the same FP100 ultrafiltration membranes using low TMP. In this case, the permeate increases with the flow velocity as well as the TMP applied. However, the latter is less significant. In addition, over 1.5 m/s of feed velocity, the increase in permeate flux stopped.

Figure VI-29 presents the results obtained when the concentrate MWF20% was filtered with FP100. In this case, the TMP has no effect on the permeate flux as the cross flow velocity does. At 1.2 m/s cross flow velocity, an increase in TMP from 1.5 to 3.5 bar sees an improvement in the permeate flux of 24% (which is the best of the 5 cases presented). When the cross flow velocity reaches 1.5 m/s the permeate flux improved by 50%.

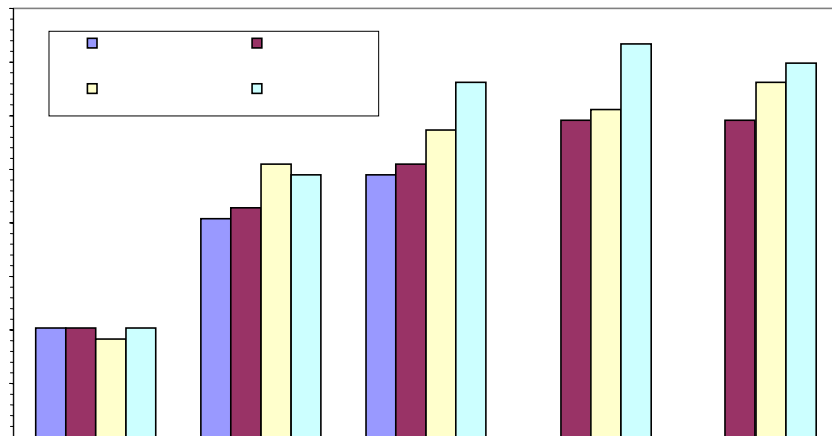


Figure VI-28: Influence of feed velocity on initial permeate flux feed MWF5% using UF membrane FP100 at low TMP

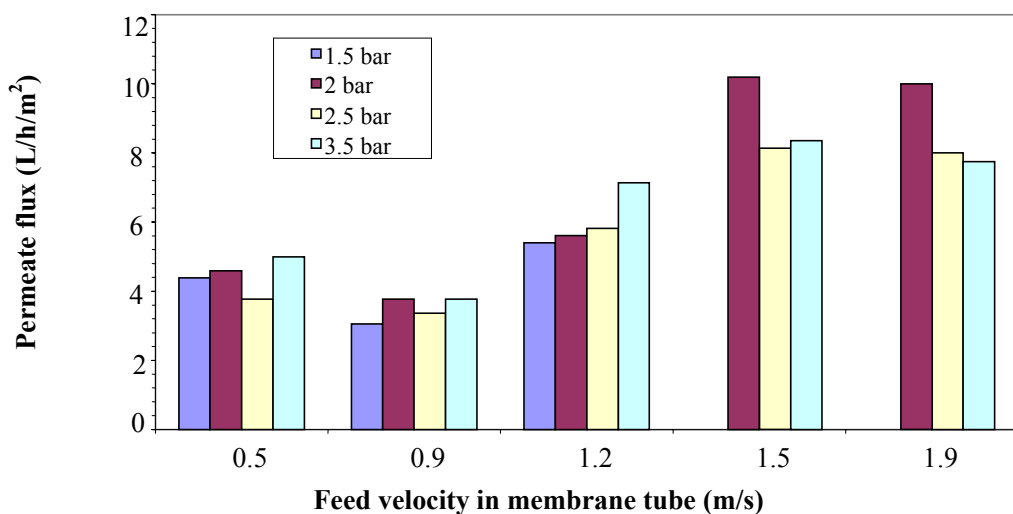


Figure VI-29: Influence of feed velocity on initial permeate flux with feed MWF20% using UF membrane FP100

Figure VI-31 and Figure VI-30 show the cross flow velocity results obtained using the ultrafiltration membrane FP200 with low TMP applied. A similar behaviour as for FP 100 can be observed. Throughout, at low feed concentration, the effect of TMP and of cross flow velocity are mixed. On one hand, at a TMP of 4 bar, the permeate flux improves with the increase of cross flow velocity. On the other hand, at a flow velocity of 1 and 1.6 m/s, the TMP has little effect. This effect is attributed to the relationship between membrane cross flow velocity and TMP.

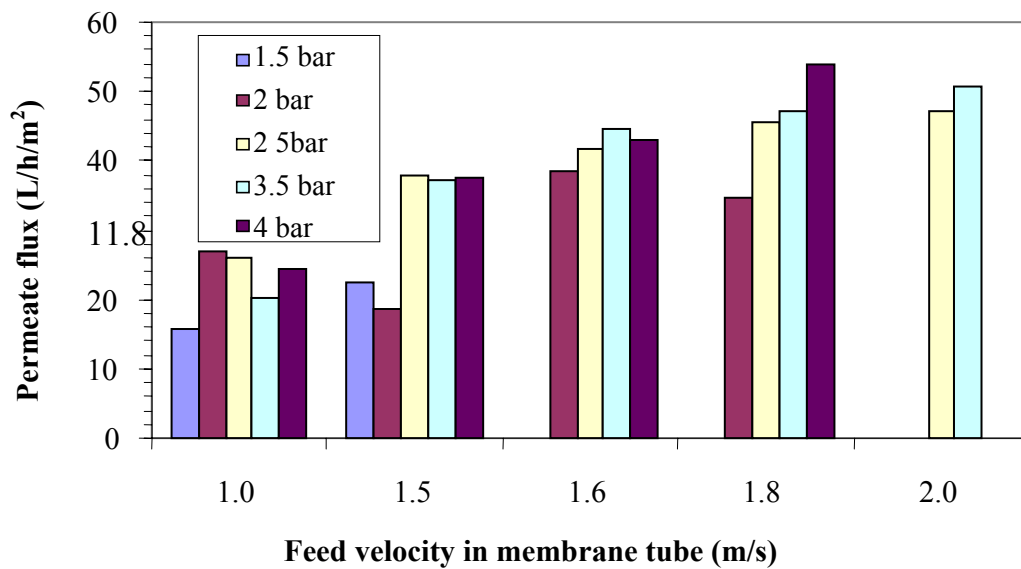


Figure VI-30: Influence of feed velocity on initial permeate flux with feed MWF5% using UF membrane FP200

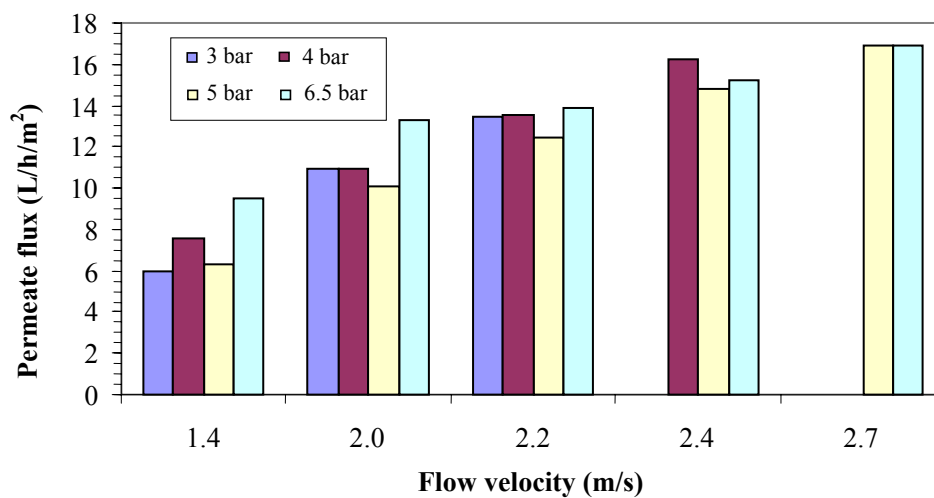


Figure VI-31: Influence of feed velocity on initial permeate flux with feed MWF16% using UF membrane FP200

In both cases for FP100 and FP200, behaviours observed can be explained by the fact that for a given TMP, the increase in fluid velocity increases turbulences and shear stress at the membrane surface results in a disturbance in the concentration polarisation layer and a decrease of the gel layer thickness. Therefore, in the cases where the gel layer governs the permeate flux, an increase in cross flow velocity improves the permeate flux. When the gel resistance is weak, the TMP controls the permeate flux and the cross flow velocity has little effect.

An identical effect of feed velocity on UF of oily wastewater was found (Benito *et al.* 2002). They observed an increase in permeate flux with velocity when the permeate flux is controlled by the concentration polarisation for a TMP above 2 bar for their experimental conditions.

VI.4.2.2 Nanofiltration membrane

Figure VI-32 and Figure VI-33 present the nanofiltration permeate flux for a feed concentration of 5% and a feed concentrate at 20% respectively versus the feed velocity at different TMPs.

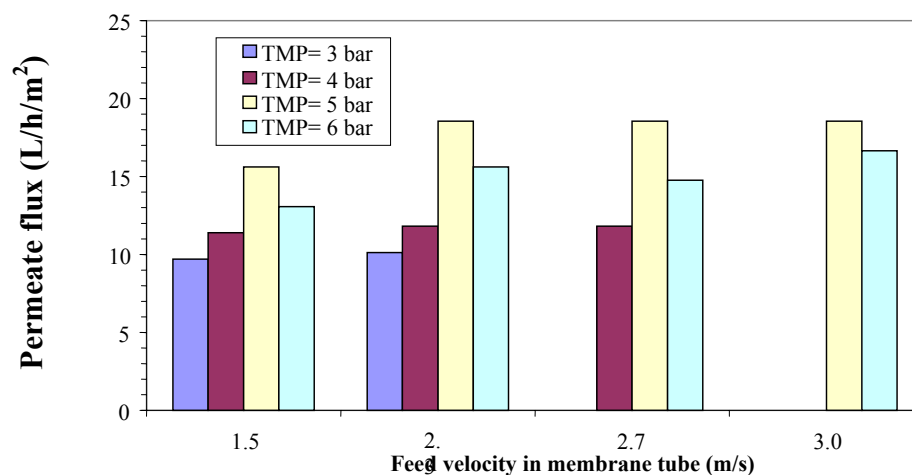


Figure VI-32: Influence of feed velocity on initial permeate flux with feed MWF5% using NF membrane AFC30

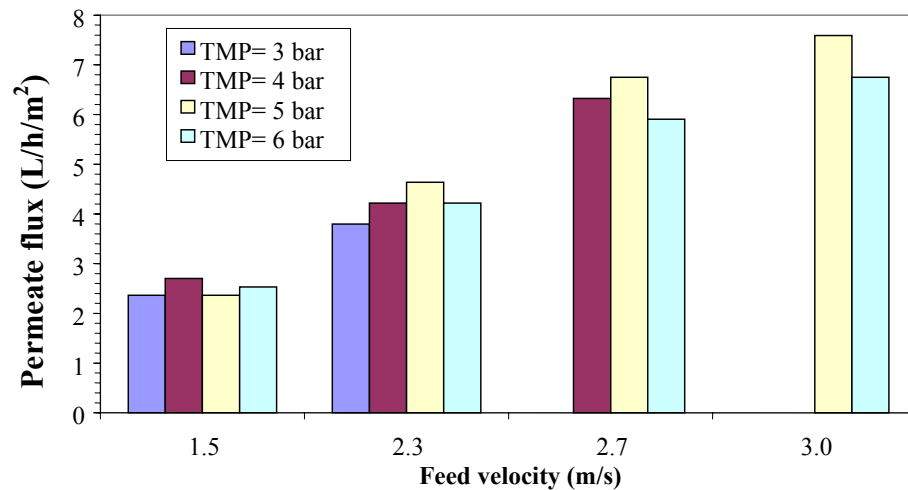


Figure VI-33: Influence of feed velocity on initial permeate flux with feed MWF20% using NF membrane AFC30

Two different behaviours can be observed. Firstly, at low concentrations when the MWF5% is filtered, the increase in feed velocity over 1.5 m/s does not increase the permeate flux. For each category of feed flow velocity, the permeate flux increases with the TMP until it reaches 6 bar. Secondly, filtration of the concentrate MWF20%, the increase in flow velocity improves the permeate flux, whereas for each category of feed flow velocity the TMP has a minor effect on the permeate flux. This is explained by the fact that the nanofiltration of MWF5% is controlled by the TMP (Figure VI-23) and the gel layer resistance R_g is small. In the case of the concentrate MWF20%, the permeate flux is controlled by the gel layer, and increasing the feed velocity increases the shear stress at the membrane surface, that reduces the effect of the gel layer.

VI.5 COMBINATION ULTRA-AND NANOFILTRATION

One of the objectives of the study was to show that using ultrafiltration as a pretreatment would enhance the nanofiltration process by significantly removing the oil content of the waste MWF (Kim, *et al.* 2002). Figure VI-34 shows a comparison of the permeate flux versus time between MWF emulsion pretreated with a FP200 and FP100 ultrafiltration membrane and direct MWF emulsion without pretreatment. The data is taken over three separate days in which filtration runs are started the next day at

the point that they finished the day before. Figure VI-34 shows a decrease in the flux to a minimum point followed by an increase to a maximum by the end of the day (point A at the end of day one, B at the end of day two and C at the end of day three). The increase in the flux is most probably due to the rise in temperature of the feed; this rise results from the energy of the pump. The start of the next day's filtration gives a lower permeate than the previous day (point A' for the second morning, B' for the third morning and C' for the fourth morning); this is likewise due to a lower temperature of the feed. Figure VI-34 shows that at the start of the filtration, a reduction in permeate flux results from membrane fouling over consecutive days, as shown by the dotted line. Similar behaviour is observed when pretreatment is included using FP100 ultrafiltration, in which the nanofiltration permeate flux is enhanced by 15 % when compared to FP200 pre-treatment case. The data representing the nanofiltration of the MWF with pretreatment in Figure VI-34 can also be divided into three successive experiments. After the 9th, 17th and 27th hours, the filtration is stopped and the feed allowed to cool down. When the filtration is started again the next day, the flux measured at points D, E, F (at 20 °C), is lower for the same reason as given previously. The dotted line shows the behaviour of the permeate flux at 20°C at the start of each run. Figure VI-34 shows a clear advantage of using ultrafiltration as pretreatment prior to the nanofiltration; the use of pretreatment leads to considerably less fouling of the nanofiltration membrane and therefore improves the quality of the final permeates.

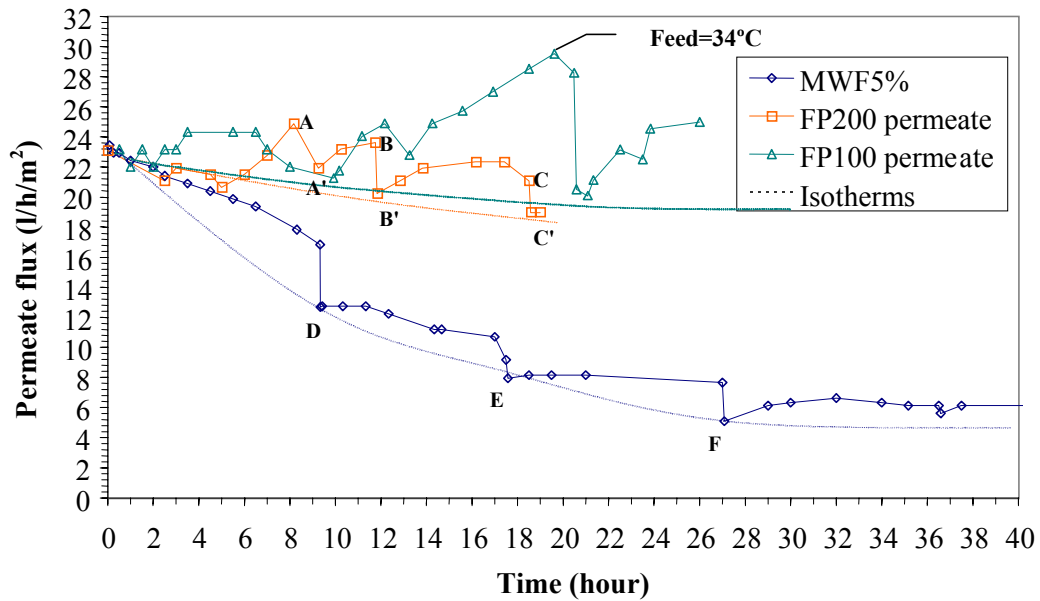


Figure VI-34: Nanofiltration runs, comparison between UF pre-treated feeds and direct filtration using MWF5% over 40 hours

Table VI-5 shows an analysis of permeates from direct nanofiltration and from the combinations of ultrafiltration and nanofiltration. In both cases the nanofiltrations pretreated with ultrafiltration performances are superior.

The advantages of using the pretreatment are that oil droplets foul the nanofiltration membrane less. The turbidity of the nanofiltration permeate stays low during filtration, indicating that no oil gel layer is formed on the membrane surface. This implies that after 400 litres of FP100 permeate were filtered through the nanofiltration membrane, the turbidity of the nanofiltration permeate was 0.2 NTU. In addition, the nanofiltration removed the excess COD.

Feed tested		Nanofiltration permeate data			
		Turbidity (NTU)	Range over filtration	COD (mg/l)	Permeate flux (L/h/m ²) TMP=7 bar
MWF	5%	0.5	0.18 to 2	8860	15
	20%	3.9	1 to 6	10150	8
FP 200 permeate		0.26	0.1 to 0.5	6690	21
FP 100 permeate		0.12	0.1 to 0.23	6400	24

Table VI-5: Typical nanofiltration performances values

Another interest in using FP100 over FP200, other than having a better permeate at high concentration, is that the volume of the concentrate can be reduced to produce a concentrate of 20% in oil although for the FP200 when the concentrate achieves 16 % in oil, the quality of the permeate and the permeate flux decrease dramatically.

VI.6 MODEL

Modelling the filtrations of MWF using the data found during large-scale filtration under industrial conditions is challenging. The feed is changing over time; parameters such as temperature, concentration and even the nature of the feed are changing. Nevertheless, in most cases the model based on Equation VI-2 has been found to fit the experimental data obtained. (Hu, *et al.* 2004) applied the model to ultrafiltration of stable oil emulsion. There are two differences between their work and the data presented. In industrial conditions for waste metalworking fluids filtration, the feed temperature is not controlled. The range of concentration is higher, the purpose of the filtration being to concentrate the emulsion as much as possible in order to reduce the volume of the waste. They were looking at concentrations of 0.5 and 5% in oil, whereas this work investigates concentrations of 5 to 20% in oil. In addition, the emulsion at 20% is in fact the retentate of the filtration and not a fresh MWF made at 20%. As it has been seen, the nature of the concentrate at 20% is different from the fresh MWF5%.

Equation VI-2 can be rearranged as follows:

$$J = (D/\delta) * \ln(C_g) - (D/\delta) * \ln(C_b) \quad \text{Equation VI-4}$$

Equation VI-4 is used to fit the permeate flux vs. bulk concentration data collected using large-scale filtration; without temperature control, with extreme feed oil concentration up to 23% and feed stream reload. Equation VI-4, when plotting the permeate flux versus the retentate concentration, allows the calculation of the gel concentration, C_g , the ratio D/δ . The comparison of these calculated parameters related to the permeate flux and oil retention, under the different filtration conditions, allows a better understanding of the filtration process.

VI.6.1 Ultrafiltration FP200

Figure VI-35 shows the evolution of the permeate flux during MWF ultrafiltration using FP200. Logarithmic curves have been fitted to the different part of the curve using Equation VI-2. The quality of the fit is good and shows that the filtration is effectively controlled by the gel layer at low and at high feed concentration. Three curves are needed to fit the filtration because of the large span of the emulsion concentration. Changes include larger droplet viscosity, leading to a variation in particles diffusion coefficient (D) and destabilisation, leading to oil droplet aggregation and gel formation. The model reflects these changes as it can be seen in Table VI-6. Nevertheless, the result may be affected by the feed temperature variation and the membrane pore blocking and fouling. Therefore, the membrane was regenerated and the filtration restarted using the concentrate as feed. Figure VI-36 shows the results and the logarithmic fitting found is excellent. From the fitted curves the gel concentration C_g and the ratio D/δ can be calculated. These calculations are reported in Table VI-6.

Figure VI-37 presents the MWF5% filtration at a TMP of 3.5 bar. In this case, a good logarithm fitting is found over the full range of feed concentrations. In this case, the result indicates that the filtration is controlled by the gel layer formation, over the whole range of feed concentrations. The gel concentration and ratio D/δ are calculated and reported in Table VI-6.

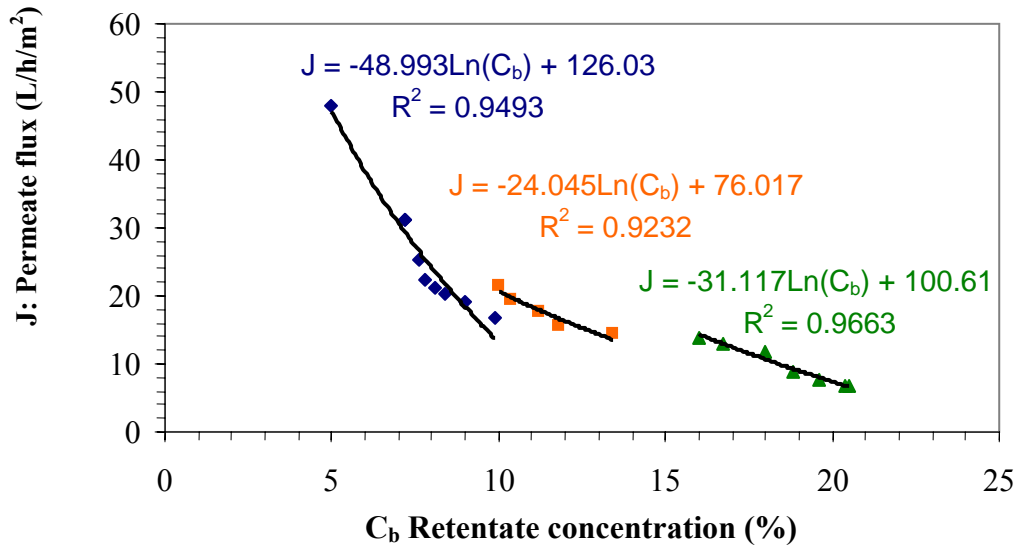


Figure VI-35: Permeate flux plotted against retentate concentration during ultrafiltration using FP200 with a TMP of 2.75 bar and 3 different logarithm fitting curves

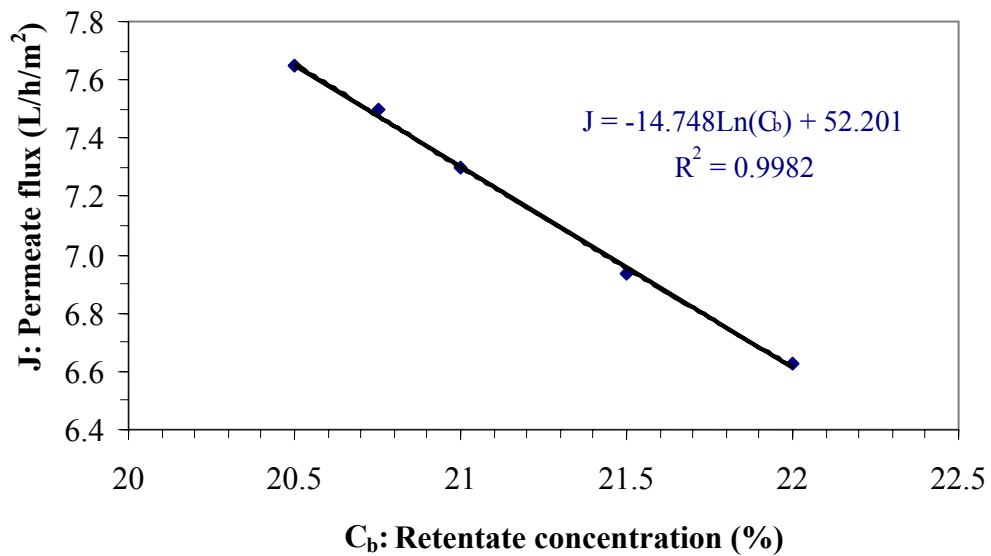


Figure VI-36: Permeate flux plotted against retentate concentration during ultrafiltration using FP200 with a TMP of 2.75 bar at high feed concentration after regenerating the membrane surface

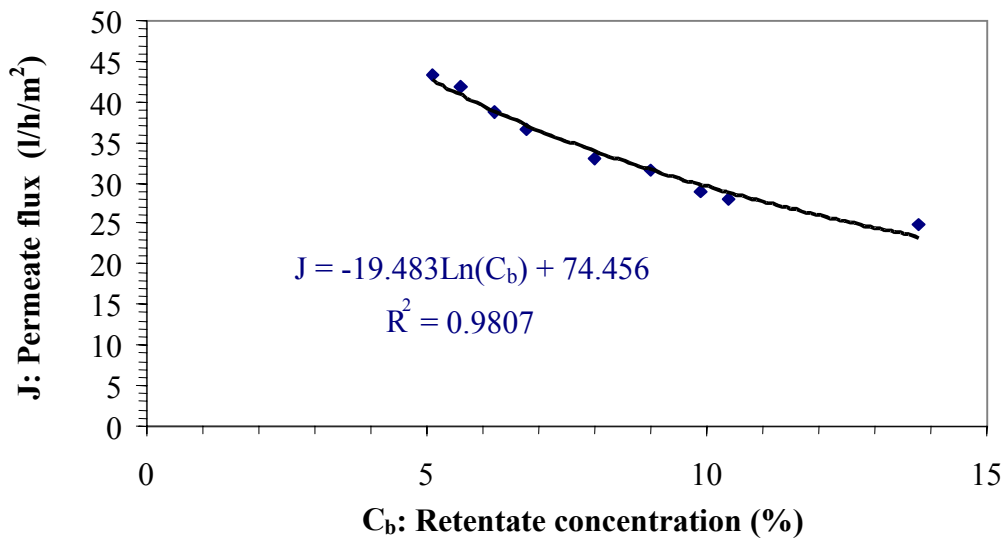


Figure VI-37: Permeate flux plotted against retentate concentration during ultrafiltration using FP200 with a TMP of 3.5 bar

TMP (bar)	Range of retentate concentration (%)	Gel concentration C_g (%)	Ratio D/δ	Permeate turbidity at maximum feed concentration (NTU)
2.75	5 to 10	13	49	182
	10 to 18	26.6	24	600
	18 to 20	28	31	3286
	20 to 22	34.5	14	4780
3.5	5 to 15	45	19	2200

Table VI-6: Values calculated from model when filtering MWF using ultrafiltration membrane FP200

It can be seen from Table VI-6 that the ratio D/δ decreases during the filtration. This indicates that the diffusivity of the oil droplet decreases. This is due to the aggregation of the droplets that becomes larger and to the increase in retentate viscosity. The difference in ratio D/δ between the filtration at 2.75 and 3.5 bar (from 31 to 19) can be

attributed to the increase in gel layer thickness δ , considering that the diffusivity is not affected by the pressure. The gel concentration increases during filtration because of the change in physical-chemical properties of the retentate. The emulsion is destabilised and the gel becomes more compact (C_g increases) until a phase inversion occurs. The fouling gel concentration is found to be in the same range as in (Lee, *et al.* 1984). Once the concentration of the oil at the membrane surface reaches the phase inversion limit, the surface is coated by oil that permeates through the pores.

VI.6.2 Ultrafiltration FP100

In case of FP100 MWF filtration, the issue is a more complex. Firstly, at a low feed concentration and low TMP of 2.75 bar, the model poorly fits the evolution of the permeate. This is due to the fact that, with light operating, (low TMP and low oil concentration) the gel concentration model cannot be applied because the gel concentration at the membrane surface is not reached. The permeate flux is controlled by the resistance of the concentration polarisation, R_g , (Equation VI-1). Besides, R_g increases during filtration due to the increases in retentate concentration. This produces the linear decrease in permeate flux during filtration when the gel concentration is reached. Once the gel concentration at the membrane surface is reached, (depending on TMP and retentate physical-chemical conditions) the decline in permeate flux can be fitted to a logarithmic curve.

Figure VI-38 and Figure VI-39 show that with the FP100 MWF filtration at 3.5 and 6 bar respectively, a good logarithmic fit was found. The value calculated for gel concentration and D/δ are reported in Table VI-7. In the case of filtration at 6 bar, the curve has been fitted using isothermal points.

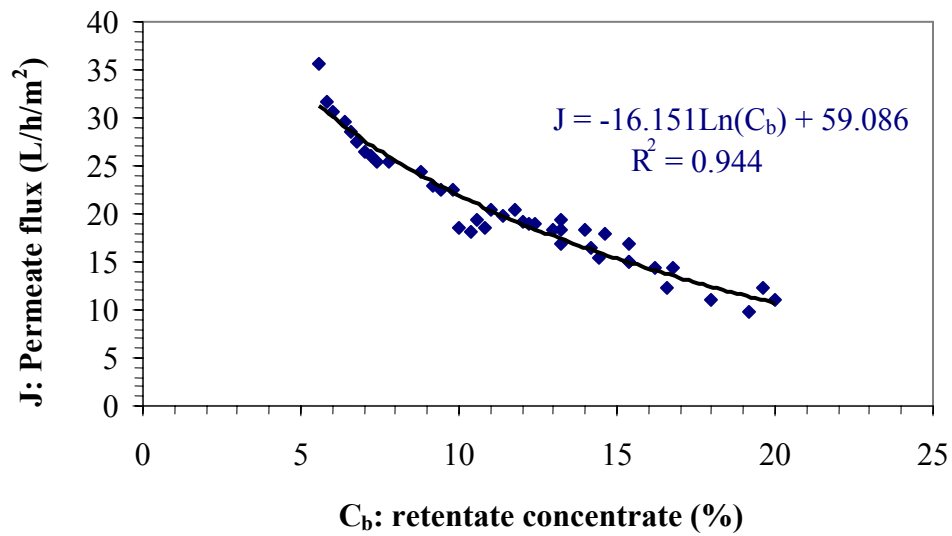


Figure VI-38: Permeate flux plotted against retentate concentration during ultrafiltration using FP100 with a TMP of 3.5 bar

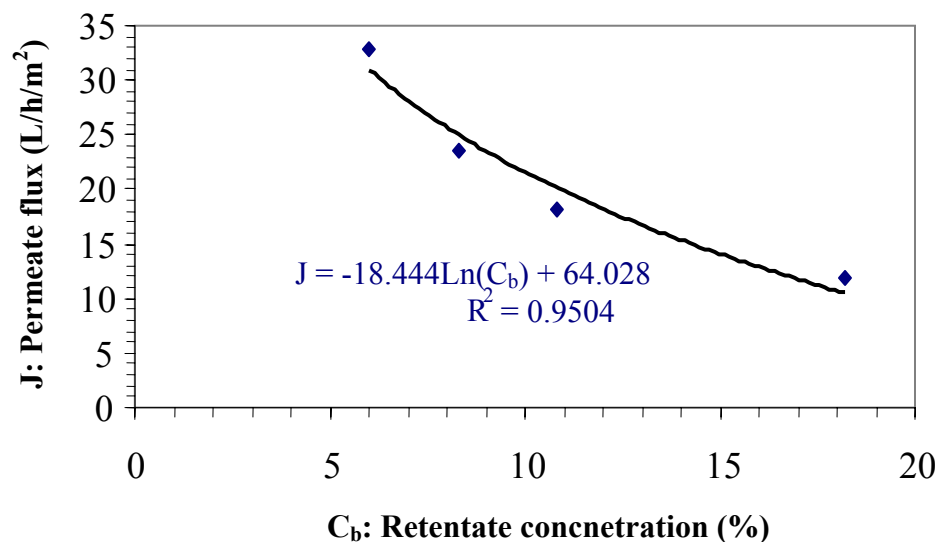


Figure VI-39: Permeate flux plotted against retentate concentration during ultrafiltration using FP100 with a TMP of 6 bar

Figure VI-40 shows the results and the logarithmic fitted curve (orange part) of FP100 filtration at high retentate concentration. Below 13% in oil concentration, the permeate flux decreases a little, independently from the increasing feed concentration. At low concentration (below 13%) the permeate flux decreases because the R_g from Equation VI-2 increased. Two stages can be observed in Figure VI-40. In the early stage of filtration (between 5 and 6%), the concentration polarisation is establishing, a

rapid and sharp permeate flux decrease is observed. During the second stage, (between 6 and 13%) the permeate flux decreases steadily. In these two regions, the membrane works in a pressure controlled region. The gel model used to fit the experimental filtration data cannot predict the flux behaviour in this region under the experimental conditions. The decrease in the second case is because of membrane fouling and retentate viscosity increase. Above 13% in retentate concentration, the gel layer takes control of the permeate flux and can be fitted with the logarithmic curve.

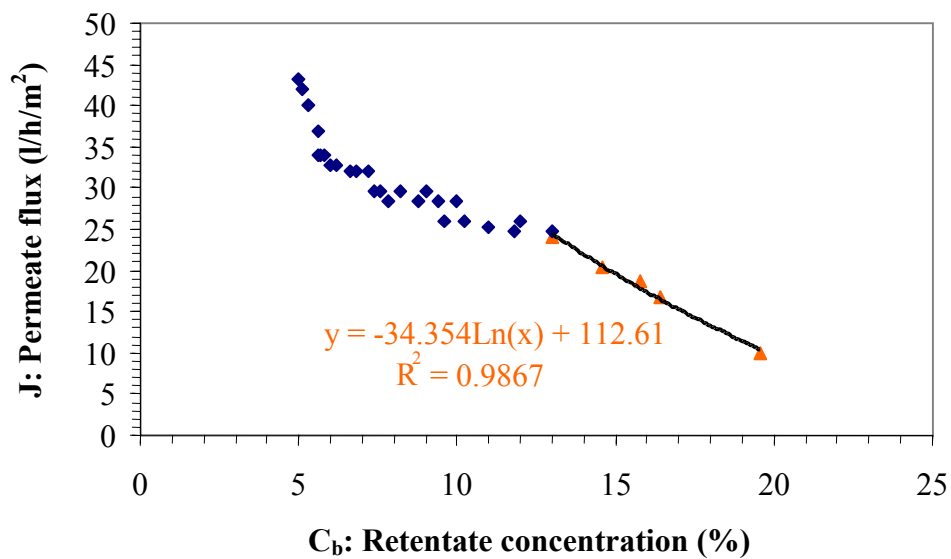


Figure VI-40: Permeate flux plotted against retentate concentration during ultrafiltration using FP100 with a TMP of 2.75 bar for high retentate concentration

TMP (bar)	Range of retentate concentration (%)	Gel concentration C_g (%)	Ratio D/δ	Permeate turbidity at maximum feed concentration (NTU)
3.5	5 to 20	38.8	16	516
6	5 to 18	32.2	18.5	285
2.75	5 to 13	Not calculated	Not calculated	5
	13 to 19.6	26.5	34.35	31.4

Table VI-7: Values calculated from model when filtering MWF using ultrafiltration membrane FP100

It can be seen from Table VI-7 that D/δ value doubles when low TMP (2.75 bar) is used. The difference in ratio D/δ between the filtration at 2.75 and 3.5 bar is due to the increase in gel layer thickness δ . D/δ and C_g values found for FP100 are comparable to those found for FP200, presented in Table VI-6. Nevertheless, the permeates turbidity is 100 times lower when using FP100. In the latter case, despite gel formation at low pressure, the oil permeates less the membrane because of the difference in pore size.

VI.6.3 Nanofiltration AFC30

Nanofiltration models have been carried out using the isotherm points of the direct filtration.

Figure VI-41 and Figure VI-42 show the results and the logarithmic fitted curve of direct nanofiltration of MWF. They present filtration at low concentration (starting with MWF5%) and filtration at high concentration (after membrane surface was regenerated and retentate was used as the feed) respectively. The results of the fit are reported in Table VI-8. The gel concentration is lower than in the cases of ultrafiltration, despite the much higher TMP used. The permeate flux is lower, so less oil droplets are coming towards the membrane surface during filtration. Between low and high retentate concentration, the gel concentration increases from 16.8% to 25.5%. This shows that the gel concentration increases with the retentate concentration. The ratio D/δ stays stable despite the decrease in diffusion coefficient meaning that the gel layer thickness δ increases (the gel layer builds-up). The turbidity of the permeate is lower than in the case of ultrafiltration membrane, but increases during retentate concentration. Despite the higher TMP, 6 bar against 2.75 bar, for the ultrafiltration membrane the turbidity is 550 and 5.5 times lower than the turbidity obtained with FP200 and FP100 respectively. These results show the importance of pore size in the oil retention performances. This is not because oil droplets are able to go through the membrane, but because of the mechanism that allows the oil to pass the membrane. This mechanism is illustrated in Figure VI-43.

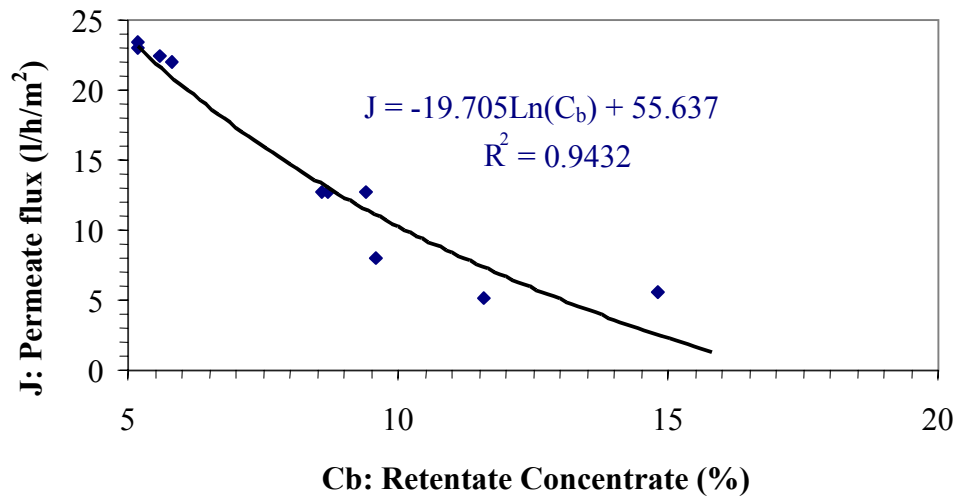


Figure VI-41: Permeate flux plotted against retentate concentration during direct nanofiltration using AFC30 with a TMP of 6 bar

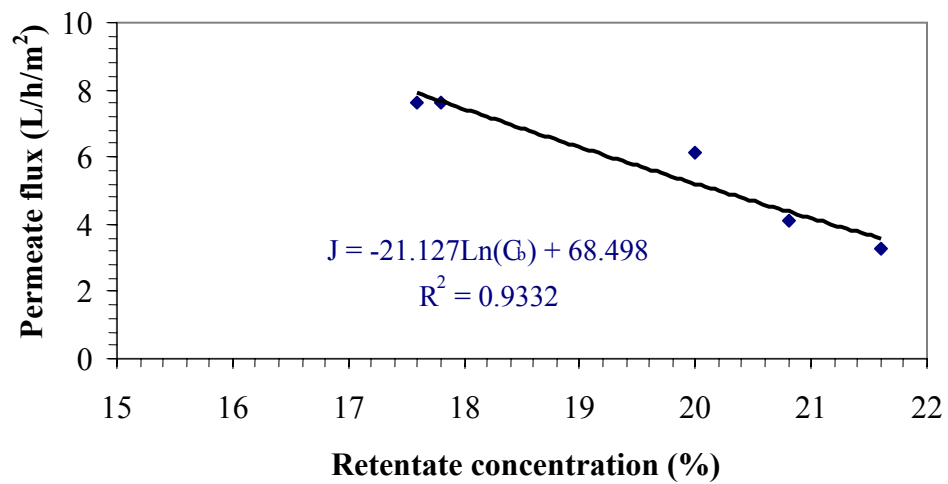


Figure VI-42: Permeate flux plotted against retentate concentration during direct nanofiltration using AFC30 with a TMP of 6 bar after regenerating the membrane surface and using the concentrate as feed.

TMP (bar)	Range of retentate concentration (%)	Gel concentration C_g (%)	Ratio D/δ	Permeate turbidity (NTU)
6	5 to 15	16.8	19.8	0.3
6	18 to 22	25.6	21	6

Table VI-8: Values calculated from model when filtering MWF using nanofiltration membrane AFC30

VI.6.4 Oil permeation mechanism

During filtration, the TMP creates concentration polarisation layer towards the membrane surface. The retentate concentration increases until the gel concentration C_g reaches the concentration of phase inversion, at which point a layer of oil covers the surface of the membrane.

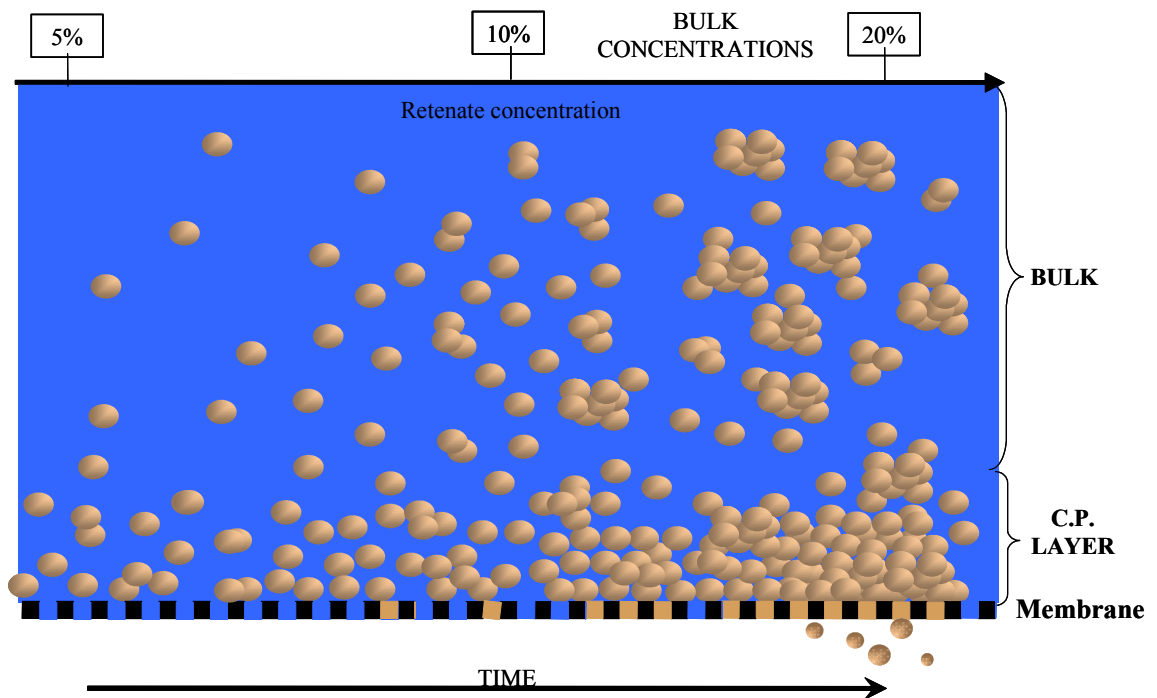


Figure VI-43: Illustration of gel formation relative to feed concentration increase.

Concentration polarisation permeate flux drop during CP formation
 Oil droplet aggregation in bulk
 Gel formation on membrane surface from C_g 35%
 Phase inversion /oil permeates

Phase inversion of the emulsion oil in water is illustrated in Figure VI-44 and leads to the formation of emulsion of water in oil. In Chapter V (Figure V-7), the phase inversion occurs between 25 and 30% in oil in the mix, leading to the formation of a thick gel. In the concentration polarisation, layer another factor influences the phase inversion, which is the depletion in surfactant in the feed during filtration. This emulsion destabilisation can explain the formation of the oil layer.

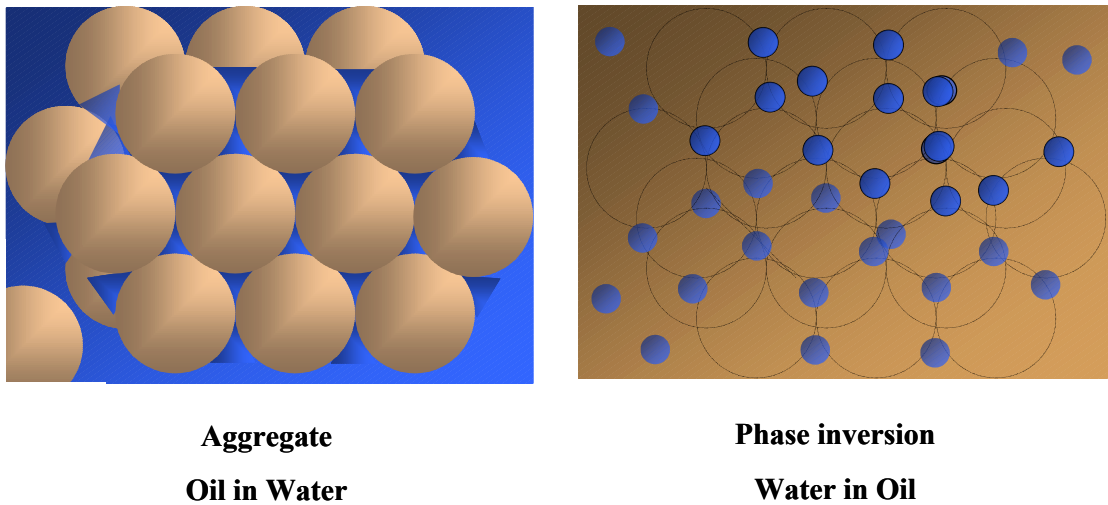


Figure VI-44: Phase inversion principle due to oil droplet compaction

VI.7 SYNTHESIS

The seventh part presents a synthesis of the chapter. The results found on metalworking fluid filtration are summarised and key factors of the MWF filtrations are pointed out.

VI.7.1 Small-scale results

These experiments helped in the understanding of each step of the completed process, giving indications on the nature of the waste effluent and its behaviour. The system proposed in this study is based on membrane filtration. Preliminary small-scale trials

of membrane filtration show that it is a satisfactory method of treating waste as semi-synthetic metalworking fluids. With the membrane filtration system, three problems occur; the production of a concentrate, membrane fouling and the quality of the permeate.

A solution for the production of a concentrate emulsion was given in Chapter V

The second problem arising from membrane filtration technology is fouling. The oily wastewater heavily fouls the membrane surface, reducing its separation performances. This issue was addressed in this chapter with the optimisation of the washing cycle and tests on the enhancement of filtration by gas injection.

The nature of the membrane permeate was also investigated. Its flux and organic content depend mainly on the membrane used UF or NF. NF membranes allow a polishing of the permeate that does not contain any more oil droplets (low turbidity). However, UF membranes tend to produce a permeate that increases in turbidity values during filtration. The second factor studied was feed temperature that has a dramatic effect on permeate quality. The third factor is transmembrane pressure that has been studied, giving a good basis for scaling up the process. Further investigations will be carried out in the large-scale filtration chapter to improve filtration process. The permeate biodegradability is investigated in the biological process chapter.

VI.7.2 Large-scale ultrafiltration

The filtration of the MWF at high emulsion concentration (from 5% to 20%) indicates that for any method employed, the permeate flux decreases with the concentration of the retentate. Therefore, reloading the retentate with fresh MWF5% can be used to dilute the retentate concentration. The reload should take place when the filtration starts to be controlled by the gel layer. In addition, avoiding the gel formation during the filtration process will avoid the oil fouling the membrane and blocking the pores. A semi-batch process may help to minimize the effect of feed concentration ratio during the UF filtration.

The membrane molecular weight cut off is of importance when looking at the oil retention. This is not because of a “sieving” effect, but because of the capacity of oil layer to pass through different size pore.

VI.7.3 Large-scale nanofiltration

An increase in transmembrane pressure can improve the permeate flux. At a lower emulsion concentration, (5%) the concentration polarisation is not obvious, the permeate flux increases with an increase in the pressure until it reaches 6 bars. At very high oil concentration (20%) the concentration polarisation totally controls the permeate flux. It has been shown that the filtration of MWF using a nanofiltration membrane follows the resistance model, and that above a TMP value of 6 bar the gel polarisation takes over. In addition, at high oil concentration, the filtration is controlled by the gel polarisation.

In both cases UF and NF direct MWF, the concentration in oil droplets and the degradation of the emulsion stability during filtration is responsible for the membrane surface fouling and pore blocking and therefore, oil retention. The filtration parameters such as temperature, TMP and MWCO are driving factors that influence the fouling phenomenon and the oil retention.

VI.7.4 Combining UF and NF

The filtration efficiency of the combination UF and NF is very beneficial. Three types of advantages can be summarised. From Figure VI-34, it can be calculated that over 40 hours of filtration, the volume of NF permeate, using FP100 pre-treated effluent, is 760 L/m² whereas the NF permeate flux using MWF5% is only 315 L/m². This corresponds to an increase of 240% in volume treated. The second benefit is the better control of the permeate quality, because the oil droplets are removed during the UF pre-treatment. The third benefit is the low NF fouling also due to the oil droplet removal, over 40 hours of filtration, the loss in permeate flux with UF pre-treatment was 21% whereas for the direct NF filtration the loss was 74%.

VI.7.5 Model

The model of filtration at large scale demonstrates that feed concentration influences the gel layer and effect on membrane fouling. Traditionally, in a more simple system, the gel layer model shows that the gel concentration is constant (Cheryan and Rajagopalan, 1998) and (Guadix, *et al.* 2004). However, in this case the gel layer concentration increases during filtration (Figure VI-35 and Table VI-6) and this is due to the change in feed physico-chemical properties during filtration. The model also shows that the NF membrane used to treat MWF5% is also subject to a gel layer controlled filtration under the experimental conditions.

VI.1	Introduction	147
VI.2	Small-scale filtration	148
VI.2.1	Flat sheet membranes	148
VI.2.1.1	Dead-end filtrations	149
VI.2.1.2	Cross flow flat sheet membrane	152
VI.2.2	Tubular membrane	152
VI.2.2.1	Effect of temperature	153
VI.2.3	Washing cycles	157
VI.2.4	Gas injection	162
VI.2.4.1	Gas injected during reverse osmosis (RO) water filtering	163
VI.2.4.2	Gas injected in during MWF5% filtration	167
VI.3	Results obtained with initial instructions	171
VI.3.1	Permeate flux	171
VI.3.2	Permeate quality	173
VI.3.3	Effect of reloading the main tank	175
VI.4	Direct filtration	177
VI.4.1	Effect of transmembrane pressure (TMP)	178
VI.4.1.1	Permeate flux	178
VI.4.1.2	Permeate quality	181
VI.4.2	Effect of feed velocity	185
VI.4.2.1	Ultrafiltration membranes	186
VI.4.2.2	Nanofiltration membrane	189
VI.5	Combination ultra-and nanofiltration	190
VI.6	Model	193
VI.6.1	Ultrafiltration FP200	194
VI.6.2	Ultrafiltration FP100	197
VI.6.3	Nanofiltration AFC30	200
VI.6.4	Oil permeation mechanism	202
VI.7	Synthesis	203
VI.7.1	Small-scale results	203
VI.7.2	Large-scale ultrafiltration	204
VI.7.3	Large-scale nanofiltration	205
VI.7.4	Combining UF and NF	205
VI.7.5	Model	206

Chapter VI

Figure VI-1: Water flux and effluent flux for BM-05D nanofiltration membrane	151
Figure VI-2: Water flux and effluent flux for BM-20D nanofiltration membrane	151
Figure VI-3: Permeate flux of ultrafiltration membrane FP100 at 3 different temperatures	153
Figure VI-4: Permeate flux of ultrafiltration membrane FP200 at 3 different temperatures	154

Figure VI-5: Permeate flux vs. feed temperature after 1-hour filtration	155
Figure VI-6: Permeate TOC vs. feed temperature after 1 hour filtration	155
Figure VI-7: Permeate turbidity vs. feed temperature after 1 hour filtration	156
Figure VI-8: Comparison of permeates flux between re-circulation and concentration regime	157
Figure VI-9: Permeate flux during washing cycle and effect of applying pressure	160
Figure VI-10: Filtration of MWF5% after successive washing cycle	161
Figure VI-11: Effect of surfactant used during washing on metalworking fluid filtration	162
Figure VI-12: Permeate flux of Demineralised water filtered with FP200 when gas is injected	164
Figure VI-13: Permeate flux when using a two phase flow	167
Figure VI-14: Filtration of metalworking fluid after gas injection has been stopped	168
Figure VI-15: Turbidity of MWF5% when air has been injected at 3.5 bar for 15 min	169
Figure VI-16: Picture of clear tube after MWF filtration with (left) and without (right) gas	170
Figure VI-17: Permeate flux of MWF5% filtration with “cardev filtration conditions”	172
Figure VI-18: Evolution of the permeate turbidity with “cardev filtration condition”	173
Figure VI-19: Permeate turbidity compared to temperature increase during “cardev filtration conditions”	174
Figure VI-20: Permeate turbidity compared to feed concentration increase during “cardev filtration conditions”	174
Figure VI-21: Permeate quality and flux decline during “cardev filtration conditions”	175
Figure VI-22: 3 Semi-batch UF filtrations with “cardev conditions”, comparison between permeate flux, indicating fouling, and feed turbidity, indicating oil permeation	176
Figure VI-23: Permeate flux at different TMP for UF FP100, FP200 and NF AFC 30 membranes using MWF5% and MWF20% as feed	179

Figure VI-24: Evolution of permeate turbidity with feed concentration for FP100 at low TMP	182
Figure VI-25: Evolution of permeate turbidity with feed concentration for FP200 at low TMP	182
Figure VI-26: Evolution of permeate turbidity with feed concentration for AFC 30 at 6 bar	183
Figure VI-27: Influence of feed velocity on initial permeate flux with feed MWF5% using UF membrane FP100	186
Figure VI-28: Influence of feed velocity on initial permeate flux feed MWF5% using UF membrane FP100 at low TMP	187
Figure VI-29: Influence of feed velocity on initial permeate flux with feed MWF20% using UF membrane FP100	187
Figure VI-30: Influence of feed velocity on initial permeate flux with feed MWF5% using UF membrane FP200	188
Figure VI-31: Influence of feed velocity on initial permeate flux with feed MWF16% using UF membrane FP200	188
Figure VI-32: Influence of feed velocity on initial permeate flux with feed MWF5% using NF membrane AFC30	189
Figure VI-33: Influence of feed velocity on initial permeate flux with feed MWF20% using NF membrane AFC30	190
Figure VI-34: Nanofiltration runs, comparison between UF pre-treated feeds and direct filtration using MWF5% over 40 hours	192
Figure VI-35: Permeate flux plotted against retentate concentration during ultrafiltration using FP200 with a TMP of 2.75 bar and 3 different logarithm fitting curves	195
Figure VI-36: Permeate flux plotted against retentate concentration during ultrafiltration using FP200 with a TMP of 2.75 bar at high feed concentration after regenerating the membrane surface	195
Figure VI-37: Permeate flux plotted against retentate concentration during ultrafiltration using FP200 with a TMP of 3.5 bar	196
Figure VI-38: Permeate flux plotted against retentate concentration during ultrafiltration using FP100 with a TMP of 3.5 bar	198

Figure VI-39: Permeate flux plotted against retentate concentration during ultrafiltration using FP100 with a TMP of 6 bar	198
Figure VI-40: Permeate flux plotted against retentate concentration during ultrafiltration using FP100 with a TMP of 2.75 bar for high retentate concentration	199
Figure VI-41: Permeate flux plotted against retentate concentration during direct nanofiltration using AFC30 with a TMP of 6 bar	201
Figure VI-42: Permeate flux plotted against retentate concentration during direct nanofiltration using AFC30 with a TMP of 6 bar after regenerating the membrane surface and using the concentrate as feed.	201
Figure VI-43: Illustration of gel formation relative to feed concentration increase.	202
Figure VI-44: Phase inversion principle due to oil droplet compaction	203

Chapter VI

Table VI-1: Explicit experimental plan and CWF response	159
Table VI-2: Evaluation of the average effect of washing condition on the CWF	159
Table VI-3: Two phases flow pattern corresponding to the gas flow rate	165
Table VI-4: High feed concentration filtration results for the three membranes	184
Table VI-5: Typical nanofiltration performances values	193
Table VI-6: Values calculated from model when filtering MWF using ultrafiltration membrane FP200	196
Table VI-7: Values calculated from model when filtering MWF using ultrafiltration membrane FP100	199
Table VI-8: Values calculated from model when filtering MWF using nanofiltration membrane AFC30	202

CHAPTER VII

ACTIVATED CARBON

CHAPTER VII

Activated carbon

VII.1 INTRODUCTION

Increasingly stringent legislation on the decontamination of wastewater has created an interest concerning the use of activated carbons. Adsorption systems are rapidly gaining prominence as treatment processes, which produce high quality effluents that are low in concentration of dissolved organic compounds, such as dyes. However, activated carbons are expensive; their use may imply carrying out regeneration and reactivation procedures. Liquid-phase adsorption has been demonstrated to be a promising option for non-biodegradable organic molecules removal. Therefore, polishing the effluent coming from the bioreactor can be proved to be a solution to eliminate all COD from the effluent. This would enable the treatment system to produce water for reuse or even to allow discharge in surface water.

The use of activated carbon to eliminate dissolved organic compounds is well known as a unit process in water treatment. In this work, it is tried to reduce the COD level obtained after different stages of the wastewater treatment of metalworking fluid. The adsorption experiments were carried out in two modes. First, a batch system is used to check the adsorption capacity of the adsorbent and model isotherms. Then, fixed continuous systems are set up, and the feasibility of a real treatment of these effluents is assessed.

The aim of the present work is to use activated carbon to reduce the COD of the effluent obtained after different treatment stages of a waste metalworking fluid. The treatment consists of four stages. The first two are membrane separation: after coarse filtration 100 μ m, the waste metalworking fluid is ultrafiltered and the resulting permeate is then filtered with a nanofiltration unit. The next stage is bioremediation of the nanofiltration permeate. The fourth stage is to remove microorganisms using a

0.45 μm microfiltration membrane. Activated carbon treatment was introduced independently after three different stages of the process described previously. The tests that were carried out after nanofiltration to treat nanopermeate (effluent *e*), after bioreactor to treat biopermeate that contains biological material (effluent *eB*) and finally after microfiltration to treat the biopermeate without microorganisms (effluent *eBF*). Adsorption tests were carried out both in a discontinuous and in a continuous mode in liquid phase. The results of the three activated carbon tests were compared. The effect of the presence of microorganisms in the adsorption process and the comparison of bioremediation versus activated carbon used both after nanofiltration stage are discussed.

The effluent resulting from each system were used to prepare fresh metalworking fluid in order to simulate the reuse of water in the manufacturing process. Characterisation tests, such as foaming and emulsion stability, are compared for the same metal-working emulsion when made with tap water in order to assess the feasibility of such water re-use.

VII.2 BATCH TESTS ADSORPTION TRIALS

Batch tests allow an estimation of the feasibility of the treatment. They also give an indication of the activated carbon employed capacity to adsorb the effluent COD. The experimental isotherms found are fitted to Langmuir and Freundlich isotherms to measure the COD adsorption capacity of the activated carbon used.

VII.2.1 Adsorption isotherms

Figure VII-1 shows the adsorption isotherms obtained for each batch experiment. Figure VII-1 plots q_e quantity of effluent COD adsorbed per gram of activated carbon versus the concentration of the effluent in the batch (C_e). Their size depends of the initial concentration used. It is going to be different because it has to be taken into account that effluents from different parts of the process are used. Initially, all

the isotherms look very similar. However, the effluent-*e* seems to be adsorbed a little better than effluent-*eB*, which is more than effluent-*eBF*. The rate of adsorption reached is good. For the effluent-*e*, it is possible to adsorb more than 550 mg of its COD per gram of activated carbon. The adsorption in stirred batch system is different to the continuous trials because the latter system is static, so the diffusion inside the carbon is lower. However, these batch experiments are the best way to understand the maximum adsorption capacity of an adsorbent.

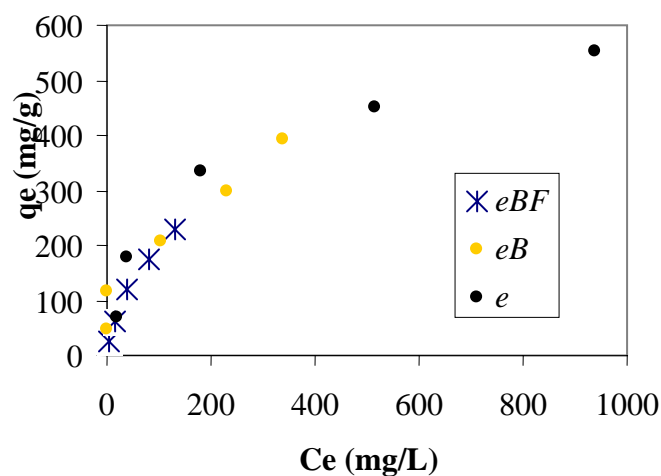


Figure VII-1: Adsorption isotherms

VII.2.2 Fittings to isotherms

Langmuir's well-known equation (Equation VII-1) is based on a theoretical model and supposes that maximum adsorption consists in a saturated monolayer of molecules of adsorbate on the surface of the adsorbent, considered energetically homogenous from the point of view of adsorption.

$$q_e = \frac{Q^{\circ} K_L C_e}{1 + K_L C_e} \quad \text{Equation VII-1}$$

Where Q° (mg/g) is the maximum adsorption capacity per unit of mass necessary for the formation of a complete monolayer on the surface and K_L (L/mg) is a constant.

On the other hand, Freundlich's isotherm Equation VI-2 is an empirical equation, which takes into account the heterogeneity of the adsorption energies of the surface.

$$q_e = K_F C_e^{1/n} \quad \text{Equation VII-2}$$

Where K_F ($[\text{mg} \cdot \text{L}^{1/n}] / [\text{g} \cdot \text{mg}^{1/n}]$) and n are the Freundlich constants characterising the system and indicating respectively the capacity and intensity of the adsorption. The value of n indicates favourable adsorption when $1 < n < 10$, being more favourable the lower its value within this range.

Final fittings to these models are shown in Table VII-1. Although the isotherms look similar Figure VII-1, the parameters calculated from the models are different. This can be due not only to different adsorption capacities, but also due to the different nature of the effluent treated. The difference in adsorption capacity between the $-eB$ and $-eBF$ can be attributed to the fact that micro-organisms do not totally adsorb onto the activated carbon. The difference in adsorption capability between $-e$ and both bio-effluents $-eB$ and $-eBF$ is due to the change in nature of the effluent. Effluent $-e$ is transformed during bio-filtration; surfactants are degraded, bio polymers are produced and both its pH and COD are lowered. The yellow dye that is present in the NF permeate is not removed during the biological step but the effluent is totally transparent after activated carbon treatment.

<i>Adsorbate</i>	<i>Langmuir</i>			<i>Freundlich</i>		
	Q^o (mg/g)	K_L (L/mg)	R^2	n	K_F	R^2
<i>e</i>	345.0	0.007	0.994	2.1	23.11	0.929
<i>eB</i>	400.0	0.033	0.928	1.9	17.05	0.989
<i>eBF</i>	625.0	0.014	0.992	1.5	9.06	0.992

Table VII-1: Fittings to Langmuir's and Freundlich's models

VII.3 CONTINUOUS MODE

The results obtained for the treatment of each effluent are shown in Figure VII-2, Figure VII-3 and Figure VII-4. The inlet COD and the outlet COD measure are C_o and C_s respectively for each column. The inlet COD varies for the effluents *-eBF* and *-eB*, as a consequence of the biological activities. The average COD over the trial calculated are 1134 mg/L for *-eBF* and 1730 mg/L for *-eB*. For column-*e*, a NF permeate of COD value of 3700 mg/l was first used then after 10 litres treated a second batch of NF permeate showing a COD value of 7350 mg/L was used.

VII.3.1 Column results

The column-*e* totally removed the COD and colour of the effluent-*e* until the second batch at 7350 mg/L was used. Then the column starts to saturate and COD started to appear in the treated effluent. After 28 litres of effluent treated the level of COD reaches 1000mg/L and at that point the column reaches the same performance as the bioreactor and is no longer competitive. Microbial development is observed at the top of the column. This development induces a decrease in effluent pH from 9.1 down to 7.95 over the 28 litres of effluent treated. It also contributes to the blockage of the column. Therefore, this column had to be stopped after 30 litres of effluent had been treated.

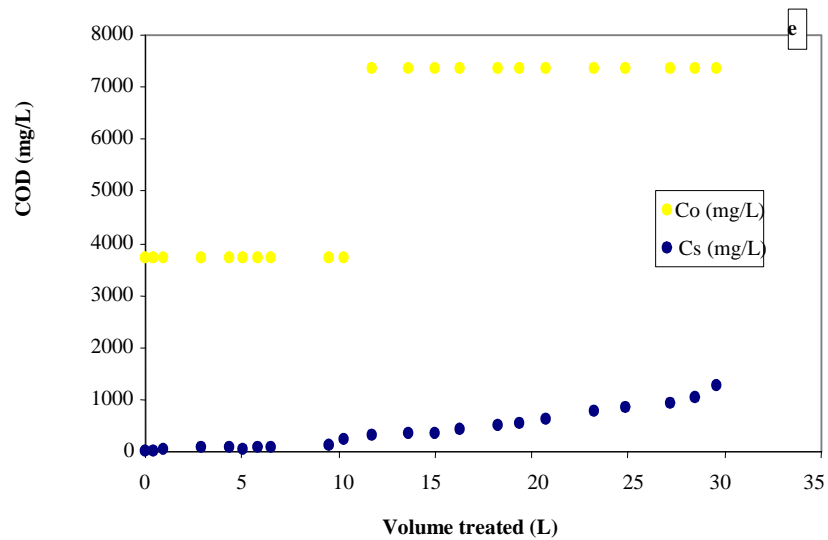


Figure VII-2: Concentration treated (C_o) and breakthrough curves for the adsorption process of effluent- e

Figure VII-3 presents the performance of column- eBF . The column treating the effluent- eBF shows better performance than the column using directly NF permeates, because the C_0 of the filtered bio-permeate is 5.5 times smaller than the NF permeate. Nevertheless, after 25 litres of effluent- eBF passed through the column the COD measured is only half compared to column- e .

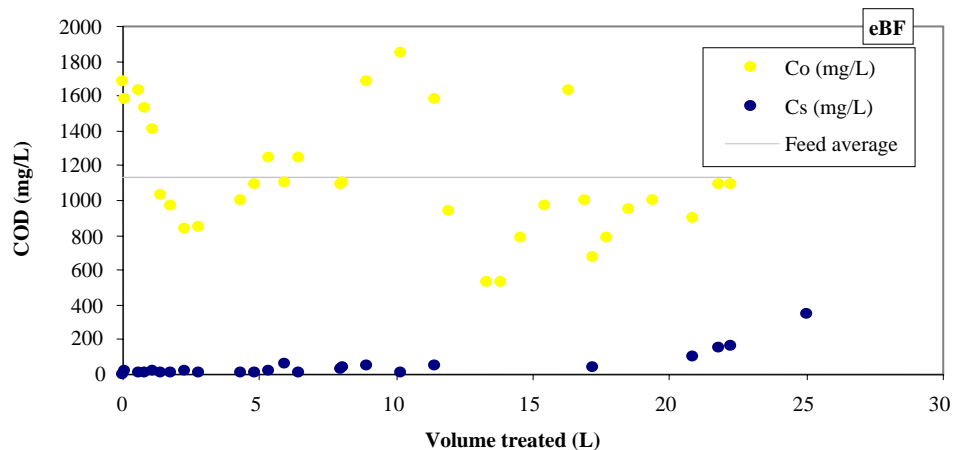


Figure VII-3: Concentration treated (C_o) and breakthrough curves for the adsorption process of effluent- eBF

The performances of column-*eB* are presented in Figure VII-4. Column-*eB* shows the best performance of the three columns. After 25 litres of effluent was treated, no COD was detected. It is after 28 litres that COD was measured at a value of 100mg/l and after 40 litres that the COD started to breakthrough. Effluent-*eB* contains micro-organisms that come from the bioreactor; contrary to the effluent-*eBF*, in which case the micro-organisms have been removed by the microfiltration membrane. A synergetic effect can be seen between adsorption onto the activated carbon and the biodegradation due to micro-organisms added to the column. However, the microbial development in column-*eB* does not block the flow of the column and this may be attributed to the fact that they do not colonise the column as for the column-*e* probably because of the low inlet COD (when compare to column-*e*). In addition, the turbidity of the effluent coming from column-*eB* has the same level as the bioreactor outlet. This is because micro-organisms are not fully retained within the column-*eB*, because the non-filtered bio-permeate contains micro-organisms. However, the inlet COD is insufficient for the microorganism to produce a biofilm within the column. The turbidity of the column -*eB* and -*e* were consistent through out the column tests and was not due to activated carbon particles presents in the filtrate.

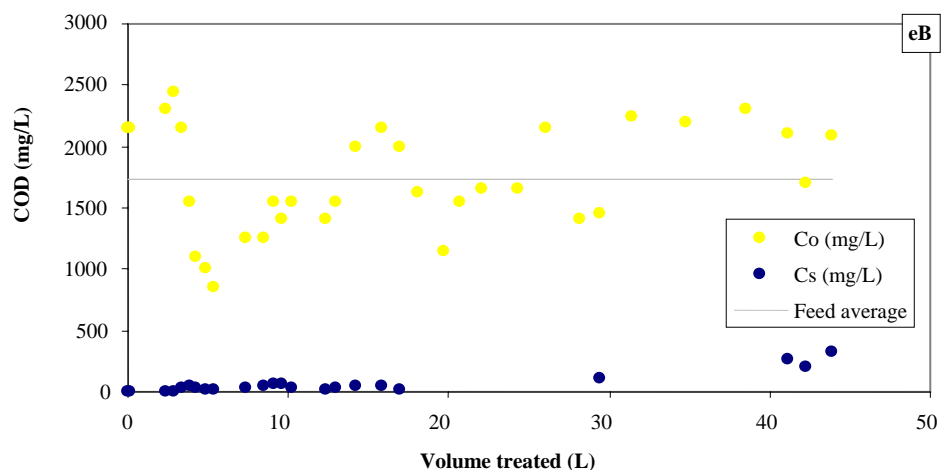


Figure VII-4: Concentration treated (C_o) and breakthrough curves for the adsorption process of effluent-*eB*

The action of the micro-organisms across the column can be seen in the lowering of the effluent pH as it can be seen in Figure VII-5. The column-*e* drops the pH of the NF permeate down to 7.9 after 35 days. This shows that the microbial development observed in the column has an effect on the effluent-*e*. The column-*eBF* shows no drop in pH when compared to the bio-permeate (blues curves). The column-*eB* (yellow curve) shows a drop in pH compared to the bioreactor outlet. This demonstrates that biological activity continues in the column for effluent-*eB*.

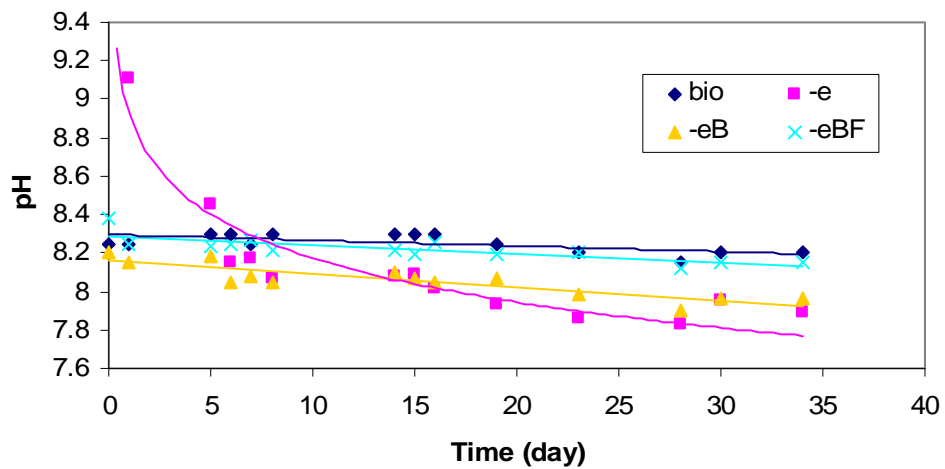


Figure VII-5: pH of the effluent collected at the outlet of each activated carbon column

Under the experimental conditions, more than 40 litres of effluent-*eB* can be treated with 212 grams of activated carbon, producing a clear effluent showing an average turbidity value of 15 NTU (average over 35 days). The differences in effluents aspect are shown on Figure VII-6.

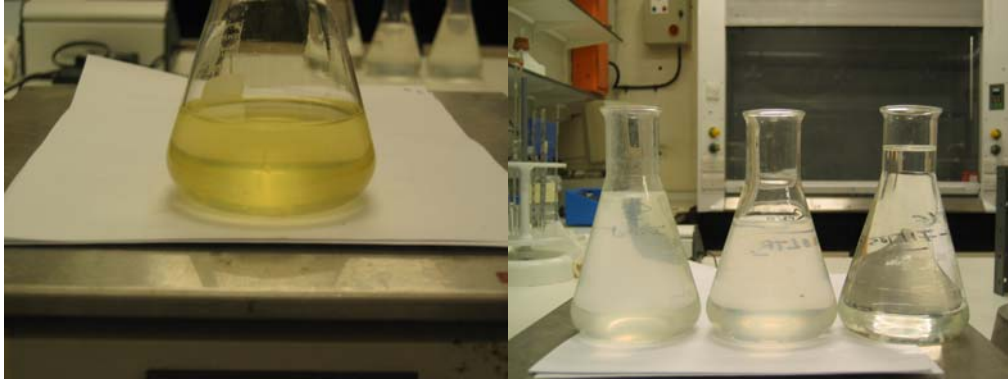


Figure VII-6: picture of effluent bioreactor permeate on the left and the three effluent after activated carbon on the right in order from left to right (-e; -eB and eBF)

The left picture (Figure VII-6) shows the different results after 25 litres of effluent have been passed through each column. In all cases the effluent colouration disappears after activated carbon. The COD is considerably reduced. Nevertheless, the turbidity of the effluent *eB* remains and increases for effluent *e*. This is because the micro-organisms that developed in both columns *e* and *eB* are not totally retained.

VII.4 SUMMARY

Figure VII-7 and Table VII-2 show the performance of the activated carbon columns for each effluent. The activated carbon is very efficient in removing the all effluents colour and COD effluents.

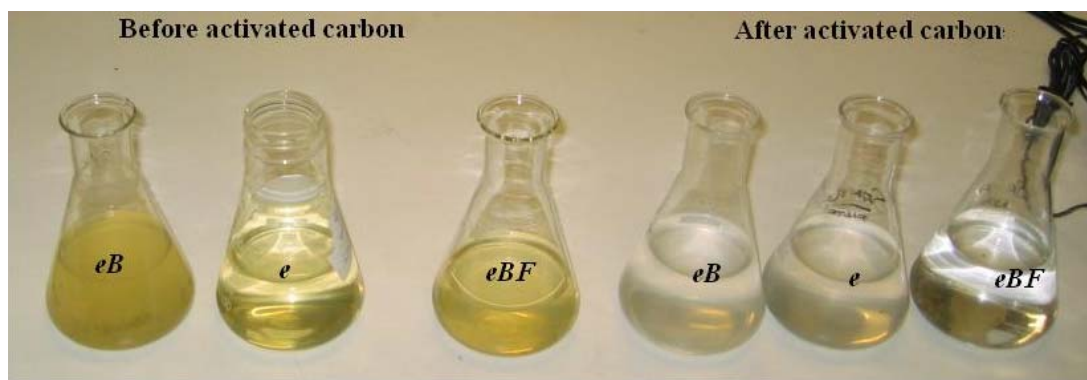


Figure VII-7: Efficiency of activated carbon on the different effluent tested after 25 litres passed through each column

Effluent	Before activated carbon			After activated carbon		
	<i>-eB</i>	<i>-e</i>	<i>-eBF</i>	<i>-eB</i>	<i>-e</i>	<i>-eBF</i>
pH	8.2	9.2	8.2	7.9	7.7	8.2
Turbidity (NTU)	17.6	1.3	0.05	15	5.5	1.1
COD (mg/l)	1150	7300	1000	85	840	350

Table VII-2: Recapitulation of effluent before and after activated carbon treatment after 25litres passed through each column

From Table VII-2 it can be seen that treating effluent that comes out directly from the bioreactor (effluent-*eB*) gives the best performances in terms of COD removal. The turbidity in both cases for the non-filtered effluent show that the microorganisms are not totally retained. Nevertheless, the synergetic action of the activated carbon and the microbes present in effluent-*eB* was demonstrated. In addition, no significant blockage occurs in this case (compared to effluent-*e*), so it can be anticipated that less or no back wash would be needed.

The aspect of scaling-up the activated carbon column is discussed in Chapter IX.

CHAPTER VII Activated carbon	208
VII.1 Introduction	208
VII.2 Batch tests adsorption trials	209
VII.2.1 Adsorption isotherms	209
VII.2.2 Fittings to isotherms	210
VII.3 Continuous mode	212
VII.3.1 Column results	212
VII.4 Summary	216

CHAPTER VII

Figure VII-1: Adsorption isotherms	210
Figure VII-3: Concentration treated (C_0) and breakthrough curves for the adsorption process of effluent- e	213
Figure VII-5: Concentration treated (C_0) and breakthrough curves for the adsorption process of effluent- eBF	213
Figure VII-7: Concentration treated (C_0) and breakthrough curves for the adsorption process of effluent- eB	214
Figure VII-9: pH of the effluent collected at the outlet of each activated carbon column	215
Figure VII-11: picture of effluent bioreactor permeate on the left and the three effluent after activated carbon on the right in order from left to right (- e ; - eB and eBF)	216
Figure VII-13: Efficiency of activated carbon on the different effluent tested after 25 litres passed through each column	217

CHAPTER VII

Table VII-1: Fittings to Langmuir's and Freundlich's models	212
Table VII-3: Recapitulation of effluent before and after activated carbon treatment after 25litres passed through each column	217

CHAPTER VIII

BIOLOGICAL PROCESS

CHAPTER VIII

Biological Process

VIII.1 INTRODUCTION

The microbiology of MWF plays an important role in the degradation of the product and could be advantageously used for its disposal. Bio-remediation is an economic and easy on-site way to dispose of the exhausted product. It is also a sensitive tool to operate. Therefore, its robustness has to be assessed.

The aim of this part of the work was to evaluate the biodegradability of metalworking fluids and its application in a waste treatment system. This aim was achieved by isolating and growing micro-organisms able to survive in the effluent and capable of digesting the organic components. The consortium extracted from waste metalworking fluid (Mobil cut 232) was tested with different effluent.

This chapter is divided into three parts. The first part presents work done in Oxford. The second part presents the development of a bio-consortium. Finally, the efficiency of the consortium was tested and enhanced in a fixed film bioreactor.

VIII.2 EXPERIMENTS CARRIED OUT IN OXFORD

Three days spent in the team of Dr Ian Thompson (Microbial Degradation and Exploitation Laboratory CEH, Oxford) enabled information to be collected about the microbiology of the waste fluid.

The set of experiments were used to assess the biodegradability of the UF permeate and to obtain information on the flora present in the waste metalworking fluid. In addition, the three days in Oxford were used to become more familiar with microbiology laboratory techniques.

VIII.2.1 Plate counting

Table VIII-1 shows the results of the bacterial count of 3 samples of three types of effluent. Raw Waste 1, 2 and 3 are waste metal working fluid Mobil cut 232. Clear UF is the ultrafiltration permeate of fresh MWF5%. Fresh MWF5% is the fresh prepared Mobil cut 232 at a concentration of 5% in oil.

MEDIUM	Bacteria (million per ml)			Results
Raw Waste1	1.25	1.2	1.35	1.27
Raw Waste2	0.8	0.8	1.1	0.90
Raw Waste3	1.95	1.5	1.6	1.68
Clear UF	0	0	0	no growth
Fresh MWF 5%	0	0	0	no growth

Table VIII-1: Bacteria count

The average number of bacteria for the 3 samples of raw waste is 1.28 million cells per ml of exhausted fluid. This is a typical level of microbes that may be found in a waste metalworking fluid.

The fact that there was no growth in neither the ultrafiltration (UF) permeates nor in the fresh MWF does not mean that they did not contain micro-organisms. It indicates that Mobil cut 232 and its UF permeate are quite resistant to bacteriological attack.

VIII.2.2 Bacteria consortia test

Two types of bio consortia have been used for the bioremediation the waste effluent. The first type is a bio consortium developed by Microbial Degradation and Exploitation Laboratory CEH Oxford named here “Oxford consortia” The second one is “home made consortium” extracted and improved from a waste Mobil cut 232 source and tested in SChEME, University of Nottingham.

Oxford consortium was composed of five chosen strains of bacteria. The strains of bacteria were selected and found in various waste metalworking fluid. The authors, (van der Gast *et al.* 2001) and (van der Gast *et al.* 2002) give more details about the selection of the strategy adopted to assemble the consortium. The tests have been carried out in batch over 7 days to degrade the ultrafiltration permeate of Mobile cut 232 that has been diluted to three times showing an original COD of 18000 mg/L to 6000mg/L. Figure VIII-1 shows the results of COD reduction obtained using a 5 litres suspended batch bioreactor.

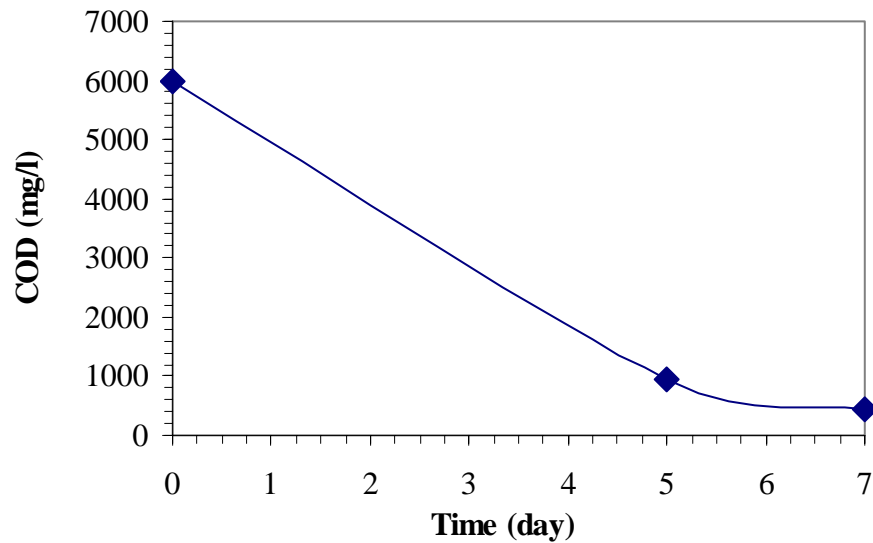


Figure VIII-1: Oxford bio consortia with dilute UF-permeate

Figure VIII-1 shows the COD evolution of Mobile cut 232 ultrafiltration permeate diluted three times with distilled water when 5 litres batch suspension conditions reactor is set with Oxford bio-consortium. A 92% COD reduction can be achieved in 7 days. This consortium is very effective in degrading the diluted UF permeate MWF. It was developed using other MWF. These results show that the Oxford consortium has a broad range of activity. This test also demonstrates that a lower level of COD than the level obtained by ultrafiltration is needed to achieve effective biodegradation.

The results obtained gave precise indications for the application of a bioremediation process. A plan to build and test a home made bio-consortium is shown in the next paragraph.

VIII.3 EXPERIMENTS CARRIED OUT IN NOTTINGHAM

The development and the enrichment of the Indigenous Community (IC) took place in 4 stages. The first stage consists of the extraction of the IC present in the waste metalworking fluid Mobil cut 232. The second stage enabled the evaluation of the feasibility of the bioremediation and gives indications of what level of pre-treatment of

the waste metalworking fluid would require. Therefore, the IC is inoculated to different strength of effluents, respectively NF, UF permeate and UF permeate diluted with RO water. The potential fast growth of the micro-organisms was assessed. The third stage was to collect the micro-organisms that have grown during the first stage and to inoculate a continuous suspended bioreactor. The bioreactor was fed with the suitable effluent found during the second stage investigation. This stage enables the adaptation and the enrichment of the IC to improve its degradation capability (reduction of the effluent's COD). It also results in the harvest of a consortium named IC2. The fourth stage consisted of a fixed bed bioreactor being inoculated with IC2.

This stage can be considered an improvement of the bio-consortium in its remediation function. This improvement is because micro-organisms that survive in batch, but do not multiply significantly fast, would leave the bioreactor by being washed out.

In Nottingham, it was decided to use a home made bio-consortium that would treat the nanofiltration permeate.

VIII.3.1 Development of a home made bio-consortium

The second consortium was developed, improved and tested at the University of Nottingham. It was developed from the extraction of biological material present in a waste metalworking fluid Mobil cut 232. The development was carried out during 10 months and consists of 4 stages as described previously. This paragraph gives the results obtained during the enrichment of the consortium and discusses the options taken to achieve effective biodegradation.

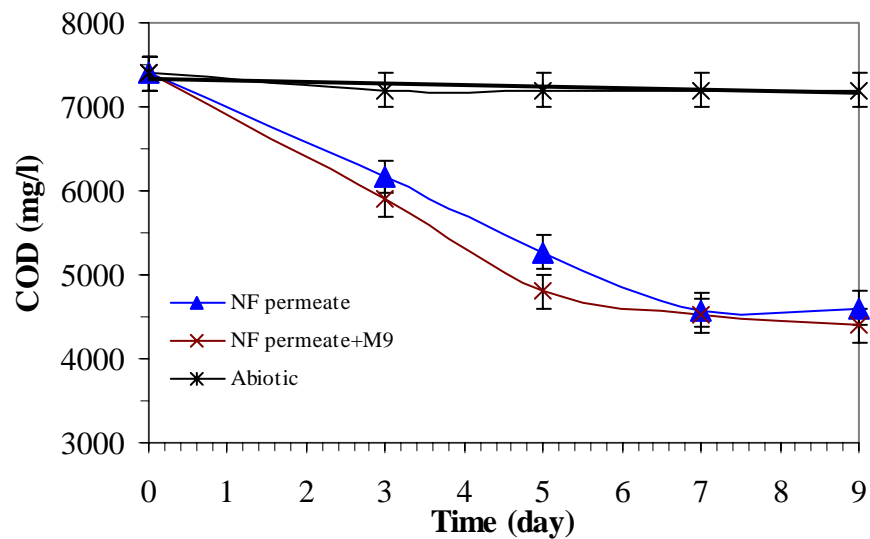
VIII.3.2 Culturing the Indigenous Community

The micro-organisms that have been extracted from waste metalworking fluid (IC) are grown in triplicate in 100ml solution batch suspension conditions and the growth and the level of COD is checked. Table VIII-2 shows the experimental plan that has been used. Parts of the trial were carried out using a general minimum media, M9. The

composition of the media is given in Chapter IV Section III 7.2. 3% in volume of full strength M9 is added in the flask.

Effluent	Effluent+ M9	Effluent
UF permeate at 100% 18 g/l COD	3	3
UF permeate 33% + RO water 6 g/l COD	3	3
NF permeate at 6 g/l COD	3	3
Non inoculated flask for each cases	1	1

Table VIII-2: Experimental plan



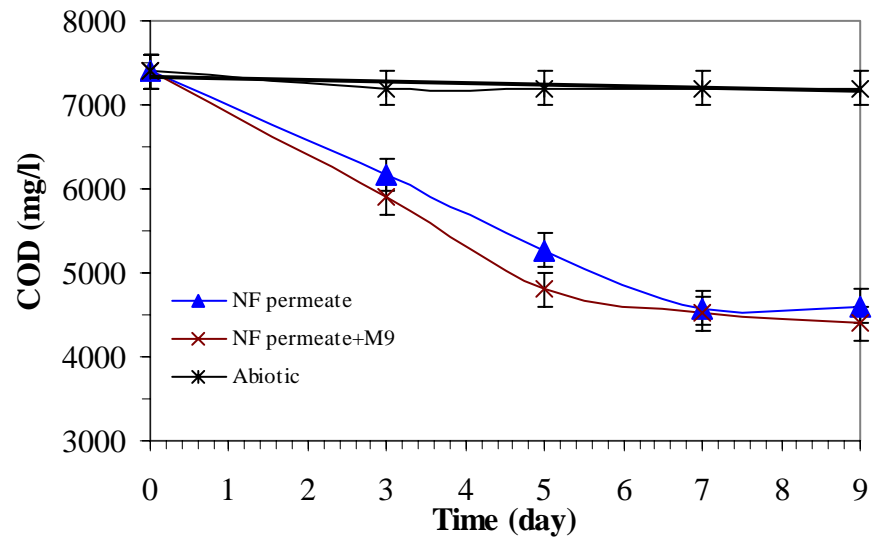


Figure VIII-2

shows the evolution of the COD when nanofiltration permeate is inoculated with the IC. Results obtained were encouraging. After 7 days the dilute broth showed a COD reduction of 40%.

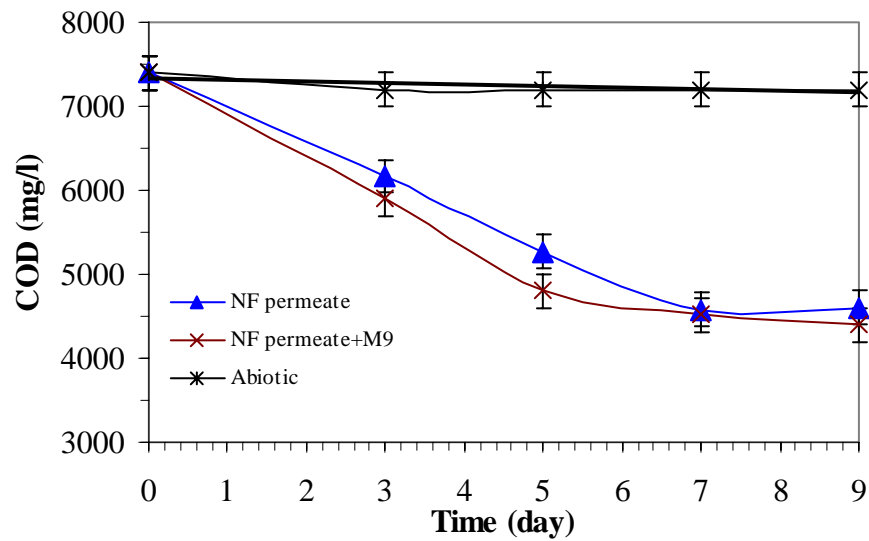


Figure VIII-2: Nanofiltration permeate test with IC

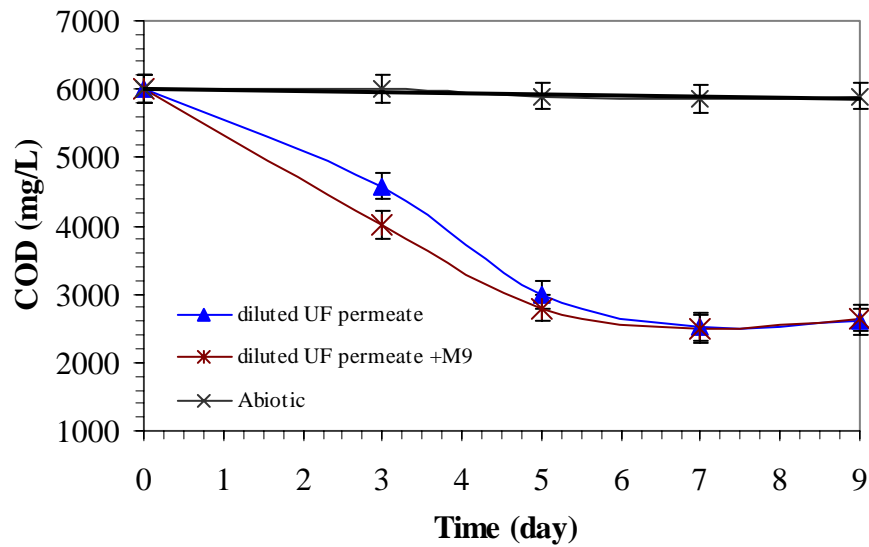


Figure VIII-3 shows the evolution of the COD when the diluted ultrafiltration permeate is inoculated with the IC. After 7 days, the dilute broth showed a COD reduction of 38%.

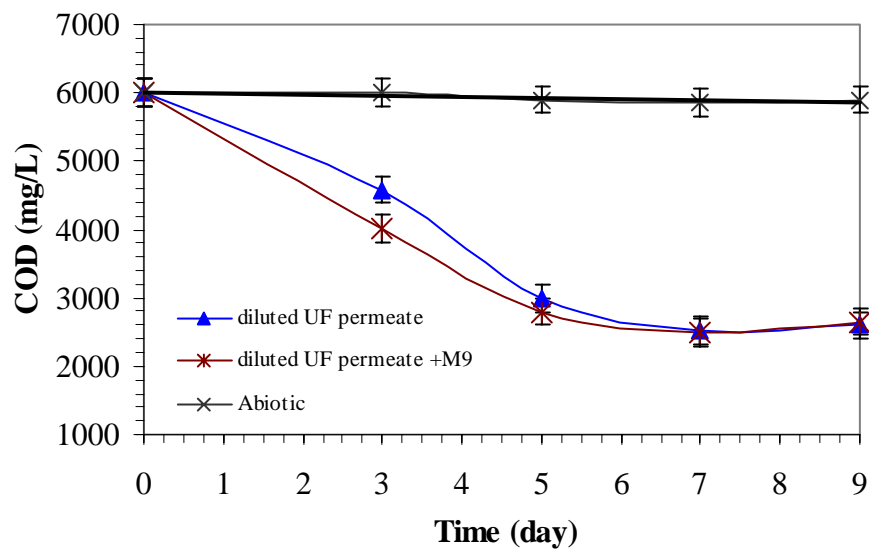


Figure VIII-3: Diluted ultrafiltration permeate flask test with IC

No significant COD reduction was measured in the case of none diluted UF permeate. However, bacterial growth did occur in the flasks. These results confirm the test done in Oxford using the Mobil cut 232 UF permeate diluted from 18,000 to 6,000 mg/L of

COD, that an acceptable maximum level of COD has to be used to feed an aerobic system.

In the three cases, no difference in COD drop was observed between trials using the bacterial minimal media and the trial without. Therefore, the development of the consortium was continued without using the minimal media M9.

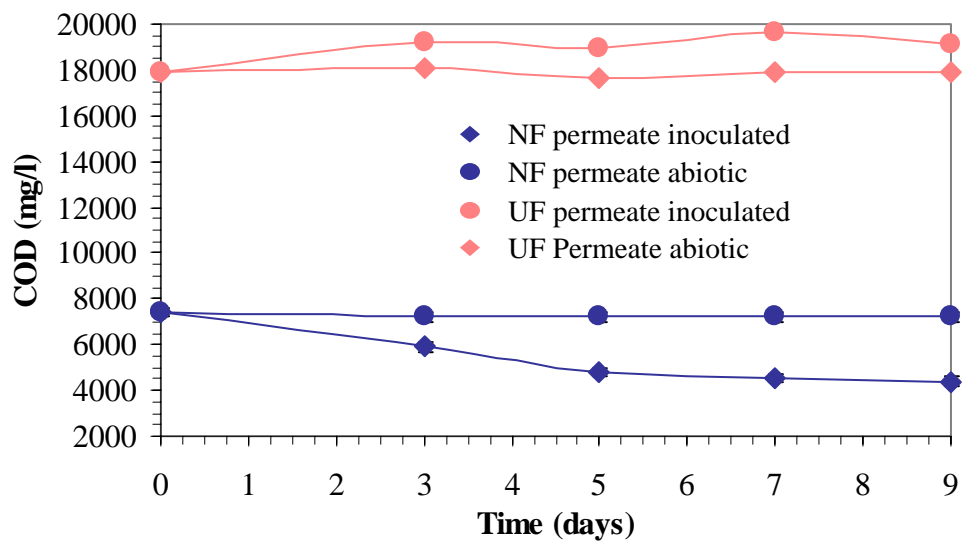


Figure VIII-4: Biodegradability comparison between NF and UF permeate

The results obtained with the bacteria extracted from the waste metalworking fluid are not as good as the one obtained with the Oxford built consortium. Two reasons can be given for this. The first reason is that the indigenous community is not selected to target the UF permeate specifically and needs to be adapted to this environment. It is difficult to colonise, as shown by the bacterial count in paragraph VIII.2.1. The second reason is that the bacteria used in Oxford were tested in a diluted media (UF plus distilled water). Therefore, the biocide that maybe found in the UF and NF permeate were accordingly diluted. During the test carried out with the Mobil cut 232's indigenous community, microbes were exposed to a full strength biocide that may be present in both permeates.

VIII.3.3 Enrichment

Enrichment aims to improve the tolerance and capability of the indigenous community.

VIII.3.3.1 Definitions

Bioremediation is defined as being the use of micro-organisms to accomplish a biological clean up of a specified contaminated area such as soil or water. Enrichment is the selection of micro-organisms to enhance the microbial populations of the operating waste treatment plant in order to improve its performances and the application of such selected micro-organisms.

This technique of enrichment applied to enhance the treatment facilities is because microbes that populate a system (soil or wastewater) become acclimated to the influent. Therefore, to start with, microbes collected from the waste effluent are specific and an excellent basis to implement enrichment. The IC is already adapted to survive in the targeted environment. These micro-organisms are well-suited to handle the contaminants in this specific waste influent and maybe acclimated to provide best performances, assuming a steady state of operation is approximated.

This approach assumes that the indigenous population introduced via routes such as windblown solids, rainwater and the plant influent stream will always contain the best-suited organisms. In practice, even though the natural population may develop into an acceptable one, there may be performance limitations that only can be overcome by the introduction of superior strains of micro-organisms.

The worked that has been proposed over a month is the continuous suspended bioreactor which aims at helping microbes that develop well (in numbers) and quickly. The population that is needed to enhance the bioremediation of the nanofiltration permeate is selected.

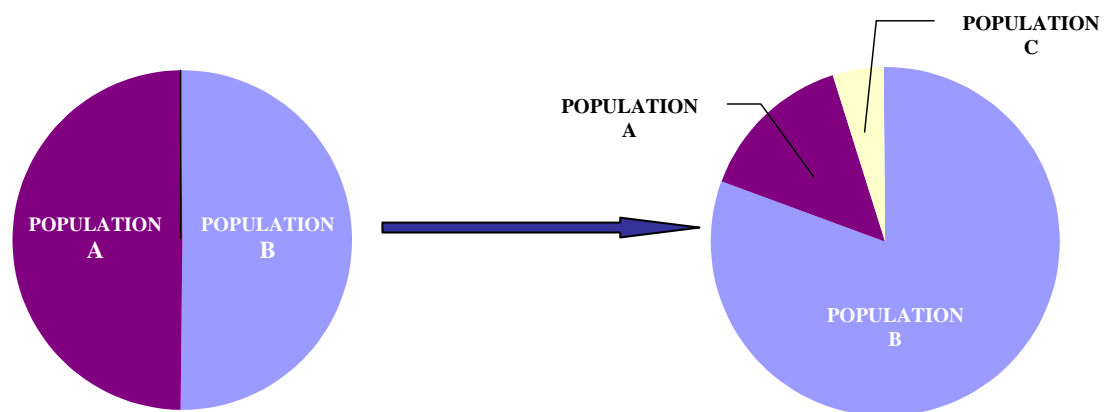


Figure VIII-5: Illustration of the impact of enrichment on indigenous population.

Figure VIII-5 illustrates the impact that enrichment can have on a microbial population (A and B) in a system. In this case, the population wanted is **Population B**. **Population B** is constituted of fast growing microbes that adapted well from their original environment, the waste MWF (with a very high COD content, with little available oxygen) to the new environment, the NF permeate. The NF permeate has a very little oil content and a COD of 7300mg/L. The system operates in continuous mode and oxygen is not limited. **Population A** represents the fraction of the population that does not adapt to the new conditions. They are slow growing and are discarded by the wash out effect. They do not adapt to the new oxygen level, to the permanent renewal of feed stream or to the utilisation of molecule that are not present in the new environment. **Population C** represents the fraction of new organism able to grow in the NF permeate, selected by enrichment. The purpose of the trials is to

enhance the growth of **Population B**, minimise **Population A** and allow the establishment of the **Population C**. The net result is to improve both the quality and quantity of the bacterial population for it to reduce the COD level of the influent in a minimum period of time.

VIII.3.3.2 Strategy adopted

The strategy adopted uses a stirred suspended continuous bioreactor. This bioreactor consists of a continuous open 1.75 litre bioreactor, used at a constant volume. The bioreactor is continuously stirred and thin air bubbles are constantly pulsed. All inner flux passed through a filter 0.45 μm to prevent any bacterial contamination. The bioreactor is described in Chapter III. Micro-organisms that develop and have a growth rate fast enough to stay in the bioreactor at a given dilution rate will be selected. The others will be washed out. Therefore, by scaling the feed rate, it is expected that the most adapted micro-organisms survive and develop the best ability to biodegrade the NF permeate. The decrease in COD at the bioreactor outlet is measured.

When a maximum COD is transformed, the consortium surviving in the bioreactor will be introduced into a 5 litres bioreactor load with a plastic matrix to encourage biofilm growth. It is likely that the fixed film bioreactor will have a better performance than the bioreactor.

The IC growth rate was measured before starting the bioreactor in order to prevent any premature and total washing out of the micro-organisms. 200ml NF permeate was inoculated with IC and left agitated in incubator. 200 μl samples were taken regularly and a bacterial count using a haemocytometer was carried out.

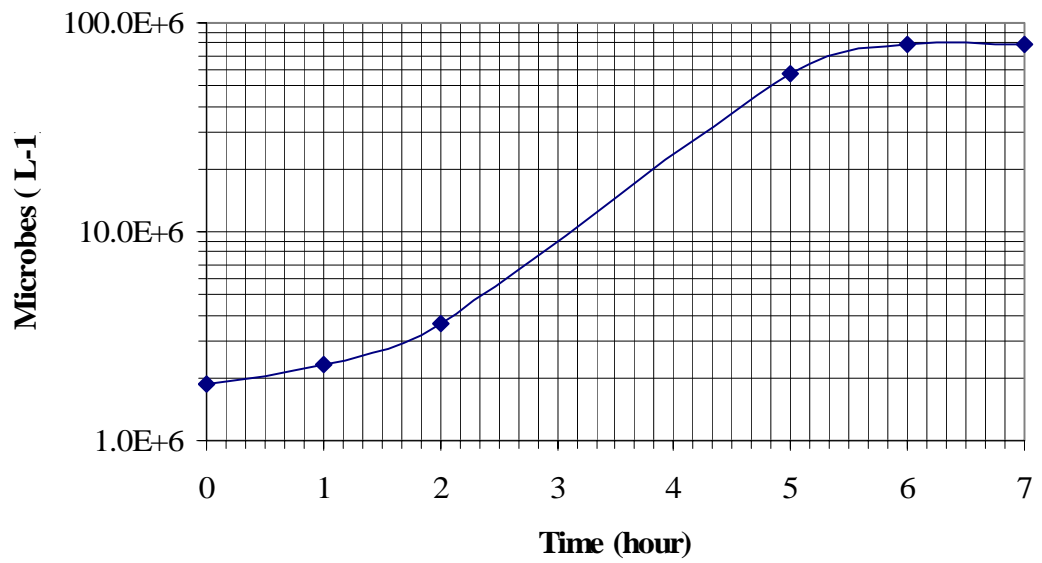


Figure VIII-6 shows the growth rate of the indigenous community. On

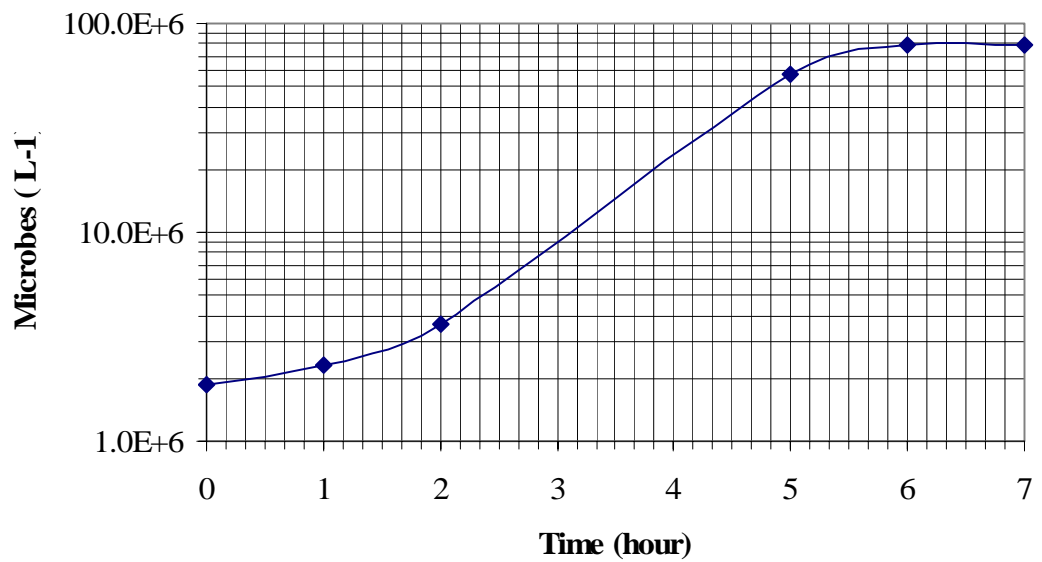


Figure VIII-6 a short lag phase of 1 hour can be seen; then the IC starts to increase. After the second hour, exponential growth is measured. The exponential growth stops after the fifth hour. The IC's generation time was calculated to be 45 minutes from

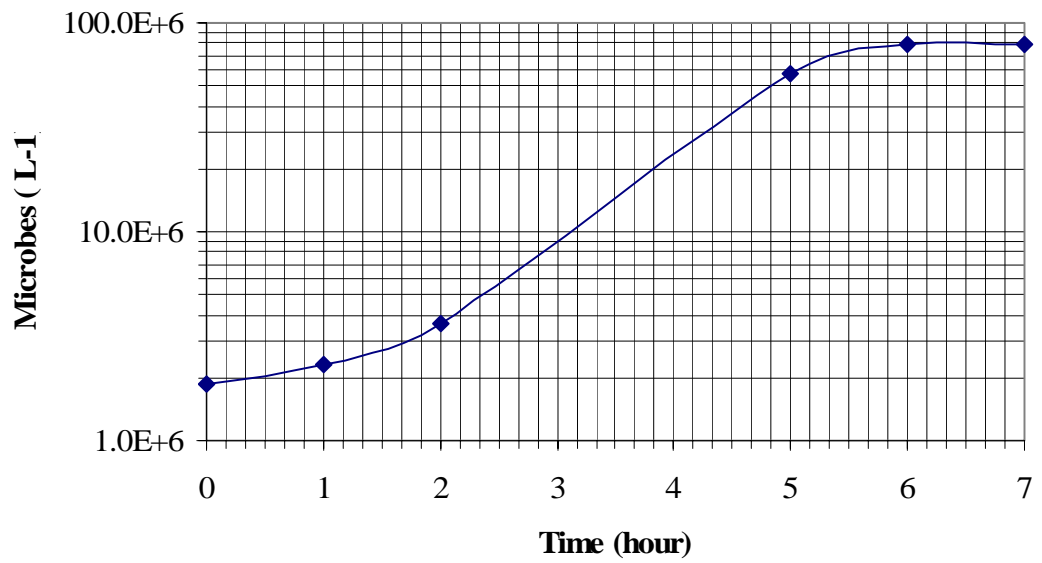


Figure VIII-6. The lag phase is very short in this measurement due to the fact that the IC cultivated in nanofiltration permeate was transferred at 10% in volume to the new flask where the growth rate measurement took place. Therefore, the IC was ready to colonise the new environment.

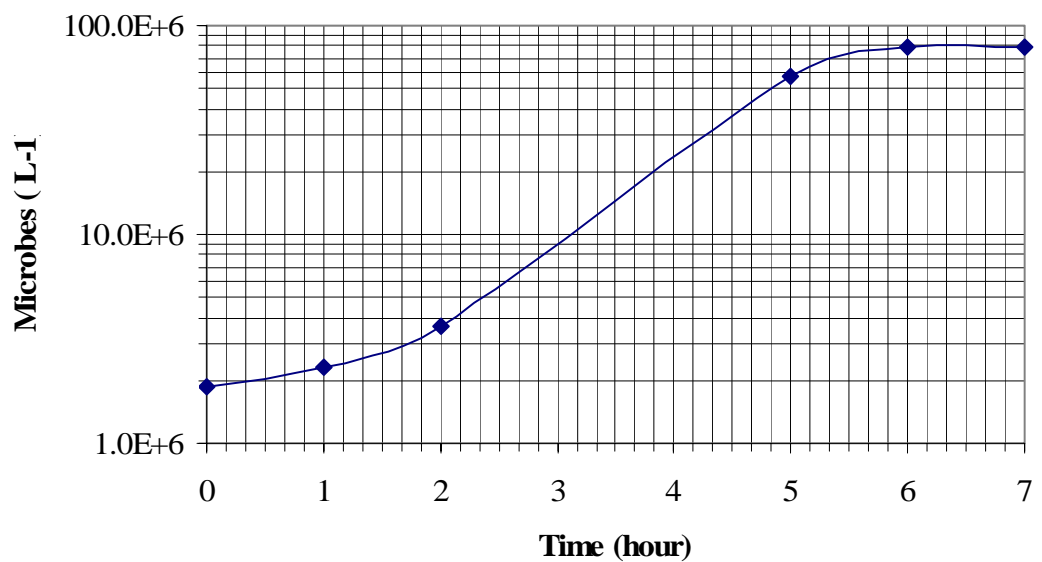


Figure VIII-6: Indigenous community growth curve

The continuous suspended bioreactor is filled up with nanofiltration permeate, adjusted to 6000 mg/L COD. The IC from the broth used to measure growth rate is used to inoculate the bioreactor. The bioreactor stands in batch mode for 3 days before the continuous mode is started.

VIII.3.3.3 *Continuous suspended bioreactor*

After 3 days in batch, the continuous mode is started at a rate of 800 ml/day, so the retention time was 2.2 days. Different retention times were tested. Figure VIII-7 shows the COD reduction achieved in suspended continuous bioreactor according to the retention time. At 2.2 days the micro-organisms grew well and a decrease in COD of 20% is observed, but after the third day, an increase in COD and pH occurred. In addition, a drop in turbidity was indicative that the bioreactor started to wash out. Micro-organisms were leaving the bioreactor quicker than they were multiplying. Therefore, after the fifth day, the feed rate was reduced, giving a retention time of 4.4 days in order to avoid total wash out of the micro-organisms.

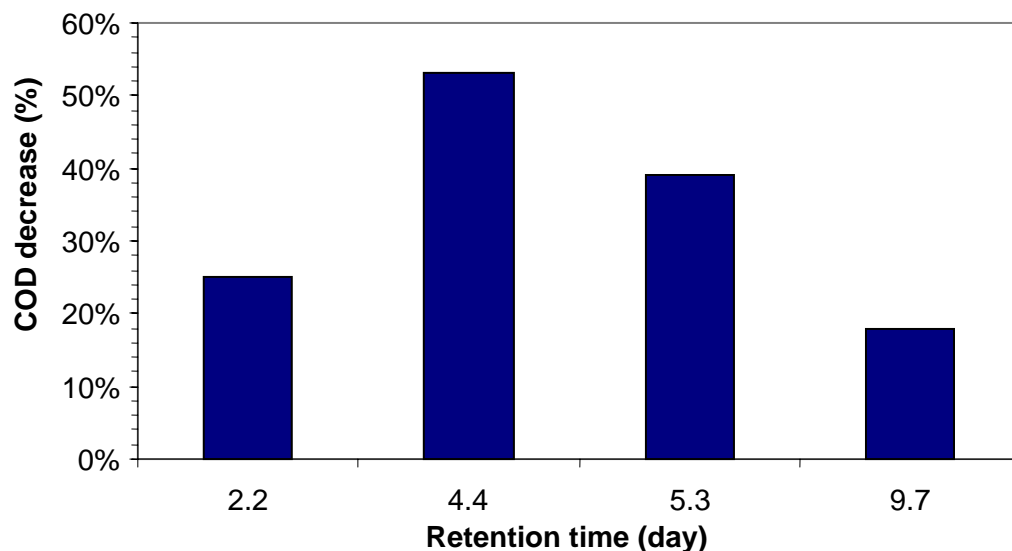


Figure VIII-7: Influence of the retention time on the COD removal

At best, the results are 53% COD decrease and a pH stabilised at 7.8 against a pH 9.2 for the NF permeate. This result is obtained with a retention time of 4.4 day and in inlet COD of 6000mg/L. This regime corresponds to an organic load of 2400 mg of COD per day. Increasing the retention time further does not improve the biodegradation. Figure VIII-7 at a retention time of 5.3 day and 9.7 day the performances are reduced. At 9.7 day retention time, the biological process stops after 24 hours. During the 24 hours the COD level and the pH increase respectively from 3180 to 3600 mg/L and from 7.9 to 8.3. After 5 days, the COD level measured is 4750mg/L which is less than 20% of COD reduction. The biological process has stopped. This is due to the non-removal of waste produced by the micro-organisms and by an impoverishment of the bioreactor in fresh nutrients.

These results show that the indigenous community does not totally reduce the COD level of the effluent. Nevertheless, through the 30 days of being cultivated in the suspended continuous bioreactor, the culture has improved its ability to degrade the nanofiltration permeate. Figure VIII-8 shows the performances of the suspended bioreactor over 1 month. The inlet flow rate is indicated with horizontal bars. When the retention time is 4.4 days the best performances are achieved. After a dramatic decrease in performance due to the high retention time set-up of 9.7 days, a return to a retention time of 4.4 days leads to a performance improvement.

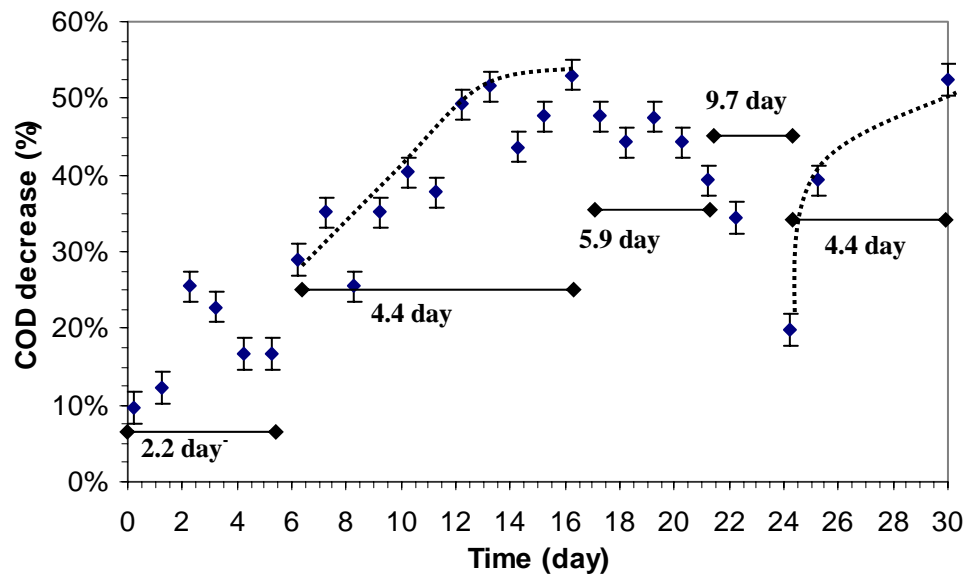


Figure VIII-8: COD reduction ability of the IC (retention times indicated in day)

Figure VIII-8 shows the evolution of the bioreactor outlet COD relative to the retention time. The dotted lines shown on Figure VIII-8 represent the improvement in COD reduction performances when the residence time is set-up at 4.4 day. During the month of growth in the continuous reactor, 960 generations of micro-organisms were produced, basing this calculation on the cell count shown in

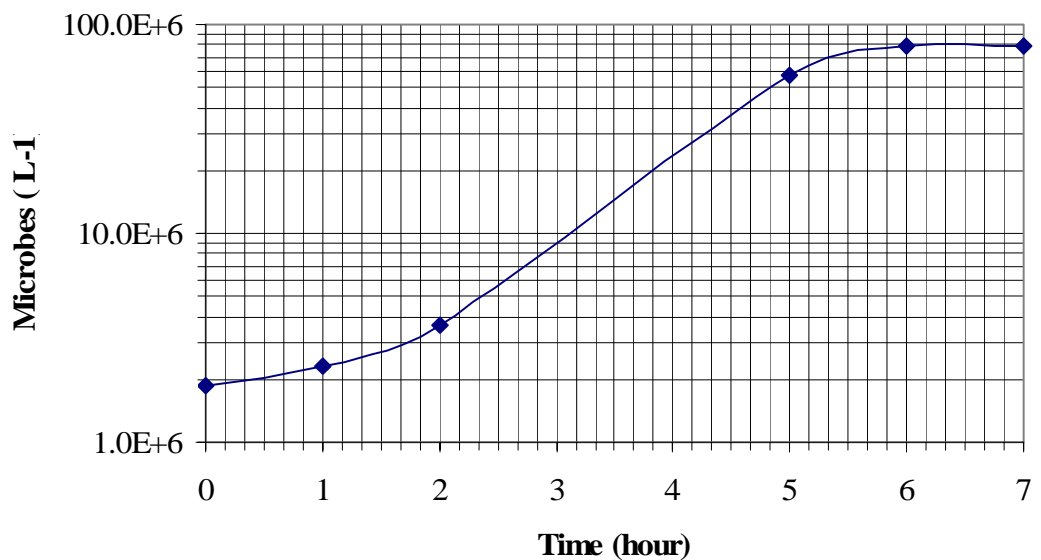


Figure VIII-6. The IC is adapted and specialised to degrade the nanofiltration permeate. In batch,

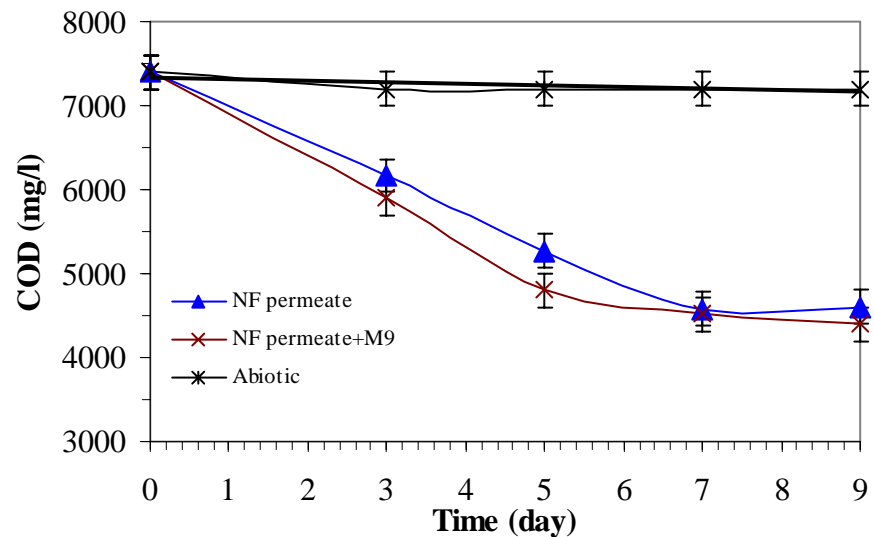
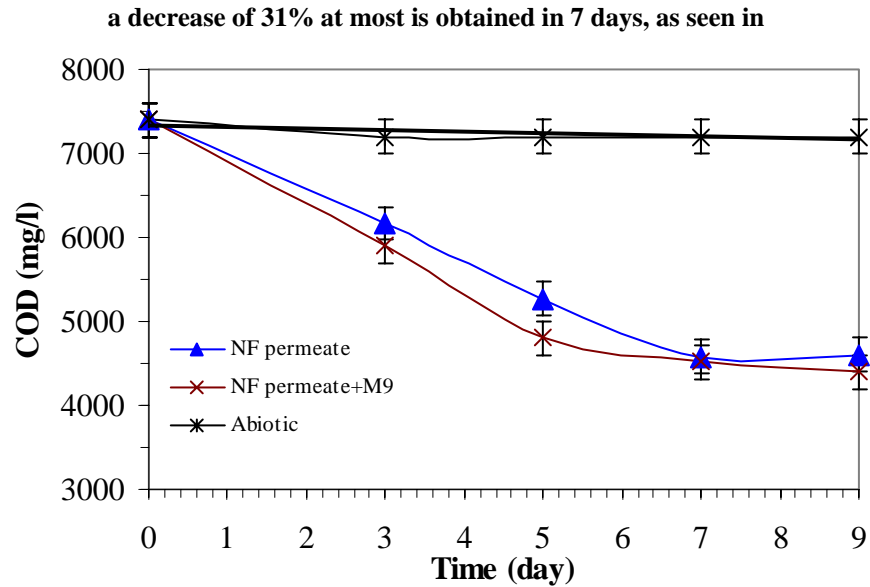


Figure VIII-2

, whereas a decrease of 53% in 4.4 days is obtained in continuous mode. The culture of the continuous bioreactor is harvested and frozen at -80°C to be used in the next stage. The new culture is named IC2. The bioreactor is sensitive to the retention time and the optimum is found to be 4.4 day or may be slightly below with a feed of 6000mg of COD per litre. The optimum retention time will be found using the fixed bed bioreactor.

VIII.4 FIXED BED BIOREACTOR

A fixed bed bioreactor was used to perform the biodegradation of the nanofiltration permeate. This bioreactor was described in Chapter III Experimental Equipment and Procedures paragraph 6.4. The fixed bed bioreactor is inoculated with the IC2. They establish themselves and colonise the plastic matrix rapidly (batch process). The outlet is opened, the feed is dripping at the open top of the bioreactor and the flow rate is controlled by a peristaltic pump. The trial lasted 240 days.

The effect of the feed flow rate on the bioreactor performance was studied and related to the feed COD load. The feed organic load corresponds to feed COD (mg/L) multiplied by the feed rate giving a value of COD per day that feed to the bioreactor. Figure VIII-9 shows the evolution and variations of the bio-permeate. It can be seen on the figure that globally and independently of the feed load, the performances of the bioreactor have significantly improved, from 40% to 90% of COD reduction, over the 240 days.

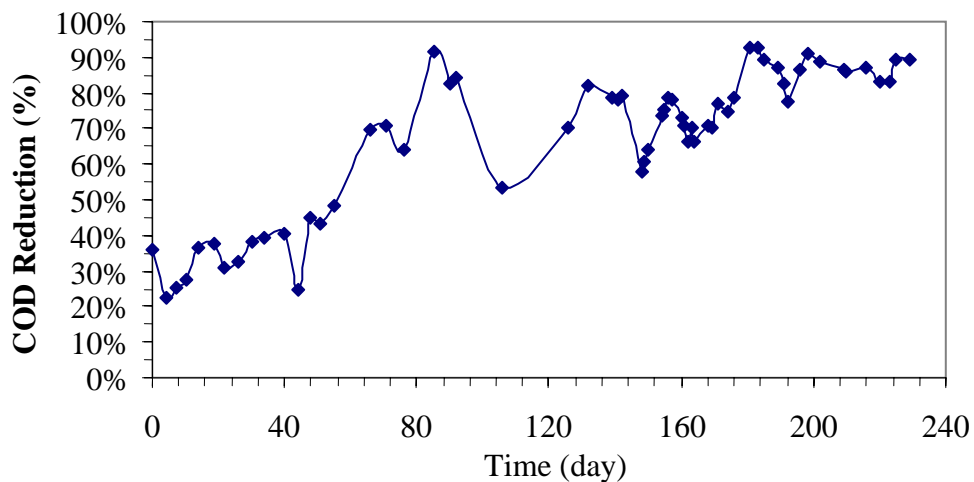


Figure VIII-9: Reduction in effluent COD

The performance improvement is attributed to two factors. The first reason is that the bioreactor feeding was optimised. By optimising feed loading and recycling loop of bio-permeate into the bioreactor permeate was introduced. The second reason is that the consortium has evolved and improved, giving better performances with time. This

last point is justified by the fact that during the 20 first days, the COD feed loading was set at 8550 mg/day of COD and the reduction of COD was 40%, similar to the results obtained previously with the suspended bioreactor. At the end of the period trial when the COD feed loading time was optimised, 8500 mg/day of COD, a reduction in COD of 90% was obtained. Figure VIII-9 shows that after day 181, the optimum feed loading and the recycling loop are implemented the reduction in COD is optimum and more consistent.

VIII.4.1 Optimisation of the ratio COD/flow rate

The nanofiltration permeate's COD evolved with time. This is mainly because the permeate is vulnerable to biodegradation and due to the filtration conditions such as fouling, temperature and nanofiltration feed concentration. The control of the nanofiltration permeate was discussed in chapter V. The fact that the permeate is vulnerable to contamination means that it cannot be stored too long without experiencing microbial growth. Therefore, the nanofiltration permeate that is used for the bioreactor feed is stored at +4°C. This inhibits microbial growth at least for one month. Nevertheless, the tank to feed the bioreactor is a 5 litre container, and regardless of the fact that it is washed with a biocide solution prior each feed reload, sometimes microbial growth was observed and lower pH and COD values were measured. This can be explained by the fact that the feed flow rate is very low at the study scale and microbes from the bioreactor may contaminate the feed tank.

The feed COD load is an important factor to optimise the fixed bed bioreactor. When this COD load is known, the feed flow rate may be tuned to the feed COD. Figure VIII-10 shows the relation between the COD load (Orange curve) and the COD measured at the bioreactor outlet. The line across the diagram represents the optimum level of feed COD load for the system. It can be seen that when the feed load varies from the value of 8550 mg/day, the COD removal decreases. The blue arrow show the point at which the recirculation loop was started at 0.5 l/day. At the optimum, a COD reduction of 90% can be observed.

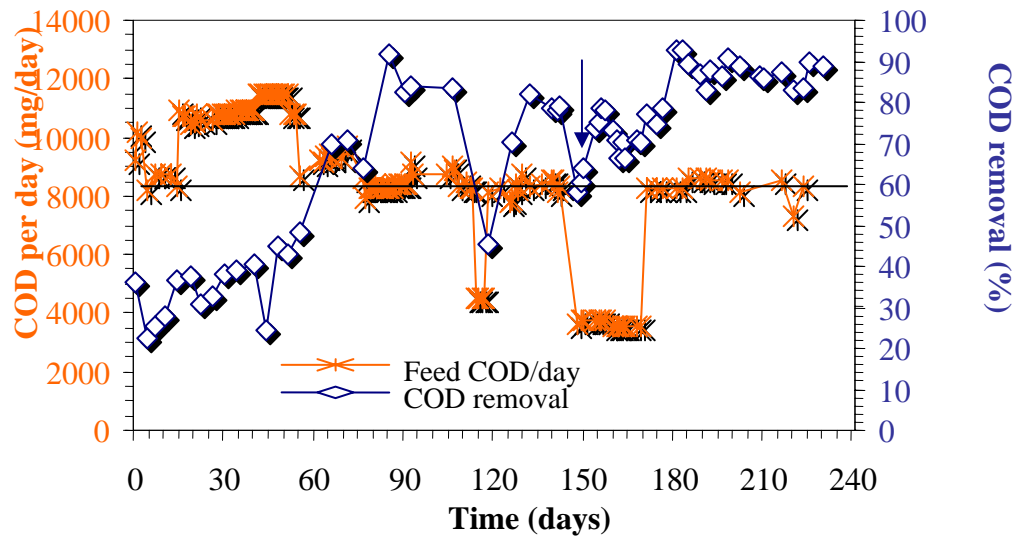


Figure VIII-10: Feed COD load and COD removal

During the 240 days, COD varied from 3700 to 9100 mg/L with an average of 7332 mg/L. This average value is in the average of the nanofiltration permeate that can be obtained when an ultrafiltration system is used as pre-treatment. The best ratio feed COD/retention time found to be between 8500 to 8600 mg of COD per day from day 170 to day 240.

VIII.4.2 Recycling loop

The recycling loop was introduced at day 148. The effect is to add more mixing to the fixed bed. This technique enables the dilution of the feed concentration and to recycle biological material back into the reactor.

Recirculation helps distribute the loading evenly throughout the depth of the bioreactor. It also helps to manage the variation in loading while maintaining a minimum wetting rate throughout the day. It is generally admitted that the higher recirculation ratios (recirculation flow rate/influent flow rate) the better the effluent quality, at least to the point where the hydraulic retention time in the bioreactor bed becomes too short. The recycling loop over-all allows the system to reach and maintain a steady state.

The effect of the recycling loop in the bioreactor inlet had an immediate effect on the bio outlet. Over night the 7 litres is recycled into the bioreactor. The turbidity value of the bioreactor outlet considerably decreased from an average value of 65 NTU before recycling down to 12 NTU after recycling. The explanation is that the biological fixed bed acts as a filter that retains particles, extra-cellular polysaccharides and detaches micro-organisms. The second effect is the effluent buffering effect, although large variations of COD inlet (down to 3700mg/L and up to 7350 mg/L), the outlet has not varied widely as seen on Figure VIII-10 from day 141 to day 171. 70-75% of the COD was reduced. After that period, the bioreactor was provided with a constant organic load of 8550 mg/day of COD and its performances improved.

VIII.5 SYNTHESSES

The fifth section summarises the chapter on biological process and points out the improvement of the biological system used. In addition, further improvements are proposed.

VIII.5.1 Achievements

A bio consortium was developed from a batch of waste metalworking fluid. It has been proven over several months to be efficient to remediate the NF permeate of the waste effluent. Table VIII-3 summarises the bioreactor parameter optimised.

COD in (mg/L)	Feed flow (l/day)	COD (mg/day)	Effluent Recycled	Turbidity (NTU)	COD outlet (mg/L)
6000-9000	1.38-1.08	8550	Yes (0.5 l/h)	10-15	800-1200
			No	65 – 90	700-2000

Table VIII-3: Summary of the bioreactor optimum parameters and performances

More than 90% of the COD is removed from the effluent when the bioreactor is used in optimum conditions with the developed bio consortium.

The difficulties to set correctly the bioreactor arose due to the fact that the COD inlet is not always known and well controlled. This represents the situation that maybe encountered in an industrial environment. The study showed that the variation can be buffered by adding a recycling loop.

An optimum of 90% of COD reduction with a single stage trickling filter is a very good achievement when compared with level of removal found in literature (Benfield and Randall 1980).

VIII.5.2 Additional improvements

Adding a second stage to the filtration will enhance the performance of the biological system and reduce the total reactor volume. The performance achieved with the system proposed lowering the COD of the effluent down to 800 mg/L. This performance may be enhanced by adding a second bioreactor in series. According to (Benfield and Randall, 1980), the addition of another reactor in series with identical volume and recirculation ratios will improve the overall performances of the system. The second benefit is that a new microbial population can establish itself in the second bioreactor more adapted to a lower level of COD and pH. This is the effect was explained in encouragement of a new microbial colonisation (Population C shown in Figure VIII-5).

The media used to grow the microbes is of importance too and choosing a better growth media than the pall ring used in the small-scale reactor. In Chapter III are the details of the Bio-deck used in the large-scale bioreactor.

The feed temperature is a factor not studied in this work. An increase in feed temperature can have a beneficial effect on the bioremediation performances. Designed for an industrial scale, it would be economically difficult to justify the heating of the media. Nevertheless, when on line with the filtration process, the permeate is flowing at a higher than ambient temperature during continuous filtration mode. It was observed that the permeate temperature varies from ambient, when starting filtration,

to a temperature of 30°C. This range of temperature could be beneficial to the biodegradation process.

CHAPTER VIII Biological Process	219
VIII.1 Introduction	219
VIII.2 Experiments carried out in Oxford	220
VIII.2.1 Plate counting	220
VIII.2.2 Bacteria consortia test	221
VIII.3 Experiments Carried out in Nottingham	222
VIII.3.1 Development of a home made bio-consortium	223
VIII.3.2 Culturing the Indigenous Community	223
VIII.3.3 Enrichment	227
VIII.3.3.1 Definitions	227
VIII.3.3.2 Strategy adopted	229
VIII.3.3.3 Continuous suspended bioreactor	230
VIII.4 Fixed bed bioreactor	233
VIII.4.1 Optimisation of the ratio COD/flow rate	234
VIII.4.2 Recycling loop	235
VIII.5 Syntheses	236
VIII.5.1 Achievements	236
VIII.5.2 Additional improvements	237

CHAPTER VIII

Figure VIII-1: Oxford bio consortia with dilute UF-permeate	222
Figure VIII-2: Nanofiltration permeate test with IC	224
Figure VIII-3: Diluted ultrafiltration permeate flask test with IC.....	225
Figure VIII-4: Biodegradability comparison between NF and UF permeate	226
Figure VIII-5: illustration of the impact of enrichment on indigenous population.....	228
Figure VIII-6: Indigenous community growth curve.....	230
Figure VIII-7: Influence of the retention time on the COD removal.....	231
Figure VIII-8: COD reduction ability of the IC (retention times indicated in day)....	232
Figure VIII-9: Reduction in effluent COD.....	233
Figure VIII-10: Feed COD load and COD removal.....	235

CHAPTER VIII

Table VIII-1: Bacteria count	220
Table VIII-2: Experimental plan.....	224
Table VIII-3: Summary of the bioreactor optimum parameters and performances....	236

CHAPTER IX

SYSTEM DESIGN

CHAPTER IX

System Design

IX.1 INTRODUCTION

This chapter concentrates on the design aspects of a full process bringing together all different processes that have been discussed in the previous chapters. Starting with the initial design proposed by CARDEV Ltd, the different options are investigated and a final design is proposed. Modifications to the process and procedures also are proposed.

IX.2 INITIAL DESIGN

The initial design proposed by Cardev Ltd, was composed of 4 different main components; a waste storage tank, ultrafiltration unit including holding tank 180 litres, a 2m³ bioreactor and a nanofiltration unit including a 600 litres holding tank. The 4 units have been described in more details in Chapter III, and the schematics are presented in Appendix C. Some general problems have been identified with this design, and are discussed below.

IX.2.1 Liquid handling

One of the general problems when dealing with emulsion and oily wastewater is the phase separation and one has to avoid the mixing effect. On the original design, it can be seen that the effluent before going into the coalescer tank is often mixed, this allow the free oil and aggregates to be re-emulsified. The floating pickup point in both the waste coolant tank and the main tank are the first problems to be solved. Floating pickup draws preferentially the floating oil that separates naturally by gravity into the system, and remixes it. This affects the filters increasing their clogging, and re-mixing

of the oil with the effluent that once tries to separate in first place. In addition more liquid than necessary is handling by the different pumps; to pass the free oil through the all system from coolant tank to the membrane inlet. The pumps energy is not used efficiently. This problem can be solved by using sinking pick-up points, so the pump draws only the emulsion, leaving the free oil in the coolant and main tank. A tap should be added on the side of the coolant tank to enable the drainage of the free oil.

The inlet of the coalescing tank was designed to spray the effluent on the top of the coalescing media. This increases the mixing of the effluent and diminishes the efficiency of the coalescing media regarding that type of media separates large oil droplets but not emulsified oil. The effluent must be introduced into the coalescing tank under the liquid level to avoid turbulence. Therefore, any oil droplets arriving at that point would be removed by the coalescing media.

The return of the effluent from the membrane into the process tank makes this tank over flow into the main tank. The return of the retentate into the process tank is necessary to maintain the process tank full, in addition the over flow into the main tank is beneficial to re-dilute the retentate with the main tank effluent. Nevertheless, the over flow returns the main tank creates turbulence and mixing. This over flow should be collected and drained to the main tank under the liquid level arriving smoothly against a wall of the tank.

All these measures can protect the filters and the coalescing media because oil plus particle tend to clog filters. The membranes are also protected; free oil and particles entering the membrane tubes have a great fouling and damaging potential. They reduce the overall running cost of the system. In addition they do not add any additional manufacturing cost, actually only a tap was added to the coolant tank and a pipe collecting the over flowing concentrate return from the process tank to the main tank.

IX.2.2 Concentrate tank and bioreactor feed

On the design of membrane filtration system 1, the concentrate tank receives all concentrated emulsion and recovered oil. This again causes the mixing of two streams

that have been separated by the process. These two streams have different nature and are of different interest. It has been seen in Chapter V-3 that the oil has a calorific value, which makes it valuable as a fuel or at least could be supplied to waste contractors at no cost. The second problem is that the mixed oil concentrated tank is transferred to the bioreactor. This was unrealistic because whatever the efficiency of the bioreactor used, this part of the process denied absolutely the all separation process. If a bioreactor can be designed to sustain the COD charge of the raw effluent, there would be no reason to propose a separation process prior to the bioreactor. It has been seen in Chapter IV that the direct aerobic biodegradation of the emulsion is not feasible due to oil content COD charge and emulsion nature. Therefore, separation process was set-up to enable the biodegradation of the MWF by using the permeate as feed for the bioreactor. The membrane filtration is used to remove the oil droplets from the bioreactor feed stream and to lower its COD.

The solution was therefore to use effectively the membrane separation process to enable good functioning of the bioreactor, providing a consistent permeate flux. On the other hand, the recovered oil from the coalescing tank as well as the steeling oil recovered from the cooling tank is kept separate from the concentrate stream. The concentrate stream can be disposed of or be chemically treated on site as it has been proposed in Chapter V-3. This matter is discussed later, it involves an additional tank to be built a motor to stir the emulsion, a holding tank for the concentrated acid used to treat the retentate and a dosing pump to progressively inject the amount of acid needed. It has been found in Chapter V that with sulphuric acid at 5 Normal 10 ml were needed to treat 500 ml of UF concentrate MWF20.8%.

IX.2.3 Post bioreactor treatment

The post bioreactor treatment proposed in the original design was to use a nanofiltration membrane including a 600 litre holding tank. Two major remarks can be made here the nanofiltration is not the usual type of membrane chosen to use with a bioreactor. On one hand, NF membranes have a great retention potential and a low flow rate when compare to microfiltration system. On the other hand the biological

system is used in this system to polish the permeate, this is why when using a NF system to clarify a biological effluent where the primary purpose would be to retain the micro-organisms, for this task microfiltration would be the right choice. The second remark concerns the size of the holding tank; 600 litres takes a lot of space and holding so much biological effluent creates odorous problems due to micro-organisms development in eventual anaerobic conditions. Therefore, as a post treatment, an online microfiltration system should be preferred, allowing the recirculation of the retentate to the bioreactor. It has been seen in Chapter VI that activated carbon columns can be used as a post bioreactor treatment the scale-up and feasibility being discussed in IX.6 later.

IX.3 CHOICE OF FILTRATIONS

In Chapter IV and V the results of the filtration of metalworking fluid using mobil cut 232 with 3 different filtration systems were presented. It has been seen that coupling UF and NF filtration enhances the whole filtration process enabling the production of a constant feed stream for the bioreactor. Therefore, the solution chosen is the use of ultrafiltration FP100 of the raw effluent in a semi-batch system followed by an on line nanofiltration using AFC30 tubular membrane. The system is shown in Figure IX-1 and the filtration parameters are shown in Table IX-1.

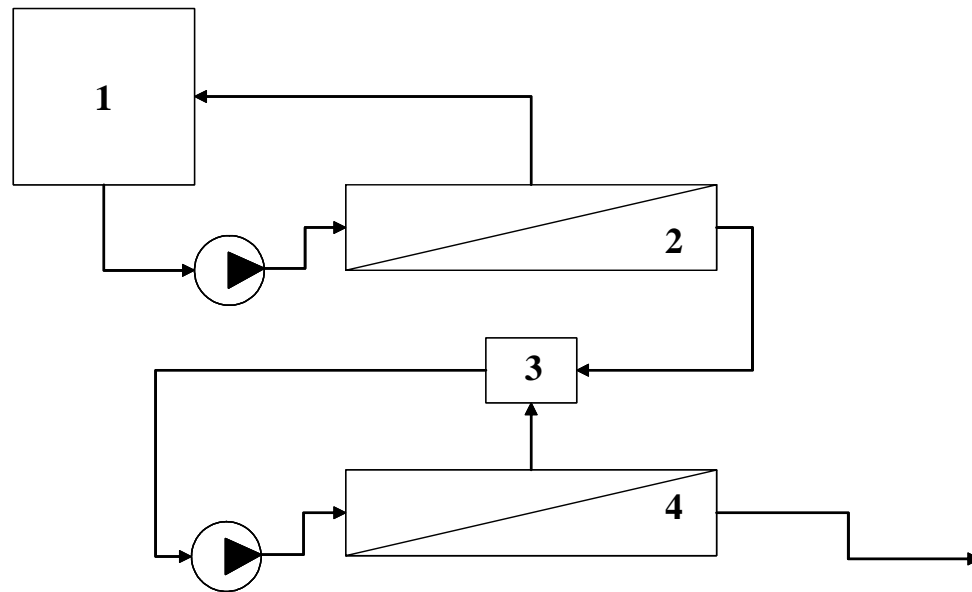


Figure IX-1: Filtration system

1: UF process tank; 2: FP 100 ultrafiltration membrane 3: UF permeate tank/NF process tank;

4: AFC30 nanofiltration membrane;  pump

Membrane	Inlet P (bar)	Outlet P (bar)	TMP (bar)	Flow velocity (m/s)	Permeate flux (L/h/m ²)	Permeate Turbidity (NTU)
FP100	4	1.5	2.75	2.5	45 to 25	5
AFC30	8	6	7	2-2.5	23-19	0.2

Table IX-1: Filtration parameters

The TMP of 2.75 bar allows the best permeate flux for the best oil retention for feed concentration between 5 and 20% to be obtained. When using The UF permeate in semi-batch instead of batch system the retentate is maintained at a lower concentration which enhance the permeate flux and the permeate quality. The choice of using UF membrane pre-treatment is in the view of removing the oil droplets is positive and this study can be related to the study carried out by (Kim et al. 2002). They used membrane filtration to treat a secondary effluent from a sewage mixed industrial and municipal wastewater treatment works. They studied the effect of pre-treating the stream for a reverse osmosis system. In the study, the authors compared three pre-treatment

systems; UF, activated carbon and dual media filtration combined with coagulation. The first system shows best performances with the least RO permeate flux decline by removing the feed turbidity. The removal of the effluent turbidity is an important factor to take into account when designing a pre-treatment system for a RO/NF filtration. Therefore, the FP100 ultrafiltration membrane is chosen to reduce the turbidity of the nanofiltration effluent.

The effect is immediate on the overall filtration treatment, the nanofiltration system. The working cycle is longer and NF unit shut-down for washing and cleaning is less frequent.

IX.4 TREATING THE CONCENTRATE

The UF concentrate consists of an emulsion of oil in water at 20% of oil and is a residue of the membrane process. Whatever the membrane process used UF, NF or combination of both the separation is limited by the concentration and the physical-chemical change of the feed. The limit of retentate concentration has been found to be 20%. Over this limit the membrane is severely fouled and oil permeates through. Nevertheless, a chemical treatment of the concentrate has been found to be effective. The chemical treatment has been studied in Chapter V and consists of slow acidification at low shear rate of the UF concentrate.

IX.4.1 UF concentrate

20% of the initial volume of waste treated remains as concentrate. Therefore, a 200 litres tank can be used to coagulate the concentrate it required a mixing unit and an acid injection point. Baffles may be added to the wall of the tank in order to avoid gel formation. The principle is to avoid mixing the coagulated oil and to neutralise the pH of the aqueous phase. Figure IX-2 present the arrangement for the acidification process.

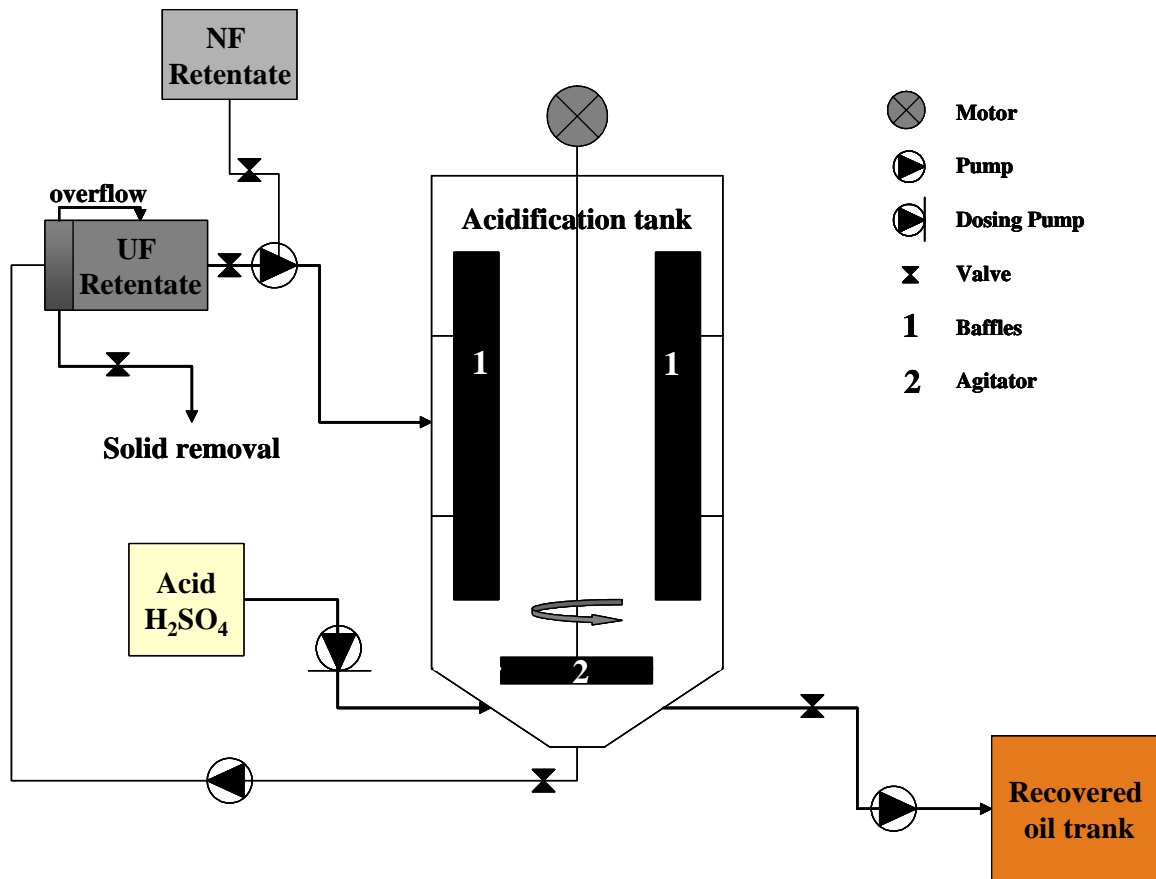


Figure IX-2: Acidification process

The aqueous phase recovered from the chemical treatment is re-directed to the UF unit. A white precipitate was formed when the acidic aqueous phase was returned to caustic pH values. This precipitate must be removed which can be done by adding a buffering tank on the side of the UF unit main tank as shown on Figure IX-2.

IX.4.2 NF concentrate

The turbidity of the nanofiltration concentrate increased during filtration, this is essentially due to the accumulation of residual oil droplets that comes from the UF separation stage. Therefore, it is possible to send this concentrate to the chemical treatment with the UF concentrate as shown in Figure IX-2. The aqueous phase is returned to the UF filtration system. In the case of the nanofiltration the acidification is

not a polishing treatment, but a purge of the NF filtration system to be returned to the UF filtration system in order to remove the oil that was concentrated during the nanofiltration process.

Concentrate volume (litre)	FP 200		FP 100	
	Turbidity (NTU)	COD (mg/l)	Turbidity (NTU)	COD (mg/l)
600	127	7989	75	6700
400	325	11098	247	9246
300	500	12995	419	10848
200	764	15058	653	12529
100	1978	20436	1403	17139

Table IX-2: Evolution of the concentrate quality during the nanofiltration of the UF permeates FP200 and FP100 respectively

Table IX-2 show the increase in NF concentrate during filtration of FP200 and FP100 permeates. The nanofiltrations have been carried out separately using 600 litres of both UF permeates. The increase in COD is not linear with the volume of concentrate treated because the nanofiltration permeate contains part of the original COD and this part increases with the concentration ratio. In addition the sharp increase in concentrate turbidity may indicate a change in particle size because turbidity is related to particle size and concentration. At the end of the nanofiltration it has been seen in chapter V that in both case the permeate flux and permeate quality do not worsen dramatically. Therefore the purge does not need to take place after only 500 litres of permeate treated. Maintaining a good UF permeate quality enhances the nanofiltration system and reduces the frequency of purge to be made.

IX.5 THE BIOLOGICAL TREATMENT

The biological treatment using an indigenous community of micro-organisms has been proven to be effective to treat the NF permeate of MWF5%. In this section the functioning parameter of the bioreactor are summarised and the scale-up of the bioreactor investigated.

IX.5.1 Functioning parameters of the bioreactor developed

The bioreactor was developed at a scale of 4.5 litres and had worked for 8 months. Table IX-3 shows the optimised biodegradation parameters found for the bioreactor used. The bioreactor was used at 21°C

Parameters	Values
Feed temperature (°C)	21
Feed Flow (l/h)	0.054
COD load COD/flow rate (mg of COD/day)	8550
Recirculation rate (litre per hour)	0.5

Table IX-3: 4.5 litres bioremediation optimised parameters

The bioreactor feed is the nanofiltration permeate produced by the system NF combined with UF. This filtration unit produced a fairly constant stream with the flowing characteristics using FP100 (from Table V-2) turbidity between 0.1 and 0.23 NTU a COD level of 6400 mg/L at 20°C the COD varies between 5900 and 8200 mg/L mainly depending on feed temperature and concentration the flux is 24 L/h/m². The bioreactor feed has to be set at 1.34 L/day when using the 4.5 litre bioreactor (1.45 to 1.05 L/day)

IX.5.2 Bioreactor scale-up

The bioreactor is scaled-up to treat 500 litres per day of NF permeate. A very important factor related to the bioreactor performances is the feed COD load. Equation IX-1 reminds the definition of the feed COD load.

$$\text{Feed COD load [mg/day]} = \text{Feed flow rate [L/day]} \times \text{Feed COD [mg/L]} \quad \text{Equation IX-1}$$

Therefore, the new COD load based on the optimum parameter of the small-scale bioreactor is recalculated to fit a similar bioreactor able to treat 500 litres per day of NF permeate.

With an average feed flow rate of 1.34 L/day and a volume of 4.5 L the retention time is 3.36 days using a bioreactor of 1.679 m³ of effective volume enable to treat 500 litres of NF permeate per day. Therefore, the feed flow is 20.8 L/hour and the COD load 3200 grams of COD per day. This COD load calculated corresponds to the best performance of the small-scale bioreactor. This allows the set-up of the bioreactor feeding flow rate, which may depend on the actual feed COD. Nevertheless, the feed load must be maintained at 3200 grams of COD per day.

In Chapter III, the large-scale bioreactor has been presented and has an internal matrix with different parameters from the small scale bioreactor. Therefore, changing the growth media may influence bioreactor performances. New functioning parameters are given in Table IX-4. These parameters are recalculated in order to maintain the bioreactor COD removal performances. Taking into account the feed flow rate and its strength, enable the bioreactor scale-up with a constant recirculation ratio.

Parameters	Values
Feed temperature (°C)	20 to 35
Flow rate (L/h)	20.8
Feed load COD/flow rate (g of COD/day)	3200
Recirculation rate (litre per hour)	192.6

Table IX-4: Large-scale bioreactor functioning parameters

IX.6 SCALING UP ACTIVATED CARBON COLUMN

Activated carbon unit has been described in chapter VII. It was found that using 212g of activated carbon in a column of 0.935 m high and 3 cm in diameter was able to treat over 50 litres of bioreactor effluent fed at a rate of 0.7 litres per day. The column performances were such that all colour and COD were removed. To scale-up the AC column the surface area of the column and the quantity of AC are recalculated relatively to the flow rate of effluent to be treated. The column high is brought to 1m (instead of the 0.935m) in order to simplify the calculation. Nevertheless, increasing the column height may seriously affect its performances; the risk of compaction to be compacted leading to column blockage. In the following calculations, it is assumed that each drop of effluent arriving at the inlet of the column surface takes a random vertical path through the column. This is the reason that the surface of the scaled-up column is re-calculated relative to the flow rate of the effluent, in order to simulate the quantity of effluent going through a given surface of activated carbon column and following a drop of 1 meter. With the column dimensions given above, it can be calculated that 0.99m^3 per day passes through 1m^2 . The principle of scale-up based on constant column flux is explained in Figure IX-3.

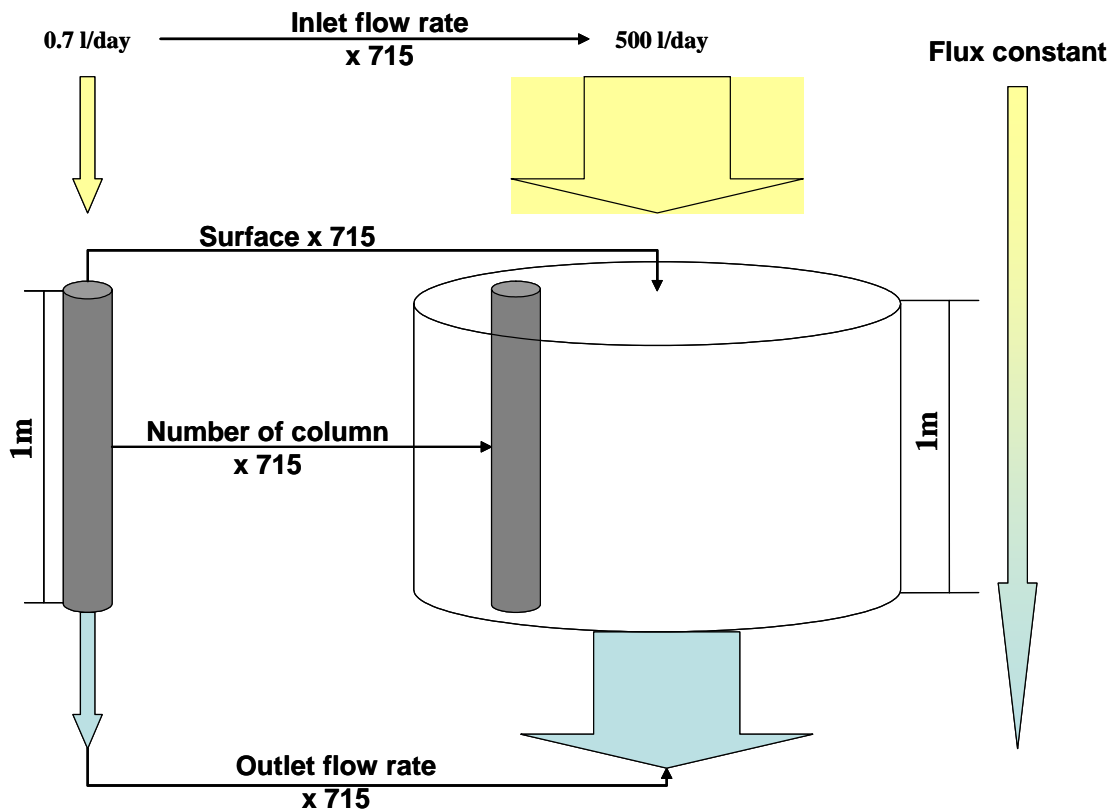


Figure IX-3: Activated carbon column scale-up

Therefore, based on a system treating 0.5 m^3 per day, when compared to the performances of the bench-scale column, 715 similar columns should be used that correspond to a larger column of inlet surface of 0.5 m^2 .

Column parameters	Values
Height (m)	1
Diameter (m)	45×10^{-2}
Volume (m^3)	0.16
Quantity of activated carbon (kg)	151

Table IX-5: Parameters of the large activated carbon filter

With 151.6 kg of activated carbon in the column, it can be calculated that a minimum of 28.6 m^3 bio-permeate can be treated before the column starts to saturate. A trickling distributor must be mounted at the activated carbon filter inlet to enable homogenous

distribution of the effluent. An additional back washing system can be used to remove eventual microbial growth at the top of the column. Figure IX-4 shows the activated carbon assembly and expected performances.

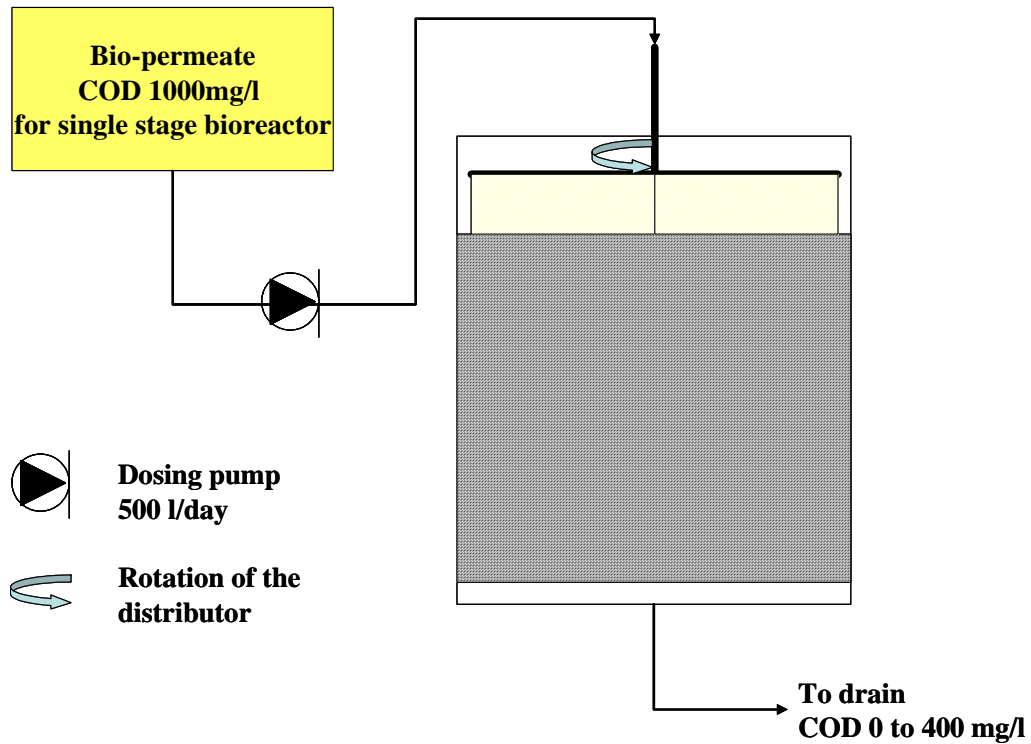


Figure IX-4: Activated carbon assembly

IX.7 SCALE-UP OF THE WHOLE PROCESS

This section will consider that 500 litres of waste metalworking fluids with an initial concentration in emulsified oil of 5% is treated through the system per day. The complete integrated design which takes into considerations all investigated process throughout this thesis is shown in Figure IX-5

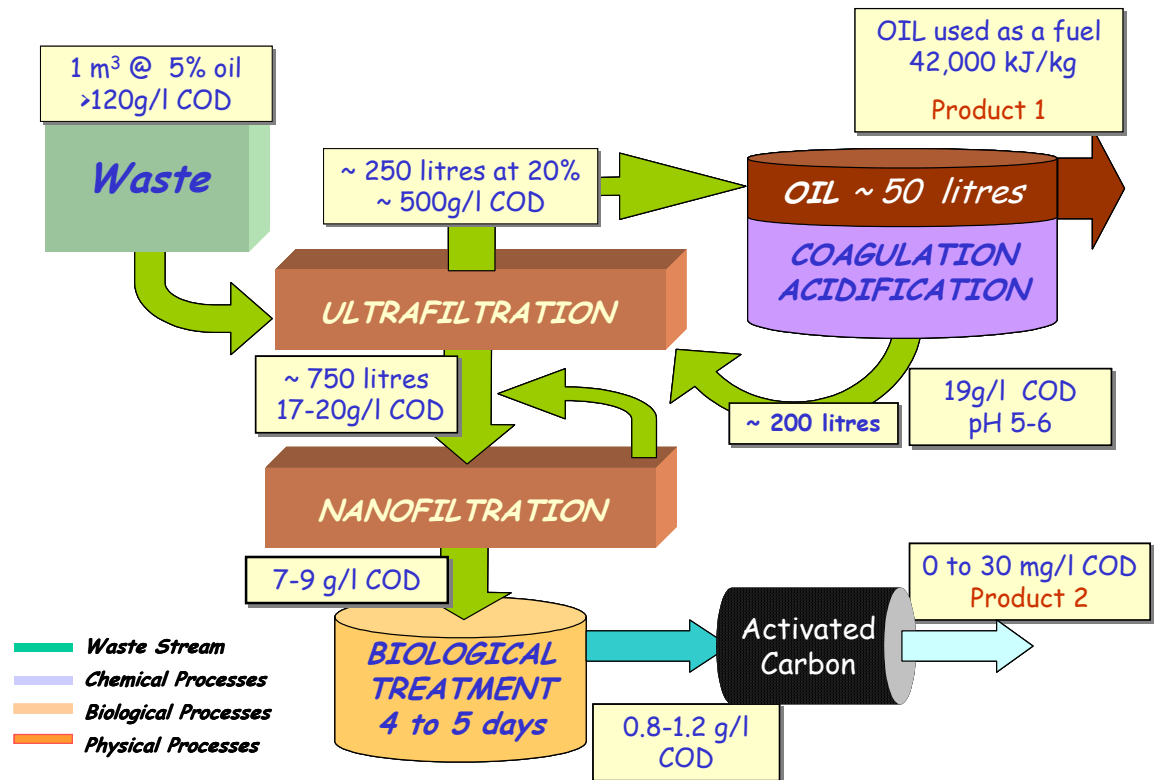


Figure IX-5: Final integrated process

It can be seen that the integrated process generates two final products: (i) recovered oil with high calorific values of 42,000kJ/kg, which can be used as fuel, and (ii) an aqueous phase with very low COD value satisfies the regulation. This aqueous phase can either be drained to sewer system or can be used to dilute the original MWF. Each component of this design and the whole setting were recognised as an enormous benefit for potential clients and the environment (see Appendix A).

IX.8 SYNTHESIS

Both the bioreactor and activated carbon filter, can be scaled up to suite the stream flux that is provided by the membrane unit provided originally by Cardev International Ltd.

When integrated to the system UF/NF the performances of FP100 are better then FP200. There are 4 benefits of using FP100 over FP200:

- ❖ The retentate obtained has a much higher concentration 20%
- ❖ More raw effluent can be treated by filtration using FP100 76% of the initial volume
- ❖ The enhancement of the NF filtration is greater by 5%
- ❖ The quality of the permeate produce implies that less nanofiltration concentrate will be treated chemically.(seeIX.4.2)

Over the period of the contract between Cardev International Ltd and the University of Nottingham, a prototype using a strategic combination of membrane filtration and biodegradation technologies has been developed.

What does the platform do?

- ❖ This prototype transforms the waste metalworking fluid into two products: Water, which can be used to mix new coolant and
- ❖ Oil which could be a saleable commodity.
- ❖ It reduces the waste volume by 95 %
- ❖ The system is modular and has been combined with two complimentary processes allowing this to:
- ❖ Recover oil from concentrate (for semi-synthetic fluids) and further reduce the waste volume
- ❖ Polish the aqueous phase using Activated carbon
- ❖ Numerous technical key points of the original filtration system have been improved.
- ❖ The new system improves the operation of the traditional membrane filtration
- ❖ It has been tested with semi-synthetic fluid with some success.
- ❖ The use of Activated Carbon further reduces the COD to approximately 0-30 mg/L removing the need for a post bio-separation process.
- ❖ A Recycling loop in the biological process enhances the performance of the Bioremediation system. This further reduces the final COD and cuts down on the turbidity)

Benefit of the system can be seen for potential clients and for the manufacturer and environment.

For the client

- ❖ After polishing permeate may be sent to drain or recycled as process water (30mg/l COD) depending on the application.
- ❖ Concentrate can be treated on site, at low cost due to volume reduction, to less than 20% of the original volume with the aqueous phase being recycled back into the filtration system i.e. No Disposal cost.
- ❖ Waste volume reduction of 95% (based on an initial concentration of 5% oil)

For Cardev

- ❖ The new system has taken the previous system tested by Cardev Intenatioanl Ltd. and made it work!
- ❖ Smaller unit can reduce manufacturing costs thereby increasing margin and/or enabling Cardev to enter new markets. Unit can be marketed has having a smaller footprint.
- ❖ Process is easily adaptable for other MWF than Mobilcut 232 and for synthetic fluids.
- ❖ There is a market for replacement consumables which are added to the system.
 - Replacement membrane elements
 - Acidification process (A specific Cardev brand may be formulated)
 - Activated carbon to be regularly regenerated/replaced

Other benefits

- ❖ The platform can be sold as an on site total remediation system
- ❖ Good press, marketing bioremediation as environmentally friendly
- ❖ The modular nature of the system makes it easy to integrate into an existing MWF maintenance program including MWF recycling.
- ❖ The system can be adapted to other suitable applications such as waste effluent from food industries.

CHAPTER IX System design	240
IX.1 Introduction	240
IX.2 Initial Design	240
IX.2.1 Liquid handling	240
IX.2.2 Concentrate tank and bioreactor feed	241
IX.2.3 Post bioreactor treatment	242
IX.3 Choice of filtrations	243
IX.4 Treating the concentrate	245
IX.4.1 UF concentrate	245
IX.4.2 NF concentrate	246
IX.5 The biological treatment	248
IX.5.1 Functioning parameters of the bioreactor developed	248
IX.5.2 Bioreactor scale-up	249
IX.6 Scaling up activated carbon column	250
IX.7 Scale-up of the WHOLE process	252
IX.8 Synthesis	253
Figure IX-1: Filtration system	244
Figure IX-2: Acidification process	246
Figure IX-3: Activated carbon column scale-up	251
Figure IX-4: Activated carbon assembly	252
Figure IX-5: Final integrated process	253
Table IX-1: Filtration parameters.....	244
Table IX-2: Evolution of the concentrate quality during the nanofiltration of the UF permeates FP200 and FP100 respectively.....	247
Table IX-3: 4.5 litres bioremediation optimised parameters	248
Table IX-4: Large-scale bioreactor functioning parameters	250
Table IX-5: Parameters of the large activated carbon filter.....	251

CHAPTER X
CONCLUSIONS AND
RECOMMENDATIONS

CHAPTER X

Conclusions and Recommendations

The present investigation into treatment of metalworking fluids aimed at the development of a robust, effective treatment system to treat liquid waste material produced in engineering industry. Not only did the research culminate in a pilot model, which would be suitable for on-site treatment, but also produced a combination of technologies, which treated the full volumes of waste fluids and separated the components into two streams.

One stream is the concentrated oil which was reduced in volume but could be suitable for use as a fuel and the other was a low chemical oxygen demand aqueous phase which could go to the drain via municipal sewage system at very low disposal cost. Alternatively, this source of water which when polished through activated carbon could be of suitable quality to recycle back as feed water into a new mixture of coolant.

The experimental programme of this study has been designed to test a number of processes that can be used for the treatment of metal working fluids. The programme covered a wide range of experimental variables to find optimal conditions for each process. A design of integrated process has been developed, the final process is suitable for on-site treatment and is being developed commercially by Cardev International Ltd (see Appendix A).

The following conclusions were made from this research:

The waste stream used was a stable oil microemulsion when mixed under 20% of oil. The concentrate of the emulsion produce during the filtration stage is still an emulsion of oil in water, but is less stable than the original oil. This is attributed to a phenomena of oil aggregation due to oil concentration and surfactant impoverishment. Two methods of chemical treatment have been studied. The chemical treatment finds its

justification in completing the filtration system by treating the irreducible concentrate produced during the ultrafiltration process. At the stage using acidification, a valuable product is recovered. This product is recovered oil with a calorific value of 42,000 kJ/kg that may be used as fuel.

This research showed that ultrafiltration was suitable to remove the oil droplets of the waste stream. Different factors have been investigated for the filtration of the waste stream. These factors were trans-membrane pressure, fluid velocity, temperature and stability of the emulsion in the feed stream. For ultrafiltration and nanofiltration, low TMP, low feed temperature (ambient), high feed velocity and stable emulsion produced a best permeate flux and quality. If TMP and feed velocity can be optimised, feed temperature and concentration cannot be technically maintained during filtration. The feed stream tends to heat-up and the emulsion deteriorates with the concentration ratio during filtration. Therefore, fouling appears and oil permeates both UF and NF membranes. This limits in the experiment to a concentration ratio of concentrate at 20% of oil. Above this limit even after membrane regeneration, oil permeates through the membrane and the permeate flux declines rapidly.

Membrane fouling was addressed by three means; optimisation of membrane surface regeneration using surfactant solution, gas injection during MWF filtration and ultrafiltration of the waste stream in order to improve the nanofiltration system.

At large scale, it was shown that for any method and filtration parameters the permeate flux declines during filtration.

It has been shown that the combination of UF and NF modules to treat the waste stream is very beneficial for the overall filtration and an increase of 240% in volume treated was calculated when using UF/NF instead of nanofiltration alone.

The feed concentration and stability greatly influence the effect on membrane fouling. The gel layer model applied to the filtration curve shows that the concentration of the gel layer increases during filtration. This phenomenon is attributed to the change in bulk concentration and nature of the emulsion.

The permeation of the oil through the membrane is attributed to the phase inversion that occurs in the gel layer.

The research has also shown that activated carbon is very efficient in removing the effluent COD and colour for the three different effluents investigated. Best performances were for the effluent coming directly from the bioreactor and containing microorganisms. This attributed to a synergetic effect between carbon adsorption and a continuity of microbial activity.

A bio consortium may be developed using microorganisms extracted from waste metalworking fluids. A fixed bed bioreactor using the bio-consortium was run successfully over 8 months and its performances were improved. 90% of the chemical oxygen demand was removed from the nanofiltration permeate, lowering its value from 7300 mg/L down to 800 mg/L using a one stage fixed bed reactor.

An integrated design including the different processes tested in this work. This design clearly shows the enormous benefits for potential clients and the environment. Cardev International Ltd have recognised the huge benefits from the proposed integrated system and are in the process of developing it (see Appendix A).

The following recommendations for further work can be suggested.

- 1- The study of the coalescence of semi-synthetic metalworking fluid concentrate and coalescing media performances could be investigated.
- 2- Use of a two stages bioremediation process for the treatment of nanofiltration permeates of metalworking fluid.
- 3- Modelling of full scale filtration (micro)emulsion at high oil concentration.
- 4- Developing the design to suit new markets such as food processing industry.

REFERENCES

Atsushi, M. and Mitsutoshi, N. 2002, "Membrane process for emulsified waste containing mineral oils and nonionic surfactants (alkylphenoethoxylate)", *Water Research*, vol. 36, no. 15, pp. 3889-3897.

Asenjo, J.A. and Merchuk J.C. 1995 *Bioreactor system design*, Marcel Dekker c1995

Baker, J. S. and Dudley, L. Y. 1998, "Biofouling in membrane systems - A review", *Desalination*, vol. 118, no. 1-3, pp. 81-89.

Baker, R.W. 1992, *Membrane Handbook* Kluwer Academic Publishers 1st May 1992

Baker, R. W. 2000, *Membrane Technology and Applications*. McGraw-Hill Companies; December 16, 1999 pp 528

Belkacem, M., Matamoros, H., Cabassud, C., Aurelle, Y., and Cotteret, J. 1995, "New results in metal working waste water treatment using membrane technology", *Journal of Membrane Science*, vol. 106, pp. 195-205.

Benefield, L. D. and Randall, C. W. 1980, "Attached growth biological treatment processes," in *Biological process design for wastewater Treatment*, G. H. Sewell, ed., London, pp. 391-456.

Benito, J. M., Ebel, S., Gutierrez, B., Pazos, C., and Coca, J. 2001, "Ultrafiltration of a waste emulsified cutting oil using organic membranes", *Water Air and Soil Pollution*, vol. 128, no. 1-2, pp. 181-195.

Benito, J. M., Rios, G., Ortea, E., Fernandez, E., Cambiella, A., Pazos, C., and Coca, J. 2002, "Design and construction of a modular pilot plant for the treatment of oil-containing wastewaters", *Desalination*, vol. 147, no. 1-3, pp. 5-10.

Benito, J. M., Rios, G., Pazos, C., and Coca, J. 1998, "Methods for the separation of emulsified oil from water: a state-of-the-art review ", *Trends in chemical engineering*, vol. 4, pp. 203-231.

Bhaskar, T., Uddin, M. A., Muto, A., Sakata, Y., Omura, Y., Kimura, K., and Kawakami, Y. 2004, "Recycling of waste lubricant oil into chemical feedstock or fuel oil over supported iron oxide catalysts", *Fuel*, vol. 83, no. 1, pp. 9-15.

Bilstad, T. and Espedal, E. 1996, "Membrane separation of produced water", *Water Science and Technology*, vol. 34, no. 9, pp. 239-246.

Bio-Wise 2001, *A Guide to Biological Treatment for Metalworking Fluids Disposal*. published by Detpartment of Trade industry

Bottero, J.Y., 1989, "Aluminium chemistry in aqueous solution", *Nordic Pulp and Paper Research* Vol. 4 (2) pp. 81-90.

Bowen, W. R. and Sharif, A. O. 2002a, "Prediction of optimum membrane design: pore entrance shape and surface potential", *Colloids and Surfaces A-Physicochemical and Engineering Aspects*, vol. 201, no. 1-3, pp. 207-217.

Bowen, W. R., Hilal, N., Lovitt, R. W., and Williams, P. M. 1996a, "Visualisation of an ultrafiltration membrane by non-contact atomic force microscopy at single pore resolution", *Journal of Membrane Science*, vol. 110, no. 2, pp. 229-232.

Bowen, W. R., Hilal, N., Lovitt, R. W., and Wright, C. J. 1998, "A new technique for membrane characterisation: direct measurement of the force of adhesion of a single particle using an atomic force microscope", *Journal of Membrane Science*, vol. 139, no. 2, pp. 269-274.

Bowen, W. R., Hilal, N., Lovitt, R. W., and Wright, C. J. 1999b, "Characterisation of membrane surfaces: direct measurement of biological adhesion using an atomic force microscope", *Journal of Membrane Science*, vol. 154, no. 2, pp. 205-212.

Bowen, W. R., Mohammad, A. W., and Hilal, N. 1997, "Characterisation of nanofiltration membranes for predictive purposes - Use of salts, uncharged solutes and atomic force microscopy", *Journal of Membrane Science*, vol. 126, no. 1, pp. 91-105.

Burke, J. M. 1991, "Waste treatment of metalworking fluids - a comparison of 3 common methods", *Lubrication Engineering*, vol. 47, no. 4, pp. 238-246.

Busca, G., Hilal, N., and Atkin, B. P. 2003, "Optimisation of washing cycle on ultrafiltration membranes used in treatment of metalworking fluids", *Desalination*, vol. 156, no. 1-3, pp. 199-207.

Butt, H. J., Jaschke, M., and Ducker, W. A. 1995, "Measuring surface forces in aqueous electrolyte solution with the atomic force microscope", *Bioelectrochemistry and Bioenergetics*, vol. 38, no. 1, pp. 191-201.

Calvo, J. I., Pradanos, P., Hernandez, A., Bowen, W. R., Hilal, N., Lovitt, R. W., and Williams, P. M. 1997b, "Bulk and surface characterization of composite UF membranes Atomic force microscopy, gas adsorption-desorption and liquid displacement techniques", *Journal of Membrane Science*, vol. 128, no. 1, pp. 7-21.

Cathalifaud, G., Ayele, J., and Mazet, M. 1997, "Etude de la complexation des ions aluminium par des molecules organiques: Constantes et stoechiometrie des complexes. Application au traitement de potabilisation des eaux: Aluminium ions/organic molecules complexation: Formation constants and stoichiometry. Application to drinking water production", *Water Research*, vol. 31, no. 4, pp. 689-698.

Chang, I. S., Chung, C. M., and Han, S. H. 2001, "Treatment of oily wastewater by ultrafiltration and ozone", *Desalination*, vol. 133, no. 3, pp. 225-232.

Chen, J. P., Kim, S. L., and Ting, Y. P. 2003, "Optimization of membrane physical and chemical cleaning by a statistically designed approach", *Journal of Membrane Science*, vol. 219, no. 1-2, pp. 27-45.

Cheryan, M. and Rajagopalan, N. 1998, "Membrane processing of oily streams. Wastewater treatment and waste reduction.", *Journal of Membrane Science*, vol. 151, pp. 13-28.

Chidlers, J. C. 1994, "The chemistry of metalworking fluids," in *Metalworking fluids*, J. P. Byers, ed., Marcel Dekker, Cincinnati, pp. 165-245.

Cui, Z. F. and Wright, K. I. T. 1996, "Flux enhancements with gas sparging in downwards crossflow ultrafiltration: performance and mechanism", *Journal of Membrane Science*, vol. 117, no. 1-2, pp. 109-116.

Darko, M. K., N.T.Miodrag, D.C.Marijana, and D.M.Spasenija 2002, "The effect of turbulence promoter on cross-flow microfiltration of skim milk", *Journal of Membrane Science*, vol. 208, no. 1-2, pp. 303-314.

Department of the Environment, "Guidance note for the implementation of small-scale packaged combine heat and power" Good Practice Guide 1

Faibish, R. S. and Cohen, Y. 2001, "Fouling-resistant ceramic-supported polymer membranes for ultrafiltration of oil-in-water microemulsions", *Journal of Membrane Science*, vol. 185, no. 2, pp. 129-143.

Fillaudeau, L. and Carrere, H. 2002a, "Yeast cells, beer composition and mean pore diameter impacts on fouling and retention during cross-flow filtration of beer with ceramic membranes", *Journal of Membrane Science*, vol. 196, no. 1, pp. 39-57.

Gabelich, C. J., Yun, T. I., Coffey, B. M., and Suffet, I. H. 2002, "Effects of aluminium sulfate and ferric chloride coagulant residuals on polyamide membrane performance", *Desalination*, vol. 150, no. 1, pp. 15-30.

Guadix, A., Sorensen, E., Papageorgiou, L. G., and Guadix, E. M. 2004, "Optimal design and operation of continuous ultrafiltration plants", *Journal of Membrane Science*, vol. 235, no. 1-2, pp. 131-138.

Hamza, A., Pham, V. A., Matsuura, T., and Santerre, J. P. 1997, "Development of membranes with low surface energy to reduce the fouling in ultrafiltration applications", *Journal of Membrane Science*, vol. 131, no. 1-2, pp. 217-227.

Hilal, N. and Bowen, W. R. 2002, "Atomic force microscope study of rejection of colloids by membrane pores", *Desalination*.

Hilal, N., Bowen, W. R., and Wright, C. J. 2002, "(bio)fouling of polymeric membranes: Atomic Force Study", *Engineering Life Science*, vol. 2, no. 5, pp. 1-5.

Hilal, N., Kochkodan, V., Al Khatib, L., and Busca, G. 2002, "Characterization of molecularly imprinted composite membranes using an atomic force microscope", *Surface and interface analysis*, vol. 33, no. 8, pp. 672-675.

Hilal, N., Kochkodan, V., Busca, G., Kochkodan, O., and Atkin, B. P. 2003, "Thin layer composite molecularly imprinted membranes for selective separation of cAMP", *Separation and Purification Technology*, vol. 31, no. 3, pp. 281-289.

Hilal, N., Victor Kochkodan, Lail Al-Khatb, and Busca, G. 2002, "Characterisation of molecularly imprinted composite membranes using an atomic force microscope", *Surface and interface analysis*, vol. 33.

Hu, X. G., Bekassy-Molnar, E., and Vatai, G. 2002, "Study of ultrafiltration behaviour of emulsified metalworking fluids", *Desalination*, vol. 149, no. 1-3, pp. 191-197.

Hu, X., Bekassy-Molnar, E., and Koris, A. 2004, "Study of modelling transmembrane pressure and gel resistance in ultrafiltration of oily emulsion", *Desalination*, vol. 163, pp. 355-360.

Hurlbut C. and Klein C. 1999 "Manual of mineralogy" Publisher John Wiley and Sons (WIE) september 1998 pp 704

Kajdas, C. 1997, "Industrial lubricants," in *Chemistry and technology of lubricants*, 2 edn, R. M. Mortier and S. T. Orszulik, eds., pp. 228-262.

Kim, J. P., Kim, J. J., Min, B. R., Kun, Y. C., and Jong-Hoon, R. 2002, "Effect of glass ball insertion on vortex-flow microfiltration of oil-in-water emulsion", *Desalination*, vol. 143, no. 2, pp. 159-172.

Kim, S. L., Chen, P. J., and Ting, Y. P. 2002, "Study on feed pretreatment for membrane filtration of secondary effluent", *Separation and Purification Technology*, vol. 29, no. 2, pp. 171-179.

King, M. R. and Hammer, D. A. 2001, "Multiparticule adhesive dynamics: Hydrodynamic recruitment of rolling leukocytes", *Biophysics*, vol. 98, pp. 14919-14924.

Lanteri and Longaray. 1998, "Chemometrics: Tools of XXth century, methods of XXIst century?" *Analysis*, vol. 26, no. 8, p. M15-M18.

Le Thi, T. 2000, *Analyse des contaminations microbiennes des surfaces et mise au point de revêtements Anti-Biofilms*, Thèses INSA de Lyon.

Lee S.B., Aurelle, Y., and Roques, R. 1984, "Concentration polarisation, membrane fouling and cleaning in ultrafiltration of soluble oil", *Journal of Membrane Science*, vol. 19, pp. 23-28.

Li, Q. Y., Cui, Z. F., and Pepper, D. S. 1997, "Effect of bubble size and frequency on the permeate flux of gas sparged ultrafiltration with tubular membranes", *Chemical Engineering Journal*, vol. 67, no. 1, pp. 71-75.

Li, Q. Y., Ghosh, R., Bellara, S. R., Cui, Z. F., and Pepper, D. S. 1998, "Enhancement of ultrafiltration by gas sparging with flat sheet membrane modules", *Separation and Purification Technology*, vol. 14, no. 1-3, pp. 79-83.

Lijinsky, W. J. 2004, *Report on the toxicology of metalworking fluids*. Canadian centre for Occupational Health and Safty Can be accessed at <http://www.canoshweb.org/odp/html/liss.htm>

Linnikov, O. D. 2003, "About seed concentration for prevention of scale", *Desalination*, vol. 157, no. 1-3, pp. 235-240.

Lissant K.J. 1973, "Making and breaking emulsions," in *Emulsions and Emulsion technology*, vol. 6. Kenneth J Lissant, ed., Marcel Dekker, new york, pp. 71-124.

Lu, W. M., Tung, K. L., Pan, C. H., and Hwang, K. J. 2002, "Cross flow microfiltration of mono-dispersed deformable particle suspension", *Journal of Membrane Science*, vol. 198, no. 2, pp. 225-243.

Magonov, S. N. and Myung-Hwan, W. 1996, *Surface Analysis with STM and AFM*.

Mahdi, S. M. and Skold, R. O. 1991, "Membrane filtration for the Recycling of water-based synthetic metalworking fluids", *Filtration and Separation*, vol. 28, no. 6, pp. 407-414.

Manttari, M., Nuortila-Jokinen, J., and Nystrom, M. 1997, "Influence of filtration conditions on the performance of NF membranes in the filtration of paper mill total effluent", *Journal of Membrane Science*, vol. 137, no. 1-2, pp. 187-199.

McCoy, J. S. 1994, "introduction: Tracing the historical development of metalworking fluids," in *Metalworking fluids*, J. P. Byers, ed., Marcel Dekker, Cincinnati, pp. 1-23.

Munson-McGee, S. H. 2002, "An approximate analytical solution for the fluid dynamics of laminar flow in a porous tube", *Journal of Membrane Science*, vol. 197, no. 1-2, pp. 223-230.

Noble, R.D. and Stern, S.A.1995, *Membrane Separation Technology: Principles and Applications*. (January 31, 1995) Elsevier pp 738

Noordman, T. R., de Jonge, A., J.A.Wesselingh, Bel, W., Dekker, M., E.Voorde, and Grijpma, S. D. 2002, "Application of fluidised particles as turbulence promoters in ultrafiltration; Improvement of flux and rejection", *Journal of Membrane Science*, vol. 208, no. 1-2, pp. 157-169.

Nuortila-Jokinen, J., Mänttari, M., and Nystrom, M. 2003, "Industrial waters," S. Judd and B. Jefferson, eds., Elsevier, pp. 75-170.

Ochoa, N. A., Pradanos, P., Palacio, L., Pagliero, C., Marchese, J., and Hernandez, A. 2001, "Pore size distributions based on AFM imaging and retention of multidisperse polymer solutes; Characterisation of polyethersulfone UF membranes with dopes containing different PVP", *Journal of Membrane Science*, vol. 187, no. 1-2, pp. 227-237.

Office of water services 2004, *Tariff structure and charges 2004-05 report*.

Panpanit, S. and Visvanathan, C. 2001, "The role of bentonite addition in UF flux enhancement mechanisms for oil/water emulsion", *Journal of Membrane Science*, vol. 184, no. 1, pp. 59-68.

Pasmore, M., Todd, P., Smith, S., Baker, D., Silverstein, J., Coons, D., and Bowman, C. N. 2001, "Effects of ultrafiltration membrane surface properties on *Pseudomonas aeruginosa* biofilm initiation for the purpose of reducing biofouling", *Journal of Membrane Science*, vol. 194, no. 1, pp. 15-32.

Plackett and Burman 1946, "Design of optimum multifactorial experiments", *Biometrika*, vol. 33, pp. 305-325.

Rios, G., Pazos, C., and Coca, J. 1998, "Destabilization of cutting oil emulsions using inorganic salts as coagulants", *Colloids and Surfaces A-Physicochemical and Engineering Aspects*, vol. 138, no. 2-3, pp. 383-389.

Ripperger, S. and Altmann, J. 2002, "Cross flow microfiltration - state of the art", *Separation and Purification Technology*, vol. 26, no. 1, pp. 19-31.

Rossmore, H. W. and Rossmore, L. A. 2003, "Metalworking fluid Microbiology," in *Metalworking Fluids*, 2 edn, J. P. Byers, ed., Marcel Dekker, Cincinnati, pp. 247-271.

Scott, K. and Hughes, R. 1996, *Industrial Membrane Separation Technology*, 1st edition 1996 edn, Blackie Academic and Professional, an imprint of Chapman and Hall.

Shakesheff, K. 1995, *The application of Atomic Force Microscopy in the surface analysis of Polymeric Biomaterials*, University of Nottingham.

Sheikholeslami, R. and Ong, H. W. K. 2003, "Kinetics and thermodynamics of calcium carbonate and calcium sulphate at salinities up to 1.5 M*1", *Desalination*, vol. 157, no. 1-3, pp. 217-234.

Sillman, J. D. 1992, *Cutting and Grinding Fluids: Selection and Application*, 2nd edn, Society of Manufacturing Engineer.

Simon, M. J. and Tragardh, G., 2000, "Membrane emulsification -- a literature review", *Journal of Membrane Science*, vol. 169, no. 1, pp. 107-117.

Skerlos, S. J., Rajagopalan, N., DeVor, R. E., Kapoor, S. G., and Angspatt, V. D. 2000, "Ingredient-wise study of flux characteristics in the ceramic membrane filtration of uncontaminated synthetic metalworking fluids, part 2: Analysis of underlying mechanisms", *Journal of Manufacturing Science and Engineering-Transactions of the Asme*, vol. 122, no. 4, pp. 746-752.

Sokoavic, M. and Mijanovic, K. 2001, "Ecological aspects of the cutting fluids and its influence on quantifiable parameters of the cutting processes", *Journal of Materials Processing Technology*, vol. 109, no. 1-2, pp. 181-189.

Stevenson, D. G. 1997, "Other treatment process," in *Water treatment unit processes*, 1 edn, D. G. Stevenson, ed., Imperial college Press, pp. 189-195.

Sur, H. W. and Cui, Z. F. 2001, "Experimental study on the enhancement of yeast microfiltration with gas sparging", *Journal of Chemical Technology and Biotechnology*, vol. 76, pp. 477-484.

Sutton, P. M. and Mishra, P. N. 1994, "Waste treatment," in *Metalworking fluids*, J. P. Byers, ed., Cincinnati, pp. 367-393.

Tardieu, E., Grasmick, A., Geaugey, V., and Manem, J. 1998, "Hydrodynamic control of bioparticle deposition in a MBR applied to wastewater treatment", *Journal of Membrane Science*, vol. 147, no. 1, pp. 1-12.

Thomas, G. and King, R. 1991, *Advances in water treatment and environmental management* Elsevier science.

Turano, E., Curcio, S., De Paola, M. G., Calabro, V., and Iorio, G. 2002, "An integrated centrifugation-ultrafiltration system in the treatment of olive mill wastewater", *Journal of Membrane Science*, vol. 209, no. 2, pp. 519-531.

Um, M. J., Yoon, S. H., Lee, C. H., Chung, K. Y., and Kim, J. J. 2001, "Flux enhancement with gas injection in crossflow ultrafiltration of oily wastewater", *Water Research*, vol. 35, no. 17, pp. 4095-4101.

van de Ven, T. G. M. 1998, "The capture of colloidal particles on surfaces and in porous material: basic principles", *Colloids and Surfaces A-Physicochemical and Engineering Aspects*, vol. 138, no. 2-3, pp. 207-216.

van der Gast, C. J., Knowles, C. J., Starkey, M., and Thompson, I. P. 2002, "Selection of microbial consortia for treating metal-working fluids", *Journal of Industrial Microbiology and Biotechnology*, vol. 29, no. 1, pp. 20-27.

van der Gast, C. J., Knowles, C. J., Wright, M. A., and Thompson, I. P. 2001, "Identification and characterisation of bacterial populations of an in-use metal-working fluid by phenotypic and genotypic methodology", *International Biodeterioration and Biodegradation*, vol. 47, no. 2, pp. 113-123.

Viadero, J., Vaughan, J., and Reed, B. E. 1999, "Study of series resistances in high-shear rotary ultrafiltration", *Journal of Membrane Science*, vol. 162, no. 1-2, pp. 199-211.

Walstra 1996, "Emulsion stability," in *Encyclopedia of emulsion technology volume 4*, vol. 4 Paul Becher, ed., Marcel Dekker; NY, pp. 1-62.

Wang, W. K. 2001, *Membrane separation in Biotechnology*, 2 edn.

Weatherley, L. R. 1994, "*Engineering processes for bioseparations*", (January 1995) Butterworth-Heinemann Ltd. pp 208 pages

Willing, A. 2001, "Lubricants based on renewable resources - an environmentally compatible alternative to mineral oil products", *Chemosphere*, vol. 43, no. 1, pp. 89-98.

Xing, C. H., Wen, X. H., Qian, Y., and Tardieu, E. 2001, "Microfiltration-membrane-coupled bioreactor for urban wastewater reclamation", *Desalination*, vol. 141, no. 1, pp. 63-73.

APPENDICES

APPENDIX A

CARDEV Letter

02/09/2004 11:30 FAX 01423530043

CARDEV

01

Cardev International Ltd

Ripon Way, Harrogate, HG1 2AU Tel: 01423 522911 Fax: 01423 530043
e-mail: admin@cardev.co.uk web: www.cardev.co.uk



Mr Gerald Busca
SCHeME
Nottingham University

2nd September 2004
Ref: Bio-Filtration Unit

Dear Gerald,

I am writing to thank you on behalf of Cardev International for the excellent work you have carried out during your PhD studentship on the prototyping and development of a Bio-Filtration system for the treatment of waste metalworking fluids.

You commenced with little existing information and practical models to help you and proceeded to carry out detailed development of a laboratory based system including the nurturing of a bio bacteria culture, which have become the basis for a platform design for a full sized system capable of being manufactured and installed in an industrial working environment.

The platform design shows quite clearly the enormous benefits for potential clients and the environment that the system will offer.
Briefly they are:

- 1) Transforming waste metalworking fluid into two product streams, a permeate which is suitable for reuse, and a high calorific oil which can be used in factory heating systems etc.
- 2) Process the waste to a very low COD level for disposal to drain.
- 3) Enable waste to be treated on site at a much lower cost to the industry.
- 4) Reduces the levels of waste fluids currently going to landfill with all the huge benefits that bring to our future environment.

The work that you have carried out over the last three years has been invaluable from our perspective and will enable the system to be developed commercially for sale in the UK and Europe.

Thank you once again and our best wishes for the future.

Kind Regards

John Willcock
Sales & Marketing Director



Registered in England No: 1753106
VAT No: 386 0916 27

02-SEP-2004 THU 10:53 01423530043

D

Appendix B

MOBIL CUT 232 DATA SHEET

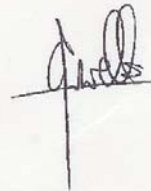
24/07 '02 15:02 FAX 01372 223870

ESSO PETROLEUM

001/011

*Facsimile***ExxonMobil**
*Lubricants & Specialties***To :** GERARD BUSCA**From :** FRED WELLS, Technical Advisor**Company :** UNIVERSITY OF NOTTINGHAM**Date :** 24 / 7 / 2002**Fax :** 0115 846 6095**cc :****Re :** MOBILCUT 232**Pages :** 11 (including this cover page)

As requested here are our Product Data Sheet, refractometer chart & Material Safety Data Bulletin for Mobilcut 232.

**Important Notice**

This facsimile may contain information intended for receipt and use solely by the addressee(s) named above. If you are not an intended recipient, any disclosure, copying or use of this information is prohibited. If you have received this facsimile in error, please notify us immediately.

ExxonMobil Lubricants & Specialties

ExxonMobil House
Ermy Way
Leatherhead, Surrey KT22 8UX

Telephone: +44 (0) 1372 222558
Facsimile: +44 (0) 1372 222368

24-JUL-2002 WED 15:12 01372 223870

P.01

24/07 '02 15:02 FAX 01372 223870

ESSO PETROLEUM

002/011

Product Data Sheet

Mobilcut 232 Semi Synthetic Metalworking Fluid

Product Description

Mobilcut 232 is a high oil content biostable semi-synthetic water emulsifiable metalworking fluid.

Mobilcut 232 is specially formulated to meet machine tool manufacturers minimum 40% oil content requirements and to offer a high performance level over a wide range of machining operations. Mobilcut 232 has been designed to exhibit low maintenance properties.

Benefits

Mobilcut 232 offers the following benefits:

- High oil content emulsion gives excellent change life
- Low foaming tendency in soft water
- Excellent machine tool lubrication - no sticky deposits or lacquers on slides and fixtures
- Wide application range including machining of ferrous metals some stainless steels and certain non-ferrous metals
- Resistant to bacterial and tramp oil degradation
- Suitable for a wide range of operations therefore allows product rationalisation in most machine shops

Applications

The high oil content and excellent biostability, together with the wide range machining capability, make Mobilcut 232 a cost effective product for most machine shops.

Recommended Dilutions

General Machining	
ferrous metals	5 - 10%
non ferrous metals	4 - 7%

Consult your local Mobil Sales Engineer for a precise concentration recommendation based on the application.

Note

Use dilute emulsion, 1-2% for top up. Never top up with water.

Storage

Mobilcut 232 concentrate must be stored in frost free conditions, minimum temperature 5°C.

9361 (05/2000)

24-JUL-2002 WED 15:12 01372 223870

P.02

24/07 '02 15:03 FAX 01372 223870

ESSO PETROLEUM

003/011

Health and Safety

Based on available toxicological information, it has been determined that this product poses no significant health risk when used and handled properly.

Details on handling, as well as health and safety information, can be found in the Material Safety Data Bulletin which can be obtained through Esso Petroleum Company Ltd., by telephoning 01372 22 2000.

Typical physical characteristics are given in the table. These are intended as a guide to industry and are not necessarily manufacturing or marketing specifications.

Product Characteristics

Mobilcut 232

Appearance	Amber
Specific Gravity at 20°C	0.99
pH at 5% Emulsion	9.0 - 9.4
Emulsion Type	Semi translucent
Corrosion Test (IP 287)	2% Break Point

Due to continual product research and development, the information contained herein is subject to change without notice

Esso Petroleum Company Limited
ExxonMobil House, Ermyn Way
Leatherhead, Surrey, KT22 8UX
Telephone: 01372 22 2000



9361 (05/2000)

24-JUL-2002 WED 15:12 01372 223870

P.03

24/07 '02 15:03 FAX 01372 223870

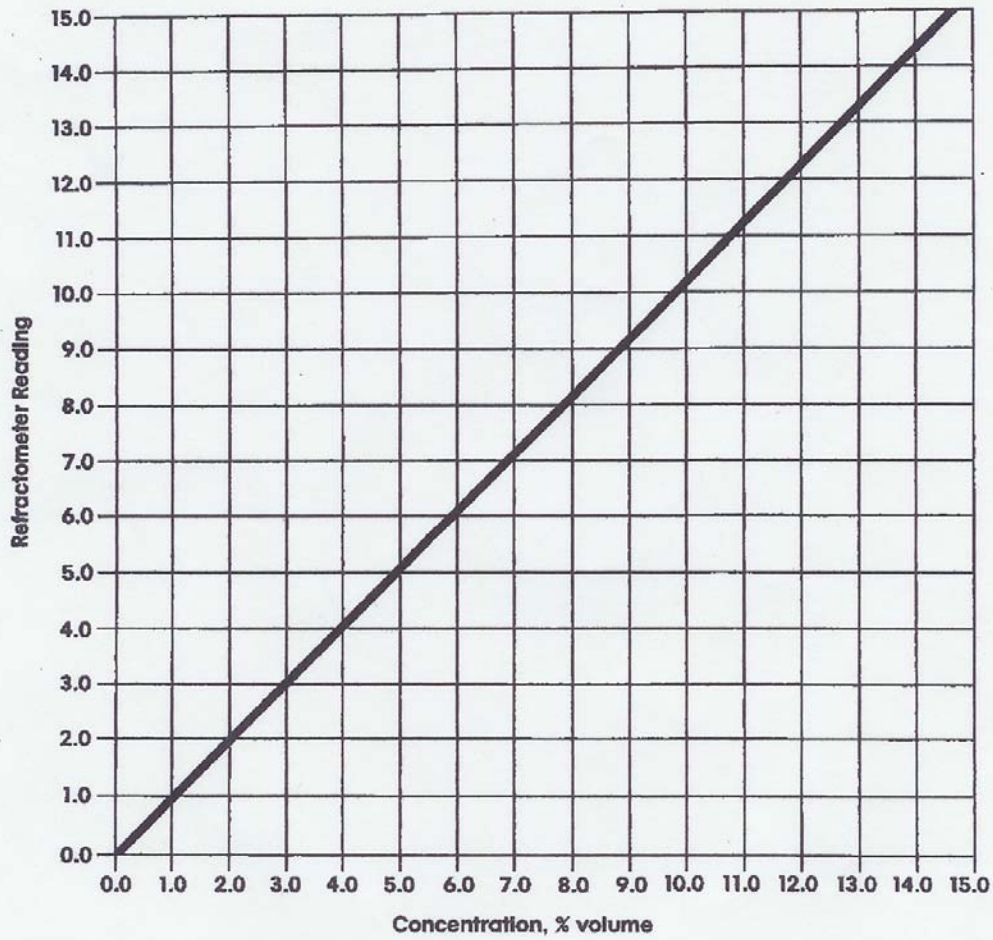
ESSO PETROLEUM

004/011



Mobilcut 232

Refractometer Calibration Chart



24-JUL-2002 WED 15:13 01372 223870

P.04

24/07 '02 15:03 FAX 01372 223870

ESSO PETROLEUM

005/011

MATERIAL SAFETY DATA BULLETIN

ELIS: 403035

Revision Date: 30/10/01

TRN:670455-60

MOBILCUT 232**1. PRODUCT AND COMPANY IDENTIFICATION**

PRODUCT NAME: MOBILCUT 232
 SUPPLIER: Esso Petroleum Company Limited
 ExxonMobil House
 Ermyr Way
 Leatherhead, Surrey
 KT22 8UX

Health Emergency Telephone: 01372 22 2000 (UK)
 00 44 1372 222 000 (IRELAND)

2. COMPOSITION/INFORMATION ON INGREDIENTS

CHEMICAL NAMES AND SYNONYMS: SEVERE TREAT MIN. OILS & ADDITIVES

GLOBALLY REPORTABLE MSDS INGREDIENTS:

Substance Name	Approx. Wt%	EU Classification
ALKANOLAMINE ESTERS AND REACTION PRODUCTS	15-25	Xi;R36/38
DIETHANOLAMIDE ESTERS OF RAPESEED OIL (68187-80-4)	5-15	Xi;R36/38
ALKYLENE ALKYL OXAZOLIDINE (66204-44-2)	1-5	Xn;R22 Xi;R36/37/38

3. HAZARDS IDENTIFICATION

This product is considered hazardous according to regulatory guidelines (See Section 15).

POTENTIAL HEALTH EFFECTS: Strong eye irritation. Skin irritation.
 EFFECTS OF OVEREXPOSURE TO DILUTE PRODUCT: No significant effects expected when used as recommended under normal conditions.

For further health effects/toxicological data, see Section 11.

GLIS No: 403035, Revision Date: 30/10/01, MOBILCUT 232 - Page: 1
 24/07/2002

24-JUL-2002 WED 15:13 01372 223870

P.05

24/07 '02 15:03 FAX 01372 223870

ESSO PETROLEUM

006/011

4. FIRST AID MEASURES

EYE CONTACT: Flush thoroughly with water for at least 15 minutes. Get immediate medical assistance. If medical assistance is not immediately available, flush an additional 15 minutes. Instill local anaesthetic eyedrops to facilitate irrigation, if available.

SKIN CONTACT: Wash contact areas with soap and water. Remove contaminated clothing. Launder contaminated clothing before re-use.

INHALATION: Remove from further exposure. If respiratory irritation, dizziness, nausea, or unconsciousness occurs, seek immediate medical assistance. If breathing has stopped, assist ventilation with bag-valve-mask device or use mouth-to-mouth resuscitation.

INGESTION: Not expected to be a problem. However, if greater than 1/2 litre (pint) ingested, seek medical attention.

5. FIRE-FIGHTING MEASURES

EXTINGUISHING MEDIA: Carbon dioxide, foam, dry chemical and water fog.

SPECIAL FIRE FIGHTING PROCEDURES: Water or foam may cause frothing. Use water to keep fire exposed containers cool. Water spray may be used to flush spills away from exposures. Prevent runoff from fire control or dilution from entering waterways or drinking water supply.

SPECIAL PROTECTIVE EQUIPMENT: For fires in enclosed areas, firefighters MUST use self-contained breathing apparatus.

UNUSUAL FIRE AND EXPLOSION HAZARDS: None.

COMBUSTION PRODUCTS: Fumes, smoke, carbon monoxide, sulfur oxides, aldehydes and other decomposition products, in the case of incomplete combustion.

Flash Point C(F): > 100(212) (IP 34 / ASTM D-93).

Flammable Limits (approx.% vol.in air) - LELNE, UEL: NE

NFPA HAZARD ID: Health: 1, Flammability: 1, Reactivity: 0

6. ACCIDENTAL RELEASE MEASURES

NOTIFICATION PROCEDURES: Report spills as required to appropriate authorities such as the local Environmental Health Officer or Fire Brigade. If spills are likely to enter any drain, waterway or groundwater, contact the Area Water Authority. In case of accident or road spill, contact the Police and Fire Brigade and, if appropriate, the Area Water Authority.

PROCEDURES IF MATERIAL IS RELEASED OR SPILLED: Contain and adsorb on fire retardant treated sawdust, diatomaceous earth, etc. Shovel up and dispose of at an appropriate licensed waste disposal site in accordance with current applicable laws and regulations and product characteristics at time of disposal. Personnel performing clean up must use protective equipment.

ENVIRONMENTAL PRECAUTIONS: Prevent spills from entering storm sewers or drains and contact with soil.

PERSONAL PRECAUTIONS: See Section 8

GLIS No: 403035, Revision Date: 30/10/01, MOBILCUT 232 - Page: 2
24/07/2002

24-JUL-2002 WED 15:13 01372 223870

P.06

24/07 '02 15:04 FAX 01372 223870

ESSO PETROLEUM

007/011

7. HANDLING AND STORAGE

HANDLING: Avoid inhalation of vapours or mists. Avoid contact with eyes. Avoid contact with skin. Do not add other materials to this product or its emulsions unless recommended by the supplier - doing so may adversely effect the health and safety characteristics.

STORAGE: Keep from freezing. Store above 4 deg C.

SPECIAL PRECAUTIONS: Prevent small spills and leakages to avoid slip hazard.

EMPTY CONTAINER WARNING: Empty containers retain residue (liquid and/or vapour) and can be dangerous. DO NOT PRESSURIZE, CUT, WELD BRAZE, SOLDER, DRILL, GRIND OR EXPOSE SUCH CONTAINERS TO HEAT, FLAME, SPARKS, STATIC ELECTRICITY OR OTHER SOURCES OF IGNITION; THEY MAY EXPLODE AND CAUSE INJURY OR DEATH. Do not attempt to refill or clean container since residue is difficult to remove. Empty drums should be completely drained, properly bunged and returned to a drum reconditioner. All containers should be disposed of in an environmentally safe manner and in accordance with governmental regulations.

8. EXPOSURE CONTROLS/PERSONAL PROTECTION

OCCUPATIONAL EXPOSURE LIMITS:

When mists/aerosols can occur, the following are recommended: 5 mg/m³ (as oil mist) - ACGIH Threshold Limit Value (TLV), 10 mg/m³ (as oil mist) - ACGIH Short Term Exposure Limit (STEL)

VENTILATION: Adequate ventilation MUST be provided to ensure personal exposure to mineral oil mist does not exceed 5mg/m³, 8-hour TWA.

RESPIRATORY PROTECTION: Approved respiratory protective equipment MUST be used when vapour or mist concentrations exceed recommended exposure standards.

EYE PROTECTION: Chemical type goggles MUST be worn.

SKIN PROTECTION: Impervious gloves MUST be worn.

OTHER: DILUTE PRODUCT HANDLING: Normal industrial eye protection practices should be employed. If prolonged or repeated skin contact is likely, impervious gloves should be worn. Good personal hygiene practices should always be followed.

GLIS No: 403035, Revision Date: 30/10/01, MOBILCUT 232 - Page: 3
24/07/2002

24-JUL-2002 WED 15:14 01372 223870

P.07

24/07 '02 15:04 FAX 01372 223870

ESSO PETROLEUM

008/011

9. PHYSICAL AND CHEMICAL PROPERTIES

Typical physical properties are given below. Consult Product Data Sheet for specific details.

PHYSICAL STATE: Liquid
COLOUR: Amber
ODOUR: Mild
ODOUR THRESHOLD-ppm: NE
pH: 9.7
BOILING POINT C(F): > 100(212)
MELTING POINT C(F): NE
FLASH POINT C(F): > 100(212) (IP 34 / ASTM D-93)
FLAMMABILITY (solids): NE
AUTO FLAMMABILITY C(F): > 150(302)
EXPLOSIVE PROPERTIES: NA
OXIDIZING PROPERTIES: NA
VAPOUR PRESSURE-mmHg 20 C: NE
VAPOUR DENSITY: NA
EVAPORATION RATE: NE
RELATIVE DENSITY, 15/4 C: 0.97
SOLUBILITY IN WATER: Emulsifies
PARTITION COEFFICIENT: NE
VISCOSITY AT 40 C, cSt: NE
VISCOSITY AT 100 C, cSt: NE
POUR POINT C(F): < 0(32)
FREEZING POINT C(F): NE
DMSO EXTRACT, IP-346 (WT.%): <3, for mineral oil only
NA=NOT APPLICABLE NE=NOT ESTABLISHED D=DECOMPOSES

FOR FURTHER TECHNICAL INFORMATION, CONTACT YOUR MARKETING REPRESENTATIVE

10. STABILITY AND REACTIVITY

STABILITY (THERMAL, LIGHT, ETC.): Stable.
CONDITIONS TO AVOID: Heat or freezing temperatures. Do not heat above 60 C (140 F) in the presence of aluminum to avoid possible release of hydrogen gas.
INCOMPATIBILITY (MATERIALS TO AVOID): Strong acids and oxidisers.
HAZARDOUS DECOMPOSITION PRODUCTS: Product does not decompose at ambient temperatures.
HAZARDOUS POLYMERISATION: Will not occur.

GLIS No: 403035, Revision Date: 30/10/01, MOBILCUT 232 - Page: 4
24/07/2002

24-JUL-2002 WED 15:14 01372 223870

P.08

24/07 '02 15:05 FAX 01372 223870

ESSO PETROLEUM

009/011

11. TOXICOLOGICAL DATA

---ACUTE TOXICOLOGY---

ORAL TOXICITY: Practically non-toxic (LD50: greater than 2000 mg/kg). ---Based on testing of similar products and/or the components.

DERMAL TOXICITY: Practically non-toxic (LD50: greater than 2000 mg/kg). ---Based on testing of similar products and/or the components.

INHALATION TOXICITY: Not established

EYE IRRITATION: Strong irritant. (Draize score: greater than 35 but 55 or less). ---Based on testing of similar products and/or the components.

SKIN IRRITATION: Irritant. (Primary Irritation Index: 3 or greater but less than 5). ---Based on testing of similar products and/or the components.

---CHRONIC TOXICOLOGY (SUMMARY)---

The base oils in this product are severely solvent refined and/or severely hydrotreated. Chronic skin painting studies of severely treated oils showed no evidence of carcinogenic effects.

---OTHER TOXICOLOGY DATA---

Dilute material expected to be non-irritating to eyes and skin.

Nitrites or nitrite-containing materials should not be added to this product due to the risk of forming nitrosamines, some of which have been shown to be carcinogenic in animals.

12. ECOLOGICAL INFORMATION

ENVIRONMENTAL FATE AND EFFECTS: Not established.

13. DISPOSAL CONSIDERATIONS

WASTE DISPOSAL: Product is suitable for burning in an enclosed, controlled burner for fuel value or disposal by supervised incineration. Such burning may be limited by the controlling authority. In addition, the product is suitable for processing by an approved recycling facility or can be disposed of at any licensed waste disposal site. Use of these methods is subject to user compliance with applicable laws and regulations and consideration of product characteristics at time of disposal.

EUROPEAN WASTE CODE: 12 01 07 (mineral-based machining oils free of halogens (except emulsions and solutions)) Waste generated from the intended use of this product is assigned the above waste disposal code. However, deviation from the intended use and/or the presence of any potential contaminants may require an alternative waste disposal code to be assigned by the end user. This waste is considered as a hazardous waste pursuant to Directive 91/689/EEC on hazardous waste, and subject to the provisions of that Directive unless Article 1(5) of the Directive applies.

14. TRANSPORT INFORMATION

USA DOT: NOT REGULATED BY USA DOT.

RID/ADR: NOT REGULATED BY RID/ADR.

IMO: NOT REGULATED BY IMO.

IATA: NOT REGULATED BY IATA.

GLIS No: 403035, Revision Date: 30/10/01, MOBILCUT 232 - Page: 5
24/07/2002

24-JUL-2002 WED 15:14 01372 223870

P.09

24/07 '02 15:05 FAX 01372 223870

ESSO PETROLEUM

010/011

15. REGULATORY INFORMATION

EU Labelling: Product is dangerous as defined by the European Union Dangerous Substances/Preparations Directives.

Symbol: Xi Irritant.

Risk Phrase(s): R36/38.
Irritating to eyes and skin.

Safety Phrase(s): S25-26.
Avoid contact with eyes. In case of contact with eyes, rinse immediately with plenty of water and seek medical advice.

Contains: Alkanolamine Esters and Reaction Products.

THE FOLLOWING PRODUCT INGREDIENTS ARE CITED ON THE LISTS BELOW:

CHEMICAL NAME	CAS NUMBER	LIST CITATIONS
*** NO REPORTABLE INGREDIENTS ***		
--- REGULATORY LISTS SEARCHED ---		
1=IARC 1	6=NO ALLERGI	11=DE TERAT B 16=DE CARC B 21=CH CARC
2=IARC 2A	7=SE ALLERGY	12=DE TERAT C 17=AT TERAT A
3=IARC 2B	8=SE CARC	13=DE TERAT D 18=AT TERAT B
4=NTP CARC	9=DK CARC	14=DE CARC A1 19=AT TERAT C
5=NTP SUS	10=DE TERAT A	15=DE CARC A2 20=AT TERAT D

CARC=CARCINOGEN; SUS=SUSPECTED CARCINOGEN; TERAT=TERATOGENIC

AT = Austria	DE = Germany	NO = Norway
CH = Switzerland	DK = Denmark	SE = Sweden

GLIS No: 403035, Revision Date: 30/10/01, MOBILCUT 232 - Page: 6
24/07/2002

24-JUL-2002 WED 15:15 01372 223870

P.10

24/07 '02 15:05 FAX 01372 223870

ESSO PETROLEUM

011/011

16. OTHER INFORMATION

USE: Metal process oil

NOTE: EXXONMOBIL PRODUCTS ARE NOT FORMULATED TO CONTAIN PCBS.

Health studies have shown that many hydrocarbons pose potential human health risks which may vary from person to person. Information provided on this MSDS reflects intended use. This product should not be used for other applications. In any case, the following advice should be considered:

INJECTION INJURY WARNING: If product is injected into or under the skin, or into any part of the body, regardless of the appearance of the wound or its size, the individual should be evaluated immediately by a physician as a surgical emergency. Even though initial symptoms from high pressure injection may be minimal or absent, early surgical treatment within the first few hours may significantly reduce the ultimate extent of injury.

NOTE: This product should not be used for any other purpose without expert advice.

COSHH Regulations: Product reviewed and considered to be potentially hazardous to health. The Regulations must be followed and measures to control exposure may be necessary.

Any sections of this Material Safety Data Sheet which are printed in bold text highlights recent significant changes which have been made to the advice or information given.

 For Internal Use Only: MHC: 1* 1* NE 3* 2*, MPPEC: D, TRN:
 670455-60, ELIS: 403035
 EHS Approval Date: 17JAN2002

Information given herein is offered in good faith as accurate, but without guarantee. Conditions of use and suitability of the product for particular uses are beyond our control; all risks of use of the product are therefore assumed by the user and WE EXPRESSLY DISCLAIM ALL WARRANTIES OF EVERY KIND AND NATURE, INCLUDING WARRANTIES OF MERCHANTABILITY AND FITNESS FOR A PARTICULAR PURPOSE IN RESPECT TO THE USE OR SUITABILITY OF THE PRODUCT. Nothing is intended as a recommendation for uses which infringe valid patents or as extending license under valid patents. Appropriate warnings and safe handling procedures should be provided to handlers and users. Alteration of this document is strictly prohibited. Except to the extent required by law, republication or retransmission of this document, in whole or in part, is not permitted. Exxon Mobil Corporation and its affiliated companies assume no responsibility for accuracy of information unless the document is the most current available from an official ExxonMobil distribution system. Exxon Mobil Corporation and its affiliated companies neither represent nor warrant that the format, content or product formulas contained in this document comply with the laws of any other country except the United States of America.

 Copyright 2001 Exxon Mobil Corporation, All rights reserved

END OF DOCUMENT

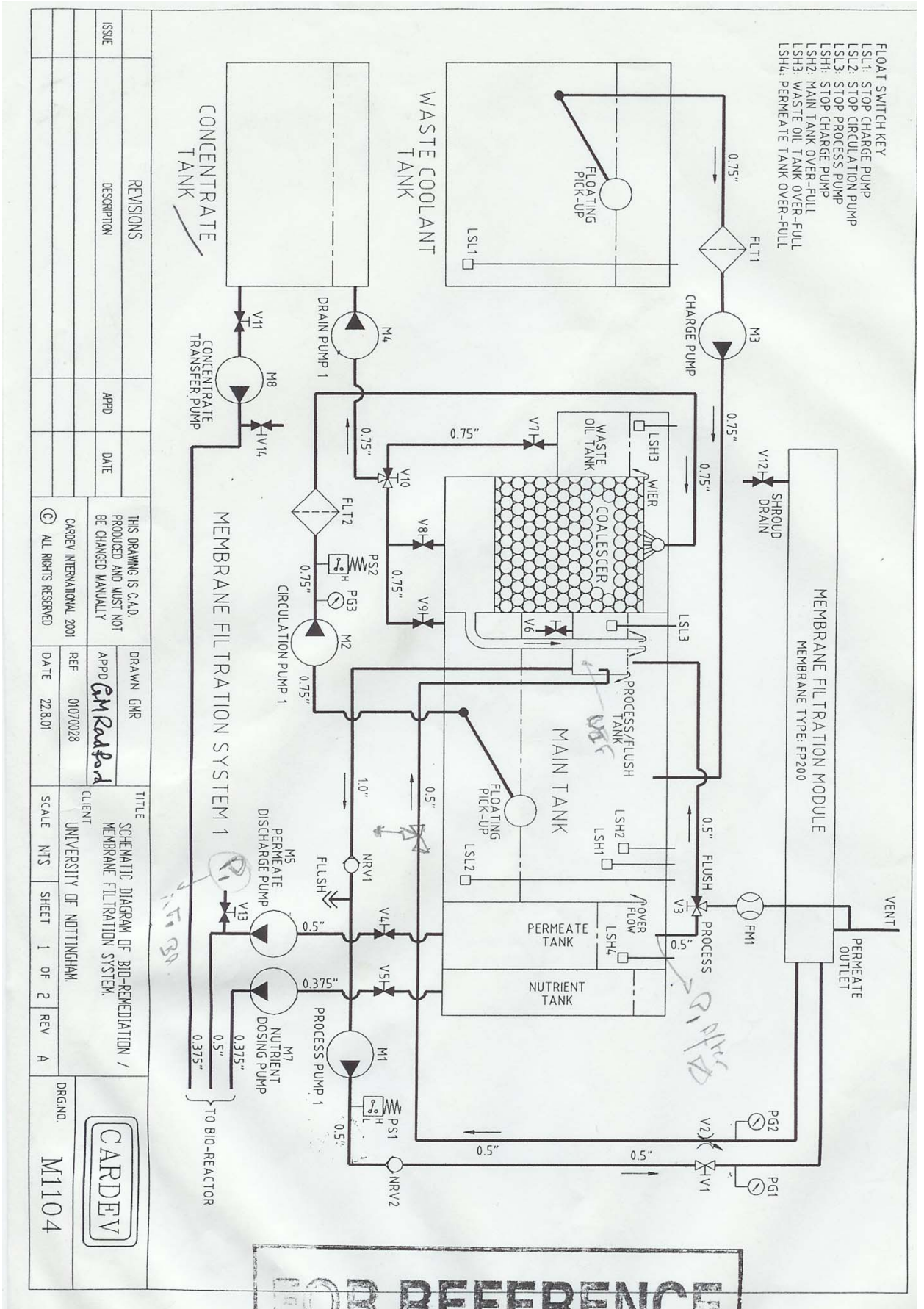
GLIS No: 403035, Revision Date: 30/10/01, MOBILCUT 232 - Page: 7
 24/07/2002

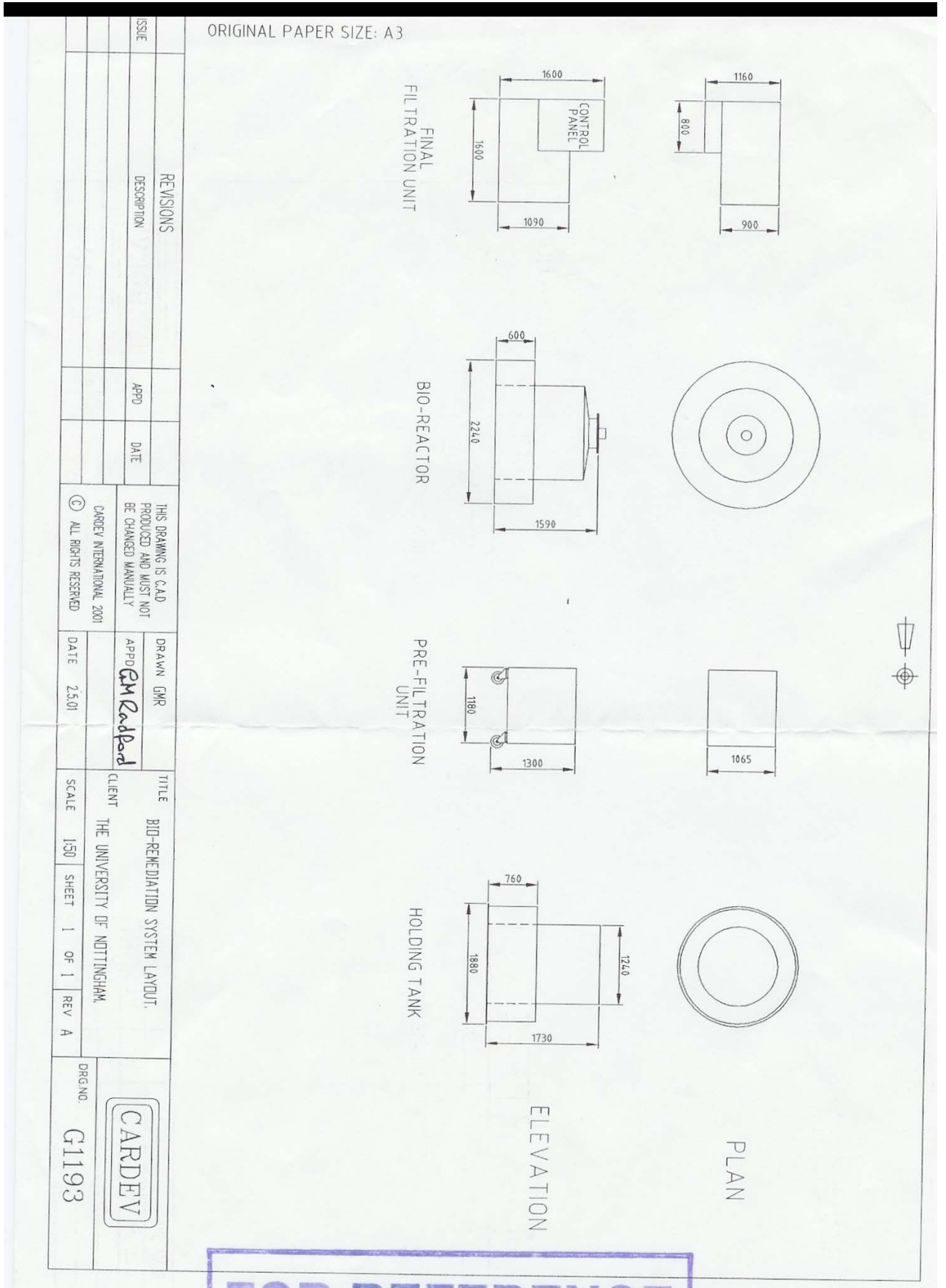
24-JUL-2002 WED 15:15 01372 223870

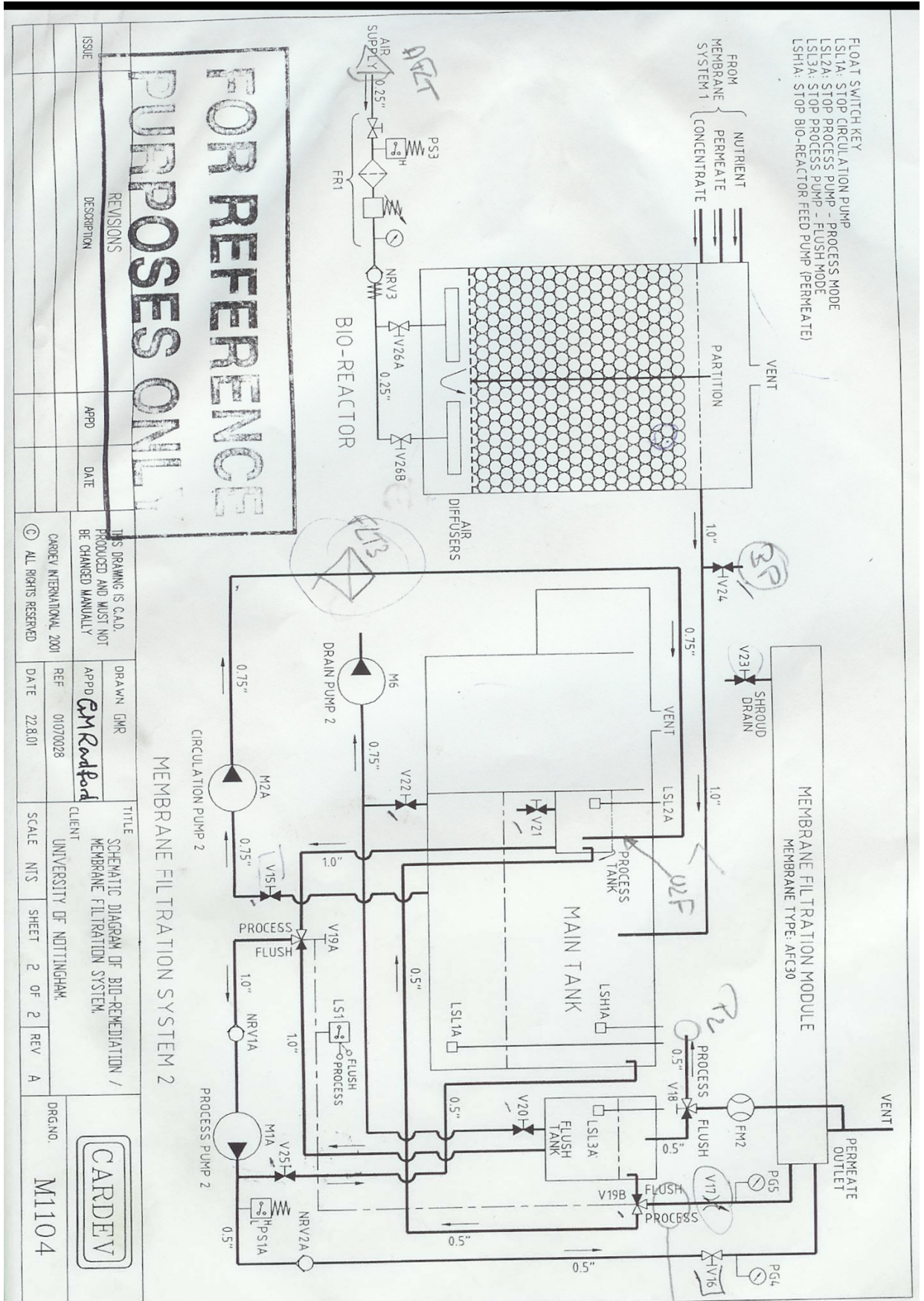
P.11

APPENDIX C

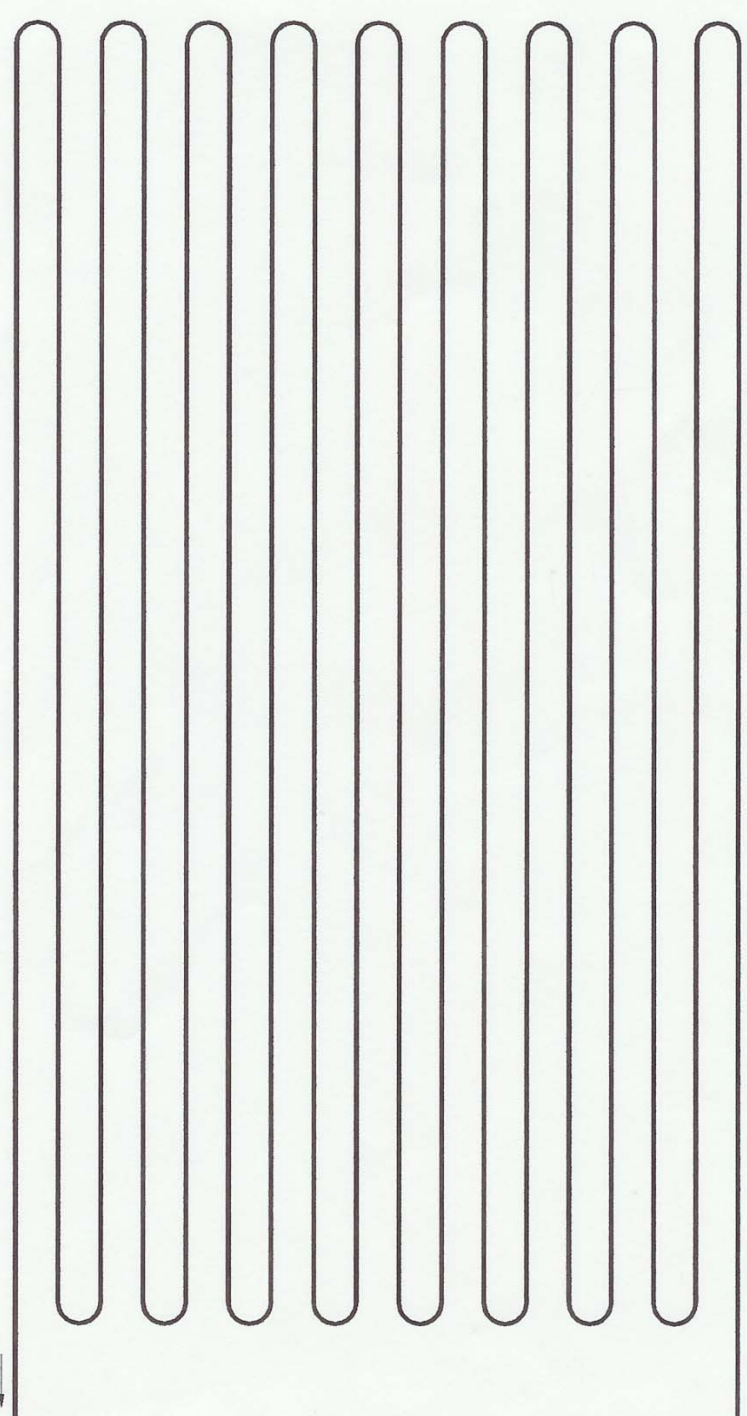
INITIAL DESIGN







ISSUE		REVISIONS		THIS DRAWING IS C.A.D. PRODUCED AND MUST NOT BE CHANGED MANUALLY		DRAWN GMR		TITLE				
		DESCRIPTION		APPD DATE		APPD DATE 28.9.03		CONFIGURATION OF SINGLE ENTRY BI RD MEMBRANE MODULE.				
								SCALE NTS		SHEET 1 OF 1		REV A
				© ALL RIGHTS RESERVED CARDEY INTERNATIONAL 2003								DRG NO. B1SE



APPENDIX D

PALL RINGS DATA SHEET

KOCH-GLITSCH UK**INTALOX® PRODUCTS DIVISION****Stoke on Trent Operations:**

King Street, Fenton, Stoke on Trent, Staffordshire. ST4 2LT. Tel: +44 (0) 1782 744561 Fax: +44 (0) 1782 744330

Product Specification: 25mm Plastic Pall Rings

Specification No. PS

Revision: 3 01.1

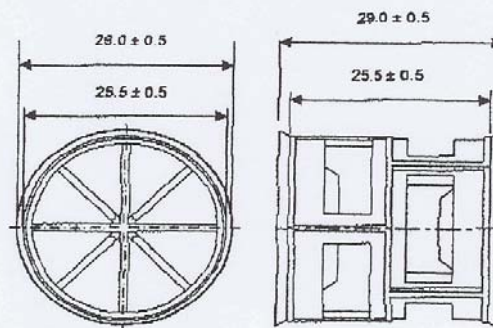
Material Classification: Plastic Packings

Product Code: 25mm Plastic Pall Rings

Part Description: 25mm Plastic Pall Rings

Product Line: Plastic Packings

Responsible Engineer: Pat Heath

1.0 Product Specification:

All Dimensions in mm

Please note:

- a) Product may be supplied with or without the flange in accordance with the dimensions specified above
 b) * Piece counts / bulk densities based on nominal values for polypropylene

Size mm	Number / Std m ³	Bulk Density Kg/m ³
25 nominal	50854*	73*
28 nominal	33640*	76*
Material Grades	Polypropylene, LTHA Polypropylene, PVDF, PVC, CPVC, PFA, PPS, ECTFE, ETFE Glass filled varieties of most Polymers available	
Forming	Spokes - 100 % formed Unformed areas (shorts) not > 25% of any linear dimension not > 5% of any circumferential dimension Not more than one point of shortage per item	
Flash (excess visible material)	Windows - 5% Max Cross sectional area - 5% Max	
General Finish	External Surfaces - maximum protrusion - 1.0 mm Free from grease, dirt and contaminants	

A Division of Koch Chemical Technology Group Limited
 Incorporated in London No. 3321082
 Registered Office: Dolphin House



INVESTOR IN PEOPLE

APPENDIX E

ACTIVATED CARBON BET SURFACE

Full Report Set

ASAP 2010 V4.02 C Unit 1 Serial # 201Page 1

Sample: Act Carbon - Phil Windsor
Op: K.S.
Submitter Id: E.L.
File Name: C:\ASAP2010\DATA\KARL\X66369.SMP

Started: 07/01/80 16:26:18 Analysis Adsorptive: N2
Completed: 08/01/80 05:31:14 Analysis Bath: 77.35 K
Report Time: 10/01/80 12:15:26 Thermal Correction: No
Sample Weight: 0.5616 g Smoothed Pressures: No
Warm Freespace: 28.3408 cm³Cold Freespace: 92.1340 cm³
Equil. Interval: 10 secs Low Pressure Dose: None

Analysis Log

RelativePressure	Vol Adsorbed	Elapsed Time	Saturation
Pressure (mmHg)	(cm ³ /g STP)	(HR:MN)	Press.(mmHg)
01:11	759.89935		
0.0100063607	61194207.044103	:28	
0.015992580	12.16875216	.844004	:00
0.025038053	19.05574226	.899104	:29
0.049997956	38.05969244	.265404	:55
05:16	761.34924		
0.075019372	57.11544255	.436005	:20
0.100052279	76.17119263	.681105	:37
0.135221300	102.94244272	.477405	:52
0.162854447	123.97622277	.877206	:03
0.208426874	158.66493285	.214806	:15
0.261891915	199.36034292	.112306	:26
0.314059503	239.06665297	.917106	:36
0.364888512	277.75290303	.015406	:45
0.400212724	304.63290306	.526506	:58
0.502882470	382.77179315	.794207	:11
07:19	761.14209		
0.650286243	494.89511331	.212207	:28
0.801519818	609.79401355	.180807	:50
0.953063563	724.79114392	.620208	:18
0.991596233	753.58716409	.626809	:04
09:20	759.79578		
1.000137079	759.83728415	.426409	:23
0.990948464	752.19427412	.105409	:55
0.952032852	721.83978401	.873610	:36
0.852832391	645.82379380	.718311	:21
11:24	757.20667		
0.800034161	605.79120370	.347912	:01
0.699288752	529.50610352	.376712	:16
0.598987883	453.55762337	.171012	:31
0.499699139	378.37552324	.953412	:47
0.398550218	301.78488306	.775413	:06

Full Report Set

ASAP 2010 V4.02 C Unit 1 Serial # 201Page 3

Sample: Act Carbon - Phil Windsor

Op: K.S.

Submitter Id: E.L.

File Name: C:\ASAP2010\DATA\KARL\X66369.SMP

Started: 07/01/80 16:26:18 Analysis Adsorptive: N2
Completed: 08/01/80 05:31:14 Analysis Bath: 77.35 K
Report Time: 10/01/80 12:15:26 Thermal Correction: No
Sample Weight: 0.5616 g Smoothed Pressures: No
Warm Freespace: 28.3408 cm³ Cold Freespace: 92.1340 cm³
Equil. Interval: 10 secsLow Pressure Dose: None

BET Surface Area ReportBET Surface Area:846.4151±30.6184 m²/g

Slope: 0.005253 ± 0.000182

Y-Intercept:-0.000109 ± 0.000039

C:-46.983317

VM: 194.435209 cm³/g STP

Correlation Coefficient: 9.958251e-01

Molecular Cross-section: 0.1620nm²

Relative Vol 1/

Pressure Adsorbed [VA*(Po/P - 1)]

(cm³/g STP)

0.049997956	244.26540.000215
0.075019372	255.43600.000318
0.100052279	263.68110.000422
0.135221300	272.47740.000574
0.162854447	277.87720.000700
0.208426874	285.21480.000923
0.261891915	292.11230.001215
0.314059503	297.91710.001537
0.364888512	303.01540.001896

Full Report Set

ASAP 2010 V4.02 C Unit 1 Serial # 201Page 5

Sample: Act Carbon - Phil Windsor
 Op: K.S.
 Submitter Id: E.L.
 File Name: C:\ASAP2010\DATA\KARL\X66369.SMP

Started: 07/01/80 16:26:18 Analysis Adsorptive: N2
 Completed: 08/01/80 05:31:14 Analysis Bath: 77.35 K
 Report Time: 10/01/80 12:15:26 Thermal Correction: No
 Sample Weight: 0.5616 g Smoothed Pressures: No
 Warm Freespace: 28.3408 cm³Cold Freespace: 92.1340 cm³
 Equil. Interval: 10 secs Low Pressure Dose: None

t-Plot Report

Micropore Volume:	0.262755 cm ³ /g
Micropore Area:	445.8341m ² /g
External Surface Area:	400.5811m ² /g
Slope:	25.897407 ± 1.672441
Y-Intercept:	169.870173 ± 7.029130
Correlation Coefficient:	9.93802e-01
Thickness Range:	3.5000 to5.0000 A

$$t = [13.9900 / (0.0340 - \log(P/P_0))] 0.5000$$

Surface Area Correction Factor:	1.00
Density Conversion Factor:	0.001547
Total Surface Area (by BET):	846.4151

Relative Statistical Vol Adsorbed
 Pressure Thickness, (A) (cm³/g)

0.010006360	2.6228207.0441
0.015992580	2.7649216.8440
0.025038053	2.9248226.8991
0.049997956	3.2371244.2654
0.075019372	3.4746255.4360
0.100052279	3.6787263.6811
0.135221300	3.9362272.4774
0.162854447	4.1250277.8772
0.208426874	4.4233285.2148
0.261891915	4.7661292.1123
0.314059503	5.1042297.9171
0.364888512	5.4452303.0154
0.400212724	5.6926306.5265
0.502882470	6.4862315.7942
0.650286243	7.9582331.2122
0.801519818	10.3704355.1808

Full Report Set

ASAP 2010 V4.02 C Unit 1 Serial # 201Page 7

Sample: Act Carbon - Phil Windsor
Op: K.S.
Submitter Id: E.L.
File Name: C:\ASAP2010\DATA\KARL\X66369.SMP

Started: 07/01/80 16:26:18 Analysis Adsorptive: N2
Completed: 08/01/80 05:31:14 Analysis Bath: 77.35 K
Report Time: 10/01/80 12:15:26 Thermal Correction: No
Sample Weight: 0.5616 g Smoothed Pressures: No
Warm Freespace: 28.3408 cm³ Cold Freespace: 92.1340 cm³
Equil. Interval: 10 secs Low Pressure Dose: None

Options Report

Analysis Adsorptive: Nitrogen @ 77.35 K
Maximum manifold pressure: 925.00 mmHg
Non-ideality factor: 0.000062
Density conversion factor: 0.0015468
Therm. tran. hard-sphere diameter: 3.860 A
Molecular cross-sectional area: 0.162 nm²

Fast evacuation: No
Unrestricted evac from: 5.0 mmHg
Leak test: Yes
Leak test duration: 120 secs
Evacuation time: 0.1 hours
Backfill Gas: Analysis
Equilibration interval: 10 secs
Maximum volume increment: No
Target tolerance: 5.0 % or 0.0 mmHg
Min. equil. delay at P/Po >= 0.995:0 secs

Free space group: Measured
Lower dewar after free space: No
Evacuation time: 0.1 hours
Leak test: Yes
Leak test duration: 180 secs

Low pressure dosing: No
Dose amount: 0.00 cm³/g STP
Minimum equilibration delay: 0.00 hours
Maximum equilibration delay: 999.00 hours

Po type: Measured
Temperature type: Entered
Temperature: 77.35 K
Measurement interval: 120 minutes

Inside diameter of sample tube: 9.530 mm

Full Report Set

ASAP 2010 V4.02 C Unit 1 Serial # 201Page 9

Sample: Act Carbon - Phil Windsor
Op: K.S.
Submitter Id: E.L.
File Name: C:\ASAP2010\DATA\KARL\X66369.SMP

Started: 07/01/80 16:26:18 Analysis Adsorptive: N2
Completed: 08/01/80 05:31:14 Analysis Bath: 77.35 K
Report Time: 10/01/80 12:15:26 Thermal Correction: No
Sample Weight: 0.5616 g Smoothed Pressures: No
Warm Freespace: 28.3408 cm³ Cold Freespace: 92.1340 cm³
Equil. Interval: 10 secsLow Pressure Dose: None

Summary ReportAreaSingle Point Surface Area at P/Po 0.31405950 : 889.5909m²/gBET Surface Area: 846.4151m²/gBJH Adsorption Cumulative Surface Area of pores
between 20.000000 and 500.000000 A Diameter: 115.7807m²/gBJH Desorption Cumulative Surface Area of pores
between 20.000000 and 500.000000 A Diameter: 153.2664m²/gVolumeSingle Point Total Pore Volume of pores less than
429.7189 A Diameter at P/Po 0.95306356: 0.607305 cm³/gBJH Adsorption Cumulative Pore Volume of pores
between 20.000000 and 500.000000 A Diameter:0.223796 cm³/gBJH Desorption Cumulative Pore Volume of pores
between 20.000000 and 500.000000 A Diameter:0.246212 cm³/gPore Size

Average Pore Diameter (4V/A by BET): 28.7001A

BJH Adsorption Average Pore Diameter (4V/A):77.3170A

BJH Desorption Average Pore Diameter (4V/A):64.2572A

APPENDIX F

Cardev Equipment Manual

CARDEV BIO-REMEDIATION / MEMBRANE FILTRATION SYSTEM

Power

Power for the entire system is provided via one 415V “3-phase and neutral” plug, which is located on the first membrane system, and is connected to the socket underneath the stairwell. Power to membrane system two is switched on via the main control panel.

Waste Coolant tank

The waste coolant tank has a capacity of approximately 2000 litres, with a sight glass indicating fluid level. Fluid is drawn from the waste oil tank via a floating pick up (drawing fluid for the top prevents a build up of separated free/tramp oil. The fluid then passes through the clear hose, along the side of the stairs, and into the long stainless steel pre-filter on system 1. This pre-filter is fitted with a reusable nylon mesh bag filter rated at 300 microns.

Processing (system 1)

From the pre-filter, the fluid is drawn through the charge pump (pump M3, operated via charge pump stop/start buttons on main control panel) and into the main tank of system 1. The charge pump will continue to run until the fluid level in the main tank rises to the bottom of the internal process tank, at which point the high level float switch is made and the pump is stopped.

Once the main tank of membrane system 2 is full, the circulation pump (M2) should be started (circulation pump start button on the main control panel). The circulation pump draws from the floating pick up in the main tank of system 1 and through the pump. Fluid is then pumped through the large blue filter (fitted with a reusable bag rated at 100 microns) and into the coalescing tank. A pressure switch is fitted to the pump to stop the pump when the pressure reaches approx 3.5 bar (i.e. when the blue filter is blocked) as well as a pressure gauge to give visual confirmation.

Once fluid is in the coalescer, it passes down through the coalescing media, returns up through the rear chamber and floods into the internal process tank.

Once the internal process tank has filled, processing can be started. Before starting the process pump (M1) ensure that the membrane pressure control valve is fully open (ie fully turned anti-clockwise) and that the membrane valve opposite is set to “membrane open”.

The process pump (M1) can now be started (process pump start button on main control panel). Once running, the membrane pressure control valve can be carefully closed until the membrane inlet pressure gauge reads 9 Bars, and the membrane back pressure gauge reads 7 Bars. The process pump will now feed from the internal process tank and pump through the membranes, returning the concentrate to the main tank and the permeate (via a flowmeter & valve V3) to the permeate tank (if V3 set to process mode), or back to the internal process tank (if V3 is set to flush mode).

During normal operation, processing will continue until the level in the main tank drops to the bottom float switch. At this point, the circulation pump will stop, and the process tank level will slowly drop until the process tank float switch is no longer made, at which point the process pump will also stop.

System 1 - Flushing

– A hose pipe should be attached to the cam-lock fitting on the inlet of the process pump. Clean water should be passed through until the water spilling out of the internal process tank is relatively clean. 500 ml of surfactant should then be added to the process tank, and the process pump started in the usual manner. Valve V3 should be turned to the flush position to divert permeate back into the process tank. This processing will continue until you decide to turn the system off (usually 30 – 60 mins is sufficient).

The concentrated solution can then be drained from the system by using pump m4 (drain pump 1) via valve V10 – when V10 is turned fully clockwise, the coalescer is drained. When the valve is turned fully anticlockwise the main tank is drained. (The internal process tank should be drained into the main tank via valve V6)

Permeate, nutrient & air – Bio

Permeate is pumped from the permeate tank on the first membrane unit into the bioreactor via pump M5 (permeate pump start). The rate at which the permeate is delivered is variable (via the knob adjuster) between 0 and 100% of its maximum flow rate, which is 1.8 litres per minute.

Nutrient is pumped from the nutrient tank in the first membrane unit via pump M7 (nutrient pump start). Again, the rate at which the nutrient is delivered is variable

(via the knob adjuster) between 0 and 100% of its maximum flow rate, which is 4 litres per hour.

Air is delivered to the bioreactor via the air regulator mounted on the first membrane unit: air pressure/volume can be adjusted via the knob on the top of the regulator. Air passes through one-way valves and into each side of the bioreactor, where the air is infused through a ceramic air stone (one air stone each side of the central partition).

The Bioreactor

The bioreactor has 3 x ½ " inlets, and 1 x 1" outlet, which is set slightly lower in the tank to allow a gravity feed on the outfall. The tank is partitioned across the middle of the tank meaning all fluids must feed in through the top, flow down through the bio-decking and then back up through the bio-decking before they can escape.

Sample points are fitted to the permeate inlet and the reactor outlet – open the tap to take a sample.

System 2

(NOTE – the second membrane system has its own control panel (local to the unit) and an external flush tank. The large double valve under the external flush tank must be facing outwards during normal operation i.e. processing, and towards the ground during flushing)

From the bioreactor, fluid is gravity fed through the sleeved pipe on the wall to the second membrane unit (note – the 2nd membrane unit will not overflow – the high level float switch in the main tank of the second system will cut out the permeate and nutrient dosing pumps which will in turn stop the flow from the bioreactor.

When the second membrane system is "full" (i.e. level just meets bottom of internal float tank), the circulation pump (M2A) should be started. This pump draws from the bottom of the main tank and into the internal process tank.

When the internal process tank is full, the process pump can then be started. Before starting the process pump ensure that the membrane pressure control valve is fully open (ie fully turned anti-clockwise) and that the membrane valve opposite is set to "membrane open". Once running, the membrane pressure control valve can be carefully closed until the membrane inlet pressure gauge reads 8 Bar, and the membrane back pressure gauge reads 6 Bar.

Fluid from the main tank is pumped through the membrane pod. Concentrate is returned to the main tank, whilst permeate is fed into an IBC, via a flow meter. This process will continue until the low-level float switch is reached. At this point, the process pump will cut off and the level in the internal float tank will drop until its float switch breaks contact – this will cut off the process pump. The resulting concentrate can then be drained via drain pump 2 (M6), which is controlled from the main panel. Valve 22 must be opened to drain the system.

System 2 - Flushing

To flush system 2, the external flush tank must be used. Fill the external flush tank with fresh water until the top float switch is made. Add 500ml surfactant to the water. Valve V?? should be turned to divert permeate back into the process tank.

(NB the large double valve underneath the flush tank must be pointing to the floor for flushing. This diverts the feed and return of the process pump from the internal flush tank to the external flush tank, and changes over the float switches that are in operation).

Before starting the process pump ensure that the membrane pressure control valve is fully open (ie fully turned anti-clockwise) and that the membrane valve opposite is set to “membrane open”. Once running, the membrane pressure control valve can be carefully closed until the membrane inlet pressure gauge reads 8 Bar, and the membrane back pressure gauge reads 6 Bar. Flushing will continue for as long as necessary (usually 30-60 minutes).

The external flush tank can be drained via V19B, using drain pump 2 (controlled on main panel).

APPENDIX G

Weighing Factor

Band	Content of discharge	Factor (C)
A	<p>Where the consent conditions contain numeric conditions for any of the following; (excluding any condition for total oil and grease)</p> <p>pesticides, herbicides, fungicides</p> <p>polyhalogenated biphenyls</p> <p>polynuclear aromatic hydrocarbons; aliphatic, aromatic, heterocyclic and halogenated hydrocarbons</p> <p>alcohols (except methanol, ethanol, butanol, propanol and glycols)</p> <p>aromatic nitrogen compounds</p> <p>phenolic compounds (except total and monohydric phenols)</p> <p>esters; ethers; ketones; aldehydes (except formaldehyde)</p> <p>viruses; effluents where consent requires toxicity tests (other than rapid bacterial toxicity tests)</p>	14
B	<p>Except where the consent falls in Band A or authorisation falls in a Band A substance -</p> <p>Where the consent conditions contain numeric conditions for any of the following:</p> <p>metals, metalloids</p> <p>cyanides; sulphides</p> <p>total and monohydric phenolic compounds</p> <p>methanol, ethanol, butanol, propanol; glycols</p> <p>carboxylic acids</p> <p>organic nitrogen compounds (except those in Band A, urea and</p>	5

	<p>quaternary ammonium salts)</p> <p>bacteria</p> <p>effluent where consent requires rapid bacterial toxicity tests</p>	
C	<p>Except where the consent falls into A or B</p> <p>sewage and organic trade effluent with numeric consent conditions (except those specified in Bands E or G)</p> <p>all discharges of trade effluent of an organic nature with numeric conditions other than included in Band E,F,G and H.</p>	3
D	<p>Except where consent falls into A,B,or C</p> <p>sewage with no numeric conditions; trade effluent not specified in E</p> <p>all other discharges of trade effluent other than those specified in bands E, F, G and H</p>	2
E	<p>Except where consent falls into A,B,C, or D</p> <p>site drainage from trade premises</p> <p>storm and emergency discharges at treatment works, pumping stations and from drainage systems</p> <p>all trade effluents of direct cooling water other than those specified in Band G</p> <p>trade effluent from prevention of interference with mining, etc, other than those specified in band F</p>	1
F	<p>surface water (not containing trade effluent)</p> <p>trade effluent from prevention of interference with mining, etc, for</p>	0.5

	<p>which only conditions are volume, suspended solids, iron, pH and chloride</p> <p>trade effluent where the consent permits the discharge of water abstracted from the controlled water after use in a trade, subject to limits only in the increase of concentration of biological oxygen demand, suspended solids, and ammonia</p> <p>any effluent not identified elsewhere</p>	
G	<p>cooling water where only conditions are volume, temperature, pH, chlorine</p> <p>trade effluent where the consent permits the discharge of water after use for cultivation of plants</p>	0.3
H	<p>Any effluent or substance with no numeric conditions other than volume discharged,</p> <p>a maximum daily volume of 5m³ or less per day</p> <p>a discharge on not more than 6 days per year or any such equivalent</p> <p>a discharge only at specific periods of the year</p>	1.5

Volume of discharge (m ³ /day)	Factor (V)	Volume of discharge (m ³ /day)	Factor (V)
0 – 5	0.3	> 1,000 – 10,000	3.0
> 5 – 20	0.5	> 10,000 – 50,000	5.0
> 20 – 100	1.0	> 50,000 – 150,000	9.0

> 100 – 1,000	2.0	> 150,000	14.0
---------------	-----	-----------	------

Type of receiving water	Factor (RW)
Surface	1.0
Coastal	0.8
Ground	0.5